SOURCE APPORTIONMENT OF URBAN CONTAMINANTS

ABIDA USMAN

(Bachelor Environ. Sci; MPhil Environ. Sci)

Thesis submitted to the University of Nottingham for the degree of

Doctor of Philosophy

September 2018

Dedication

This work is dedicated to my lovely son

‘**Muhammad Mahad Ali**’

Acknowledgment

I owe my sincere gratitude to my supervisors Dr Scott Young, Dr Liz Bailey, Dr Simon Chenery and Dr Louise Ander for their meaningful supervisions and encouragement. I feel myself very fortunate to have such caring supervisors who were very kind and helpful throughout my research studies.

I want to thank the University of Nottingham for awarding me the 'Vice Chancellor Scholarship' that allowed me to undertake this research work.

I would like to extend my gratitude to all my colleagues in the division of Agricultural and Environmental sciences, University of Nottingham for their support and friendly behaviour. My sincere thanks goes to 'Emma Hooley' for her administrative support and 'Saul' for providing technical assistance. A very special thanks to Abdul Mossa Wahab and Saeed Ahmad for always being ready to help me.

Also this work would have never been accomplished without the prayers of my loved ones. A very big thanks to all my family, my parents, my son, brothers, sisters, brothers in law, sisters in law, nieces and nephews for their unconditional support and love.

Last but not the least, I heartiest acknowledge contributions of 'Jawad Hussain' my husband, who had to put up with my mood swings and frustrations during time of pressure and his support to my success here.

List of acronyms and abbreviations

AR	Analar
ANOVA	Analysis of variance
BECs	Background equivalent concentrations
BLLs	Blood lead levels
CA	Cluster analysis
CPS	Counts per second
CRC	Collision reaction cell
DC	Direct current
Df	Dead time correction factor
DLs	Detection limits
EFs	Enrichment factors
GIS	Geographic information system
HI	Hazard Index
HREEs	Heavy rare earth elements
IAs	Isotopic abundances
ICP-QMS	Quadrupole based inductively coupled plasma mass spectroscopy
ICP-QQQ-MS	Triple quadrupole inductively coupled plasma mass spectroscopy
ID	Isotopic dilution
IR	Isotopic ratio
IUPAC	International Union of Pure and Applied Chemistry
KED	Kinetic energy discrimination
Kf	Mass bias correction factor
LREEs	Light rare earth elements
MC-ICP-MS	Multi-collector inductively coupled plasma mass spectroscopy
NBCs	Normal background concentrations
NERC	National Environmental Research Council
NIST	National Institute of Standard and Technology
PCA	Principal component analysis
PFA	Perfluoro Alkoxy
PGEs	Platinum group elements

PMF	Positive matrix factorization
PTEs	Potentially toxic elements
Pzc	Point of zero charge
QL	Quantification limit
REEs	Rare earth elements
RF	Radio frequency
SCP	Suspended colloidal particles
SEPs	Sequential extraction procedures
SEM	Scanning electron microscopy
SGVs	Soil guideline values
SOC	Soil organic carbon
SOM	Soil organic matter
TAG	Trace analysis grade
TDS	Total dissolved solids
TIMS	Thermal ionization mass spectrometry
UCC	Upper continental crust
XAFs	X-ray absorption fine structure

Abstract

Urban soils are major recipients of large amount of contaminants from multiple sources of both natural and anthropogenic origins. Accumulation of heavy metals at trace levels can be hazardous to human health and to the environment due to their ubiquity, high toxicity and persistent bioavailability. In order to mitigate the adverse effects of contaminants in soil, it is essential to have a better understanding of their characteristics and sources. Knowledge of contaminant sources is a prerequisite for developing appropriate prevention and control regulations. The overall aim of this research work was to undertake a forensic analysis of urban soil contaminants. The methodology included determination of Pb isotopic ratios in combination with a spectrum of associated elements. The experimental objectives utilized a sequential extraction procedure (SEP) and isotopic dilution (ID) to assess the fractionation and reactivity of pollutants and thereby reveal source-associations.

A key part of the project was to refine experimental and instrumental protocols for accurate and precise measurement of Pb isotope ratios using a current generation inductively coupled plasma quadrupole based mass spectrometer (ICP-QMS). This is a widely available and relatively inexpensive instrument providing a rapid assay of isotope ratios. However, ICP-QMS is subject to various interferences which limit the accuracy and precision of Pb isotope signals. The protocol developed on the ICP-QMS benchmarked very well against multi-collector inductively coupled plasma mass spectrometry (MC-ICP-MS) assays on the same sample material. The protocol was then applied to a range of samples, including soils from urban locations, sewage-amended arable fields and allotments, in order to determine soil Pb source apportionment. The characterization of Pb isotopes were helpful in confirming that Pb from petrol and local geological (coal, ore) sources were the dominant sources

of Pb in soils. The examination of Pb isotopic ratios in allotment topsoils and subsoils was useful in revealing the extent to which labile Pb_{petrol} migrated down the soil profile into the subsoils. The evaluation of trends of Pb_{petrol} with total soil Pb (Pb_{total}) further helped in identifying allotment sites where the main influence was from vehicular emissions and coal burning.

The determination of Pb isotopes in the individual fractions of SEP was a useful approach in giving more insight regarding the estimation of Pb_{petrol} and $Pb_{geogenic}$ associated with different phases. The relative proportion (%) of $Pb_{geogenic}$ in all fractions was greater (>67%) than the Pb_{petrol} whereas highest proportion Pb_{petrol} was observed associated with the most labile fraction (F1). Measurement of Pb isotopes also helped in assessing the behaviour of Pb_{petrol} across different fractions of SEP. An interesting finding was the presence of Pb_{petrol} (24%) in the most resistant fraction (F5), which was unexpected. The proportion of Pb_{petrol} in F5 was greatest in soils with greater concentration of organic matter, available P and Pb_{total}. This may represent transformation of initially soluble Pb_{petrol} to more resistant forms through reaction with soil constituents or, it might be an artefact arising from resistant anthropogenic (non-petrol) Pb that does not have a typical isotopic signature of 'geogenic Pb'.

The measurement of labile (isotopically exchangeable) trace metals including Ni, Cu, Cd, Zn and Pb in allotment soils showed that the reactivity of these five trace metals were below 50% and followed a consistent decreasing order of Cd> Pb≥ Zn> Cu> Ni. The overall weak influence of soil properties on lability of trace metals suggested a lasting impact from the original contaminant sources. Furthermore, the relative contribution of $Pb_{geogenic}$ (coal Pb) to both labile and non-labile fractions was greater whereas surprisingly the intrinsic lability of Pb_{petrol} was observed lower. The

greater lability of $Pb_{geogenic}$ was unexpected which reflected that the particulate coal-derived Pb arrived as aerial deposition were in more reactive form.

The comparison of E-values for Ni, Cu, Zn, Cd and Pb with SEP data showed no consistent agreement between the labile fractions and any single fraction although a reasonable correspondence was found between metals extracted in combined fractions (i.e., F1+F2) and E-values for Zn and Ni. In case of Cu, the non-isotopically exchangeable fraction correlated with the sum of the most resistant two fractions (i.e., F4+F5).

Approach such as cluster analysis (dendrogram) using the full range of trace elements with source apportioned Pb (Pb_{petrol} and $Pb_{geogenic}$) in all sets of soils (urban soils, sewage amended soils and allotment soils) was to some extent helpful in understanding the likely origins of key contaminant metals and metalloids. In allotments, the variation observed in the concentration of trace metals at different sites was partly associated with the location, age and history of sites. For example, site BH, relatively new allotment and remote was less contaminated compared to other allotments which were near to major pollutant sources.

Forensic analysis of trace elements including REEs and PGEs in allotment soils was of limited use in identifying other specific sources of contaminants. It revealed that REEs mainly originated from natural sources whereas, the EFs values and comparison of isotopic abundance ratios with the mean upper continental crust (UCC) showed a small influence from anthropogenic sources such as fertilizers. The concentration of PGEs were below detection limit following sample preparation. This revealed two possibilities, first there was no substantial influence of PGEs on allotment soils. Secondly the method used for soil digestion and resulting dilutions would have produced solution with very low concentrations of PGEs. An optimised

analytical approach (e.g. digestion of samples with Aqua regia and pre-concentration) is therefore suggested for determination of PGEs in soils.

Contents

Dedication ____ *i*

Acknowledgment ____ *ii*

List of acronyms and abbreviations ____ *iii*

Abstract ____ *v*

1 Chapter 1: Introduction ____ *1*

1.1 Lead in the environment ____ **2**

1.1.1 Natural abundance of Pb isotopes ____ 2

1.1.2 History of Pb use ____ 3

1.1.3 Current sources of Pb contamination ____ 4

1.2 Soil Pb ____ **5**

1.2.1 Urban soils ____ 5

1.2.2 Agricultural soils ____ 8

1.2.3 Forest soils ____ 10

1.2.4 Peat deposits ____ 12

1.3 Environmental forensics ____ **14**

1.4 Rare earth elements (REEs) ____ **15**

1.5 Platinum group elements (PGEs) ____ **16**

1.6 Approaches to source apportionment ____ **17**

1.6.1 Elemental ratios ____ 18

1.6.2 Binary models ____ 19

1.6.3 Soil extractions and measurement of E-values ____ 20

1.7 Measurement of Pb isotopes ____ **21**

1.7.1 Principles of ICP-QMS ____ 22

1.7.2 Limitations of ICP-QMS 26

1.8 Study aims and thesis structure 26

2 Chapter 2: General Materials and methods 29

2.1 Overview 29

2.2 Soil selection 29

2.3 Reagents 33

2.4 Soil preparation and digestion 33

2.5 Sequential extraction 33

2.6 Major and trace element analysis by ICP-QMS 35

2.7 Measurement of REEs and PGEs 36

2.7.1 REEs 36

2.7.2 PGEs 36

2.8 Isotopically exchangeable Cu, Ni, Zn, Cd and Pb 38

2.8.1 Stock solutions 38

2.8.2 Sample preparation 39

2.8.3 Resin purification method 39

2.9 Analysis of Cu, Ni, Zn, Cd and Pb isotopic abundances 40

2.10 Lead source apportionment 40

2.11 Preliminary development of a method for accurate measurement of Pb isotopes using ICP-QMS 41

2.11.1 Dead time correction 42

2.11.2 Mass bias correction 44

2.11.3 Dwell time 45

2.11.4 Peak Compression 47

2.12 Quality control 49

2.13 Statistical analysis 49

3 Chapter 3: Benchmarking current generation ICP-QMS against MC-ICP-MS spectrometry for the determination of lead isotope ratios in soils *51*

3.1 Introduction 52

3.2 Experimental 56

3.2.1 Preparation of samples 56

3.2.2 Instrumentation and optimisation procedures 59

3.3 Procedures for optimising measurement of Pb isotopes using ICP-QMS 61

3.3.1 Evaluation of detector dead time correction factor 61

3.3.2 Mass bias correction 63

3.3.3 Quadrupole dwell time 65

3.3.4 Optimising the number of scans (quadrupole peak visits) 66

3.4 Results and discussion 68

3.4.1 Comparison of Pb isotope ratios ($^{207}/^{206}$Pb, $^{208}/^{207}$Pb and $^{208}/^{204}$Pb) measured by ICP-QMS and MC-ICP-MS 68

3.4.2 Comparison of Binary plots 74

3.5 Conclusions 76

3.6 Conflicts of interest 77

3.7 Acknowledgements 77

4 Chapter 4: Identification of pollutant sources in urban soils *78*

4.1 Introduction 78

4.2 Objectives 79

4.3 Material and methods 79

4.3.1 Soil sampling 79
4.3.2 Sample analysis 79
4.3.3 Statistical analysis for variation of heavy metals concentration in Pakistan sewage amended soils 80
4.3.4 Cluster Analysis (CA) 80
4.4 Results and discussion 81
4.4.1 Nottingham urban soils 81
4.4.2 Wolverhampton urban soils 87
4.4.3 Pakistan sewage amended soils 93
4.5 Conclusions 102
5 Chapter 5: Identification of contaminant sources in urban allotment soils 104
5.1 Introduction 104
5.2 Objectives 105
5.3 Materials and methods 106
5.3.1 Soil sampling 106
5.3.2 Sample analysis 111
5.3.3 Statistical analysis for variation of heavy metals concentration between allotment sites 112
5.3.4 Enrichment factors (EFs) 112
5.4 Results and discussion 113
5.4.1 Major and trace element concentrations in allotment soils 113
5.4.2 Enrichment factors (EFs) 115
5.4.3 Cluster Analysis (CA) 121
5.5 Rare earth elements 131
5.5.1 Concentration of REEs in allotment soils 131
5.5.2 Crust-normalized REEs patterns for allotment soils 133
5.5.3 REEs Enrichment Factors 136
5.5.4 Correlation analysis between REEs in soils 139

5.5.5 Sources of REEs in allotment soils 141

5.6 Platinum Group Elements 144

5.6.1 Investigation of interferences in the determination of PGEs by ICP-MS. 144

5.6.2 Concentration of PGEs in allotment soils 144

5.7 Characterisation of Pb isotopic signatures 144

5.8 The relationship between Pb_{petrol} and Pb_{total} in top and subsoils 151

5.9 Conclusions 154

6 Chapter 6: Use of common approaches to study behaviour and sources of pollutants in allotment soils 156

6.1 Introduction 156

6.1.1 Aim of chapter 162

6.2 Materials and methods 163

6.2.1 Soil sampling 163

6.2.2 Measurement of isotopically exchangeable Pb, Zn, Cd, Cu and Ni in soils using an ID technique 164

6.2.3 Calculation of isotopic abundances (IAs) of non-labile metal 165

6.2.4 Proportion of Pb_{Petrol} and $Pb_{geogenic}$ in labile and non-labile pools 166

6.2.5 Sequential extraction procedure 167

6.2.6 Analytical procedures for measurement of isotopic abundances in soils through ICP-QMS 167

6.3 Results and discussion 167

6.3.1 Lability (E-value) of trace elements (Ni, Cu, Zn, Cd and Pb) in soils 167

6.3.2 Comparison of isotopically exchangeable (E-values) pool of different trace metals measured in filtered solutions (E_{soln}) and resin – treated solutions (E_{resin}) 171

6.3.3 Fractionations of multi-elements in allotment soils using a sequential extraction procedure (SEP) 175

6.3.4 Labile and non-labile pools of Pb, Zn, Cd, Ni, and Cu: comparison of data from an isotopic dilution and SEP. 188

6.3.5 Effects of soil properties on E-value of Ni, Cu, Zn, Cd and Pb 191

6.3.6 Source apportionment of labile/non-labile pools of lead urban allotment top soils 197

6.3.7 Behaviour of Pb in individual fractions of an SEP in urban allotment topsoils 200

6.4 Conclusions 209

7 Chapter 7: General conclusions and future work 211

7.1 Overview 211

7.2 Main Findings 211

7.3 Future work 216

8 References 218

9 APPENDICIES 240

9.1 Appendix A Descriptive statistics 240

9.2 Appendix B Investigation of interferences in the determination of PGEs by ICP-MS 248

9.3 Publication 258

LIST OF TABLES

Table 1.1: Advantages and disadvantages of different mass spectrometric techniques for the determination of Pb isotopes. 22

Table 2.1: Number of soil samples collected from individual plots of urban allotments. 32

Table 2.2: Potential interfering species in the determination of PGEs 37

Table 2.3: Different reference materials used as test materials in different experiments 41

Table 3.1 Studied soil samples from Nottingham (Ng) and Wolverhampton (Wv) 57

Table 3.2 Operational parameters selected for measurement of Pb isotopic ratios using ICP-QMS 60

Table 3.3 Configuration of the Nu Plasma HR 'Zircon' collector block, used for Pb isotope analysis 61

Table 3.4 Evaluation of significance of slope (multiplicative) and offset (additive) when regressing the difference between measured ICP-QMS and MC-ICP-MS against MC-ICP-MS ratios, showing the significant differences occurring in the offset for $^{207}/^{204}$Pb and $^{208}/^{204}$Pb ratios. 73

Table 3.5 Statistical comparison of within sample measurement precision with between sample precision and evaluation for Pb isotope ratios determined both by ICP-QMS and MC-ICP-MS. Note: the greater the F-statistic is over the critical F value, the greater the power of the measurement to discriminate true sample variation from analytical "noise". 73

Table 4.1: Description of individual sites in Nottingham soils 82

Table 4.2: Location of Wolverhampton soil sampling sites 88

Table 5.1: Nottingham allotment sites and their descriptions 106

Table 5.2 Average concentration ratios of Pb_{petrol} to Pb_{coal} in topsoils 121

Table 5.3: Speculative association of elemental clusters with soil and contaminant sources for nine allotment sites 127

Table 5.4: Correlation coefficients (r-values) between REEs (LREEs and HREEs) in allotment topsoils at $p \leq 0.001$. 140

Table 5.5: Correlation coefficients (r-values) between REEs (LREEs and HREEs) in allotment subsoils at $p \leq 0.001$. 140

Table 5.6: Ratio of La to other REEs and V in topsoils and subsoils of individual allotment sites 143

Table 6.1: Isotopic ratios (spiked and unspiked) and their natural isotopic ratio values 165

Table 6.2: Comparison of apparent labilities (%E-values), average standard deviations and average differences for Ni, Cu, Zn, Cd and Pb between resin-treated (E_{resin}) and filtered solutions (E_{soln}). *174*

Table 6.3: Average percentage (%) distribution of multi-elements in different fractions of sequential extraction procedure (SEP)..... *186*

Table 6.4: Pearson correlation coefficients (r values) between %E-values of Ni, Cu, Zn, Cd and Pb with soil properties. Bold Figures represent significant r values at p values ≤ 0.05..... *192*

Table 6.5: Proportions (%) of Pb_{petrol} and $Pb_{geogenic}$ in individual fractions of SEP *204*

LIST OF FIGURES

Figure 2.1: Lead isotopic ratio $^{206}/^{207}$Pb versus concentration (µg L^{-1}) of SRM-981, NIST; symbols denote duplicate runs. 42

Figure 2.2: Isotopic ratios (a) $^{204}/^{208}$Pb, (b) $^{206}/^{208}$Pb, (c) $^{207}/^{208}$Pb versus Pb standards concentration (µg L^{-1}) all at individually optimised values of Df. The circle and triangle symbols represent repeat runs of the same samples. 43

Figure 2.3: SRM-981, NIST (external correction) for mass bias correction of all Pb isotopic ratios at different intervals. 44

Figure 2.4: SRM-981, NIST spiked with Tl for mass bias correction of all Pb isotopic ratios at different intervals. 45

Figure 2.5: Average %RSD for intensities of the four Pb isotopes (^{204}Pb, ^{206}Pb, ^{207}Pb and ^{208}Pb) as a function of quadrupole dwell time (0 - 50 ms). 46

Figure 2.6: Average %RSD of isotopes (^{204}Pb, ^{206}Pb, ^{207}Pb and ^{208}Pb) intensities as a function of quadrupole dwell time (5 - 15 ms). 46

Figure 2.7: Comparison of SRM-981, NIST (external) compression factors (Kc) for converting compressed signals for (a) ^{206}Pb, (b) ^{207}Pb and (c) ^{208}Pb intensities to equivalent uncompressed values. 48

Figure 3.1. Isotopic count ratios (CR) $^{204}/^{208}$Pb vs ^{208}Pb intensity measurements (cps) at the optimised value of Df. 63

Figure 3.2. Average RSD (%) of Pb isotope ratios against dwell time (ms) whilst retaining a constant total acquisition time. 66

Figure 3.3. Values of residual standard deviation, comparing ICP-QMS with MC-ICP-MS, for Pb isotope ratios (a) $^{207}/^{206}$Pb, (b) $^{208}/^{207}$Pb, and (c) $^{208}/^{204}$Pb against the number of quadrupole scans (peak visits). 68

Figure 3.4. Correlation of Pb isotope ratios (a) $^{206}/^{207}$Pb, (b) $^{208}/^{207}$Pb, and (c) $^{208}/^{204}$Pb measured using quadrupole (ICP-QMS) and multi-collector (MC-ICP-MS) instruments. 69

Figure 3.5. Difference between the benchmark MC-ICP-MS data and the difference between ICP-QMS and MC-ICP-MS (a), (b) and (c). 72

Figure 3.6. A binary plot using isotopic ratios $^{208}/^{207}Pb$ vs $^{206}/^{207}Pb$ for data derived from MC-ICP-MS and ICP-QMS with either 10,000 or 1,000 scans. Note error bars for MC-ICP-MS and ICP-QMS (10000 scans) are smaller than symbols for most samples. 75

Figure 3.7. A binary plot using isotopic ratios $^{208}/^{204}Pb$ vs $^{206}/^{207}Pb$ for data derived from MC-ICP-MS and ICP-QMS with either 10,000 or 1,000 scans. 76

Figure 4.1: Concentration of trace metals (a) Ni, (b) Cr, (c) Cu, (d) Zn, (e) As, (f) Cd and (g) Pb in Nottingham urban soils. Vertical bars denote the average plus/minus the standard error. The dashed line shows the normal background concentration (NBC). 83

Figure 4.2: Dendrogram for Nottingham urban soils. 84

Figure 4.3: Binary plot showing the isotopic ratios $^{206}/^{207}Pb$ versus $^{208}/^{207}Pb$ for Nottingham urban soils, with median values from UK leaded petrol, Southern Pennine Pb ore (Galena) and Nottinghamshire-Yorkshire-Derbyshire (N-Y-D) coal shown for comparison. 85

Figure 4.4: Relationship of Pb_{total} versus isotope ratio $^{206}/^{207}Pb$ in Nottingham urban soils. 86

Figure 4.5: Proportion of Pb_{petrol} in Nottingham urban soils 87

Figure 4.6: Concentration of different trace metals (a) Ni (b) Cr, (c) Cu, (d) Zn, (e) As, (f) Cd and (g) Pb in soils collected from different sites of Wolverhampton. Vertical bars denotes the average plus/minus the standard error and dashed line shows the normal background concentration values (NBCs). 89

Figure 4.7: Dendrogram of elemental analysis in Wolverhampton urban soils. 90

Figure 4.8: Binary plot for Wolverhampton urban soils. Median values of UK leaded petrol, Southern Pennine Pb ore (Galena) and Nottinghamshire-Yorkshire-Derbyshire (N-Y-D) coal shown as end members. 91

Figure 4.9: Relationship of Pb_{total} concentration with isotope ratio $^{206}/^{207}Pb$ in Wolverhampton urban soils. 92

Figure 4.10: Proportion of Pb_{petrol} in Wolverhampton urban soils. 92

Figure 4.11: Concentration (mg kg^{-1}) of Ni, Cr, Cu, Zn, As, Cd and Pb in sewage amended soils. Boxes indicate the interquartile ranges of the concentrations. Whiskers extend to the highest and lowest limits of the data. Outliers are shown as asterisks. Mean is shown as a dot (●) and the median as a line. 96

Figure 4.12: Dendrogram of cluster analysis of elements in Pakistan sewage amended soils. 98

Figure 4.13: Binary plot of isotopic ratios $^{206}/^{207}Pb$ vs $^{208}/^{207}Pb$ for sewage amended soils. 99

Figure 4.14: Lead isotopic ratio $^{206}/^{207}Pb$ in sewage amended soils of different districts of Pakistan. Mean is shown as a (●) and median as a line. Broken lines indicate the range of reference sources (Australian ore as a proxy for Pb_{petrol} and UCC for $Pb_{geogenic}$).....100

Figure 4.15: Relationship of Pb_{total} concentration and isotope ratio $^{206}/^{207}Pb$ in Pakistan sewage amended soils from different districts (a) GW (b) GT (c) LH and (d) FB. Grey and black dashed lines represents the ratios in UCC and Australian ore respectively.....101

Figure 4.16: Proportion of Pb_{petrol} in Sewage amended soils.....102

Figure 5.1: Concentration (mg kg^{-1}) of Cr, Ni, Cu, Zn, As, Cd and Pb in topsoils from 9 allotment sites are shown as box and whisker plot. Boxes indicate the interquartile ranges of the concentration of elements, whereas whiskers are the lines outside the box and extend to the highest and lowest limits of the data. Outliers are shown as asterisks. Mean is shown as a symbol (●) and median as a line. Dashed lines denote SGVs (EA, 2009) in the case of Cr, Ni, As, Cd, Pb and for Cu and Zn they indicate the 'Sludge regulation, 1989' values.....115

Figure 5.2: Average concentration ratios topsoil:subsoil (Enrichment factor, EF) for different elements in individual allotment sites. Vertical error bars denote the standard errors across all samples from individual sites.....120

Figure 5.3: Dendrograms of topsoils elemental analysis from seven individual allotment sites. 130

Figure 5.4: Concentration (mg kg^{-1}) of total REEs at different allotments sites (a) topsoils and (b) subsoils 132

Figure 5.5: Average concentration (mg kg^{-1}) of LREEs and HREEs in topsoils and subsoils of allotments. 132

Figure 5.6: Crust-normalized REEs pattern for topsoils and subsoils of individual allotments. 136

Figure 5.7: Average concentration ratio topsoil:subsoil (Enrichment factor, EF) for REEs in individual allotment sites. The vertical bars denote the average standard error.....139

Figure 5.8: Binary plots showing the isotopic ratios $^{206}/^{207}Pb$ vs $^{208}/^{207}Pb$ for individual allotment topsoils and subsoils with median values from UK leaded petrol, Southern Pennine Pb ore (Galena) and N-Y-D coal shown for comparison. 149

Figure 5.9: Lead isotopic ratio $^{206}/^{207}Pb$ in (a) topsoils and (b) subsoils of individual allotment sites are shown as box and whisker plots. Outliers are shown as asterisks. Mean is shown as a symbol (●) and median as a line. The broken lines indicates the range of reference sources (UK ore and UK leaded petrol). 150

Figure 5.10: Proportion of Pb_{petrol} in allotment topsoils and subsoils 150

Figure 5.11: Relationship between $\%Pb_{petrol}$ and Pb_{total} in topsoils and subsoils of individual allotment sites....154

Figure 6.1: Box and whisker plot showing lability (% E-value) of Ni, Cu, Zn, Cd and Pb in allotment soils (n=59); the mean value (●) is also shown and outliers are marked as an asterix. *169*

Figure 6.2: Frequency distributions of % E–value for (a) Ni, (b) Cu, (c) Zn, (d) Cd and (e) Pb in allotment soils. *170*

Figure 6.3: Comparison of $\%E_{soln}$ *and* $\%E_{resin}$ *for (a) Ni, (b) Cu, (c) Zn, (d) Cd and (e) Pb in soils. The solid line is 1:1 line.* *173*

Figure 6.4 Comparison of non-spiked isotopes (a) ^{111}Cd *and (b)* ^{208}Pb*; ICPMS intensities (cps) in resin-treated (*E_{resin}*) and filtered equilibrated soil solutions (*E_{soln}*).* *174*

Figure 6.5: Correlation between concentrations of Cu associated with SEP fraction F4 (Cu_{F4}*) and total organic matter content.* *175*

Figure 6.6: Correlation between Pb and P associated with F4 of the SEP. *178*

Figure 6.7: Correlation between SOC and concentration of P in F4 (P_{F4}*)* *178*

Figure 6.8: Comparison of Sr and Ca (mg kg^{-1}*) in different fractions (F1-F5) of SEP.* *181*

Figure 6.9: Correlation between concentration of As and P associated with F3 of the SEP. *182*

Figure 6.10: Correlation between concentration of Co and Mn held in F3. ..... *182*

Figure 6.11: Correlations between concentrations of V and Fe in different fractions (F1-F5) of SEP. *184*

Figure 6.12: Fractionation (%) of elements in urban allotment topsoils determined by a sequential extraction *187*

Figure 6.13: Comparison of individual and combined fractions of SEP (F1, F1-F2, F1-F3) with %E-value of (a) Pb, (b) Zn, (c) Cd, (d) Ni and (e) Cu in urban allotment top soils. The dashed line is 1:1 line. *190*

Figure 6.14: Average fractionation of labile and non-labile pools (% of total soil metal content) by isotopic dilution (ID) (n = 52 allotment soils). *191*

Figure 6.15: Relationships between %E-values (% of total metal content) and total soil metal concentration (mg kg^{-1}*) for (a) Cu, (b) Cd, (c) Pb, (d) Ni and (e) Zn.* *193*

Figure 6.16: Relationships between %E-values (% of total metal content) and pH of (a) Cd, (b) Ni, (c) Pb, (d) Cu and (e) Zn. *194*

Figure 6.17: Relationships between %E-values (% of total metal content) and organic matter (%) for (a) Ni, (b) Zn, (c) Cu, (d) Cd and (e) Pb. *195*

Figure 6.18: Relationships between %E-values (% of total metal content) and available P (mg kg^{-1}*) for (a) Ni, (b) Zn, (c) Pb, (d) Cu and (e) Cd.* *196*

Figure 6.19: The ratio of non-labile to labile $^{206}/^{207}$Pb ratios (IR_{NL}/IR_L) as a function of $^{206}/^{207}$Pb of Pb_{total} in topsoils. The dashed horizontal line represents an IR_{NL}/IR_L ratio of 1. ..... *198*

Figure 6.20: Proportion (%) of Pb_{petrol} and $Pb_{geogenic}$ in labile and non-labile pools in soils. *199*

Figure 6.21: Intrinsic average percentage (%) of Pb_{petrol} and $Pb_{geogenic}$ in labile and non-labile pools of allotment topsoils. *200*

Figure 6.22: Binary plots showing the isotopic ratios $^{206}/^{207}$Pb vs $^{208}/^{207}$Pb for allotment top soils with median values from UK leaded petrol and Southern Pennine Pb ore (Galena) shown for comparison. *203*

Figure 6.23: Proportion (%) of $Pb_{geogenic}$ to Pb_{petrol} in individual fractions of SEP *204*

Figure 6.24: Effect of pH on Pb_{petrol} on (a) F1/F5, (b) F2/F5, (c) F3/F5 and (d) F4/F5. ..... *205*

Figure 6.25: Effect of organic matter (mg kg^{-1}) on Pb_{petrol} on (a) F1/F5, (b) F2/F5, (c) F3/F5 and (d) F4/F5. ..... *206*

Figure 6.26: Effect of Pb_{total} content (mg kg^{-1}) on Pb_{petrol} on (a) F1/F5, (b) F2/F5, (c) F3/F5 and (d) F4/F5. ..... *207*

Figure 6.27: Effect of available P (mg kg^{-1}) on Pb_{petrol} on (a) F1/F5, (b) F2/F5, (c) F3/F5 and (d) F4/F5. ..... *208*

1 Chapter 1: Introduction

In the urban environment, trace elements are released on a daily basis from numerous human activities such as municipal, commercial, industrial, vehicular emissions and the corrosion of construction/building materials (Nriagu, 1996, Martin and Griswold, 2009, Chen et al., 2005b). Trace element emissions from coal-fired power plants, mining and smelting activities are also important contaminant sources if located in or near urban areas. Trace elements typically accumulate in surface soils and may migrate into water bodies through urban run-off (Thornton, 1993, Mielke and Reagan, 1998, Wong et al., 2006). Their presence in urban environments increases the chances of exposure via inhalation, ingestion and dermal contact (Mielke and Reagan, 1998, Mielke et al., 1999) and result in long-term environment impacts (Callender and Rice, 2000, Sutherland and Tolosa, 2000, Cui et al., 2005, Zhang et al., 2007). Lead (Pb) is considered one of the most hazardous metals to have affected the environment to a significant extent. In the human body it can enter mainly through inhalation and ingestion from variety of sources such as contaminated food, water, air and soil (Needleman, 2004, Cheng and Hu, 2010). Children are at greater risk to Pb poisoning as compared to adults due to ingestion of contaminated soils because of their hand-to-mouth behaviours (Wixson and Davies, 1994). It has been reported that adverse health effects in children at blood lead levels (BLLs) <10 μg/dL are associated with attention disorders, behavioural problems, cognitive deficits, reduced height and delayed puberty (Lanphear et al., 2000, Canfield et al., 2003, Barbosa Jr et al., 2005, Surkan et al., 2007). Exposure of children to very high level of Pb causes neurological effects, coma, death, ataxia and convulsions (ATSDR, 2007). In adults, Pb poisoning can cause neurological effects, headache, impaired concentration, fatigue, increase blood pressure and nervousness (Goyer,

1993, Sanborn et al., 2002, ATSDR, 2007). Due to its high toxicity, knowledge regarding the occurrence and behaviour of Pb in environment may be useful for developing mitigating strategies to ameliorate problems arising from Pb contamination.

1.1 Lead in the environment

1.1.1 Natural abundance of Pb isotopes

Lead has four main isotopes with a range of average natural isotopic abundances: ^{204}Pb (1.4%), ^{206}Pb (24.1%), ^{207}Pb (22.1%) and ^{208}Pb (52.4%) (Komárek et al., 2008). The minor isotope, ^{204}Pb, is the only primordial stable isotope with a constant abundance on Earth. The other three isotopes (^{206}Pb, ^{207}Pb and^{208}Pb) are both primordial (originating from supernovae) and radiogenic, the latter formed by the radioactive decay of ^{238}U, ^{235}U and ^{232}Th (Sangster et al., 2000). Different Pb ores and products derived from these ores have distinct isotopic signatures which differ from the surrounding bedrock (Faure, 1986). For example there are Pb deposits in Australia, Scandinavia and the USA that have 'extreme' isotopic compositions and their signatures are considered unique when compared to many other mines that have a narrow range of ^{206}/^{207}Pb (1.15-1.22) and ^{208}/^{207}Pb (2.42-2.50) (Sangster et al., 2000). The specific isotopic composition of an ore body depends on initial U/Pb and Th/Pb ratios of source rocks (bed rocks) and half - lives of the parent isotope (geological age) (Faure, 1998, Walraven et al., 2013). Isotopic signatures, if carefully measured, can be used as 'fingerprints' allowing the movement of Pb through the environment to be investigated.

1.1.2 History of Pb use

Lead has been released into the environment for approximately 5000 years, originally from inefficient smelting technologies, particularly the processing of sulphide ores containing Pb-Ag alloys in South Western Asia. World production of Pb at that time is estimated to be 200 t yr^{-1} (Patterson, 1971). During the 'Roman period', there was an increase in the processing of Pb, with up to 80,000 t yr^{-1} being produced by around 2000 years ago (Adriano, 2001). Following the decline of the Roman Empire there was a long period of "clean" conditions between about 400 A.D. and 900 A.D. In the Medieval period (900-1600 A.D) levels of Pb pollution again increased (Brännvall et al., 1999). The period from 900 to 1200 A.D. in Europe was one of both increasing population and economic growth during which an increasing number of Pb deposits were exploited and old mines re-opened. At the start of the 20th century, a further increase in Pb use occurred due to industrialization and increased coal burning. Lead has been extensively used in building materials such as flashing and piping because of its high ductility, it was also an important component of paints and glazes (Ahlberg et al., 2006, Walraven et al., 2013). A particular increase in Pb concentration was observed after World War II (1945 onwards) as the use of alkyl lead gasoline additives increased and became a major source of Pb pollution throughout the world (Nriagu, 1990).

Nriagu and Pacyna (1988) suggest that more than 90% of Pb emission into the environment originates from anthropogenic sources. Cumulative total world Pb production since ancient times is estimated to be 300 Mt (based on Nriagu, 1998 and updated to 2010 according to current world mine production figures) with the most intense emission within the past 500 years (Tong et al., 2000).

1.1.3 Current sources of Pb contamination

Due to its high toxicity, and the fact that it offers no benefit to human or environmental health, Pb is ranked second in a list of hazardous metals by the U.S. Agency for Toxic Substances and Disease Registry (ATSDR, 2007). As a consequence since the 1980s leaded petrol has been phased out and greater pollution controls implemented. These have resulted in a decrease in Pb pollution (Renberg et al., 2002). Despite this reduction Pb continues to enter the environment and has been found in very remote areas including the Antarctica ice sheet and snow in Greenland (Boutron et al., 1991, Vallelonga et al., 2002). Lead is still used for many commercial purposes such as sheeting, car batteries, radiation protection and cable sheathing (Ahlberg et al., 2006) and half of the total Pb use is from recycled Pb - approximately 8 Mt (Walraven et al., 2013). Current mining, smelting, industrial activities and improper disposal of electronics are sources of Pb in the environment. Lead is also applied incidentally to soils through sewage sludge application and the use of artificial fertilizers (Ahlberg et al., 2006, Walraven et al., 2013).

Resuspension and remobilization of particulates deposited from historical activities are important source of prevailing Pb pollution (Duzgoren-Aydin, 2007). Exterior sources are also responsible for indoor Pb pollution via transfer of particulates from contaminated soil or road dust (Farfel et al., 2003, Bi et al., 2015). Lead-based paints are another important source of Pb inside old houses. Clark et al. (2006) determined the Pb content of paint samples from India, China and Malaysia and found that 66% of new paint samples contained ≥5000 ppm (0.5%) Pb (the US definition of Pb based paint in existing housing) and 78% contained ≥600 ppm (0.06%) (limit for new paints). The intake of Pb through food is also considered a

common exposure route for both children and adults (Finster et al., 2004). Watanabe et al. (2000) reported that 59% and 81% of the total lead uptake of adults could be attributed to dietary sources in urban and rural areas, respectively.

1.2 Soil Pb

1.2.1 Urban soils

Urban soils generally have high levels of Pb contamination as these provide a sink for a variety of point and diffuse anthropogenic sources (Wong et al., 2006, Clark et al., 2008). Many studies have used the abundant isotopes i.e. ^{206}Pb, ^{207}Pb and ^{208}Pb to identify the origin of Pb in soil. This is possible because different sources of Pb can have characteristic ratios e.g. leaded petrol with alkyl additives from Broken Hill Type (BHT) Pb ore and Canadian ores have low isotopic ratios in the range between 1.03-1.04 (Doe and Stacey, 1974). Few studies of Pb isotopes have included consideration of the least abundant isotope ^{204}Pb, alongside the abundant isotopes i.e.,^{206}/^{204}Pb and ^{208}/^{204}Pb to assist with source identification. The use of Pb isotopes for identification of common sources of Pb in urban soils is described in the following sections.

1.2.1.1 Leaded gasoline

The emission of Pb into the urban environment in the modern era is mainly due to the use of tetraethyl lead as an anti-knock agent in leaded gasoline with a Pb contamination footprint in surface soils (Lin et al., 1998, Sutherland et al., 2000). Different studies have also shown through the characterization of Pb isotopes that surface roadside soils have a legacy of petrol-Pb in their surface layers despite the phase-out of leaded gasoline (Davies et al., 1987, Bäckström et al., 2004). For example, Gulson et al. (1981), measured ^{208}/^{206}Pb, ^{207}/^{206}Pb and ^{206}/^{204}Pb in soils

from an urban-rural transect in South Australia and observed that leaded gasoline was higher in the surface horizon compared to geogenic Pb, which was the major source of Pb at depths greater than 30-40 cm. Similarly Hansmann and Köppel (2000) used Pb isotopes ($^{207}/^{206}$Pb, $^{206}/^{204}$Pb and $^{208}/^{204}$Pb) to identify different types of anthropogenic and natural sources of Pb in urban soils of Switzerland. They found that anthropogenic sources of Pb were less radiogenic than the Pb in unpolluted soils ($^{206}/^{204}$Pb>18.8). Lead from vehicle exhausts was the least radiogenic ($^{206}/^{204}$Pb = 17.13 - 17.52).

Determination of Pb isotopes is also helpful for investigating the downward migration pattern of Pb (anthropogenic and natural) in soil profiles as anthropogenic Pb is considered to be more mobile than geogenic Pb in soils (Ettler et al., 2004). The evaluation of migration of Pb in soils using Pb isotope ratios has been investigated in several studies conducted in Europe and the Mediterranean region (Efcel and Veron, 1997). For example, Erel et al. (1997) used $^{206}/^{207}$Pb to characterize the isotopic composition of petrol Pb in roadside soils in Israel and calculated that the velocity of migration of petrol Pb in soil was 0.5 cm year^{-1}. Izquierdo et al. (2012) found the evidence of post-depositional vertical migration of petrol Pb in alluvial subsoils to a depth of 35 cm. Studies have also examined the relative contribution of different sources of Pb principally petrol derived and geogenic, in the labile and non-labile fractions of soils using Pb ratios ($^{206}/^{207}$Pb and $^{208}/^{207}$Pb) in order to investigate the influence of sources and contact time on lability. For example, Mao (2014) estimated the relative contributions of petrol Pb and geogenic Pb in the labile pool of rural roadside top soils by measuring the Pb ratios and it was evidenced that petrol Pb was more labile (35%) as compared to geogenic Pb (ore or coal) (27%). Shetaya et al. (2018) also reported similar

results with greater contribution of petrol Pb in the labile pool as compared to geogenic Pb in soils from urban and industrial locations.

In some studies, sequential extraction and isotope analysis have been used in combination to give more insight into the behaviour of mobile Pb in soils (Teutsch et al., 2001, Emmanuel and Erel, 2002, Bacon et al., 2006). For example, Teutsch et al. (2001) used this combined approach to identify the distribution of petrol Pb and natural Pb to investigate the penetration pathway of petrol Pb in Mediterranean roadside soils over a period of 40 years to be 25-30 cm depth . In the same study, it was reported that the petrol Pb was found in more labile phases of the soils whereas natural Pb was mostly associated with the more stable soil minerals. Efcel and Veron (1997) observed similar results where acid leached fractions of roadside soils were dominated with petrol Pb and the concentration of petrol Pb was observed decreased with soil depth. Lead isotopes measurements have also been used to investigate the mechanisms of mobilisation of roadside Pb into streams in an upland catchment in NE Scotland (Bacon et al., 1996).

1.2.1.2 Coal

Coal is a dominant anthropogenic source of Pb in most urban soils, and Pb in coal is generally present at concentrations between 2.0-80 mg kg^{-1} (Díaz-Somoano et al., 2007). Lead isotopes are helpful in distinguishing coal from other Pb sources. Walraven et al. (1997) identified the coal as the most radiogenic Pb isotope ratio ($^{206}/^{204}$Pb = 18.29-18.57) amongst potential Pb sources including leaded gasoline and residues of building materials. Similarly Farmer et al. (1999) identified that the isotopic composition of British coals (average 1.182 ± 0.009) is close to the isotopic composition of indigenous Pb-ore (1.16-1.18) but different from the Australian Pb-ore (approx. 1.04) 'BHT' ore used to manufacture the Pb additive in

leaded petrol. They also established that coal combustion strongly influenced the Pb ratio ($^{206}/^{207}$Pb) in the UK until the mid-1950s and was the dominant source of Pb contamination before the introduction of leaded gasoline. In China, studies have used the measurement of Pb isotopic composition and revealed that high Pb concentration in soils after the phasing-out of leaded gasoline was mostly from the coal combustion (Mukai et al., 1993, Chen et al., 2005a, Cheng and Hu, 2010). Lead isotope determination has also been considered useful for the classification of coals of different characteristics and origin because the mode of occurrence of Pb (galena, pyrite, chalcopyrite and/or carbonate) may vary from coal to coal.

1.2.1.3 Mining and smelting

Mining and smelting operations, especially Pb/Zn mining and smelting are some of the primary potential sources of metals and metalloids in the environment (Li, 2007, Zhang et al., 2012). Lead isotopes have been used to investigate the influence of Pb mining and smelters on local soils and other media (Dudka and Adriano, 1997, Ettler et al., 2004, Komárek et al., 2007). For example, Rabinowitz (2005) used Pb isotope ratios ($^{206}/^{204}$Pb, $^{206}/^{207}$Pb and $^{206}/^{208}$Pb) to identify the sources of Pb ores in soil profiles close to different historical American lead smelters and refineries, despite the complications of changing smelter feedstock sourced from mines of different geological age.

1.2.2 Agricultural soils

In agricultural soils, the accumulation of trace metals from anthropogenic sources can result in loss of soil function and their bioavailability to plants poses indirect risks to human health through the food chain (Hough et al., 2004). Therefore in recent decades, numerous studies have evaluated the content and potential

sources of trace metals in agricultural soils (Micó et al., 2006, Wei and Yang, 2010).

Atmospheric deposition has been identified as an important source of metals to agricultural soils of England and Wales, ranging from 25 to 85% of total inputs (Nicholson et al., 2003). Reimann et al. (2012) conducted a study of agricultural soils across Europe to see, at a continental scale, the variation in Pb isotopic ratios. Large variations in both the concentration of Pb and the range of Pb isotopic ratios was shown to be dominated by the underlying geology and influenced by climate. Local sources of Pb either anthropogenic or natural mineralization were considered to be more of a threat to agricultural soils than diffuse sources of Pb on a continental scale. Land use practices, differences in rate of harvesting and the ability of plants to intercept aerosol particles were also considered common reasons for different levels of contamination observed over small distances (Van Oort et al., 2001, Fernandez et al., 2008).

In agricultural soils, agricultural management practices such as liming, fertilization (especially phosphate addition), application of sewage sludge, manure, ploughing can also provide additional sources of Pb and are considered important factors that strongly influence soil characteristics and metal retention behaviour (Andersen et al., 2002, Fernandez et al., 2007). For example, Walraven et al. (2013) observed that the higher isotopic composition ($^{206}/^{207}$Pb, $^{208}/^{207}$Pb, $^{206}/^{208}$Pb) of agricultural top soils were close to the Pb isotopic composition of N-P fertilizers and animal manure samples. Wong et al. (2002) suggested that increased use of agrochemicals over several decades was the major source of heavy metal contamination on agricultural soils collected near the Pearl River Delta, China. In the same study it was also reported that anthropogenic Pb was relatively stable after deposition in soils because Pb was strongly associated with

Fe–Mn oxide and organic/sulphide phases. Isotopic characterization ($^{206}/^{204}$Pb) of sewage sludge in a study by Hansmann and Köppel (2000) found that the isotopic composition of the sludge was intermediate between that of fly-ash and leaded gasoline (i.e., 17.74-17.88). Also Pb from road run-off was considered to be a significant contributor to sewage sludge.

1.2.3 Forest soils

Atmospheric deposition is largely responsible for trace metals contamination in rural and remote areas. Forests have been considered as important sinks for trace metals because they are efficient at absorbing or scavenging pollutants from the atmosphere (Fowler et al., 1989). The potential for large rates of atmospheric deposition is mainly provided by the turbulent structure of air above and within forest canopies.

Many studies have been conducted on forest soils with the aim of identifying different sources of pollutants, including stationary and diffuse sources, with the help of Pb isotopes ratios. Atmospheric Pb deposits mostly accumulate on the surface layers of forest soils but due to their high organic matter contents a portion of the Pb can be transferred into deeper soil horizons posing a risk to ground water, streams and rivers (Wang and Benoit, 1997). Brännvall et al. (2001) in a study of boreal forests in Sweden ruled out the possibility that Pb present in the humic surface layer (mor) was from the underlying or local soil by studying Pb isotope ratios ($^{206}/^{207}$Pb). The isotope ratio $^{206}/^{207}$Pb values in the mor layer were all similar (1.152 ± 0.009) and resembled the isotopic composition of atmospheric pollution derived Pb. In a study by Yarlagadda et al. (1995) industrial emissions and coal combustion were identified as the major sources of additional Pb in mixed forest soils of Dinghushan Southern China. Hernandez et al. (2003) noted that

global atmospheric inputs from leaded gasoline were more important than regional and local industrial emissions in forests in the north and north-eastern regions of France.

Previous studies have also shown an influence of metallurgical activities on forest areas due to smelting (Rieuwerts et al., 1999). Ettler et al. (2004) investigated the Pb isotopic composition of individual horizons in forest and tilled soils, collected near a Pb smelter of Pribram, Czech Republic. Metallurgical processes were shown to be the dominant cause of the local Pb pollution in forest topsoils with isotopic compositions of $^{206}Pb/^{207}Pb \sim 1.17$. Lead in deeper soil samples had isotopic compositions closer to those of the bedrock but some downward movement of the pollution Pb was also observed. Walraven et al. (2013) also used Pb isotope ratios to reveal that the source of Pb contamination in the Southern forest region of the Netherlands was from Belgian Zn smelters, located downwind, which processed Zn ore from the former Belgian Congo.

In forest soils, Pb ratios have also been used to calculate the migration velocities of Pb into deeper soil horizons (Johnson et al., 2004, Yanai et al., 2004). For example, in Europe in soils collected from over 40 forested areas, the transfer rate of Pb has been reported to vary between 0.39-0.83 mm/yr (Dörr and Münnich, 1991). The downward movement of organic material due to the sedimentation of soil organic matter and subsequent turnover into CO_2 was identified as the controlling factor. Hernandez et al. (2003) in a study of cambic podzols in the northern part of France estimated that the anthropogenic Pb contribution was 83, 30 and 11%, respectively, for surface, intermediate and deep horizons. Similarly Hansmann and Köppel (2000) demonstrated penetration of pollutant lead to a depth of 20-30 cm in Swiss forest soils.

The mechanism of partitioning of anthropogenic and natural Pb have also been investigated in Czech forest soils through the measurement of Pb isotopes in individual fractions of a sequential extraction procedure (SEP) (Emmanuel and Erel (2002). Results indicated that natural Pb was mainly associated with residual and oxide fractions whereas anthropogenic Pb was in fractions associated with surface bound and organic matter phases.

1.2.4 Peat deposits

Peat bogs are commonly used as archives in Paleo environmental studies as they preserve atmospheric signals and are typically widespread (5% of land area) as compared to other archives such as ice-cores, which are restricted to e.g. polar and alpine regions. Lead isotopic studies of cores from ombrotrophic peat bogs are considered ideal to reconstruct the historical trends in trace metal deposition because they receive pollutants only from wet and dry deposition (Clymo, 1987, Shotyk et al., 1996, van Geel et al., 1996, Mauquoy and Barber, 1999, Vile et al., 1999). Vertical movement of Pb in the bogs is low due to the high organic matter content and anoxic conditions of peat, resulting in Pb adsorption and fixation in secondary sulphide minerals (Walraven et al., 2013).

Lead isotopic composition in deep peat profiles is helpful for reconstructing the general trend in atmospheric Pb deposition. For example Martínez-Cortizas et al. (1997) recorded Pb deposition extending back 4000 years after sampling ombrotrophic peat bogs in Spain. Similarly Shotyk et al. (1998), reconstructed Pb deposition over the past 12,000 years using peat cores from the Jura Mountains in Switzerland. Alfonso et al. (2001) studied cores used from two marshes from south-western France to study the regional variation in Pb isotope signals recorded from 6000 to 300 years. Reconstruction of Pb deposition over long periods is

helpful in determining the isotopic signals of the pre-anthropogenic period and peak periods of Pb production such as the Roman and Medieval periods.

Lead isotopes measured in peat bogs have also been beneficial for comparison of chronologies across different sites (Dunlap et al., 1999, Alfonso et al., 2001, Kylander et al., 2010). Dunlap et al. (1999) observed a correlation between the trend in isotopic composition variations in peats in Southern Norway with previously measured chronologies from France, Switzerland, England and Greenland that covered different periods of time. They also established that Pb emissions between 366 BC and the first half of the 20th century were dominated by European Pb ores and from the 1950's onward by leaded gasoline. Similarly Kylander et al. (2010) investigated Pb isotopes in pre-contamination sections of peat cores from Europe, North America, South America and Australia and revealed that peat archives only record Pb inputs from local (< 10 km) and regional (10-500 km) sources not continental scale trends.

Monitoring historical trends in the predominant sources of Pb is a useful indicator of the success of environmental policies such as the phasing-out of leaded gasoline. Novak et al. (2008) in a study of Pb emissions since the Industrial Revolution identified a rapid decrease in the percentage of gasoline derived Pb in peats in the British Isles (≤ 55%) and Czech Republic (≤ 63%) after the phasing out of leaded gasoline in 1970. Similarly Cloy et al. (2005) demonstrated the change from leaded petrol to non-leaded petrol in recent decade through variations in Sb/Pb and ^{206}/^{207}Pb ratios using two cores (dated with ^{14}C and ^{210}Pb) collected from Flanders moss ombrotrophic peat bog in Central Scotland.

1.3 Environmental forensics

In forensic studies, the use of isotopic ratios is generally preferred compared to elemental ratios because they are more sensitive tracers for characterising pollutant sources and the transport of pollutants (Aggarwal et al., 2008). Chow and Johnstone (1965) were the first researchers to demonstrate that Pb isotopic abundances could be used to identify the origin of Pb sources. Nowadays, Pb isotopes are commonly applied to local and global scale investigations to identify sources of Pb pollution (both natural and anthropogenic) and their pathways in a wide range of environmental compartments (Rosman et al., 1994). This technique helps to quantify Pb dynamics between and within biological and geochemical environments and detect temporal changes in the loading of different types of pollutant (Weiss et al., 1999, Charalampides and Manoliadis, 2003). Information regarding Pb isotope composition is important to trace the sources of pollution as the Pb isotope composition is virtually unchanged by physicochemical or biological processes (Veysseyre et al., 2001, Ettler et al., 2004). However, natural and anthropogenic Pb sources can be differentiated only if: (i) all possible sources of Pb are known and (ii) the isotopic compositions of these sources are well defined i.e. there must be a significant difference between the natural background and anthropogenic sources (Renberg et al., 2002, Reimann et al., 2008, Walraven et al., 2013).

In addition to Pb isotope measurements investigation of other trace element patterns may provide additional information that can assist in identifying sources. In particular rare earth elements (REEs) and the platinum group elements (PGEs) may be particularly useful.

1.4 Rare earth elements (REEs)

The International Union of Pure and Applied Chemistry (IUPAC) has classified rare REEs as a group of 17 elements, with similar physicochemical properties which are found together in nature (Hu et al., 2006). Rare earth elements are divided into 2 groups: the light rare earth elements (LREEs) and the heavy rare earth elements (HREEs). The LREEs (La, Ce, Pr, Nd, Pm, Sm and Eu) are present in higher concentrations in the environment than the HREEs (Dy, Er, Gd, Ho, Lu, Sc, Tb, Tm, Y, Yb) (Šmuc et al., 2012). In soils, LREEs are mostly associated with clayey soils while HREES are associated more with sandy soils (Caspari et al., 2006). Resistant minerals such as zircon that remain in the coarser fraction of the soil typically have a greater HREE contents (Ayres and Harris, 1997).

The demand for REEs in recent years has increased due to their wider use in automobile–catalysts, clean energy technologies, health care, pharmacology and modern technology e.g. mobile phones (Hirano and Suzuki, 1996, Zhu et al., 1996, Ramos et al., 2016). Various studies have reported increased accumulation of REEs in the environment due to anthropogenic activities (Ramos et al., 2016). Small quantities of REEs in soil have been reported to have positive effects on the growth of plants and animals but can lead to adverse effects if intake is excessive or prolonged (Thomas et al., 2014). Increased concentrations of REEs in soils are mostly restricted closer to industrial centres, or large cities. One of the major factors governing the concentration of REEs is the intensity of agricultural activities mostly due to the long term application of fertilizers (Smidt et al., 2011, Xie et al., 2014, Ramos et al., 2016).

1.5 Platinum group elements (PGEs)

The PGEs (Pt, Pd, Rh, Ir, Ru and Os), Au and Ag are rare in the Earth's crust and are enriched in very few natural geological rock types or minerals. Peridotite (ultramafic lithology) is an example, where the concentration of Pt and Pd are in the range 10-20 ppb (Barnes, 2004, Bogdanov et al., 2005). Over time, the concentration of PGEs have continuously increased in the environment, in both developed and developing countries (Ladonin, 2018). Platinum, Pd and Rh are commonly utilized in automobile catalytic converters in order to minimize the toxic effects of pollutants such as oxides of carbon (COx) and nitrogen (NOx), and unburned hydro-carbons by effectively converting them into less harmful forms: CO_2, N_2 and H_2O. However there has been concern that catalytic converters are also a source of PGEs to the environment. Worldwide production of PGEs has been increasing since 1970 and environmental concentrations of PGEs are expected to increase over the next few decades (Whiteley and Murray, 2003, Ek et al., 2004, Ravindra et al., 2004, Sen and Peucker-Ehrenbrink, 2012). A number of studies have already reported increased concentration of PGEs in different environmental media over time, including street dust, urban soils, sewage sludge and incinerator ash (Heinrich et al., 1996, Zereini et al., 1997, Morton et al., 2001, Djingova et al., 2003, Jackson et al., 2010, Yang and Zhang, 2015). Emission of PGEs into the surrounding environment is mainly due to the abrasion of catalytic converters and concentrations in road dust and soils have been found to decrease with increasing distance from roads (Moldovan et al., 2003). High concentrations of PGEs are of serious concern due to possible harmful effects on human populations and ecosystems and so rigorous evaluation of PGEs accumulation is required (Ek et al., 2004, Zereini and Wiseman, 2015).

Analysis of PGEs using ICP-MS is challenging due to interferences that hinder accurate measurement of very low concentrations (Bencs et al., 2003). To date several techniques have been used for removal of spectral interferences (isobaric and polyatomic) in the measurement of PGEs. These include: mathematical correction, high mass resolution or chemical resolution, separation from the analysis matrix using cation exchange resins, co-precipitation techniques and the use of O_2 as a reaction gas in ICP-MS with CRC (collision reaction cell) (Gomez et al., 2000, Simpson et al., 2001, Bruzzoniti et al., 2003, Gomez et al., 2003, Fritsche and Meisel, 2004, Rodríguez-Castrillón et al., 2009, Spada et al., 2012, Zhao et al., 2014). All these approaches are partially effective in removing interferences but cannot completely remove them at the very low concentrations at which PGEs are present in environmental materials. However, recent developments in triple quadrupole ICP-MS (ICP-QQQ) technology utilizing MS/MS reaction cell mode are providing a more effective approach in suppressing severe interferences.

1.6 Approaches to source apportionment

Source apportionment of contaminants is important because it helps in both (i) understanding the characteristics of the contaminant and (ii) in evaluating the relative contribution of each pollutant source. This information informs e.g. preventive measures in order to reduce the adverse effects of anthropogenic contaminants (Davis et al., 2001, Howard et al., 2003, Hu and Cheng, 2016). Source apportionment is also useful in approaches where controls are based upon the potential risk associated with each source (Jiang et al., 2017).

Qualitative source identification methods such as multivariate statistical analysis e.g. principal component analysis (PCA) and cluster analysis (CA), mapping based

upon geographic information systems (GIS) and determination of isotopic signatures have been used in many studies to assist with Pb source apportionment (Facchinelli et al., 2001, Zhang, 2006, Mijić et al., 2010, Nanos and Martín, 2012, Ming-Kai et al., 2013, Huang et al., 2015). There are also some studies that have used quantitative source identification methods such as receptors models e.g. chemical mass balance, multiple linear regression, PCA related methods and positive matrix factorization (PMF) (Bzdusek et al., 2006, Luo et al., 2014, Luo et al., 2015, Schaefer and Einax, 2016, Wang et al., 2016).

1.6.1 Elemental ratios

Use of elemental ratios is a common and simple approach to identify the origin of sources. Bi et al. (2006) used Zn/Cd and Pb/Cd ratios to identify the origin of heavy metals from zinc smelting and flu gas dusts in areas impacted by Zn smelting. Eckel et al. (2002) used ratios of Sb/Pb, As/Pb and Cd/Pb to investigate source of Pb contamination at eight sites in Baltimore and Philadelphia and revealed former lead smelting operations as the major source of contamination. Similarly Kimbrough and Carder (1999) identified the source of elements in contaminated sediments samples (collected downstream from a secondary lead smelter) by multi-element analysis, observing that the ratios of Pb, Sb, As and Cd in sediments were close to air and soil samples collected from similar sites. Prohaska et al. (2005) used a multi-isotope approach (i.e., Pb isotopic ratios $^{207}/^{206}$Pb in combination with ^{87}Sr/^{86}Sr) for identifying variation in anthropogenic and natural sources of Pb pollution and their mobility in soil. This approach was used with classical pedological Zr/Ti ratio to increase the certainty and to overcome the limitation of the individual approaches.

1.6.2 Binary models

In most studies the approach used for distinguishing between separate Pb sources is construction of a bivariate plot, also known as a 3-isotope biplot, with a common isotope as denominator. In environmental studies, common isotope plots include $^{206}/^{207}$Pb versus $^{206}/^{208}$Pb or Pb isotope ratios plotted against Pb concentration (Saal et al., 2005). These approaches help in precisely evaluating different Pb sources (Monna et al., 2000a, Ettler et al., 2004). The three heavier radiogenic isotopes are most commonly used due to their greater, and similar, isotopic abundances (Erel et al., 2001). A binary mixing model is the simplest form and works most satisfactorily when anthropogenic and natural background sources of Pb have distinctly different isotopic signatures (Renberg et al., 2002). Lead isotope bi-plots are not suitable where more than two sources need to be identified. However, this is not always clear given the similarity of local geogenic sources and the distinct characteristics of petrol Pb. It is reported through statistical analysis that 86% of discriminating power for source apportionment lies with ^{206}Pb, ^{207}Pb and ^{208}Pb and the relative contribution of Pb from petrol is identifiable solely with $^{206}/^{207}$Pb data (Komárek et al., 2008). Furthermore, it is acknowledged that apparent linear trends observed in bi-plots can be a consequence of the co-linearity of terrestrial Pb and can be explained by the mixing of several Pb sources (Ellam, 2010a). Inclusion of ^{204}Pb with other isotopic determinations can help in identifying intermediate isotopic composition of pollutants (Sangster et al., 2000, Ellam, 2010a). In most geological studies very precise data are required for natural source apportionment and so ^{204}Pb data are also included in the analysis: $^{206}/^{204}$Pb, $^{207}/^{204}$Pb and $^{208}/^{204}$Pb (Saal et al., 2005). Recently three end-member mixing model (tri-plot) has been used in a few studies to calculate the relative contribution of Pb from three sources (Cheng and Hu, 2010, Luo et al., 2015).

1.6.3 Soil extractions and measurement of E-values

Information on only the total elemental content of a soil is not sufficient to provide details regarding the toxicity and the potential risks associated with trace element contaminants (Nolan et al., 2003). Chemical fractionation of heavy metals in soils can provide a more detailed insight into the minerology and chemistry of the soils, as well as their potentials to release trace elements under various conditions (Tack and Verloo, 1995, Templeton et al., 2000). Trace elements from anthropogenic sources typically bind to different soil fractions such as carbonates, oxides (Fe and Mn) and organic matter through processes including ion exchange, adsorption, co-precipitation and complexation that influence their fractionation, mobility and bioavailability (Shuman, 1991, Carrillo-González et al., 2006, Hooda, 2010). Trace elements present in the residual phase are mostly within the lattice of primary and secondary soil minerals and are barely subjected to the influence of human activities (Gleyzes et al., 2002, Marzouk et al., 2013a, Marzouk et al., 2013b, Mao, 2014). Thus, chemical fractionation of heavy metals can offer valuable insight into their sources, and the relative contribution of natural and anthropogenic sources can be evident from evaluating the non-residual fractions as compared to the total concentrations (Hu and Cheng, 2016). There are different approaches that have been used to provide insight into these processes but the most widely applied approaches are sequential extraction procedures (SEPs) and isotopic dilution (ID) (please see Chapter 6 for details) (Rauret et al., 1999, Gleyzes et al., 2002, Mossop and Davidson, 2003, Gäbler et al., 2007, Favas et al., 2011, Chenery et al., 2012, Marzouk et al., 2013a, Marzouk et al., 2013b). Studies have combined Pb isotopes measurement with SEPs to provide detail regarding environmental impact as using a combination of methods gives more insight into the behaviour of Pb in soils (Teutsch et al., 2001, Bacon et al., 2006). The total content of trace

elements may be operationally divided into 'reactive' and 'non-reactive' fractions. The reactive fraction is most likely to be responsible for biologically harmful effects (Rieuwerts et al., 2006). Sequential extraction procedures are helpful in auditing the various chemical fractions of trace metals expected to be present in soil, but these methods cannot simply discriminate between 'reactive' and 'non-reactive' forms (Ottosen et al., 2009, Degryse et al., 2011). The inherent limitations of SEPs have been considered in many studies; problems include the selectivity of the extractants for a given phase and the redistribution of trace elements during the extraction procedure (Gleyzes et al., 2002, Degryse et al., 2011). By contrast, ID using an enriched stable isotope can be used to determine the isotopically exchangeable metal content or 'E-value' which represents the 'labile' or 'reactive' pool of metal. Using an ID technique is therefore preferable for risk assessment for planning and developmental purposes (Smolders et al., 1999, Young et al., 2000a).

1.7 Measurement of Pb isotopes

Isotopic ratios of Pb can be measured using thermal ionization mass spectrometry (TIMS) or by inductively coupled plasma mass spectrometry (ICP-MS). The ICP-MS instruments use either quadrupole (ICP-QMS) or magnetic sector fields (MS-ICP-MS) and can be equipped with single (SC) or multi collectors (MC), array detector (AD) or 'time-of flight' (TOF) detectors (Barbaste et al., 2002, Komárek et al., 2008, Cheng and Hu, 2010). Each of these analytical techniques has its own precision, advantages and disadvantages for the measurement of Pb isotopes (Table 1.1).

Table 1.1: Advantages and disadvantages of different mass spectrometric techniques for the determination of Pb isotopes.

Technique	Precision (RSD)	Advantages	Disadvantages
TIMS	0.001-0.01%	• Most precise and accurate technique for measuring Pb isotopes	• Needs separation of Pb from sample matrix • Long analysis time • Sample introduction and handling are not easy processes, risk of contamination
ICP-QMS	0.1-0.5%	• Relatively inexpensive • Commonly used analytical technique • Simple in terms of sample preparation, handling and operation • Higher tolerance to matrix	• Low precision and accuracy • Plasma flicker can sometimes limit the measurements
MC-ICP-MS	<0.05%	• Higher sensitivity and less noise compared to ICP-QMS • Accurate measurement of Pb isotopes	• Requires separation of Pb from sample matrix • Manual sample introduction • Plasma flicker can sometimes limit the measurements

1.7.1 Principles of ICP-QMS

Quadrupole ICP-MS instruments comprise a sample introduction system, an argon plasma to ionize elements, an interface region where ions are accelerated into a quadrupole for mass separation and finally a detector.

The sample introduction system is the 'front end' of the instrument and consists of a nebulizer and spray chamber. The nebulizer converts the sample solution into an aerosol and the spray chamber acts as a filter which only allows the smallest aerosols droplets to pass through into the plasma (Suess and Prather, 1999). The plasma is produced as a result of interaction of a radio-frequency field with argon gas. Once in the plasma particles are vaporised, atomised and ionised (Günther et al., 1999).

A small fraction of the ion cloud produced in the plasma is passed into the interface region, located between sample and skimmer cone, by negative pressure. Each cone has a small orifice at its apex (Nelms, 2005). A mechanical roughing pump is used to decrease the temperature and pressure in the interface region by creating a vacuum. Thus the interface region enables the movement of sample ions from a region of high temperature and pressure within the plasma to the quadrupole mass spectrometer where temperature and pressure are comparatively low (Walder and Freedman, 1992). The largest mass discrimination effect in ICP-QMS is produced in the low electrostatic field of the interface region due to space charge effects which reduces the total number of ions (Gillson et al., 1988, Begley and Sharp, 1994). This effect is a result of mutual repulsion of lighter positively charged ions when they pass through the skimmer cone; as a result of this repulsion, lighter ions are deflected more whereas heavier ions are left in the beam (Heumann et al., 1998).

Ions from the interface region are passed to the mass spectrometer (quadrupole) through ion lens optics. The main function of the lenses are to focus the ion beam to allow the subsequent passage of the positively charged ions to the quadrupole mass spectrometer (Hu et al., 2005). Before ions reach the quadrupole they can pass through a collision reaction cell, an advanced technology which helps in the suppression or elimination of polyatomic interferences (McCurdy and Woods, 2004). In the collision reaction cell the ion beam, prior to reaching the quadrupole mass filter, is passed through a cell pressurized with either an inert collision gas (e.g. He) or a reactive gas (e.g. H_2, NH_3 or O_2). Polyatomic interferences are reduced by kinetic energy discrimination, a phenomenon where larger polyatomic ions undergo more energy dampening collisions than the analyte ions and therefore do not pass through the cell. In reactive gas mode ions can interact with

a reactive gas to form species with different m/z than that of the analyte ions that can then be separated from the analyte within the quadrupole (Koppenaal et al., 2004, McCurdy and Woods, 2004).

The quadrupole only allows masses of interest (ions with a specified m/z ratio) to reach the detector (Nelms, 2005). It consists of four parallel metal rods in a part of the vacuum unit. Radio-frequency (RF) and direct current (DC) applied to these rods produces an electrostatic field which helps in separation of the ions on the basis of their m/z ratio. At any one time only one particular analyte ion m/z will follow a stable spiral transport pattern between the rods that comprise the quadrupole. Lighter and heavier ions will discharge against the quadrupole rods and be swept away to the vacuum pump extraction system (Miller and Denton, 1986, Dawson, 2013). Resolution of the quadrupole can be changed between standard and peak compression mode within a single run by changing the RF and DC voltage settings (Dawson, 2013).

In the quadrupole mass filter, efficiency of transmission through the mass separator system should be independent of m/z ratio, which otherwise produces mass discrimination. However this is often difficult to achieve in quadrupole mass filters. Heavier ions take longer to traverse the electrostatic field than lighter ions and so are dispersed more and transferred to the detector less efficiently; this produces a mass discrimination which is the reverse of the space charge effect (Heumann et al., 1998).

Low resolution quadrupoles can also contribute signal from neighbouring isotopic peaks to the measurement of intensity. This can affect the isotope ratio measurement producing 'low abundance sensitivity'. In ^{11}B:^{10}B ratio measurements, for example, the normally very high $^{12}C^{+}$ peak from carbon

containing impurities in the sample or plasma gas contributes to the intensity of $^{11}B^{+}$ (Demuth and Heumann, 1999).

A discrete dynode detector is used for counting the selected incoming ions from the quadrupole. The detector can operate in two ways, known as 'pulse counting' and 'analogue' modes. In pulse counting mode, secondary electrons are counted after they have travelled across all the dynodes. In this mode the detector records relatively small count rates (up to 10^6 counts per seconds, cps). When count rates exceed 10^6 cps, the detector is unable to measure all incoming ions due to the temporary effect of the measurement of the previous ion (dead time) the result of which is that the actual counts are not reliably recorded (Encinar et al., 2001). Therefore, dead time correction is important if accurate isotope intensities are to be measured. At sufficiently high count rates (cps), the detector switches to an analogue mode in which secondary electrons are collected half way down the dynode chain and in this mode there is no dead time effect (Nelms et al., 2001). During pulse counting, there is inherent uncertainty when the pulses arrive at different rates to the detector (Monna et al., 2000b). When the number of counts recorded are larger, then there is smaller statistical variation (Heumann et al., 1998, Vanhaecke et al., 1998). In ICP-MS, counting statistics are therefore based on Poissonian statistics in which the variance is approximately equal to the mean and so the standard deviation is taken as the square root of the mean (Eq. 1).

$$s.d.(x) = \sqrt{\ } mean\,(x) \qquad \text{Eq. (1)}$$

Where x is the number of counts

1.7.2 Limitations of ICP-QMS

There are significant limitations of ICP-QMS. Noise (i.e. variation in signal) is typically created when the sample matrix contains variable concentrations of total dissolved solids (TDS) and especially if sample matrices differ from the calibration standards (Wu et al., 1996, Murray et al., 2000). Noise originates in the ion source, the interface region, lens voltages, collision/reaction cell, quadrupole mass filter and detector.

Spectroscopic interferences mostly occur due to atomic and molecular ions which have similar mass to charge ratios to that of the analyte of interest. They include isobaric interference, over-lapping peaks and polyatomic interference. There are also problems with nano-particulate species which cause 'ion bursts' in the plasma however modern electronic processing on ICP instruments is typically sufficiently rapid to pick these out from background (Nelms, 2005).

1.8 Study aims and thesis structure

The main aim of this work is to undertake a forensic analysis of urban soils using Pb isotope analysis in combination with determination of other trace element signatures and approaches including sequential extraction and the measurement of metal lability. Specific objectives were to:

(i) Refine a protocol, using a current generation ICP-QMS instrument to maximise the accuracy and precise determination of Pb isotope ratios;

(ii) Apply the developed methods to a range of soils (i.e., urban soils, sewage amended soils and urban allotment soils) in order to enable soil Pb source apportionment;

(iii) Extend the source apportionment of Pb (petrol Pb and geogenic Pb) to a wider range of elements including REEs and PGEs, in order to identify other specific sources of contaminants;

(iv) Determine the fractionation of trace metals through SEPs and ID methods in selected urban allotment soils to investigate the behaviour and sources of pollutants.

The work is divided into several chapters which are summarised below:

Chapter 2: General materials and methods for the measurement of major and trace elements including REE and PGEs are described. Sequential extraction procedures and ID approaches are also presented. Preliminary tests conducted to optimize range of parameters for measurement of Pb isotopes through ICP-QMS using reference materials are also described.

Chapter 3: In this chapter, a refined instrumental and experimental protocol is presented that maximises the accuracy and precision of Pb isotopes ratio measurements in urban soil digests using a current-generation ICP-QMS instrument. Optimization includes (i) individual dilutions of samples and standards to the same Pb concentrations, (ii) dead time correction, (iii) dwell time, (iv) testing of the number of scans and (iv) correction of mass bias discrimination using sequential application of both *internal* (^{203}Tl and ^{205}Tl) and *external* (SRM-981, NIST) standards. The optimised methodology is further benchmarked against MC-ICP-MS measurements on the same sample material.

Chapter 4: Multi-element concentration and source apportioned Pb (e.g. petrol-Pb and non-petrol Pb) are used to identify likely pollutant sources in different sets of urban soils from Nottingham, Wolverhampton (UK) and sewage amended soils (Pakistan) using multivariate statistical cluster analysis.

Chapter 5: In this chapter, the range of elements investigated is extended to REEs and PGEs to look more closely at potential sources of pollutants in urban allotment soils (Nottingham). For REEs, the crust-normalized pattern for both top and sub soils are evaluated along with the enrichment factor (EF) to identify possible sources. An attempt is made to investigate concentrations of PGEs using different cell modes of ICP-QQQ-MS (He gas mode, $NH_{3(on\text{-}mass)}$ and $NH_{3(mass\text{-}shift)}$ gas modes) in order to compare results in terms of interferences removal and accuracy.

Chapter 6: Isotopically exchangeable fractions (E-value) of selected trace elements (Ni, Cu, Zn, Cd and Pb) are measured, through ID approach and metal fractionation using SEP, on selected urban allotment soils. The correspondence between these two methods (ID and SEP) is also investigated. The effect of common soil properties and the long-term effect of Pb sources on lability of metals are investigated. The relative contributions of different sources of Pb (i.e., petrol-derived and geogenic) to labile and non-labile pools of soils are evaluated to examine the influence of source and contact time on lability. The relative contributions of petrol-derived and geogenic Pb in individual fractions of the SEP are also calculated to assess the behaviour of petrol Pb in relation to common soil properties.

Chapter 7: The success of using a forensic approach for establishing the source of contaminants in soils is reviewed and areas for future work are discussed in this chapter.

2 Chapter 2: General Materials and methods

2.1 Overview

This chapter briefly describes the soils selected for study in this work. The analysis of major and trace elements including the REEs and PGEs is described together with the measurement of isotopically exchangeable metals in soils using ID and fractionation of soils using a SEP. Preliminary experiments to optimize a range of parameters for the measurement of Pb isotopes with ICP-QMS using reference materials are also described. A final developed methodology for measurement of Pb isotopes with ICP-QMS is discussed separately in Chapter 3.

2.2 Soil selection

Three different sets of soils samples; urban, urban allotment and sewage amended soils, previously collected for other studies, were selected and investigated as case studies for the study of source apportionment of contaminants.

Urban Soils

Composite urban surface (0-15cm depth) soil samples (n=50, triplicate) collected from 20-25 subsamples (area 20 x 20 m^2) from different sites in Wolverhampton and Nottingham were used. These soils were previously sampled for a National Environmental Research Council (NERC) 'URGENT' project 'Studies into metal speciation and bioavailability to assist risk assessment and remediation of brownfield sites in urban areas' by a research consortium from Imperial College, London, NERC Isotope Geosciences Laboratory, British Geological Survey and the University of Nottingham between 1999 and 2002. These urban soils samples were air dried at 30°C for 3 days and were later sieved to <2mm. The soils were selected to cover a range of toxic elements concentrations and past and contemporary land uses in terms of industrial activities, brownfield sites, waste

disposal areas, gardens and allotments, urban roadsides, recreational sites, rail transport sidings, urban nature reserves (Thums et al., 2008, Thornton et al., 2008).

Wolverhampton is located to the north east of Birmingham in the west Midlands, UK and extends on an area of 70km^2. Wolverhampton is covered mostly with periglacial deposits that exists as a widespread till sheet with subordinate sands, gravels and clays (Kelly et al., 1996). The city of Wolverhampton has a long history of industrial activity and has a legacy of mining and metal processing activities since the 16th century. Initially these activities were confined to local coal and iron stone resources. Iron industry rapidly grew during the mid-18th century and was declined in the mid-19th century, with peak production observed during 1850 to 1860 (Gale, 1966). In the industrial revolution the area was dominated by manufacturing companies, mostly associated with manufacturing of steel, metal component parts, electroplating, galvanising and the paint and pigment industry and dyestuff industries. During the mid-20th century these industrial activities declined and modern electronics and component-based industries prevailed which play an important role in the local economy (Bridge et al., 1997, Upton, 1998). The historical activities of former industries have left legacy of contamination and are responsible for elevated trace element concentrations in the area.

The city of Nottingham is unitary area in Nottinghamshire, England which is located 128 miles north of London. The earliest settlement of Nottingham may go back to Roman or even before Roman times. Afterwards it was settled continuously through the Viking and Norman periods to become a major trading centre during the middle ages. During the middle ages, the major industry was woollen manufacture (Bell et al., 2009). The city of Nottingham has a long history of industrial activity during the 19th and early 20th centuries including production

of textiles, bicycles, pharmaceuticals, telecommunications equipment and cigarettes. During the later part of 20th century, there was a gradual shift from old heavy industry to light manufacturing and service industries alongside older more traditional crafts such as lace-making. The rapid population expansion with poor city planning during 19th century resulted in the creation of appalling slums. Also coal was mined in the area for hundreds of years and has resulted in soil contamination (Charsley et al., 1990, Bell et al., 2009).

Urban Allotment Soils

Urban allotment top (~15cm depth, duplicate) and subsoils (~15cm depth in the second soil horizon, duplicate) that had been sampled in 2014-2015 and analysed for another project were selected (146 individual plots, n=269). Samples were from 9 different allotments across Nottingham; Blenheim, Canal, Mapperly, Moorfield, Old Park Farm, Sneinton Dale, St Ann's, Windmill and Woodthorpe. Of these, 5 were directly let and the other 4 sub-let through allotment associations. The city of Nottingham has had a large number of growing spaces ever since the 1980s. It has been reported that among all allotments, St Ann's (ST) was the oldest and largest site that covered 30 hectares area and contained ~550 individual plots. Whereas Woodthorpe (WT) and Mapperly (MP) were smaller sites, each of these sites contained less than 30 plots. Blenheim (BH) was comparatively new site which had recently received new topsoil covering. Details about the distribution of samples collected from individual plots is given in Table 2.1. Both top and subsoils were sampled from plots with Dutch auger using a 'W' transect approach, with samples collected at each corner in the 'W'. Replicate samples (n=5) collected were aggregated together and stored in labelled polyethylene bags. Both top and subsoils were later air dried for 2-3 days and sieved (< 2mm

in diameter) to remove large particles. Also a sub sample (~ 15 g) of both top and subsoils were ball milled (< 40 µm) using an agate ball mill (Retch: PM 400).

Table 2.1: Number of soil samples collected from individual plots of urban allotments.

Urban allotments	Total no. of plots/ no. of plots sampled	Location
Old Park Farm(PF)	~90/14	*Bilborough*
St Ann's (ST)	~550/50(38)	*St Ann's*
Canal (CN)	~200/21	*Wollaton*
Mapperly (MP)	~20/9	*City centre near forest fields*
Moorfields (MR)	~250/12	*Near Jubilee Campus*
Blenheim (BH)	~120/20	*Hucknall*
Sneinton Dale (SN)	~140/7(5)	*Sneinton*
Woodthorpe (WT)	~25/5	*Sherwood*
Windmill (WM)	~100/6	*Sneinton*

Sewage Amended Soils

Sewage amended soils (0-15 cm depth) previously sampled in a collaboration between researchers in Pakistan and the British Geological Survey (United Kingdom) for a project evaluating the 'Health risk assessment of potentially harmful elements and dietary minerals from vegetables irrigated with untreated wastewater in Pakistan' were also selected for investigation. More details about the sampling strategy is given in Zia et al. (2017). These samples had been collected from major cities (Gujranwala, Gujrat, Lahore, and Faisalabad) in upper Punjab, Pakistan. All these cities have industrial units that discharge untreated effluents into sewage drains. This wastewater is mostly used for irrigation

purposes. The soils (n=67) have been utilized in this current study as sewage amended soils are considered good representative of pollutants from different sources. A further set of sewage soils (n=38) has also been included for comparison purpose. These were collected from a sewage processing farm in Nottinghamshire, UK which has been in use for more than 100 years.

2.3 Reagents

All the chemical reagents utilized in this study were ensured to be of trace analysis grade (TAG) or Analar (AR) quality. Ultrapure water (≥ 18.2 MΩ cm^{-1}) was used throughout. All glassware was cleaned with phosphate-free biodegradable detergent and soaked in 2% HNO_3 before rinsing with deionised water prior to the start of each experiment.

2.4 Soil preparation and digestion

Soil samples were air-dried and sieved to <2mm to remove gravel sized particles and large plants roots. A small subsample of the soil was ground in an agate ball mill (Model PM400, Retsch GmbH & Co., Germany). Complete digestion of triplicate 0.2 g samples was achieved in PFA (Perfluoro Alkoxy) vials in a 48-place Teflon-coated graphite block digester (Model A3, Analysco Ltd, Chipping Norton, UK) using a mixed acid digestion process (i.e., 2 mL HNO_3 (>68%), 1 mL $HClO_4$ (70%) and 2.5 mL HF (70%)). The digested soil samples were taken up in 2.5 mL HNO3 and diluted to 50 mL with ultrapure water in plastic volumetric flasks, then transferred to polypropylene tubes for storage. Prior to analysis by ICP-QMS a 1:10 dilution with ultrapure water was undertaken.

2.5 Sequential extraction

A 5 step SEP was carried out on selected number of allotment top soil samples (n= 59) according to the modified method of Li and Thornton (2001), developed

from an approach used by Tessier et al. (1979). Initially 1.0 g soil samples (<2 mm) were weighted into 50 mL polypropylene centrifuge tubes, followed by extraction steps designated as: Exchangeable (F1), carbonate/specifically adsorbed (F2), Fe/Mn oxides, reducible (F3), organic matter/sulphide, oxidizable (F4) and residual (F5). The procedure of sequential extraction (SE) is briefly described below.

- In the first extraction step (F1), soils were extracted with 8 mL 0.5 M $MgCl_2$, shaking end over end, for 20 min.
- The residues from F1 were then extracted with 8 mL 1.0 M NaOAc for 5 hr. Adjustment of pH (i.e., 5.0) of NaOAc was made with HOAc.
- Residues from F2 were extracted with 20 mL 0.04 M $NH_2OH.HCl$ (diluted with 25% HOAc) for 6 hr.
- Fraction 4 involved extraction with 3 mL 0.02 M HNO_3 and 5 mL H_2O_2 (30%) for 2 hr before addition of 3 mL H_2O_2 (30%) and heating for 3 hr. Prior to addition of H_2O_2, the pH of H_2O_2 was adjusted to pH 2.0 using HNO_3. Finally, 5 ml 3.2 M NH_4OAc (diluted with 20% HNO_3) was added and continuously agitated for a further 30 min.
- Residues from F4 were acid digested according to the approach described in section 2.4.

All extractions were performed in duplicate and after each extraction step, the mixture was centrifuged at 2000 rpm for 30 min and the supernatant was filtered (0.22 µm, Millex® Millipore) into clean universal tubes. Prior to the next extraction step, residues were washed twice with ultrapure water and the wash solutions discarded after 20 min centrifugation. The recovery of different elements was compared to total contents of these elements measured through mixed acid digestion method according to Eq. (1).

$$\% \text{ Recovery} = \frac{\sum C_{Fi}}{C_{total}} \times 100$$

Eq.1

Where, C_{Fi} = Concentration in each fraction

C_{total} = total concentration

Concentrations of multi elements in different fractions (F1-F5) of sequential extractions in allotment soils (n= 59) were also determined with ICP-QMS. Fraction 1, 2 and 3 were diluted (1:10) with 2%HNO_3 whereas, fraction 4 and 5 were diluted (1:10) with ultrapure water before analysis with ICP-QMS.

2.6 Major and trace element analysis by ICP-QMS

All samples were analysed with quadrupole-based ICP-MS system (Model iCAPQ; Thermo Scientific, Bremen, Germany) at University of Nottingham equipped with CCTED, 'collision cell mode' (7% hydrogen in helium) with kinetic energy discrimination (KED) to eliminate polyatomic interferences. Samples entered the ICP-QMS through an auto-sampler (Cetac ASX-520) via a concentric glass venturi nebuliser (Thermo-Fisher Scientific; 1mL min^{-1}) and spray chamber. Internal standards were introduced to the sample stream via a separate line including Ge (50 µg L^{-1}), Rh (20 µg L^{-1}) and Ir (10 µg L^{-1}) in 2% HNO_3. Two sets of external multi-element calibration standards for major elements (0 – 30 mg L^{-1}) and trace elements (0 – 100 µg L^{-1}) were prepared from CertiPrep™ multi-element stock solutions. Data processing was undertaken using Qtegra software (Thermo Fisher Scientific).

2.7 Measurement of REEs and PGEs

A selected number of urban allotment top and sub soils (n=51) were also analysed for REEs and PGEs.

2.7.1 REEs

Acid digests were diluted (1:10) with 2% HNO_3 before analysis. External calibration standards of 1, 2, 5, 7 and 10 µg L^{-1} were prepared from CertiPrep™ "multi-element stock solution 3" for REE determination. An internal standard solution of 5 µg L^{-1} was prepared from Rh and Ir in 2% HNO_3. 5% HCl was used as a wash solution for REE analysis and samples were run in the 'KED' mode of ICP-QMS to minimize interferences.

2.7.2 PGEs

At BGS Keyworth, an Agilent 8900 ICP-QQQ-MS was used for the determination of PGEs in allotment soils. This instrument was equipped with a spray chamber (short Scott double pass cooled to 2°C) concentric glass nebuliser (MicroMist 400 uL/min) and auto-sampler (SP4) in combination with the ISIS2 flow injection system (2mL loop). The Agilent 8900 ICP-QQQ-MS is not strictly a "triple quad" as it has two quadrupoles as mass filters which are separated by an octopole reaction system (ORS) that can be gas filled to act either as a reaction cell or a collision cell. It may therefore perhaps be better described as ICP-MS/MS but current convention is retained by referring to it as ICP-QQQ-MS. The collision/reaction cell consists of the octopole, which is used as an ion guide within a gas cell chamber, where Helium (He) gas is used in collision cell mode or reactive gases (normally NH_3 or H_2 or O_2) in reaction cell mode. The two quadrupoles may be individually controlled to filter either the same mass or two different masses such that if NH_3 is to be used the target analyte can be determined either on-mass

$NH_{3\ (on\text{-}mass)}$ mode or mass-shift $NH_{3\ (mass\text{-}shift)}$ mode. The selection of mode depends on the relative reactivity of the analyte and interfering ions with the chosen gas. The MS/MS mode of ICP-QQQ therefore has the advantage that unwanted reaction product ions is avoided resulting in more accurate determination of PGEs (Sugiyama and Shikamori, 2015). Bencs et al. (2003) and Barefoot (1998) provided details regarding the different types of interferences in the measurement of PGEs (Ru, Rh, Pd, Os, Ir, Pt), Au and Ag. These potential interfering species in the determination of PGEs are given in Table 2.2.

Table 2.2: Potential interfering species in the determination of PGEs

Isotopes	Abundances (%)	Potential Interfering species
103Rh	100	SrO, RbO, Pb^{2+}, ZnCl, CuAr
105Pd	22.33	YO, SrOH, ZnCl, CuAr
106Pd	27.33	Cd, YOH, ZrO, ZnAr
108Pd	26.46	Cd, ZrO, MoO, ZnAr
191Ir	37.3	LuO, EuAr
193Ir	62.7	HfO, EuAr
194Pt	32.97	HfO, SmAr, GdAr
195Pt	33.83	HfO, GdAr
196Pt	25.24	Hg, HfO, GdAr
198Pt	7.163	Hg, Wo, TaOH, GdAr
197Au	100	TaO, HfOH, GdAr

For the analysis of PGEs, initially different concentrations of calibration standards (i.e., 1, 5, 10, 100ppb of Rh, Ir and 1, 5, 10, 100ppb mixture of Spex Certiprep 1, 2, 3 and 4) were prepared and run. Whereas indium (In) (10ppb) was used as an internal standard and added directly into the 7^{th} port of the ISIS2 flow injection valve. Ten different test samples were prepared from single element standards of Cu (500ppb), Pb (500ppb), Sr (500ppb), Zn (500 ppb),Ta (100 ppb), Hf (100 ppb), Zr (100 ppb), W (100 ppb), Y (100ppb) and Mo (100 ppb), (diluted from

Romil 1000 or 10000 mgL^{-1} single element standards) to examine the different range of interferences produced by these elements in the measurement of PGEs. All these test samples were run using three different modes of ICP-QQQ i.e., He, $NH_{3(on\text{-}mass)}$ and $NH_{3(mass\text{-}shift)}$. For calculation of detection limits (DLs) of PGEs, 13 blank samples were run and the values were obtained using the 3sd method (3sd=3 x standard deviation). The background equivalent concentrations (BECs) of the PGEs were also determined by calculating the sensitivity (cps/ug/L) of the instrument from the calibration standards and multiplying the raw cps of the blanks by this. Before analysis of allotment samples (HF digests) through ICP-QQQ, each sample was further diluted (1:20) with 1% HNO_3 and 0.5% HCl and each sample was run as an independent duplicate digestion.

2.8 Isotopically exchangeable Cu, Ni, Zn, Cd and Pb

The E-value of trace metals such as Ni, Cu, Cd, Zn and Pb in selected allotments top soils (n=59) were determined using a multi-element ID technique described by Marzouk et al. (2013b).

2.8.1 Stock solutions

Enriched stable isotopes of ^{65}Cu (IA = 99.0%), ^{62}Ni (IA = 98.2%), ^{70}Zn (IA = 92.7%), ^{108}Cd (IA = 69.7%) and ^{204}Pb (IA = 98.8%) were purchased from ISOFLEX, San Francisco CA, USA as metal foils. Stock solutions were prepared by dissolving these metal foils in 2% HNO_3. They were further diluted with ultrapure water to obtain solutions with concentrations of 27 mg L^{-1} (^{65}Cu), 5.5 mg L^{-1} (^{62}Ni), 48 mg L^{-1} (^{70}Zn), 0.25 mg L^{-1} (^{108}Cd), and 80 mg L^{-1} (^{204}Pb). Working spike solutions were freshly prepared from these stocks by further dilution with ultrapure water to minimise pH change of soil suspensions as a consequence of spiking.

2.8.2 Sample preparation

Three suspensions of each soil (3.0 g; < 2mm) were pre-equilibrated with 30 mL 0.01 M $Ca(NO_3)_2$ for three days on an end over end shaker. Two suspensions were then spiked with 0.4 mL of an enriched stable multi-isotope stock solution and the remaining suspension was used as control (unspiked). In order to avoid mobilization of non-labile metal in the suspensions, the volume of spike solution was keep as small as possible. To calculate the spike concentration soil samples were divided into three different groups according to their total metal concentrations. The amount of spike was calculated to increase the total soil metal content by approximately 1-5%. After spiking, all suspensions (both spiked and unspiked) were equilibrated for a further three days before the supernatant was separated by centrifugation (2000 rpm for 20 min) followed by filtration (0.22 µm, Millex® Millipore). Finally the supernatant was divided into two portions. One portion (8 mL) was acidified with 0.4 mL of 50% HNO_3 and a second portion (10 mL) was purified using resin (section 2.8.3) prior to the analysis of isotopic ratios with ICP-QMS.

2.8.3 Resin purification method

A 'resin purification method' initially described by Hamon and McLaughlin (2002) and Lombi et al. (2003) was used to detect the presence of non-labile metal on suspended colloidal particles (SCP). Analytical grade Na Chelex-100 resin (Bio-Rad laboratories, UK) was converted to a Ca^{2+} form by equilibrating it with 0.5 M $Ca(NO_3)_2$ for 2 hr to reduce pH of the Chelex resin. It was then washed twice with ultrapure water to remove any remaining Na ions. An aliquot of Ca-Chelex resin (c. 0.1 g) was added to the filtered supernatant solutions (both spiked and unspiked) and allowed to equilibrate for 2 hr. The resin was rinsed with ultrapure water three times to separate colloidal material. Finally metals were eluted from

the resin with 3%HNO_3 before filtration (0.22 µm) and isotope ratios measurement. A comparison was made between E-value calculated from isotope ratios measured in filtered samples (E_{soln}) and samples treated with resin (E_{resin}).

2.9 Analysis of Cu, Ni, Zn, Cd and Pb isotopic abundances

Isotopic abundances of Cu, Ni, Zn, Cd and Pb in isotopic dilution assays were determined by ICP-QMS. Supernatant solutions were diluted to avoid the detector tripping to analogue mode. Measurements were made in CCT-KED mode to prevent interferences from the chlorine dimer (^{35}Cl-^{35}Cl) on ^{70}Zn and other polyatomic interferences (Marzouk et al., 2013b). The isotopes ^{63}Cu, ^{107}Ag and ^{202}Hg were included as 'settle points' for the quadrupole immediately before the measurement of ^{64}Zn, ^{108}Cd and ^{204}Pb respectively. External mass bias discrimination was avoided by analysis of a mixed standard (10 µg L^{-1} of SRM-981, NIST for Pb spiked with single calibration standards for Ni, Cu, Cd and Zn) after every 12 samples.

2.10 Lead source apportionment

A simple binary model proposed by Monna et al. (1997) was used to estimate the relative contributions of Pb from different sources; principally petrol-derived (Pb_{petrol}) and geogenic Pb ($Pb_{geogenic}$) according to Eq. (2). The Pb isotopic signatures (i.e., $^{206}/^{207}Pb$ and $^{208}/^{207}Pb$) of UK leaded petrol, UK Pb ore and UK coal were used as reference values (end-members) to calculate the likely sources of Pb in the urban soils. The reference values for $^{206/207}Pb$ and $^{208}/^{207}Pb$ for UK leaded petrol were 1.067 ± 0.007 and 2.340 ± 0.011 respectively (Monna et al., 1997). The isotopic signature values of galena from Derbyshire and Leicestershire as recorded by Rohl (1996) were used as representative of UK Pb ore (i.e., $^{206/207}Pb$ = 1.182 ± 0.004 and $^{208}/^{207}Pb$ = 2.458 ± 0.002). For coal Pb the isotopic signature

values for England and Wales reported by Farmer et al. (1999) were used (i.e., $^{206/207}Pb$ = 1.184 ± 0.006 and $^{208}/^{207}Pb$ = 2.461 ± 0.012). In this research work UK Pb ore and coal Pb values were used as a proxy for $Pb_{geogenic}$.

$$Pb_{total(petrol)} = \frac{(\frac{206}{207}Pb)\,ore - (\frac{206}{207}Pb)total}{(\frac{206}{207}Pb)ore - (\frac{206}{207}Pb)petrol} \times Pb_{total} \qquad \text{Eq. (2)}$$

2.11 Preliminary development of a method for accurate measurement of Pb isotopes using ICP-QMS

Alternative approaches for improving Pb isotope ratio measurement by ICP-QMS were tested by conducting a series of experiments using certified and in-house reference materials. These test experiments are described in Table 2.3. Experiments included investigation of detector dead time correction, mass bias correction, dwell time optimization and use of peak compressed mode.

Table 2.3: Different reference materials used as test materials in different experiments

Reference Material	Details
SRM-981, NIST	Common Pb isotopic standard available from the National Institute of Standards and Technology. High purity (99.9+%) Pb metal available as an extruded wire. Used to establish optimum dwell time, dead-time correction, as an 'external' mass bias correction standard and to test peak compression approaches.
Glendenning	Made from a single Scottish crystal of galena chosen to be representative of a typical UK lead ore. Used as an in-house standard by BGS since 2007. Available in two preparations, designated Gd 'low' (L) and 'high' (H) concentrations. Used mainly to test peak compression approaches.
BCR 2	Prepared from a US Geological Survey certified reference basalt that has been extensively characterised. The powdered standard was dissolved using $HF/HClO_4/HNO_3$ before being taken up in 5% HNO_3/2.5% HCl. Available in two formulations, designated '55' and '85' at 'low' (55L, 85L) and 'high' concentration (55H, 85H). Used mainly to test peak compression approaches.

2.11.1 Dead time correction

Initially a detector dead time correction factor (Df) was determined using a restricted range of Pb standard solutions (0, 1, 2, 3, 4 and 5 µg L^{-1}) prepared from SRM-981, NIST in 2% HNO_3 using the $^{206}/^{208}Pb$ isotopic ratio. The calculated Df, where the isotope ratio $^{206}Pb/^{208}Pb$ was independent of Pb concentration, was 54 nano seconds (ns) (Figure 2.1). In a second test experiment, values of Df were calculated for different Pb isotope ratios ($^{204}/^{208}Pb$, $^{206}/^{208}Pb$ and $^{207}/^{208}Pb$) using the same standard solution concentrations. However, in this test, the slope of isotopic ratio against concentration appeared quite insensitive to Df value and no consistency was observed across the range of isotopic ratios tested (Figure 2.2). Calculated values of Df for $^{204}/^{208}Pb$, $^{206}/^{208}Pb$ and $^{207}/^{208}Pb$ were 42.2, 21.3 and 36.3 ns respectively. In a final test values of Df were calculated individually across a range of Pb isotopic ratios using an expanded SRM-981, NIST concentration range (0, 2, 4, 6, 8, 10, 12, 14, 16, 18, 20 and 22 µg L^{-1}), full details are given in Chapter 3 (Section 3.3.1).

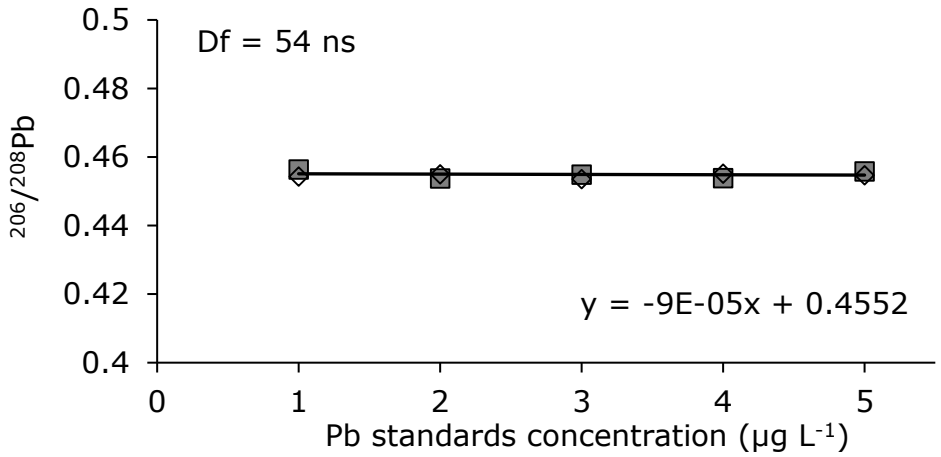


Figure 2.1: Lead isotopic ratio $^{206}/^{207}Pb$ versus concentration (µg L^{-1}) of SRM-981, NIST; symbols denote duplicate runs.

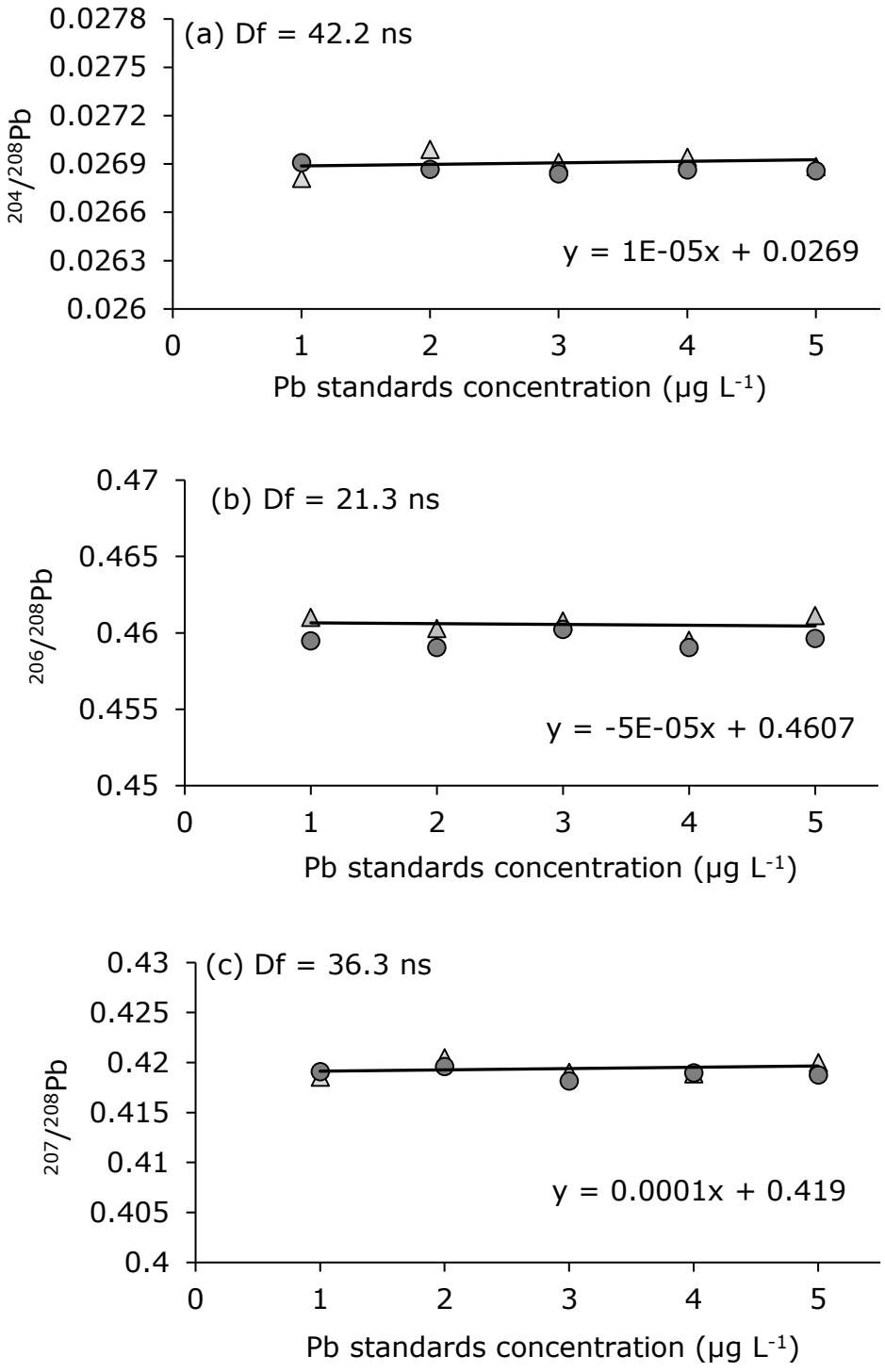


Figure 2.2: Isotopic ratios (a) $^{204}/^{208}$Pb, (b) $^{206}/^{208}$Pb, (c) $^{207}/^{208}$Pb versus Pb standards concentration (µg L^{-1}) all at individually optimised values of Df. The circle and triangle symbols represent repeat runs of the same samples.

2.11.2 Mass bias correction

The mass bias correction factor (Kf) was investigated using two sets of samples each consisting of thirty replicates of SRM-981, NIST (5 µg L^{-1}). The second set of samples was spiked with Tl (1 µg L^{-1}) and ^{203}Tl and ^{205}Tl were measured for determination of internal mass bias correction. The frequency of correction using 'standard' SRM-981, NIST was varied to examine the nature of the drift in mass bias and how frequently it was necessary to measure Kf. A dilute Tl solution (2 µg L^{-1}) was also analysed to test for possible ^{203}Tl-H or ^{204}Pb-H hydride generation and any evidence of peak overlap between ^{203}Tl, ^{204}Pb and ^{205}Tl.

For the first set of samples, mass bias correction was calculated using SRM-981, NIST at a range of (external) correction intervals (i.e. 2, 3, 4……28). It was observed that SRM-981, NIST provided a good Kf for all Pb isotopic ratios (Figure 2.3). No effect of (external) correction interval was observed.

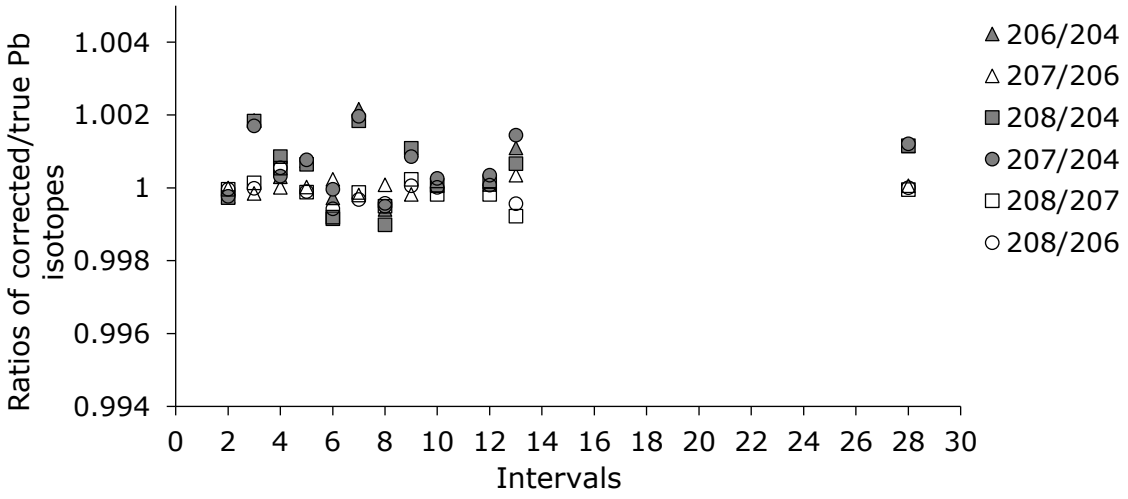


Figure 2.3: SRM-981, NIST (external correction) for mass bias correction of all Pb isotopic ratios at different intervals.

In the second set of samples spiked with Tl, no thallium hydride generation was observed to affect the ^{204}Pb signal. Mass bias correction was also calculated with

SRM-981, NIST at a range of correction intervals (i.e. 2, 3, 4……28) and compared with Tl (designated a 'zero interval'). External correction (SRM-981, NIST) was observed to be best for drift correction up to a sample interval of 13 but was significantly worse at longer intervals (Figure 2.4). It was observed that the measurements of Pb isotope ratios were closer to accepted values when Tl was not measured. This may have been due to greater plasma flicker arising from the additional isotope analysis time when Tl was included.

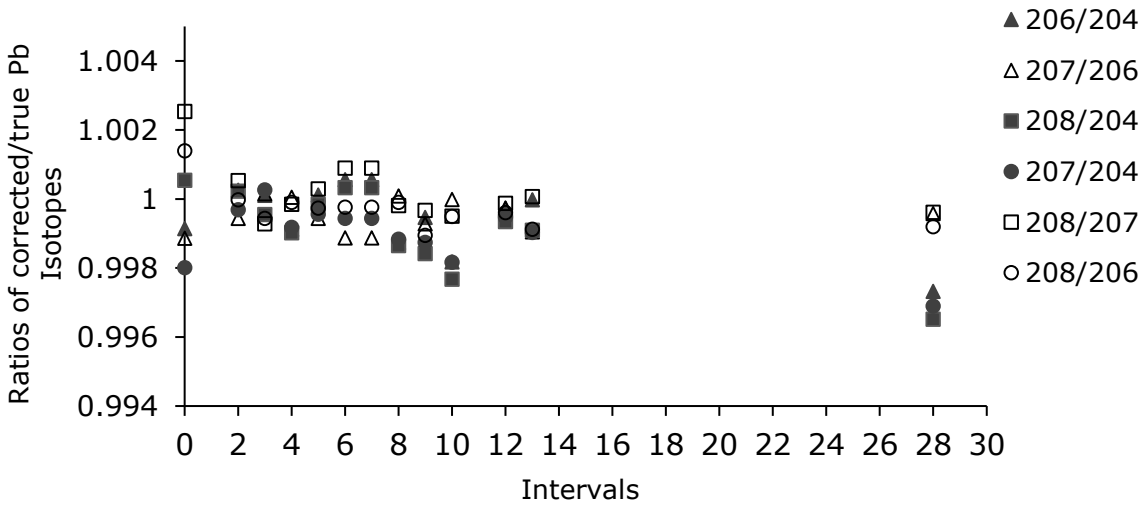


Figure 2.4: SRM-981, NIST spiked with Tl for mass bias correction of all Pb isotopic ratios at different intervals.

2.11.3 Dwell time

Replicates of SRM-981, NIST (5 µg L^{-1}) were repeatedly analysed at different dwell times (0.1, 0.5, 1.0, 5.0, 10 and 50 ms) to examine the effect on count rate precision (as % RSD) for all four Pb isotopes (^{204}Pb, ^{206}Pb, ^{207}Pb and ^{208}Pb). Initially 10 separate runs were used each with 100 sweeps to give 1000 quadrupole visits to each isotope per sample. Average %RSD values for measured intensities of the four Pb isotopes are shown as a function of dwell time in Figure 2.5.

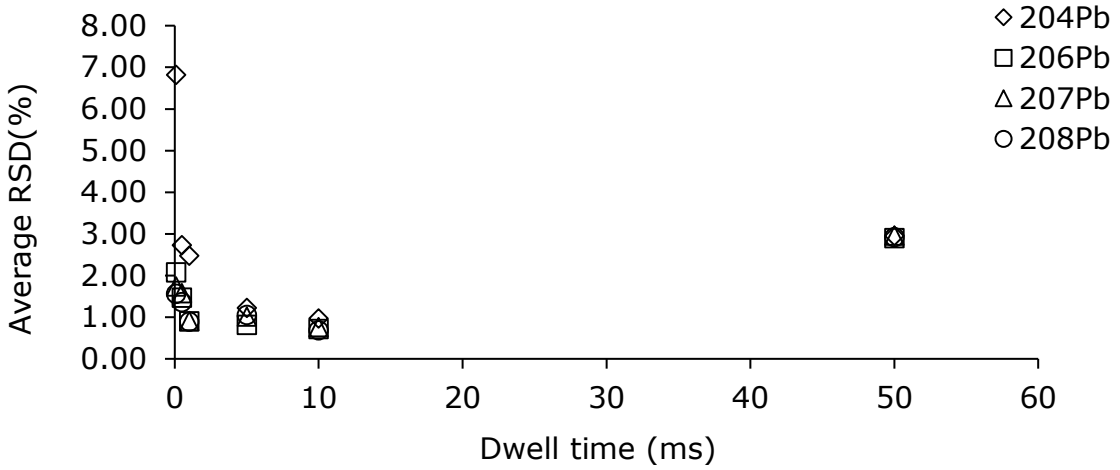


Figure 2.5: Average %RSD for intensities of the four Pb isotopes (^{204}Pb, ^{206}Pb, ^{207}Pb and ^{208}Pb) as a function of quadrupole dwell time (0 - 50 ms).

A minimum %RSD for all four isotopes is suggested corresponding with a dwell time of approximately 10 ms; the ^{204}Pb intensity values showed the sharpest minimum in %RSD. An attempt was made to refine the dwell time by repeating the experiment with a more focussed range of dwell times from 5.0 ms to 15.0 ms (Figure 2.6).

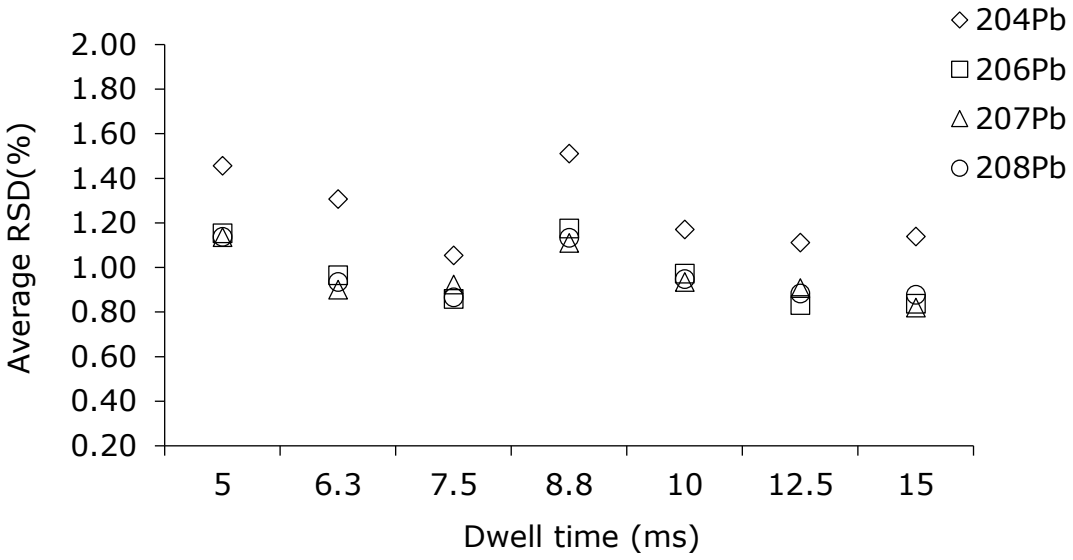


Figure 2.6: Average %RSD of isotopes (^{204}Pb, ^{206}Pb, ^{207}Pb and ^{208}Pb) intensities as a function of quadrupole dwell time (5 - 15 ms).

The trend observed in %RSD was quite flat across this more restricted range. However, in these tests the total acquisition time for each isotope was not constant which meant the effect was probably due to counting statistics for shorter dwell time rather than instrumental noise.

2.11.4 Peak Compression

In preliminary experiments three reference standards; BCR 2, Glendenning and a high concentration of NIST (24 µg L^{-1}), SRM-981 were used with Tl (internal) and SRM-981, NIST (external) correction to calculate and implement a peak compression factor (Kc) to convert compressed counts into uncompressed counts for each Pb isotope. Samples were run bracketed by external SRM-981, NIST standards (5 µg L^{-1}). Thallium (2 µg L^{-1}) was used as an internal standard and continuously delivered to the nebulizer on a separate line. One hundred sweeps with 10 separate runs was set to give 1000 quadrupole visits to each isotope per sample at a dwell time of 10 ms. In all samples and standards, the isotopes ^{208}Pb, ^{207}Pb, ^{206}Pb and ^{205}Tl were determined in both standard and peak compressed modes. When a comparison was made for ^{206}Pb counts corrected with Tl and SRM-981, NIST derived compression factors, smaller RSD values were observed using the external conversion with SRM-981, NIST. However, in the case of ^{207}Pb, smaller RSD values were observed for internal conversion with Tl. Thallium and SRM-981, NIST both produced similar results for conversion of ^{208}Pb count rates (Figure 2.7).

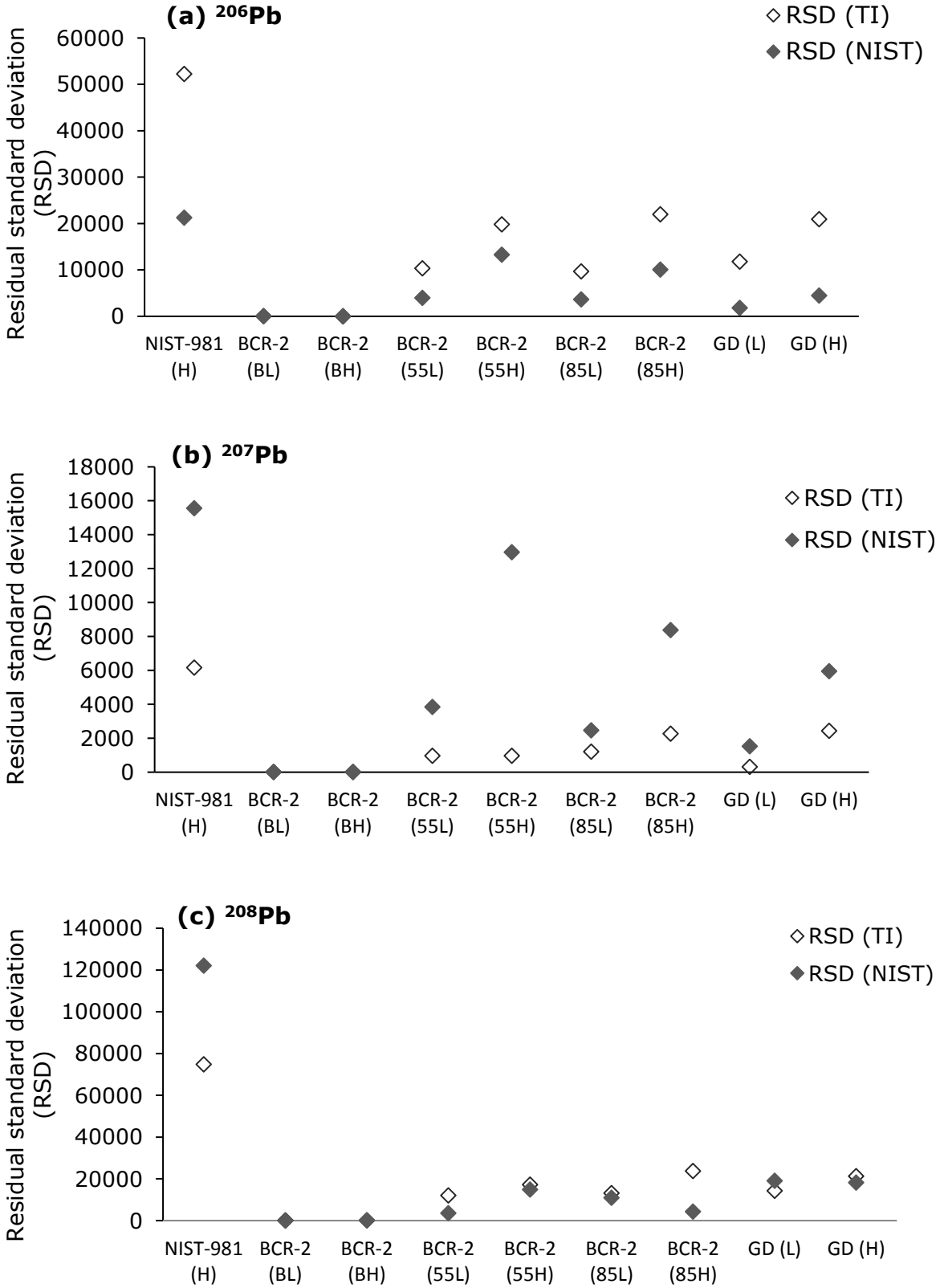


Figure 2.7: Comparison of SRM-981, NIST (external) compression factors (Kc) for converting compressed signals for (a) ^{206}Pb, (b) ^{207}Pb and (c) ^{208}Pb intensities to equivalent uncompressed values.

Development of an approach for the accurate measurement of Pb isotopes by ICP-QMS is described in Chapter 3.

2.12 Quality control

The quality of analytical procedures were monitored by using procedural blanks in each batch of samples to account for background element concentrations. All samples analysis was carried out in duplicate and in some cases triplicate. An isotopic standard reference material, SRM-981, NIST (Common lead isotope) was used to compare the accuracy and for mass bias correction of the Pb isotope ratios measured with ICP-QMS instrument in the method development. Other certified and in-house laboratory standards (i.e., BCR and Glendenning) were also used to monitor accuracy in the preliminary experiments of Pb isotope ratios measurement through ICP-QMS.

In urban allotment soils, three samples of certified reference material (Montana II soil: NIST 2711a) were included as quality control for digestion efficiency. The mean recovery of elements from the certified reference material was observed in the range of 79-106%. In case of urban soils (Nottingham and Wolverhampton) and Pakistan sewage amended soils, certified reference material was not included during the analysis of multi elements. Also for the individual sequential extraction steps, no certified reference materials were available due to inadequate agreement on standard method of extraction (Li et al., 1995).

2.13 Statistical analysis

Microsoft excel (2013) was used for basic statistical calculations such as mean, median, standard deviation and standard error. A range of statistical approaches such as analysis of variance (ANOVA), T-test, Pearson correlation and multivariate analysis (cluster analysis) were calculated using Minitab version (17.2.1). The

default level of confidence was 95% ($p<0.05$). Minitab was also used to tests normality of the raw and transformed data, prior to cluster analysis and the statistical tests (ANOVA). In this study, the Box-Cox transformation was used to make the data more normal. Pearson correlation was applied to investigate the elemental associations in the soils. Similarly cluster analysis (Ward method) was carried out to classify different elements into groups on the basis of similar geochemical features. In the method development, ANOVA *via* F-statistic was used to benchmark ICP-QMS against MC-ICP-MS for Pb isotope ratios for demonstrating 'fitness for purpose' in environmental source apportionment. Crust-normalized REEs patterns were used to evaluate enrichment of REEs relative to upper continental crust in topsoils and subsoils.

3 Chapter 3: Benchmarking current generation ICP-QMS against MC-ICP-MS spectrometry for the determination of lead isotope ratios in soils

Abida Usman[a,b], E. Louise Ander[b], Elizabeth H. Bailey[a], Simon Nelms[c], Vanessa Pashley[b], Scott D. Young[a] and Simon R. Chenery[b]

Abstract

The analytical precisions of lead (Pb) isotope measurements obtained from quadrupole-based mass spectrometers (ICP-QMS) are considered to be limited by a number of factors originating in different components of the instruments. In this study, an attempt was made to refine experimental and instrumental protocols to maximise accuracy and precision when determining lead isotope ratios in urban soil digests (n=11) using current-generation ICP-QMS. Experimental measures included individual dilution of all samples and isotopic standards (SRM-981, NIST) to a single Pb concentration intended to produce an intensity which was high enough to negate blanks and interferences (> 1 x 10^6 CPS for ^{208}Pb) but low enough to fall below the tripping point of the detector. Instrumental protocols included pre-measurement of dead time correction, optimisation of dwell time and the number of scans employed and correction of mass discrimination by sequential application of both *internal* (^{203}Tl and ^{205}Tl) and *external* (SRM-981, NIST) standards. This optimised methodology was benchmarked against multi-collector mass spectrometer (MC-ICP-MS) measurements of Pb isotope ratios using the same soil digest solutions but after these had been subjected to Pb separation using ion-exchange procedures.

Keywords*:* ICP-QMS, MC-ICP-MS, lead isotopes, soil, parameter optimisation

3.1 Introduction

Lead isotopes can be measured by a range of mass spectrometry techniques. Until fairly recently, thermal ionization mass spectrometry (TIMS) was the preferred choice for precise (0.001-0.01% RSD) measurement of Pb isotope abundances (Weiss et al., 2004, Cheng and Hu, 2010). However, TIMS involves laborious sample preparation steps, such as separation of the analyte from the matrix into a highly purified form, involving extensive chemical treatment, and stringent optimisation of vaporisation and ionisation conditions of samples, with long analysis times (~45 minutes). These measurements are not only time consuming but also incur cost factors, rendering TIMS unsuitable when analysing large numbers of samples (Thirlwall, 2001, Komárek et al., 2008). Inductively coupled plasma mass spectrometers (ICP-MS) are more appropriate for routine use with large sample numbers and are operationally simpler than TIMS (Santos et al., 2007). They are widely used for multi-element and isotopic analysis with a precision (<0.05% RSD) comparable to that of TIMS for Pb isotopes. The term 'ICP-MS' covers a range of instruments which differ in their mass filter and detector systems. These include; those that are quadrupole-based (ICP-QMS) or high resolution, magnetic sector field-based (HR-ICP-MS) and those which can utilize single-collector (SC), multi-collector (MC), array detector (AD) or 'time-of-flight' (TOF) detectors (Maréchal et al., 1999, Komárek et al., 2008).

Quadrupole-based mass spectrometers (ICP-QMS) are the most commonly used ICP-MS instruments principally because they are relatively inexpensive to produce and support, and are fast and simple in terms of sample preparation, handling and operation. As a result, the number and availability of ICP-QMS instruments far outweigh MC-ICP-MS. However, in isotope studies, specifically when high precision

ratio measurements are required, MC-ICP-MS is preferred over ICP-QMS and is considered the benchmark for accurate and precise isotope data (Wu et al., 2017). This is principally due to simultaneous measurement of all relevant isotopes, which effectively cancels out the effects of 'plasma flicker', and the flat-topped peaks produced in MC-ICP-MS, with their inherent resistance to instrument drift. This is in contrast to sequential measurement of isotopes on leptokurtic peaks in ICP-QMS (Begley and Sharp, 1997, Quétel et al., 1997, Vanhaecke et al., 1998). The sequential nature of the analysis in any single collector instrument renders the technique susceptible to variations in, for example, sample aerosol transport, RF fluctuations and perturbations within the plasma itself (plasma flicker). In essence, any signal instability results in non-sample related variation in relative isotope abundances from one microsecond to the next. To achieve the ultimate high accuracy and precision that MC-ICP-MS is capable of, does pose some extra constraints, these include the need to separate the element of interest not just to ensure minimising any spectral interferences but also to minimise mass bias effects. However, this is rarely used in ICP-QMS studies as the aims in particularly environmental research require the analysis of large numbers of samples, in the minimum time.

The accuracy and precision of isotopic ratios measured through ICP-QMS are considered limited by 'noise' (variation in signal intensity). This originates from varying conditions throughout the ion pathway, including the ion source (i.e. sample introduction system and the plasma itself), the interface region, the collision/reaction cell (if used), the quadrupole mass filter and the detector (Begley and Sharp, 1994, Quétel et al., 1997). Variation in the efficiency of nebulisation and sample transport produces low frequency noise (Carré et al., 1992); as a result it is common in MC-ICP-MS studies to use manual sample introduction with

naturally aspirating nebulisers. In the ICP ion source, noise is produced due to 'plasma flicker' that is caused by changes in energy transfer from plasma to analyte atoms. In addition to mainly random fluctuation caused by these instrumental factors, variation in 'mass bias' is a major source of systematic error, responsible for deviation of measured intensity ratios from true isotopic ratios (Appelblad and Baxter, 2000, Santos et al., 2007). The largest mass discrimination effect in ICP-MS is observed due to space charge effects (Quétel et al., 1997), which occur between the plasma torch and the skimmer cone, and cause differential deflection of lighter ions (Gillson et al., 1988, Begley and Sharp, 1994). Thus the ratio of heavier to lighter isotopes increases in the ion beam passing through the skimmer cone (Heumann et al., 1998); therefore it is common in high precision isotope ratio studies to separate the element of interest to minimise these effects. Woodhead (2002), used this variability in mass bias with matrix to propose an improved Tl bias correction by "calibrating" the small difference in mass bias for Tl and Pb. It also has been reported that mass discrimination induced by space charge effects should be minimal in magnetic sector instruments due to high accelerating voltages however this is not always the case compared to the low extraction voltages, behind the skimmer cone, in a quadrupole instrument. Heumann et al. (1998) showed that mass discrimination for bromine isotopes was smaller than for a quadrupole but was still significant leading to the suggestion that discrimination can occur between the plasma torch and the skimmer cone. Random noise originating in the ICP ion source and quadrupole mass filter is also responsible for imprecision in measuring isotope ratios because of the sequential measurement required in ICP-QMS and, to a lesser extent, single collector HR-ICP-MS.

In ICP-QMS, a discrete dynode detector is normally used which necessitates a compromise between employing large analyte concentrations to improve the counting statistics of minor isotopes while working below the point at which the detector trips to analogue mode for major isotopes. This may push the intensities of high abundance isotopes into the zone in which the detector dead time correction has a significant effect. Therefore, accurate *dead time correction* is necessary for precise measurement of isotopic ratios especially when very different isotope abundances are involved (e.g. $^{208}Pb/^{204}Pb$) (Heumann et al., 1998). The age of the detector is also considered an important factor in influencing dead time (Begley and Sharp, 1997, Vanhaecke et al., 1998, Nelms et al., 2001).

Different strategies have been employed for precise determination of Pb isotopes using different types of mass spectrometers. To minimise low frequency noise sources, Furuta (1991), Begley and Sharp (1994) and Monna et al. (1998) all recommended cycling the ICP-QMS as rapidly as possible through the measured masses. Quétel et al. (1997) used a factorial design approach to investigate the simultaneous effects of different factors (dwell time, number of sweeps/replicates, number of replicates/analysis and time factor) on the precise determination of Pb isotopes, including ^{204}Pb. To reduce the effects of mass bias in multi-collector, quadrupole and other mass spectrometers Ingle et al. (2003) demonstrated mass bias correction by modelling the underlying instrument response function in MC-ICP-MS. Reuer et al. (2003) revealed the importance of both external and internal correction for mass bias in MC-ICP-MS to improve measurements of Pb isotopes in natural samples, i.e. marine carbonates and sea water. Simultaneous assessment of several optimising parameters have also been undertaken in some studies. For regular monitoring of dead time and mass discrimination, Appelblad and Baxter (2000) presented a linear model for the simultaneous determination

of dead time and mass bias correction factor in double focusing sector field mass spectrometry (SF-ICP-MS) for regular monitoring of dead time and mass discrimination. This had the advantage of utilizing more time on the isotopes of interest. Different methods for calculating accurate detector dead times have also been demonstrated to improve the precision of isotopic ratios (Vanhaecke et al., 1998, Nelms et al., 2001).

In this study, the ability of a current-generation ICP-QMS instrument to determine Pb isotope ratios in urban soil samples was tested through a comparison with MC-ICP-MS analysis. The primary aim of this study was to refine protocols intended to maximise the accuracy and precision of ICP-QMS determination of Pb isotope ratios to enable soil Pb source apportionment. The optimised methodology was benchmarked against MC-ICP-MS measurements on the same sample material.

3.2 Experimental

3.2.1 Preparation of samples

Composite urban surface (0-15 cm) soil samples (n=11) from a range of sites in Wolverhampton and Nottingham were used. These had been sampled previously as part of a Natural Environmental Research Council (NERC) project, under the URGENT programme, conducted by a research consortium from Imperial College, London, NERC Isotope Geosciences Laboratory, British Geological Survey and University of Nottingham between 1999 and 2002 (Table 3.1).

Table 3.1 Studied soil samples from Nottingham (Ng) and Wolverhampton (Wv)

Samples	Total Pb content mg kg^{-1}	Land use	Grid ref
Ng2	385	Churchyard	455280 338770
Ng5	434	Domestic garden	457360 342370
Ng7	340	Grassland (imported)	458500 339110
Ng8	339	Grassland (racecourse)	459710 339170
Ng9	146	Vegetated colliery spoil heap	453570 344310
Ng12	893	Disused factory	455760 338550
Wv2	47.6	Grassland (Golf course)	388450 300860
Wv12	134	Grassland	388240 295750
Wv19	40.6	Grassland	395150 299140
Wv21	27.9	Brownfield	393960 299860
Wv29	271	Deciduous woodland	391680 300080

Soil samples were air-dried and sieved to <2 mm and a small subsample of the archived soil (c. 2.0 g in triplicate) was ground in an agate ball mill (Model PM400, Retch GnbH & Co., Germany). Complete digestion of 0.2 g samples was achieved in PFA vials in a 48-place Teflon-coated graphite block digester (Model A3, Analysco Ltd, Chipping Norton, UK) using a mixed acid digestion process i.e., HNO_3 (68%), $HClO_4$ (70%) and HF (70%). The dried digestate was dissolved in 68% HNO_3 and diluted to 50 mL with Milli-Q water (18.2 MΩ cm). Prior to analysis of total Pb concentration by ICP-QMS a further 1:10 dilution with 2% HNO_3 was undertaken. Internal standards were introduced to the sample stream via a separate T-line including Ge (50 µg L^{-1}), Rh (20 µg L^{-1}) and Ir (10 µg L^{-1}) in 2% HNO_3 and multi-element standards (0, 20, 40, 100 µg L^{-1}) were used to determine the Pb concentration (CLMS-2; CertPrep™). Three procedural blanks were also included in each digestion batch for quality assurance. All samples were analysed

with the ICP-QMS operating in 'kinetic energy discrimination' (KED) mode, with He as the cell gas, to eliminate polyatomic interferences.

3.2.1.1 Dilution of samples for Pb isotopes measurement (ICP-QMS)

The precision of Pb isotope ratio measurements generally improves with increasing Pb concentration as counting statistics improve (Furuta, 1991). However, at high concentrations the ion counter detector used with the ICP-QMS employed in this study trips to an analogue signal, resulting in non-linearity caused by measuring isotopes in different detector modes, with added uncertainty due to the application of a gain correction between the two detector types (Monna et al., 1998). Thus, individually tailored dilutions of each sample digest were carried out, with 2% HNO_3, using prior knowledge of the total concentrations of Pb. The objective was to work with near identical concentrations (~15 µg L^{-1}) of all samples and reference materials (SRM-981, NIST Pb wire). This approach had the advantages of (i) reducing the effect of any error in the dead time correction factor and (ii) ensuring that the intensity of the ^{204}Pb signal was as high as possible while keeping the ^{208}Pb signal below the detector trip point (c. 10^6 cps).

3.2.1.2 Lead separation method for Pb isotope measurement by MC-ICP-MS

Variations in mass bias and small interferences are known to impact on data quality in MC-ICP-MS isotope ratio determinations (Yang, 2009). Therefore, prior to the measurement of Pb isotopes in soil digests, a preliminary separation of Pb was performed using an anion exchange (AG1-X80) column (Strelow, 1967). Aliquots, containing an estimated 200 ng of Pb from each digest, were heated overnight to dryness in PFA vials on a hotplate. An aliquot of HBr (2 mL) was then added to each vial and left overnight again to solubilise the sample. Sample Pb

was separated using anion exchange resin columns (2 mL, AG1-X80). The resin was pre-cleaned with MQ quality (>18 MΩ) water followed by 6 M HCl and then equilibrated by washing the column with 2 mL 1 M HBr. All samples were then passed through individual columns adsorbing the sample Pb as $PbBr_4^{2-}$ ions. Major cations were then eluted from the columns with further HBr. The sample Pb was then eluted using 8 mL of 6 M HCl back into its original vial. Concentrated nitric acid (0.2 mL) was added to each vial as an oxidising agent and the contents evaporated to dryness on a hotplate, overnight, at 90°C. Prior to analysis by MC-ICP-MS each sample was diluted to c.5-10 ng mL^{-1} and spiked with Tl (c. 5-10 ng mL^{-1}) for instrumental mass bias correction with the aim of achieving less than the maximum 10V signal on ^{208}Pb and ^{205}Tl.

3.2.2 Instrumentation and optimisation procedures

ICP-QMS

At the University of Nottingham Pb isotope ratios were determined by current generation ICP-QMS (Model iCAP Q; Thermo Scientific, Bremen, Germany). All samples were analysed with the ICP-QMS operating in 'kinetic energy discrimination' (KED) mode, with He as the cell gas, to eliminate polyatomic interferences. Additionally, in the past it has been suggested that the use of a collision gas may "thermalize" the ion beam and improve isotope ratio precision (Bandura et al., 2000). Samples were introduced from an autosampler incorporating an ASXpress™ rapid uptake module (Cetac ASX-520, Teledyne Technologies Inc., Omaha, NE, USA), with a 5 mL sample loop, through a perfluoroalkoxy (PFA) Microflow PFA-ST nebuliser (Thermo Fisher Scientific, Bremen, Germany). The typical operational parameters selected for measurement of Pb isotopic ratios are given in Table 3.2.

Table 3.2 Operational parameters selected for measurement of Pb isotopic ratios using ICP-QMS

Detector acquisition mode	Pulse counting mode
Dead time	36.8 ns
Dwell time	10 ms
Number of runs	10
Number of scans	10000
Isotopes measured	^{202}Hg, ^{204}Pb, ^{206}Pb, ^{207}Pb, ^{208}Pb, ^{203}Tl and ^{205}Tl
Points per peak	1
Number of replicates	3
Analysis time per sample	16 minutes

MC-ICP-MS

Lead isotope analysis was conducted at the NERC Isotope Geosciences Laboratory (BGS, Keyworth, U.K.) using a Nu Instruments, Nu Plasma, MC-ICP-MS (Multi-Collector Inductively Coupled Plasma Mass Spectrometer). Prior to analysis, each sample was spiked with a Thallium (Tl) solution, to enable correction of instrument induced mass bias. Samples were then introduced into the instrument via an ESI PFA50 nebuliser attached to a de-solvating unit, (Nu Instruments DSN 100). For each sample, five ratios were simultaneously measured (^{206}/^{204}Pb, ^{207}/^{204}Pb, ^{208}/^{204}Pb, ^{207}/^{206}Pb and ^{208}/^{206}Pb) using the instruments array of Faraday detectors. The collector configuration used is illustrated in Table 3.3. Each individual acquisition consisted of 3 blocks of 25 cycles, with a 5-second integration time per cycle, following a 60 second de-focused baseline (c. 7 min. per acquisition).

The precision and accuracy of the method was assessed through repeat analysis of a SRM-981, NIST Pb reference solution, (also spiked with Tl). The average values obtained for each of the mass bias corrected SRM-981, NIST ratios were then compared to the known values for this reference material (Thirlwall, 2002): ^{206}/^{204}Pb = 16.9417 ± 29, ^{207}/^{204}Pb = 15.4996 ± 31, ^{208}/^{204}Pb = 36.724 ± 09,

$^{207}/^{206}Pb$ = 0.91488 ± 08 and $^{208}/^{206}Pb$ = 2.1677 ± 24; Precision = ppm 2sd. All sample data were subsequently normalised according to the relative deviation of the measured reference values from the true values. The analytical errors for each of the sample ratios were propagated relative to the reproducibility of the SRM-981, NIST to take into account the errors associated with the normalisation process.

Table 3.3 Configuration of the Nu Plasma HR 'Zircon' collector block, used for Pb isotope analysis

High 4	High 3	High 2	High 1	Axial	Low 1	Low 2
^{208}Pb	^{207}Pb	^{206}Pb	^{205}Tl*2	^{204}Pb ^{204}Hg	^{203}Tl*2	^{202}Hg*1

*1 Measured to allow for the correction of the isobaric interference of ^{204}Hg on ^{204}Pb.

*2 Measured to allow for the correction of instrumental mass bias.

3.3 Procedures for optimising measurement of Pb isotopes using ICP-QMS

3.3.1 Evaluation of detector dead time correction factor

A dead time correction factor (Df) was determined, according to a method described by Nelms et al. (2001), for the isotopic ratios: $^{204}/^{208}Pb$, $^{206}/^{208}Pb$ and $^{207}/^{208}Pb$. Values of Df were measured from intensity ratios determined across a range of Pb standard solutions (i.e. 0, 2, 4, 6, 8....22 µg L^{-1}) prepared from SRM-981, NIST in 2% HNO_3. Data from samples providing higher count rates for ^{208}Pb

were used so that the detector was more likely to be close to saturation; we also wanted to investigate the validity of measurements up to the point where the detector tripped to analogue signals.

The Df was initially set to zero ns. An isobaric correction factor for ^{204}Hg was determined from measurement of the signal at m/z = 202 (^{202}Hg). Intensity values (cps) were measured using a quadrupole dwell time of 10 ms with 200 sweeps and 20 separate integrations to give 4000 quadrupole visits to each isotope per sample and a total signal integration time per isotope of 40 seconds. Initially, a blank correction was made to all raw Pb isotope intensities ($I_{sample} - I_{blank}$). Sample intensity values were corrected using Eq. 1, following optimisation of the Df value (van Heuzen et al., 1989).

$$I_{corr} = \frac{(I_{sample} - I_{blank})}{1 - (I_{sample} - I_{blank})Df\,10^{-9}} \quad \ldots\ldots\ldots\ldots\ldots\ldots\ldots\ldots \quad (1)$$

The value of Df was optimised by determining the slope of individual isotope intensity ratios (i.e.$^{204}I_{corr}/^{208}I_{corr}$) against the intensity signal for ^{208}Pb (cps) and varying the value of Df until the value of the slope squared (slope^2) was minimised. This was undertaken using the Microsoft Excel *Solver* function. The optimised values of dead time calculated for Pb isotopic ratios were 37.4, 36.7 and 36.3 ns for $^{204}/^{208}$Pb, $^{206}/^{208}$Pb and $^{207}/^{208}$Pb ratios respectively. The values of Df calculated did not change systematically with mass difference between the isotopes and they were independent of mass and analyte concentration as illustrated in Figure 3.1 for the isotopic ratio $^{204}/^{208}$Pb. An average value of dead time correction was calculated (i.e., 36.8 ns) and set within the instrument software. Values of dead time were in good agreement with previous studies (Monna et al., 1998, Encinar

et al., 2001) and close to the manufacturer's factory-set value of 40 ns. Subsequently, all analytical sessions were preceded by measurement and re-setting of detector dead-time.

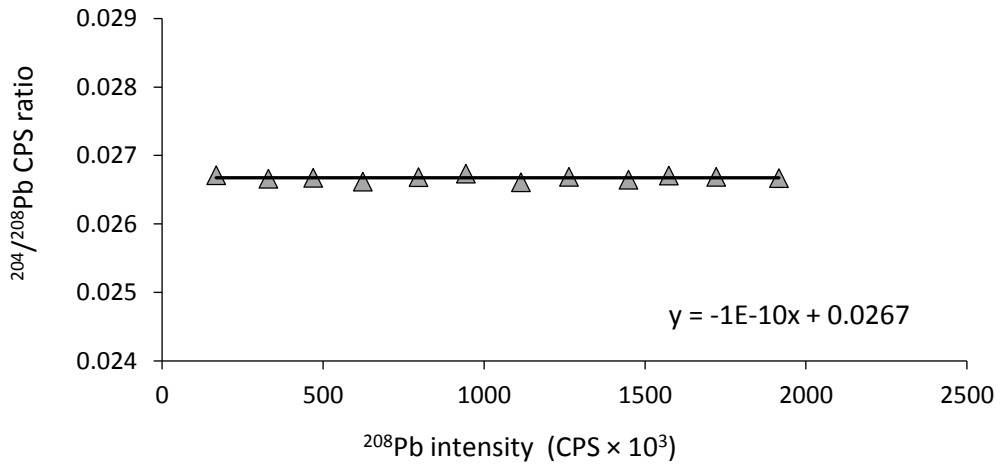


Figure 3.1. Isotopic count ratios (CR) $^{204}/^{208}$Pb vs ^{208}Pb intensity measurements (cps) at the optimised value of Df.

3.3.2 Mass bias correction

Prior to mass bias correction, Pb isotope intensities were corrected for an isobaric interference from ^{204}Hg, through measurement of ^{202}Hg, and for operational blanks. The resulting data was then corrected for mass bias using both *proxy internal* and *external* standards. Thallium (2 µg L^{-1}) was used as an internal standard because its isotopic masses (i.e., ^{203}Tl and ^{205}Tl) are sufficiently close to those of the Pb isotopes that it can be used as a proxy for continuous monitoring of mass discrimination in individual samples (Reuer et al., 2003). Thallium was continuously delivered to the nebulizer on a separate line and the bias per unit mass (ε) determined from the measured ^{205}Tl/^{203}Tl, when compared to the known, 'true', value for this ratio i.e., 2.3871 (Weiss et al., 2004).

Three equations (i.e., linear, power and exponential models; equations 2-4 below) are generally used to estimate the mass discrimination correction factor (or 'K-factor') for a pair of Pb isotopes when Tl is used as an internal standard (Taylor et al., 1995, Heumann et al., 1998). Most previous studies conducted using MC-ICP-MS have favoured a power (Eq 3.) or exponential (Eq 4.) equation over a linear relation (Eq. 2) on grounds of precision for internal standardisation (Taylor et al., 1995, Heumann et al., 1998, Weiss et al., 2004). However, a linear model (Eq. 2) is more commonly used for mass discrimination correction for quadrupole mass analysers as this has been found to be a sufficiently accurate model (Nelms and Beauchemin, 2005).

$$\mathrm{K} = 1 + (\Delta m\ \varepsilon) \quad \ldots\ldots\ldots\ldots\ldots\ldots\ldots\ldots \quad (2)$$

$$\mathrm{K} = (1 + \varepsilon)^{\Delta m} \quad \ldots\ldots\ldots\ldots\ldots\ldots\ldots\ldots \quad (3)$$

$$\mathrm{K} = \exp(\Delta m\ \varepsilon) \quad \ldots\ldots\ldots\ldots\ldots\ldots\ldots\ldots \quad (4)$$

In equations 2 – 4, Δm is the mass difference between two Pb isotopes; K is the K-factor for the ratio of those two isotopes and ε is the bias per unit mass determined for the ratio $^{205}Tl/^{203}Tl$. Preliminary data for Pb isotopes were processed using the linear (Eq. 2), power (Eq. 3) and exponential (Eq. 4) equations to assess the difference in mass bias correction factor, but very similar results were observed using the three approaches. Therefore, the most simplistic linear correction was used in this study.

Thallium-corrected data was then further normalised using the SRM-981, NIST Pb reference material to allow for any element-specific drift in instrument sensitivity during the experiment. The refined K-factor for each sample was calculated using interpolated values of the K-factor for SRM-981, NIST samples (15 μg L^{-1}) run every 10^{th} sample.

3.3.3 Quadrupole dwell time

Improvement in precision of Pb isotope ratio determinations can be achieved by decreasing the quadrupole dwell time in order to reduce low frequency noise in the plasma (Begley and Sharp, 1994), but this may result in accurately jumping to the mass peak maximum at extremely fast scanning rates (low dwell times) (Furuta, 1991). This suggests that there should be an optimum isotope dwell time at which counting precision is greatest. The influence of quadrupole dwell time was tested using a solution of SRM-981, NIST (5 μg L^{-1}) spiked with Tl (1 μg L^{-1}). The test solution was aspirated directly and the precision of Pb isotopic ratio measurements (% RSD) determined for a range of dwell times. Ten separate integrations were set with the number of sweeps changed inversely to increasing isotope dwell time (1-15 ms) to retain a constant overall signal acquisition time. Values of %RSD for individual Pb isotopic ratios were plotted against dwell time. Figure 3.2 shows that the variation in precision across the range of dwell times was neither systematic nor significantly different between dwell times, with the single outlier of ^{204}Pb ratios at 9 ms. It was therefore decided to retain a dwell time of 10 ms for further studies as suggested in the literature (Almeida and Vasconcelos, 2001).

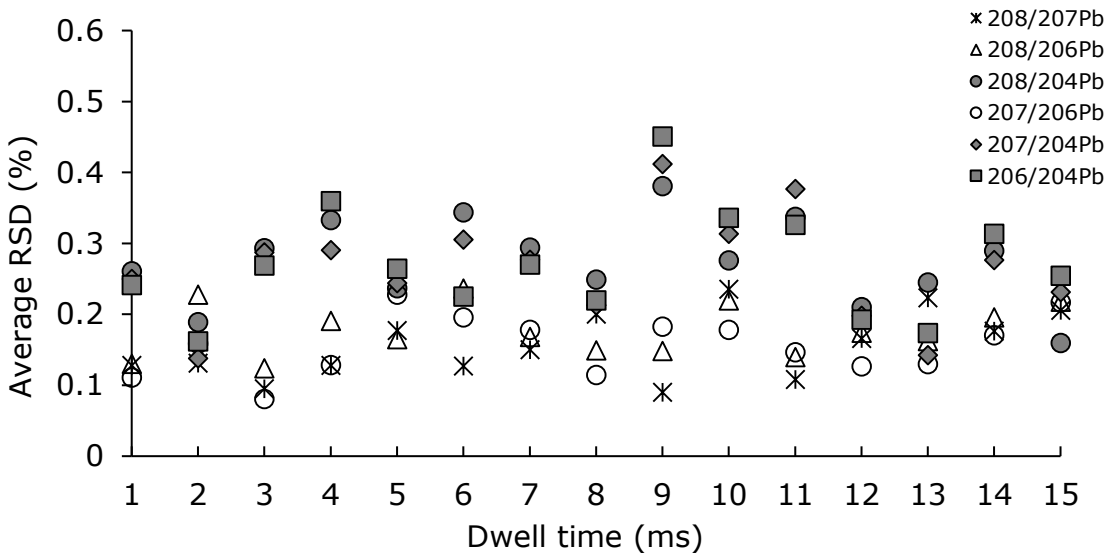
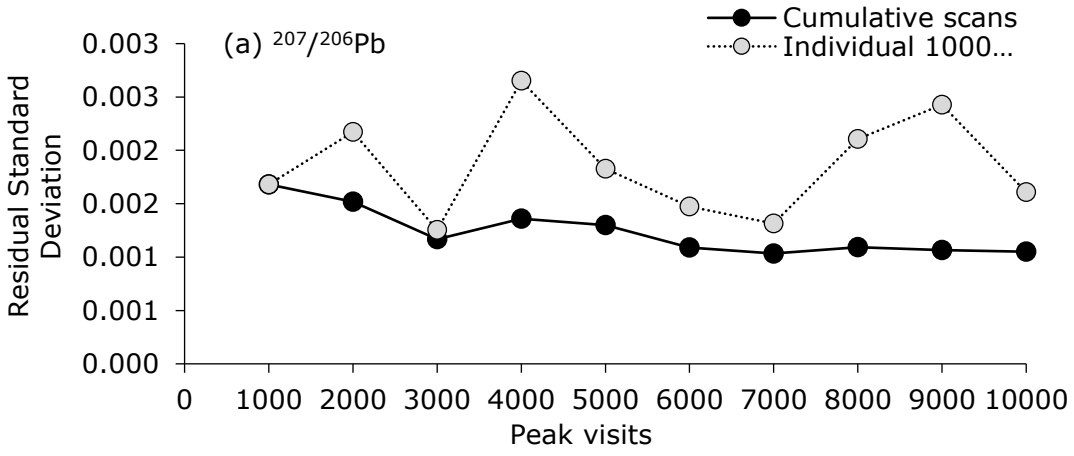


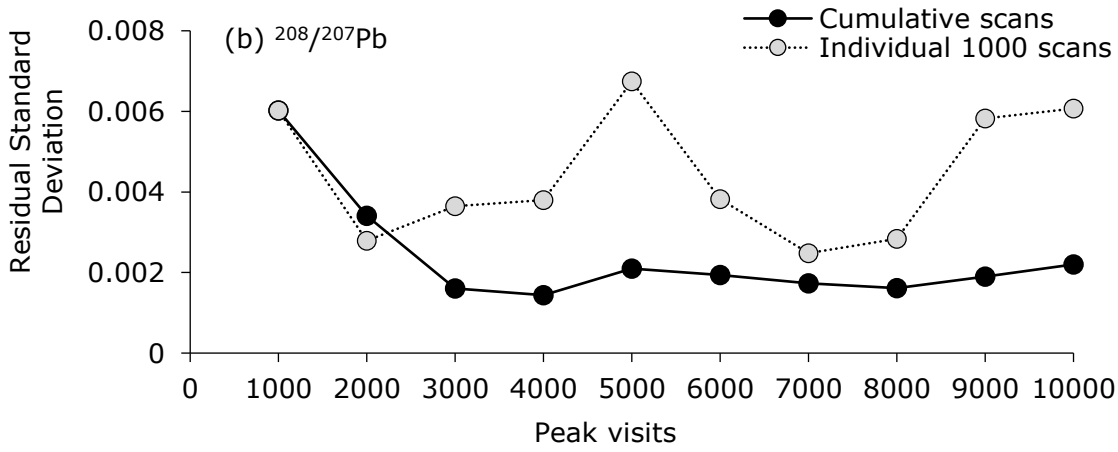
Figure 3.2. Average RSD (%) of Pb isotope ratios against dwell time (ms) whilst retaining a constant total acquisition time.

3.3.4 Optimising the number of scans (quadrupole peak visits)

To optimise the number of scans (peak visits by the quadrupole), 10 separate runs with 1000 scans per run was selected and the number of points per peak was set to one (dwell time 10 ms). The total analysis time for each sample (SRM-981, NIST) was approximately 16 minutes. To determine the effects of the number of scans on Pb isotopic ratios determination, each of the 10 runs of 1000 scans was processed (i) separately and (ii) cumulatively i.e. using 1000, 2000 scans etc. A comparison of the resulting data is shown in Figure 3.3. The error for different Pb isotopic ratios (i.e., $^{207}/^{206}$Pb, $^{208}/^{207}$Pb and $^{208}/^{204}$Pb) was assessed by comparing residual standard deviation (RSD) values against the multi-collector data. The data processed using individual groups of 1000 scans showed relatively high and variable RSD values for all isotopic ratios (grey circles). By contrast, data processed in a cumulative way showed better precision and consistency for all three isotopic ratios. Precision generally increased with increasing number of scans as shown in Figure 3.3 (a, b and c). For the current study we decided to use

10,000 scans to try to minimise variation due to counting statistics, although Figure 3.3 suggests this could potentially be reduced to 6000 scans to save time without significant loss of precision.





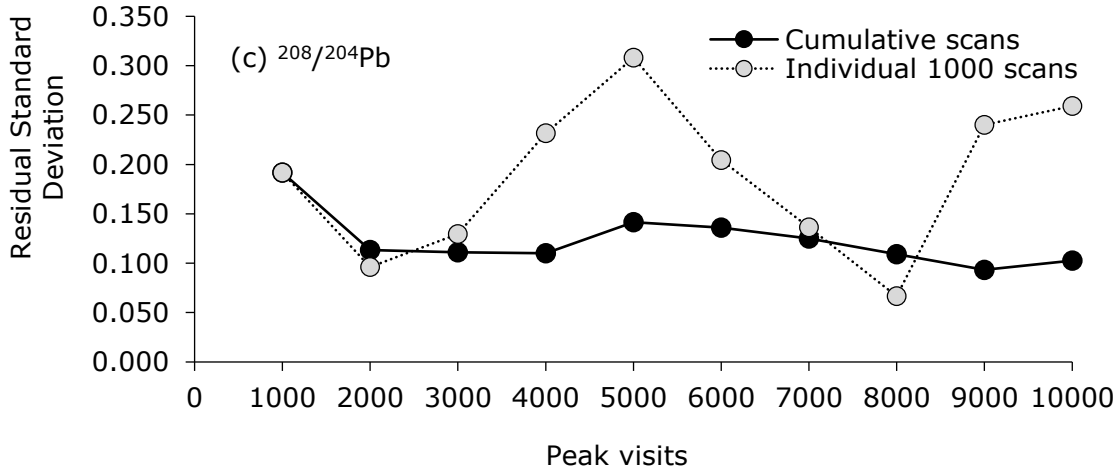


Figure 3.3. Values of residual standard deviation, comparing ICP-QMS with MC-ICP-MS, for Pb isotope ratios (a) $^{207}/^{206}$Pb, (b) $^{208}/^{207}$Pb, and (c) $^{208}/^{204}$Pb against the number of quadrupole scans (peak visits).

3.4 Results and discussion

3.4.1 Comparison of Pb isotope ratios ($^{207}/^{206}$Pb, $^{208}/^{207}$Pb and $^{208}/^{204}$Pb) measured by ICP-QMS and MC-ICP-MS

Following optimisation of the Pb isotopic ratios measurement protocol, the processed data for diluted soil sample digests analysed with ICP-QMS (10,000 scans) were compared to equivalent data for chemically separated Pb measured by MC-ICP-MS. Each of the 3 digestions for an individual sample were treated as a separate data point to achieve the most direct comparison of the two techniques. An excellent correlation (r=0.999 and r=0.998; n=36) was observed for $^{206}/^{207}$Pb and $^{208}/^{207}$Pb isotopic ratios with slope values of 1.0008 and 1.0006 respectively shown in Figure 3.4 (a and b). The correlation observed for the $^{208}/^{204}$Pb isotopic ratio was also good, albeit a little weaker than for the other ratios (Figure 3.4. c; r= 0.987, slope=1.0017). This is understandable given that: (i) there is a greater dependence on mass bias because of the mass difference of 4 amu; (ii) ^{204}Pb (isotopic abundance = 1.4%) produces a lower signal giving poorer counting

statistics and (iii) the large difference in isotopic abundance results in increased vulnerability to errors in dead time correction. There is also the need for Hg correction on ^{204}Pb, which further compromises the measurement uncertainty.

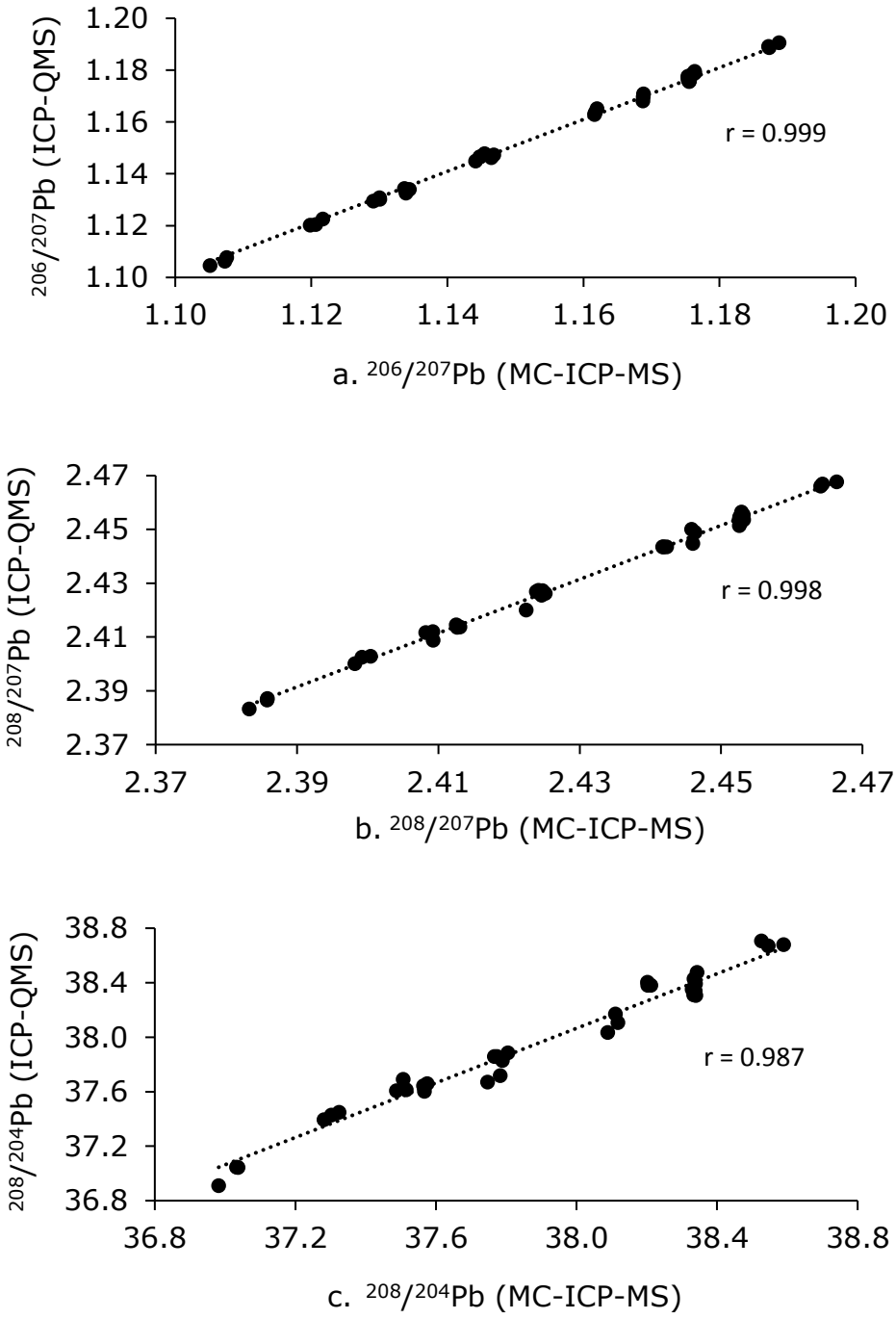


Figure 3.4. Correlation of Pb isotope ratios (a) $^{206}/^{207}Pb$, (b) $^{208}/^{207}Pb$, and (c) $^{208}/^{204}Pb$ measured using quadrupole (ICP-QMS) and multi-collector (MC-ICP-MS) instruments.

With such strong correlations it is instructive to examine the difference between the precision of the benchmark MC-ICP-MS and the ICP-QMS data (Figure 3.5 a, b and c), assuming that the MC-ICP-MS has no error for the purposes of this comparison. There may be two sources of error between the datasets: *additive* i.e. a simple offset value constant for all samples, and *multiplicative* i.e. a change in value proportional to the isotope ratio measured. For $^{206}/^{207}$Pb (Figure 3.5 a) there was a clear increase in error with increasing isotopic ratio, indicating a multiplicative bias between ICP-QMS and MC-ICP-MS. For $^{208}/^{207}$Pb and $^{208}/^{204}$Pb this was not apparent. A regression analysis of ICP-QMS on MC-ICP-MS was made and tested for significance of the slope being different to 1 for all ratios shown in Table 3.4. All slope values were statistically different from 1 except $^{208}/^{206}$Pb; however only in the 4th significant figure. To account for the effect of the very narrow range of isotope ratio values, an intercept between the ICP-QMS and MC-ICP-MS data was estimated by correcting the ICP-QMS data for the slope, then calculating the difference between the two data sets. The median difference was calculated (Table 3.4) to avoid outliers biasing the estimate. In terms of impact, the offset for $^{208}/^{204}$Pb ratio was the most significant with an absolute value of 0.02, equivalent to approximately 0.04% of the median $^{208}/^{204}$Pb ratio.

As each original soil sample was digested and analysed separately 3 times there was an opportunity to test 'fitness for purpose' for the whole method from digestion to ICP-QMS and MC-ICP-MS measurement. This was achieved using analysis of variance (ANOVA) to separate the total variance of the dataset into the analytical variance and the true variance between samples; where the analytical variance is a combination of the digestion variance and the measurement variance.

First, comparing the within sample analytical precision (as measured by RSD %) of the ICP-QMS with that of MC-ICP-MS (Table 3.5). If we assume that the MC-ICP-MS inherently has a better measurement precision but with the within sample precision essentially being equal between the techniques, then we must assume that the digestion process has limited our analytical precision. For example, for $^{207}/^{206}$Pb values of RSD for ICP-QMS and MC-ICP-MS were 0.09% and 0.07%, respectively, which suggests the data were digestion heterogeneity limited. By contrast, for $^{207}/^{204}$Pb the greater values for ICP-QMS (0.13%) compared to MC-ICP-MS (0.02%) suggests that the precision is limited by instrumental factors. This is supported by quantifying if within sample variance is different between ICP-QMS and MC-ICP-MS using the F-statistic. This demonstrated that there was no statistical difference between the two instruments for $^{207}/^{206}$Pb; but very significant differences for $^{207}/^{204}$Pb (Table 3.5). This implies that there is no advantage in using MC-ICP-MS, and chemical separation of Pb, for determination of $^{207}/^{206}$Pb ratios but the converse is true for $^{207}/^{204}$Pb.

The ANOVA, via the F-statistic, can be further used to test, for each isotope ratio, the power of the analytical technique to discriminate between samples. The greater the ratio of the "between samples" variance and the "within sample" variance which is the F-statistic, the better the discrimination i.e. when the ratio falls below the F_{crit} value we have no discrimination. For $^{207}/^{206}$Pb, a variance ratio of 615 for ICP-QMS implies that we can readily discriminate between samples; for $^{207}/^{204}$Pb with a variance ratio of 6, this was not the case, as this is barely above the F_{crit} of 2.78. Thus, values of $^{207}/^{204}$Pb ratio measured by ICP-QMS (the lowest F-value), will have little resolving power between samples and any further analytical improvements should focus on determination of this isotopic ratio. By comparison, the variance ratios for these isotope ratios by MC-ICP-MS were 1123

and 137 respectively, suggesting that MC-ICP-MS can be readily used for all isotope ratios to differentiate between samples.

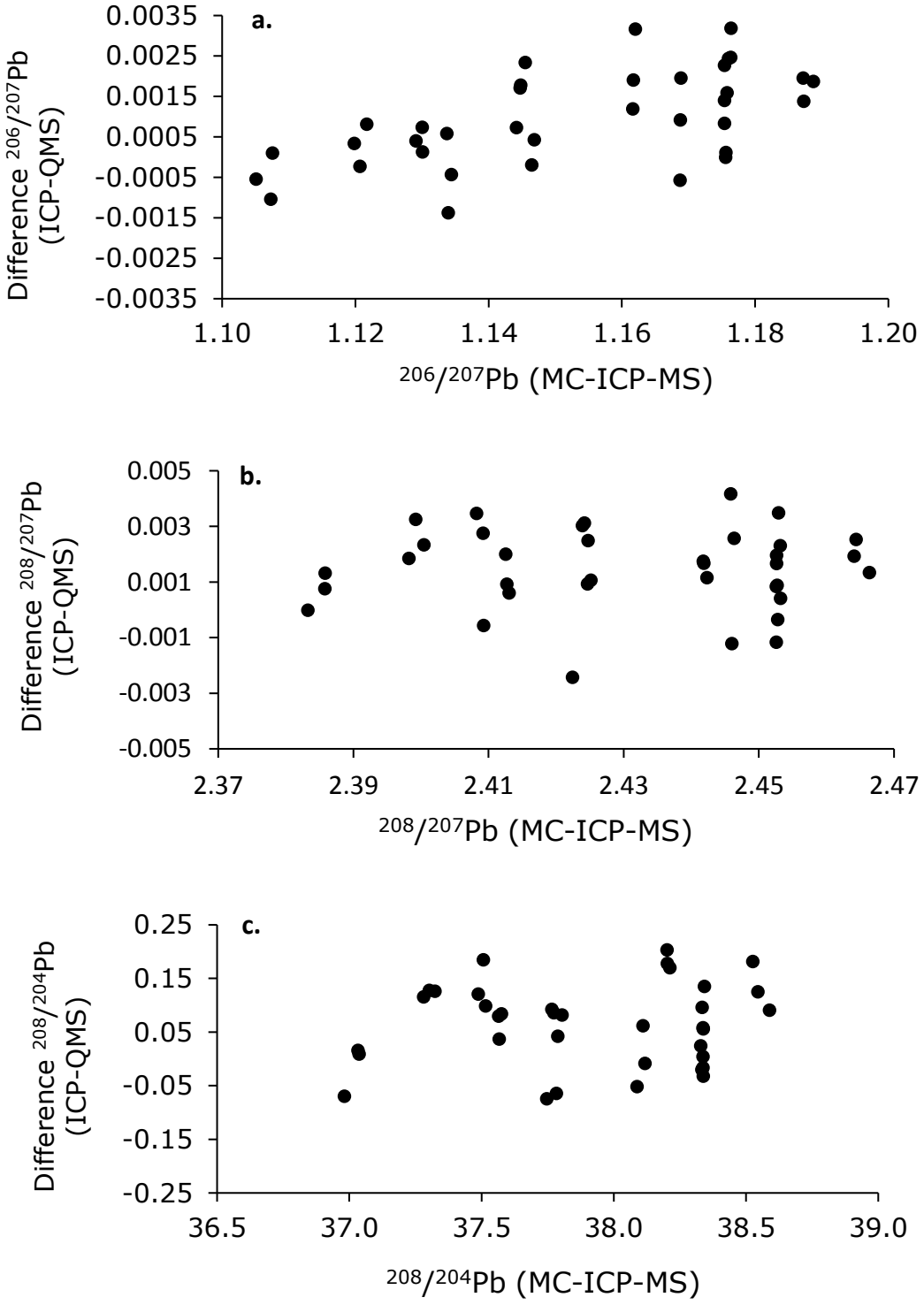


Figure 3.5. Difference between the benchmark MC-ICP-MS data and the difference between ICP-QMS and MC-ICP-MS (a), (b) and (c).

Table 3.4 Evaluation of significance of slope (multiplicative) and offset (additive) when regressing the difference between measured ICP-QMS and MC-ICP-MS against MC-ICP-MS ratios, showing the significant differences occurring in the offset for $^{207}/^{204}$Pb and $^{208}/^{204}$Pb ratios.

Ratio	Slope	95% Confidence interval	Median Offset
$^{207}/^{206}$Pb	0.9992	0.0003	0.00007
$^{206}/^{207}$Pb	1.0009	0.0003	-0.0001
$^{208}/^{206}$Pb	0.9998	0.0004	0.0001
$^{208}/^{207}$Pb	1.0006	0.0002	0.0002
$^{206}/^{204}$Pb	1.0019	0.0006	0.0008
$^{207}/^{204}$Pb	1.0011	0.0006	0.0045
$^{208}/^{204}$Pb	1.0017	0.0007	0.02

Table 3.5 Statistical comparison of within sample measurement precision with between sample precision and evaluation for Pb isotope ratios determined both by ICP-QMS and MC-ICP-MS. Note: the greater the F-statistic is over the critical F value, the greater the power of the measurement to discriminate true sample variation from analytical "noise".

		$^{207}/^{206}$Pb	$^{208}/^{206}$Pb	$^{206}/^{204}$Pb	$^{207}/^{204}$Pb	$^{208}/^{204}$Pb	$^{206}/^{207}$Pb	$^{208}/^{207}$Pb
MC-ICP-MS	Within sample RSD%	0.07	0.03	0.08	0.02	0.05	0.07	0.03
MC-ICP-MS	Between sample RSD%	2.27	1.21	2.48	0.24	1.28	2.25	1.04
ICP-QMS	Within sample RSD%	0.09	0.08	0.14	0.13	0.16	0.09	0.08
ICP-QMS	Between sample RSD%	2.34	1.28	2.58	0.31	1.32	2.31	1.04
F_{crit} 1-tail 95% (10df,10df) = 2.98	Within sample F-stat MC - ICP-MS v ICP-QMS	1.94	6.11	3.35	37.30	10.34	2.00	5.40
F_{crit} 1-tail 95% (22df,10df) = 2.78	Between v Within sample F-stat ICP-QMS	615	237	322	6	67	625	167
F_{crit} 1-tail 95% (22df,10df) = 2.78	Between v Within sample F-stat MC-ICP-MS	1123	1302	1001	137	653	1180	902

3.4.2 Comparison of Binary plots

Binary plots were used to attempt soil Pb source apportionment for the three sets of data derived from (i) MC-ICP-MS, (ii) ICP-QMS measured using 10,000 scans, and (iii) ICP-QMS using just the first run of 1,000 scans as an example of acquisition parameters used previously in the literature (Mao et al., 2014). The first comparison was made using a conventional binary plot ($^{208}/^{207}$Pb vs $^{206}/^{207}$Pb) as shown in Figure 3.6. The MC-ICP-MS data (dark circles) all fell on a single straight trend line, expected from a simple 2 isotopic end-member system. Similarly, data analysed by ICP-QMS with 10,000 scans (grey circles) fell very close to the multi-collector data. By contrast, data from ICP-QMS using 1000 scans (white circles) clearly deviated from the multi-collector data and the single mixing line in the binary plot. The standard error at each data point (n=3) was also large compared to ICP-QMS data analysed using 10,000 scans where reproducibility was very high.

A further comparison was made using a second binary plot (Figure 3.7) involving the ^{204}Pb isotope ($^{208}/^{204}$Pb versus $^{206}/^{207}$Pb) in an attempt to identify the presence of further end member sources not revealed by Figure 3.6; as Ellam (2010b) has pointed out plots based only on ^{206,207,208}Pb ratio have a limited ability to discriminate more than 2 end-members. Again, all data points determined by MC-ICP-MS fell on a single straight mixing line, providing no evidence of a 'third source' of Pb. The data determined by ICP-QMS using 10000 scans (grey circles) again fell very close to the multi-collector data. However, a few points visibly deviated from the single mixing line and the standard errors were very small, suggesting a small systematic deviation. The largest systematic deviations and standard errors (n=3) were observed for ICP-QMS data using 1,000 scans (white

circles). It is clear that although a straight line through the data would indicate 2 dominant sources, the substantial scatter around the mixing line could be erroneously interpreted as indicating multiple (> 2) sources of Pb in the current dataset. This highlights the necessity for longer total acquisition time than previously reported (Mao et al., 2014, Shetaya et al., 2018) and a fuller understanding of causes of error in determination of Pb isotope ratios.

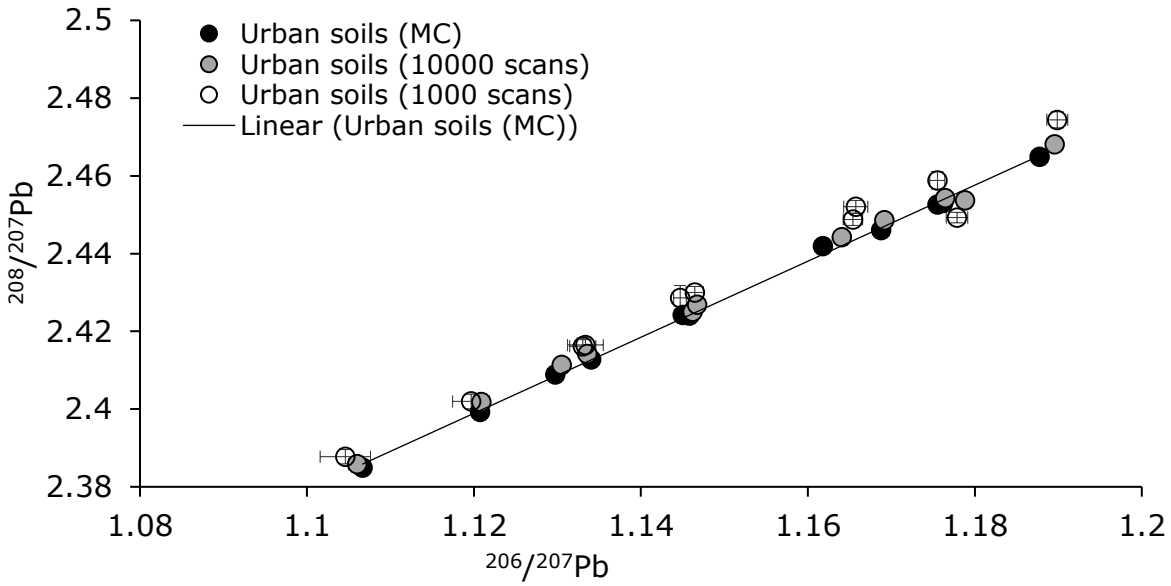


Figure 3.6. A binary plot using isotopic ratios $^{208}/^{207}$Pb vs $^{206}/^{207}$Pb for data derived from MC-ICP-MS and ICP-QMS with either 10,000 or 1,000 scans. Note error bars for MC-ICP-MS and ICP-QMS (10000 scans) are smaller than symbols for most samples.

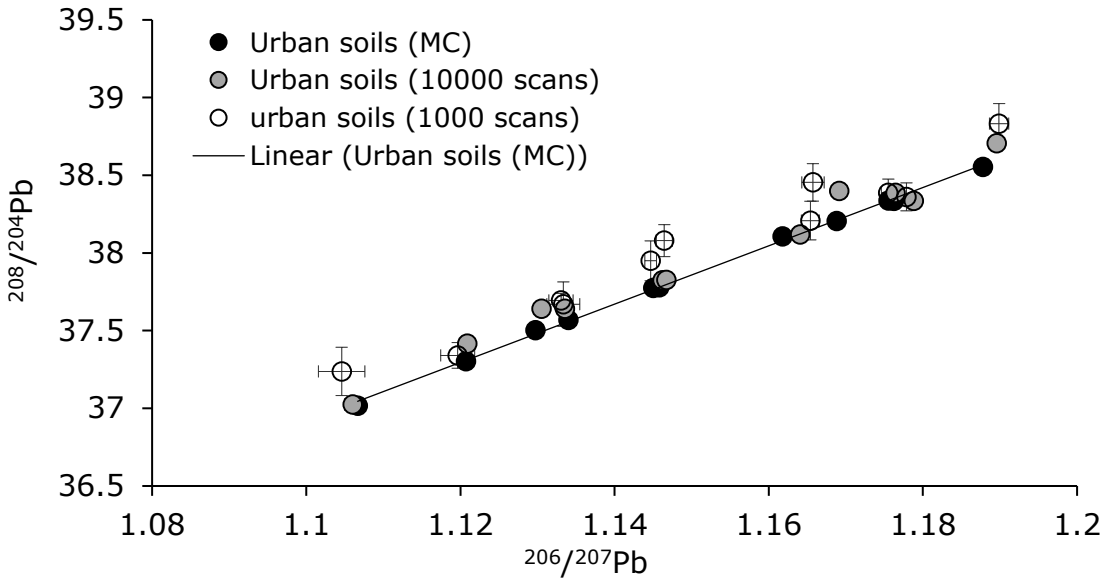


Figure 3.7. A binary plot using isotopic ratios $^{208}/^{204}$Pb vs $^{206}/^{207}$Pb for data derived from MC-ICP-MS and ICP-QMS with either 10,000 or 1,000 scans.

3.5 Conclusions

In this study a protocol is refined for accurate and precise determination of Pb isotope ratios in urban soils using current-generation ICP-QMS. The operating parameters optimised were; individual dilution of soil samples to a single Pb concentration (15 ug L^{-1}), identical to that of an external isotope standard (SRM-981, NIST), determination of dead time correction factor (Df =36.8 ns), optimisation of quadrupole dwell time (10 ms), number of scans per sample and use of both internal (Tl) and external (SRM-981, NIST) mass bias correction. No dependency of measurement precision on isotope dwell time, was observed compared to that observed in studies with previous generations of ICP-QMS instrument. High reproducibility was observed for data where the number of scans was increased to 10,000 (total analyte time per sample = 16 min). This developed protocol was further compared to Pb isotopic ratios data measured through MC-ICP-MS using the same soil sample digests. An excellent correlation was observed for $^{206}/^{207}$Pb and $^{208}/^{207}$Pb isotope ratios (r = 0.999 and r = 0.998, n = 35). The

correlation observed for $^{208}/^{204}$Pb isotope ratio was also strong but weaker than for other ratios (r=0.987). ANOVA was used to test 'fitness for purpose' for the whole method from digestion of samples to ICP-QMS and MC-ICP-MS measurement. No statistical difference was observed for $^{207}/^{206}$Pb (ICP-QMS RSD 0.09%; MC-ICP-MS 0.07%) whereas for determination of the $^{207}/^{204}$Pb isotope ratio (ICP-QMS 0.13%; MC-ICP-MS 0.02%) ICP-QMS appeared to be limited by instrumental factors. Comparison of measurement variance with that of the between-sample variance was also undertaken using the F-statistic. It was apparent that the $^{207}/^{206}$Pb ratio determined through ICP-QMS (V.R. = 615) has excellent discriminating power between samples; by contrast utilising the $^{207}/^{204}$Pb ratio (V.R. = 6) for Pb source apportionment would require further analytical improvements, for example a detector with a wider pulse counting dynamic range that would allow the accumulation of better counting statistics within a reasonable time-frame.

3.6 Conflicts of interest

SN is an employee of Thermo Corp but the study was designed and tested by the other authors independently, to avoid any conflict of interest.

3.7 Acknowledgements

A.U., L.A., V.P. and S.C. publish with the permission of the Director, British Geological Survey.

4 Chapter 4: Identification of pollutant sources in urban soils

4.1 Introduction

Urbanization results in physical, chemical and biological changes in affected soils (Rossiter and Burghardt, 2003, Micó et al., 2006, Puskás et al., 2008, Luo et al., 2014). In recent decades, anthropogenic inputs of trace elements to urban soils has far exceeded contributions from natural sources (Facchinelli et al., 2001). Anthropogenic activities with the clearest impacts on the urban environment include vehicular emission, industrial activities, combustion of fossil fuel, corrosion of old building materials, application of fertilizers, pesticides, manures and disposable of municipal waste (Nadal et al., 2004, Wong et al., 2006). Urban areas close to current or former industrial areas are commonly contaminated with metals that reflect the nature of the industrial raw materials and products being produced (Alloway, 2013).

Wear and tear of automotive parts commonly releases e.g. Pb, Cr and Cu into the environment (Blake and Goulding, 2002, Shi et al., 2008, Kadi, 2009). Chromium is used in chrome plating of automotive parts, Zn is added to tyres during vulcanization (Smolders and Degryse, 2002, Chen et al., 2012), Cu is used in lubricants and Cu alloys in mechanical parts and radiators (Sayed et al., 2003, Lu et al., 2010, Yang et al., 2011).

Urban pollutants are primarily released via atmospheric emission and their dispersal in the urban environment is highly dependent upon particle size. Particles deposited on soil can be easily re-suspended and re-located by heavy traffic movements, wind, rainfall and surface run-off (Callender and Rice, 2000, Meza-

Figueroa et al., 2007, Przybysz et al., 2014). Heterogeneity of soil also contributes to spatial variations in trace elements concentrations (Luo et al., 2007). Apportioning pollutants to natural (parent) materials and anthropogenic activities is therefore challenging in the urban environment (Gallego et al., 2002, Chen et al., 2008, Chen et al., 2012, Luo et al., 2015).

4.2 Objectives

Determination of soil Pb isotopic composition can help to establish pollutant sources and combined with in-depth analysis of other trace elements may prove to be a more powerful tool for source apportionment. The objectives of this chapter were therefore to determine the concentrations of a wide range of possible 'contaminant' elements for a range of urban soils and to combine this with (i) investigation of Pb isotopic composition ($^{206}/^{207}$Pb and $^{208}/^{207}$Pb), (ii) consideration of the relationship between total Pb (Pb_{total}) and Pb isotopic ratio ($^{206}/^{207}$Pb), and (iii) identification of the proportion of Pb_{petrol} to Pb_{total}, in order to estimate the likely origins of key contaminant metal and metalloids in the soils.

4.3 Material and methods

4.3.1 Soil sampling

Urban soils collected from sites in Nottingham (n=20) and Wolverhampton, UK (n=30) have been studied along with sewage amended soils (n=67) from four districts of Southern Punjab, Pakistan (detail given in chapter 2, section 2.2).

4.3.2 Sample analysis

Major and trace elements concentrations were determined by ICP-MS after acid digestion (see Chapter 2, Sections 2.4 and 2.5.1). Lead isotopic abundances were measured following the methodology described in Chapter 3. The relative proportion of Pb from different sources (i.e. Pb_{petrol} and $Pb_{geogenic}$) was calculated

according to the model proposed by Monna et al. (1997) (Chapter 2, Section 2.8).

4.3.3 Statistical analysis for variation of heavy metals concentration in Pakistan sewage amended soils

The variation in heavy metals concentrations between different districts sewage amended soils of Pakistan was assessed using ANOVA in in Minitab (Version: 17.2.1). The normality of data was assessed using the Anderson-Darling method (Razali and Wah, 2011) and when necessary data was transformed using the Box-Cox transformation in order to reduce the skewness of data because too high skewness causes result distortions and low level of significance. Tukey analysis was used to make comparison between heavy metals concentrations at different districts.

4.3.4 Cluster Analysis (CA)

Prior to applying CA in data sets, the normality of the data sets (i.e., urban soils of Nottingham and Wolverhampton and Pakistan sewage amended soils) were also evaluated using the Anderson-Darling method because multivariate analysis also require normal distribution of data. The concentrations of elements which were not normally distributed were transformed using the Box-Cox transformation. Cluster analysis is considered a suitable method to display correlation between variables. The similarity axis (Y-axis) represents the degree of association between variables, the lower the value on the axis, the more significant the association between the variables. In this study the results of CA for different data sets are shown as a dendrogram.

4.4 Results and discussion

4.4.1 Nottingham urban soils

4.4.1.1 Concentrations of major and trace metals in Nottingham soils

Mean concentrations of major and trace elements are presented in Table A1 (see Appendix A). Site locations and descriptions of land use are given in Table 4.1 (after Mao (2014). Total concentrations of elements including Cu, Zn, Pb, As, Cd, Ni and Cr vary considerably between sites (Figure 4.1). Urban soils of Nottingham has been impacted most in past by human activities which left a potential legacy of contamination in most of the areas therefore, concentrations of elements were compared to normal background concentrations (NBCs) for assessment of contamination, except for Zn and Cr, for which there are no assessment criteria. Normal background concentrations for the contaminated domains are defined as the upper 95% confidence limit of the 95th percentile and are used at National to regional scales as a guidance as to what are the normal levels (Ander et al., 2013). The term background includes both geogenic and anthropogenic diffuse pollution. In this study, many sites in urban Nottingham sites had trace element concentrations that were mostly at or below NBCs. Four sites exhibited concentrations of several metals significantly above NBCs. Disused factory sites Ng11 and Ng12 had elevated concentrations of Pb, As, Ni and Zn. Sewage farm soils Ng14 and Ng15 had elevated Cu, Zn, Cd, Cr and Ni reflecting long term sludge application (Singh et al., 2004, Jamali et al., 2008). Arsenic and Ni were elevated at site Ng6 which was close to a railway. Railways may have residues of scrap metal, oil and debris from rolling stock in the soil (Bacon et al., 1996). The railway line in Nottingham was also used for the transportation of coal and the trace element concentrations may also reflected coal contamination. A domestic garden Ng4 had a high concentration of Pb with some suggestion of elevated Zn.

Contamination of urban gardens and allotments with heavy metals has been reported previously in the UK (Hursthouse et al., 2004, Nathanail et al., 2004, Giusti, 2011) and may arise from factors including application of fertilizers and pesticides, burning and burial of metal-containing materials and importation of soils (Alloway, 2004).

Table 4.1: Description of individual sites in Nottingham soils

Sites	Land use	Grid ref
Ng1	Grassland (football field)	455470 336660
Ng2	Churchyard	455280 338770
Ng3	School	453760 341550
Ng4	Domestic garden	454700 343720
Ng5	Domestic garden	457360 342370
Ng6	Railway	458720 339210
Ng7	Grassland (imported)	458500 339110
Ng8	Grassland (racecourse)	459710 339170
Ng9	Vegetated colliery spoil heap	453570 344310
Ng10	Vegetated colliery spoil heap	455170 342480
Ng11	Disused factory	455770 338590
Ng12	Disused factory	455760 338550
Ng13	Grassland (amenity)	453570 344210
Ng14	Sewage Farm	464120 340530
Ng15	Sewage Farm	464130 340810
Ng16	Brownfield	462830 340800
Ng17	Brownfield	462770 340730
Ng18	Brownfield	462900 340700
Ng19	Brownfield	446800 339730
Ng20	Brownfield	447040 339240

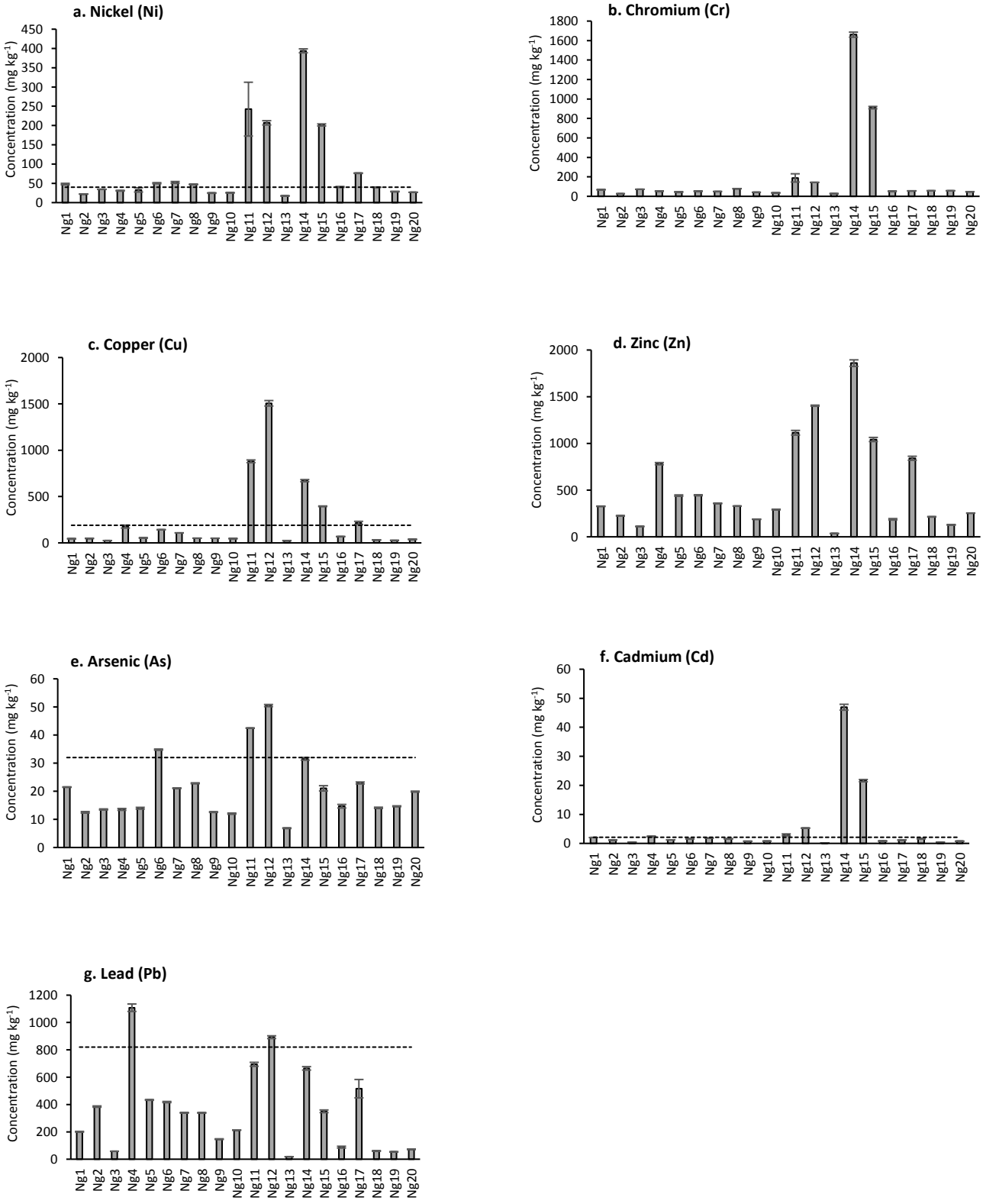


Figure 4.1: Concentration of trace metals (a) Ni, (b) Cr, (c) Cu, (d) Zn, (e) As, (f) Cd and (g) Pb in Nottingham urban soils. Vertical bars denote the average plus/minus the standard error. The dashed line shows the normal background concentration (NBC).

4.4.1.2 Cluster analysis

Cluster analysis identified two main groups (Figure 4.2). In the first group one sub group suggested that Pb_{petrol} and $Pb_{geogenic}$ were closely clustered with Ca, Zn, Sb, Ba, Mg, Se, P, Ag, Cd, Cr and Ni reflecting industrial activities, waste disposal and vehicular emissions. A second sub-group contained elements reflecting both natural and anthropogenic sources (e.g. Fe, Mn, Cu, As, Mo, Sr). The second main cluster contains elements associated with aluminosilicate and clay minerals (K, Rb, Cs, Li, Al) suggesting a natural origin.

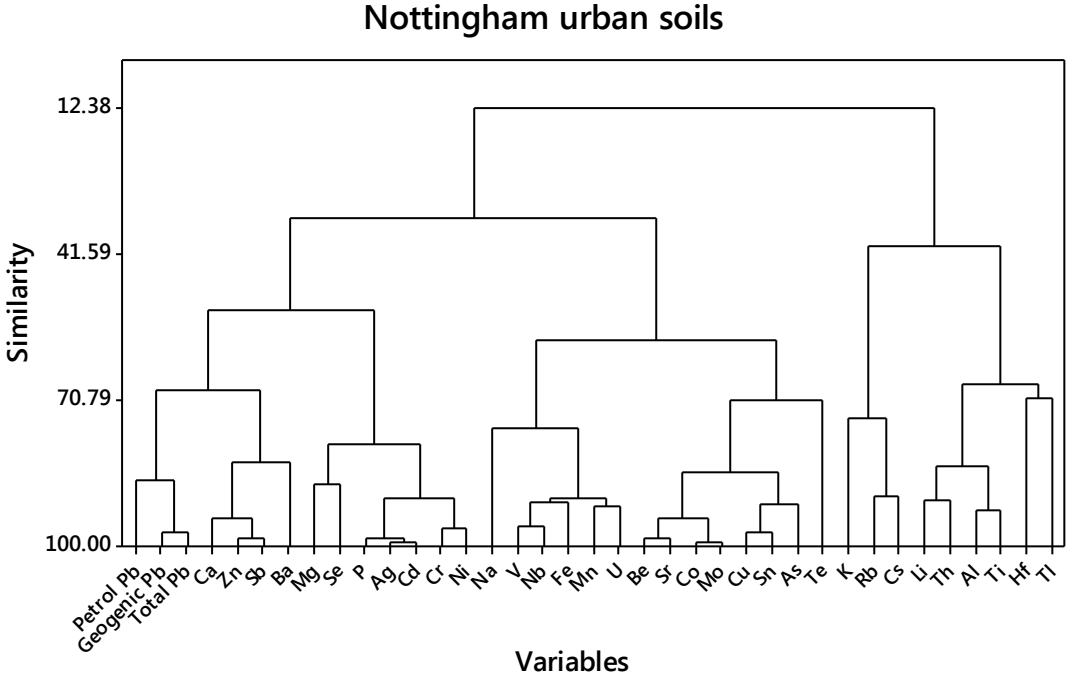


Figure 4.2: Dendrogram for Nottingham urban soils.

4.4.1.3 Nottingham urban soils: Pb isotopic composition and source apportionment

Binary plots are shown in Figure 4.3 alongside typical values for UK leaded petrol, ore (Southern Pennine) and coal (Nottinghamshire-Yorkshire-Derbyshire). Farmer et al. (1999) demonstrated that the isotopic ratio for UK coals overlaps with that

of UK ore. All the Pb isotope ratios fall on the mixing line between Pb_{petrol} and $Pb_{geogenic}$ (UK ore and UK coal). Soils had $^{206}/^{207}$Pb and $^{208}/^{207}$ Pb value in the ranges 1.11-1.18 and 2.39-2.46 respectively. These values are close to reported values for London aerosols (Noble et al., 2008) and Nottinghamshire roadside soil (Atkinson et al., 2011a) suggesting a mix of Pb from both geogenic and leaded petrol sources.

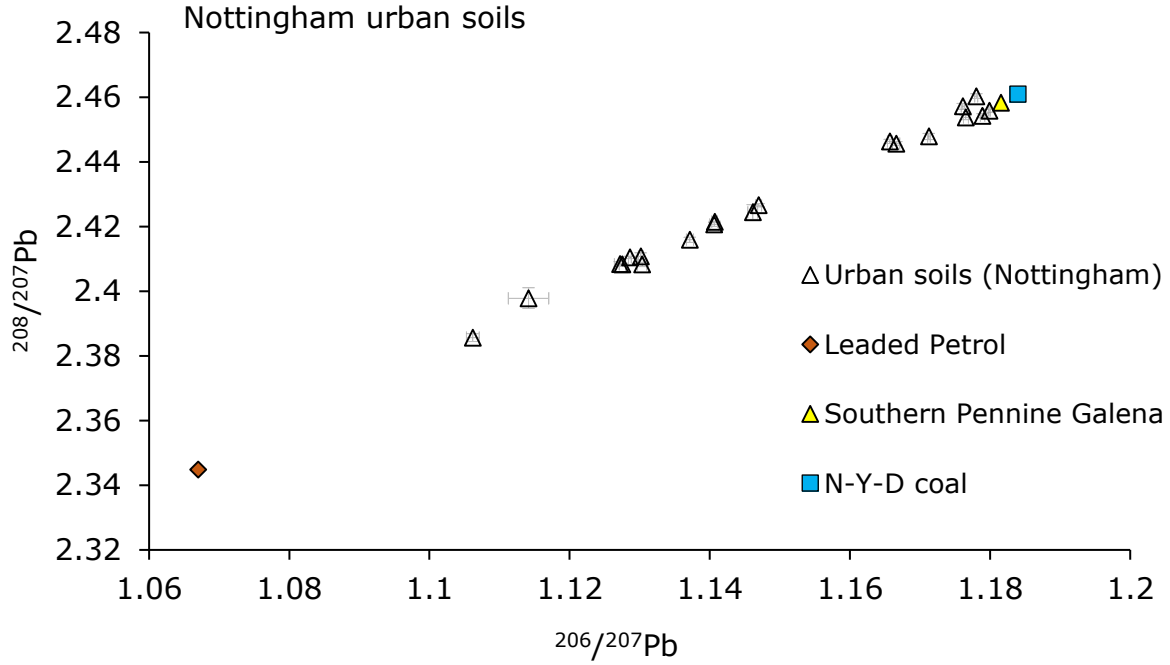


Figure 4.3: Binary plot showing the isotopic ratios $^{206}/^{207}$Pb versus $^{208}/^{207}$Pb for Nottingham urban soils, with median values from UK leaded petrol, Southern Pennine Pb ore (Galena) and Nottinghamshire-Yorkshire-Derbyshire (N-Y-D) coal shown for comparison.

The relationship of $^{206}/^{207}$Pb ratio with the Pb_{total} contents is shown in Figure 4.4. A significant correlation was observed (-0.559, $p<0.05$) between $^{206}/^{207}$Pb and Pb_{total}. Soils with lower concentrations of Pb have isotopic ratios closer to $Pb_{geogenic}$ whereas soils with higher concentrations of Pb (e.g. Ng4 and Ng12) were closer

to the Pb_{petrol} end member. A similar relationship was reported by Shetaya et al. (2018) in soils collected from Egypt.

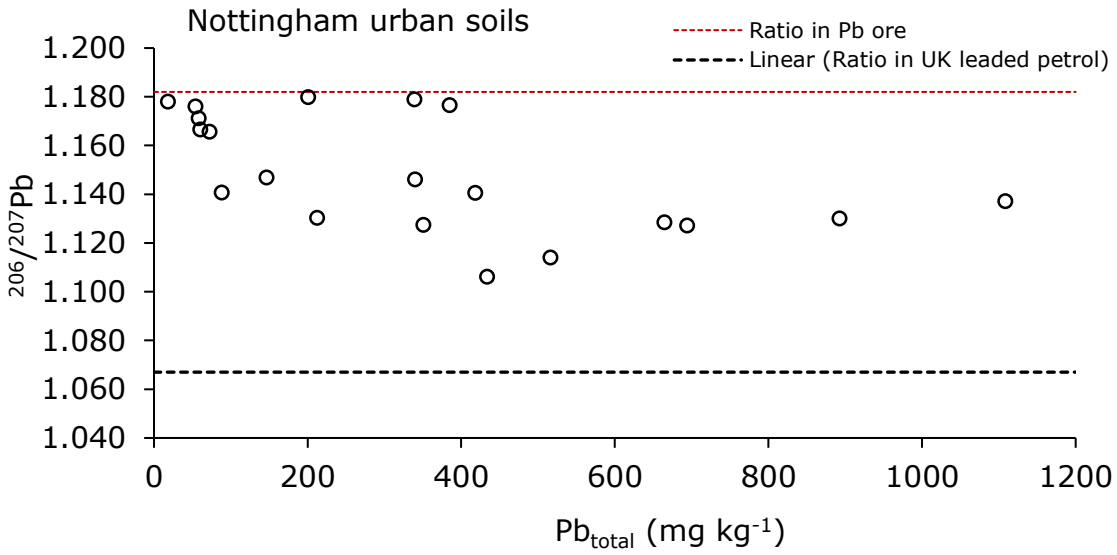


Figure 4.4: Relationship of Pb_{total} versus isotope ratio $^{206}/^{207}Pb$ in Nottingham urban soils.

Leaded gasoline was a primary source of Pb during the last century, but was phased out in most countries by 2000 (Nriagu, 1990, Oudijk, 2010). The Pb derived from petrol still remains in soils and has been reported in many different studies (Marzouk et al., 2013b, Mao et al., 2014). The contribution of Pb_{petrol} to Pb_{total} is shown in Figure 4.5 and ranges from >65% in a domestic garden (Ng5) to <5% in a football field (Ng1). Sites previously identified as having significant trace element contamination (Ng11, Ng12, Ng14 and Ng15) also have greater proportions of Pb_{petrol}.

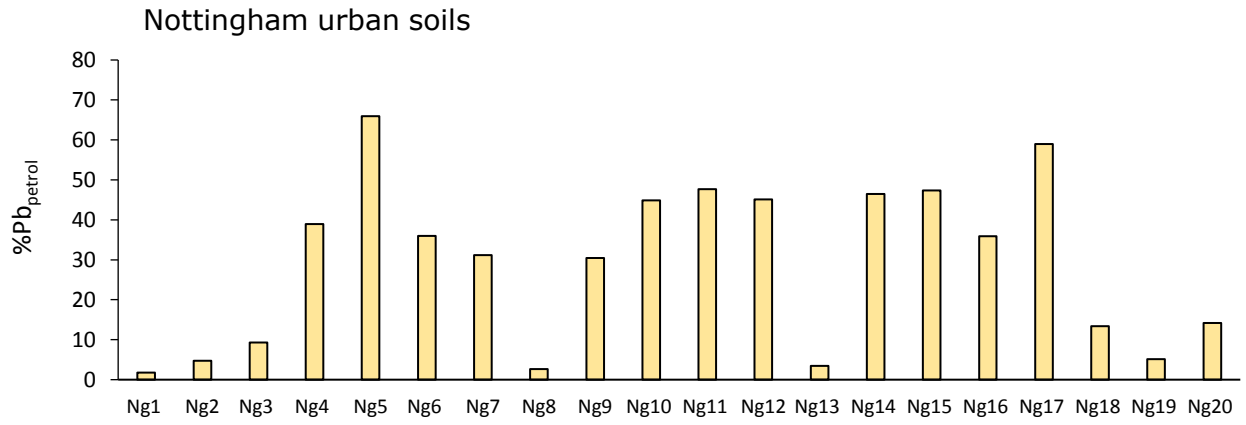


Figure 4.5: Proportion of Pb_{petrol} in Nottingham urban soils

4.4.2 Wolverhampton urban soils

4.4.2.1 Major and trace element concentrations in Wolverhampton soils

Mean concentrations of major and trace elements are presented in Table A1 (see Appendix A) and locations of individual sites are given in Table 4.2 (after Mao (2014). Trace elements concentrations were compared to NBCs (Figure 4.6). Concentrations were greatest on waste ground that had formerly been a landfill site (Wv6). In the UK up to 90% of waste from domestic and industrial activities has in the past been disposed of to landfill (Bridge et al., 1997). Elevated concentrations of Cu, Zn, Pb, Ni, Cd, Cr and As were also observed on parkland (Wv3), grassland (Wv7), former industrial sites and old gas works (Wv5), site of a former tyre factory (Wv10) and a nature reserve close to a railway (Wv14).

Table 4.2: Location of Wolverhampton soil sampling sites

Sites	Land use	Grid ref
Wv1	Grassland (Golf course)	391030 301170
Wv2	Grassland (Golf course)	388450 300860
Wv3	Park	393690 297700
Wv4	Grassland (open land)	392180 297280
Wv5	Old industrial (gas work)	393730 296530
Wv6	Wasteland (old landfill)	394490 295160
Wv7	Grassland	394960 295960
Wv8	Woodland	397060 296980
Wv9	Grassland	390170 301290
Wv10	Old industrial (tyre factory)	391330 301090
Wv11	Domestic garden	390810 296710
Wv12	Grassland	388240 295750
Wv13	Park	392760 295760
Wv14	Nature reserve (railway)	392830 299710
Wv15	Nature reserve (railway)	388910 299580
Wv16	Vegetated colliery spoil heap	392380 295460
Wv17	Old industrial (disused factory)	391240 297580
Wv18	Grassland (not maintained)	395120 299290
Wv19	Grassland	395150 299140
Wv20	Grassland	396720 301130
Wv21	Brownfield	393960 299860
Wv22	Brownfield	394390 299860
Wv23	Brownfield	395400 299670
Wv24	Brownfield	394680 299830
Wv25	Grassland (park)	394210 298970
Wv26	Grassland	394600 298750
Wv27	Brownfield	392800 298520
Wv28	Brownfield	391700 310630
Wv29	Deciduous woodland	391680 300080
Wv30	Grassland (park)	391780 300120

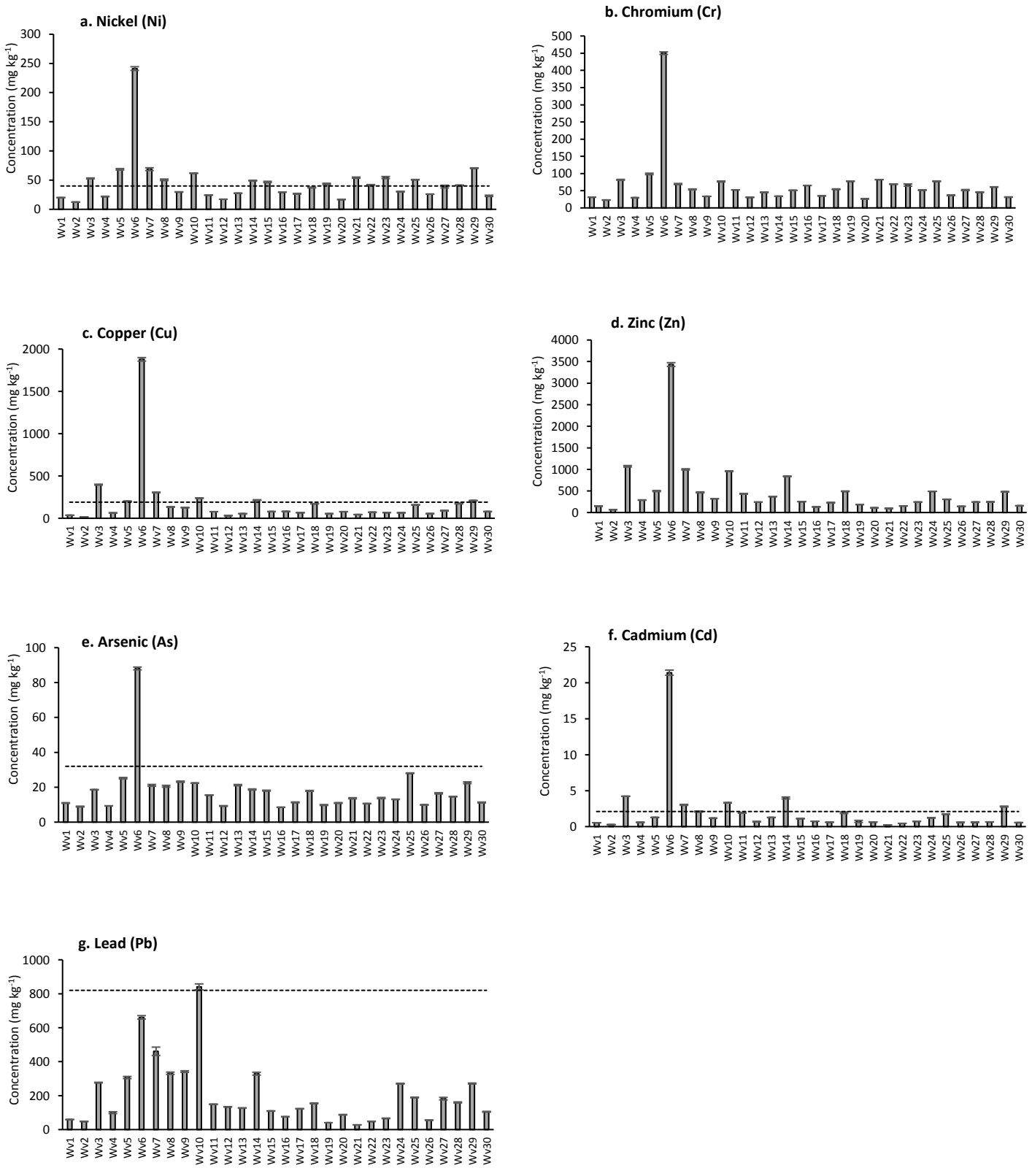


Figure 4.6: Concentration of different trace metals (a) Ni (b) Cr, (c) Cu, (d) Zn, (e) As, (f) Cd and (g) Pb in soils collected from different sites of Wolverhampton. Vertical bars denotes the average plus/minus the standard error and dashed line shows the normal background concentration values (NBCs).

4.4.2.2 Cluster Analysis

The influence of anthropogenic sources was revealed in the cluster analysis of Wolverhampton soils (Figure 4.7). Three sub-groups of elements were observed in the first cluster. The first sub-group consisted of Pb_{petrol} and $Pb_{geogenic}$ with Sb closely grouped with Sn, Be, Co, Se, Mo and Fe. Elements including As, Cu, Cd, Zn, and Cr were closely clustered in a separate sub-group. Together these two sub groups contain elements typically arising from anthropogenic activities. The third sub-group consisted mainly of group II elements such as Mg, Ca and Sr. The second cluster comprises elements including K, Rb, Li, Al, and Cs suggesting natural sources such as clay or other aluminosilicate minerals.

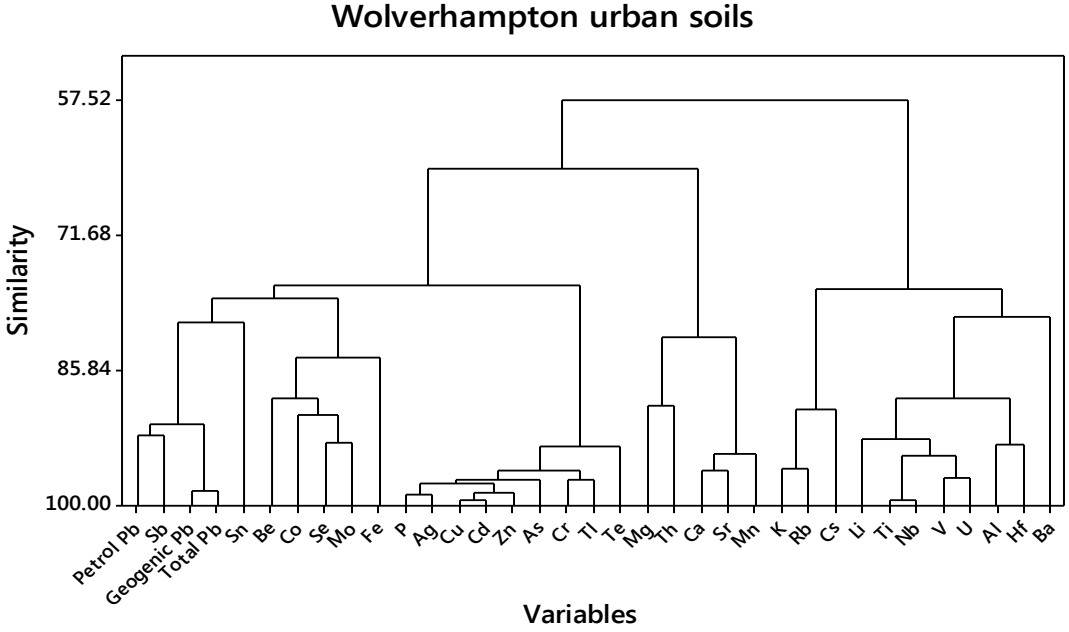


Figure 4.7: Dendrogram of elemental analysis in Wolverhampton urban soils.

4.4.2.3 Wolverhampton urban soils: Pb isotopic composition and source apportionment

Binary plots for Wolverhampton urban soils are shown in Figure 4.8. All samples sit close to a mixing line between Pb_{petrol} and $Pb_{geogenic}$ end members with $^{206}/^{207}Pb$ and $^{208}/^{207}$ Pb ratio values in the range between 1.12-1.19 and 2.40-2.47 respectively. In contrast to the Nottingham urban soils no relationship was observed between $^{206}/^{207}Pb$ and Pb_{total}, possibly suggesting a more complex mixture of Pb originating from a wide variety of sources (Figure 4.9).

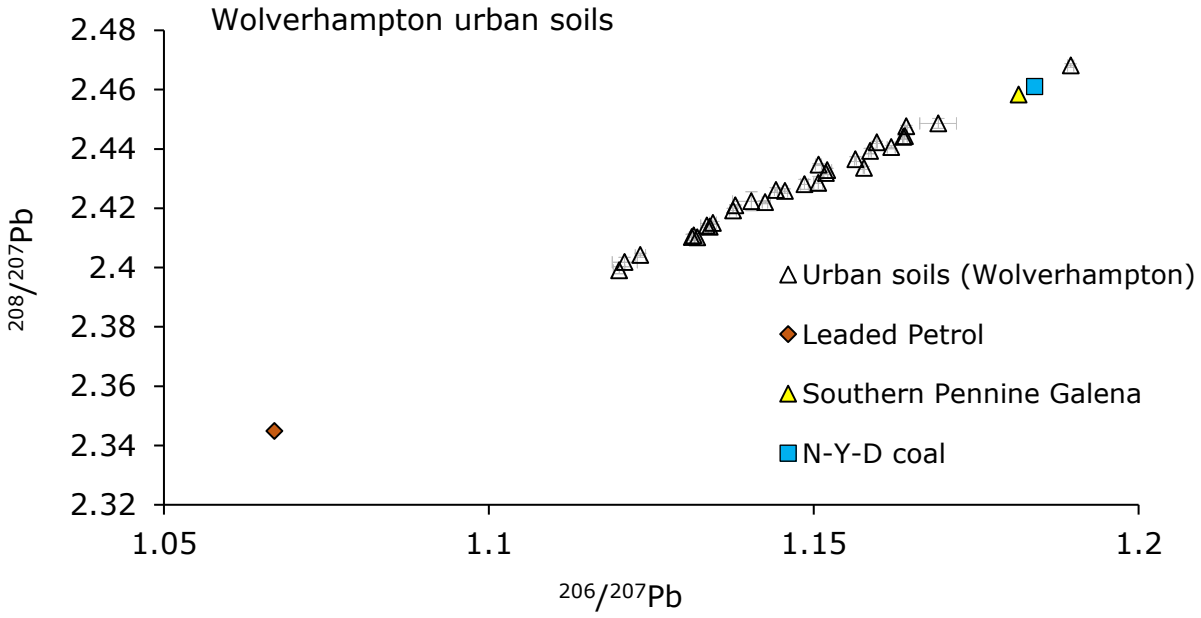


Figure 4.8: Binary plot for Wolverhampton urban soils. Median values of UK leaded petrol, Southern Pennine Pb ore (Galena) and Nottinghamshire-Yorkshire-Derbyshire (N-Y-D) coal shown as end members.

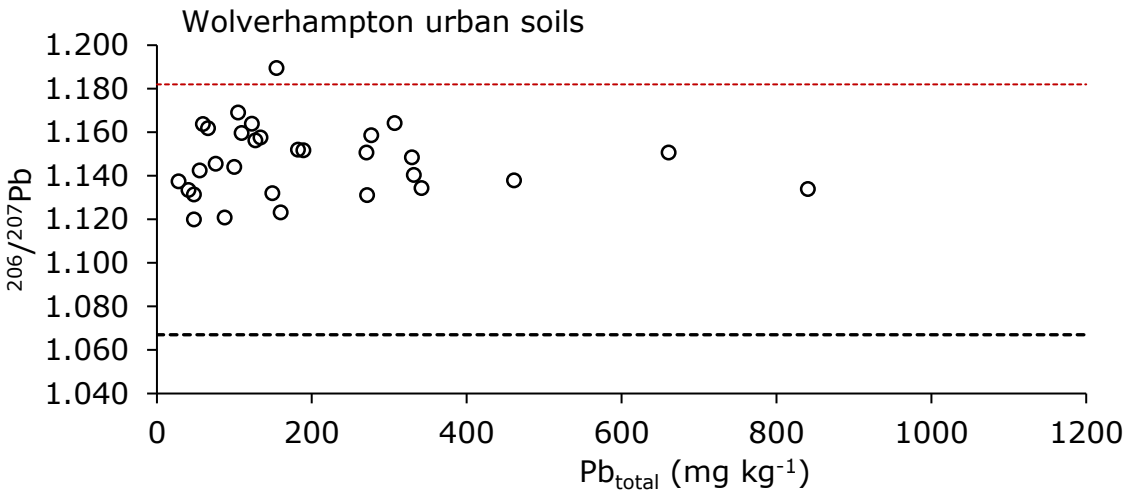


Figure 4.9: Relationship of Pb_{total} concentration with isotope ratio $^{206}/^{207}Pb$ in Wolverhampton urban soils.

The proportion of Pb_{petrol} calculated is similar to that observed in Nottingham with most samples in the range 10-55% (Figure 4.10). Sites where the greatest trace element concentrations were observed all have >30% of Pb_{petrol}. The remaining sites all have > 10% of Pb_{total} derived from petrol sources with the exception of one brownfield site (Wv21).

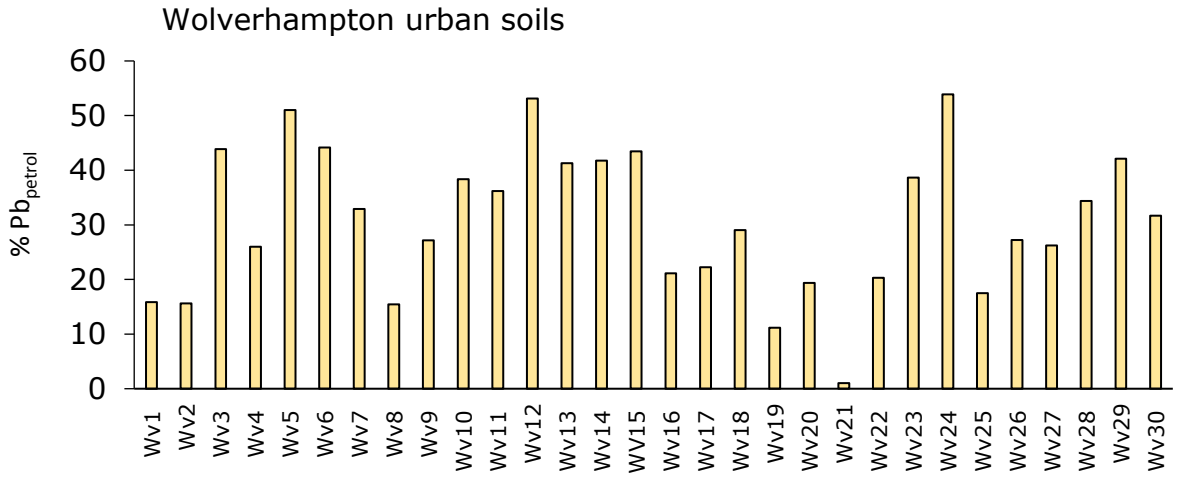


Figure 4.10: Proportion of Pb_{petrol} in Wolverhampton urban soils.

4.4.3 Pakistan sewage amended soils

Pakistan is a developing country with environmental challenges associated with an imbalance between economic and social development in recent decades. Emerging industrialization (fossil fuel burning) along with rapid urbanization (traffic and municipal waste) are important factors responsible for elevating trace element concentrations. Combustion of biomass, diesel oil, coal and furnace oil in residential areas are considered to be a severe threat to the urban environment (Waheed et al., 2006, Waseem et al., 2014).

Sewage sludge produced from industrial and municipal wastewater treatment consists of a mixture of organic compounds, macronutrients, microorganisms, organic micro pollutants, essential and non-essential trace metals (Jamali et al., 2008). Due to its high organic matter content and substantial N and P concentrations, it is considered a cost-effective fertilizer (Logan et al., 1997). However long term application can result in environmental and soil health problems as the industrial and municipal inputs are a common source of toxic elements that are then applied to agricultural land (Baveye et al., 1999, Qadir et al., 2000, Singh et al., 2004, Mapanda et al., 2005, Kadir et al., 2008). In most of developed countries, there is proper treatment of sewage sludge in order to improve its quality prior to its application to land. Like most developing countries, in Pakistan no substantive treatment of sludge occurs. Due to a lack of central policies and the cost of sewage treatment, untreated sewage and waste water is commonly used for irrigation in many urban and sub-urban areas of Pakistan, where vegetables and cereal crops are grown (Jamali et al., 2008). In total untreated sewage is estimated to be used as a fertilizer for irrigation of around 32,500 ha of land (Murtaza et al., 2010, Ensink et al., 2004).

Leaded gasoline was a major source of Pb in the urban environment of Pakistan and was identified as a potential public health problem as long ago as 1988 (Kadir et al., 2008). In 1991, the concentration of Pb reported in Pakistani leaded gasoline was the highest amongst Asian countries at 1.5–2.0 gL^{-1} and in the period 1993-1996 the reported Pb concentration in gasoline was >0.4 gL^{-1} (Murley, 1991). In 2001, the Government of Pakistan encouraged all the main refineries within the country to phase out Pb from gasoline. This commenced in October, 2001 and was completed in July, 2002 (Kadir et al., 2008).

In developing countries few studies have attempted to source apportion pollutants, typically the main focus of investigation has been to establish the total concentrations of potentially toxic elements (PTEs). No study has previously used Pb isotope ratios as tracers of Pb pollutants in Pakistan. Previous studies on Pb have been focused on determination of Pb-exposure using biomarkers such as blood, hair and nails (Eqani et al., 2016a). A recent study conducted by Ahmad et al. (2018), highlighted high levels of Pb-exposure among automobile technicians from selected towns in Khyber Pakhtunkhwa, Pakistan. Mean Pb concentrations determined in blood, hair and nails were 65.3 μg dL^{-1}, 23.6 mg kg^{-1} and 29.7 mg kg^{-1} respectively and overall 52% of the automobile technicians had blood levels higher than 50 μg dL^{-1}. In a study by Hozhabri et al. (2004) Pb levels in children's blood in the city of Karachi were above >10 μg dL^{-1} and were linked to urban activities, application of surma (a traditional eye-make-up), parental illiteracy, paternal Pb exposure at the workplace and hand-to-mouth activity. Similarly Eqani et al. (2016b) identified substantial Pb-exposure from dust in Islamabad and Swat. Lead levels from sites in Islamabad were slightly higher than those of Swat and a Hazard Index (HI) calculated for different age groups were above unity in industrial and urban areas.

This study is the first investigation of the isotopic composition of sewage amended soils collected from some of the largest cities of Southern Punjab after the phase out of leaded gasoline in Pakistan.

4.4.3.1 Concentrations of major and trace elements in sewage amended soils from Pakistan

Mean concentrations and ranges of selected elements are shown in Table A2 (see Appendix A) and Figure 4.11 for sewage amended soils from Gujranwala (GW), Gujrat (GT), Lahore (LH) and Faisalabad (FB). Concentrations of Cr, Ni, Cu, Cd, Zn, Pb and As were not normally distributed and were therefore transformed using Box-Cox transformation to reduce the skewness of data. Tukey analysis was used to make comparison between heavy metals concentrations at different districts.

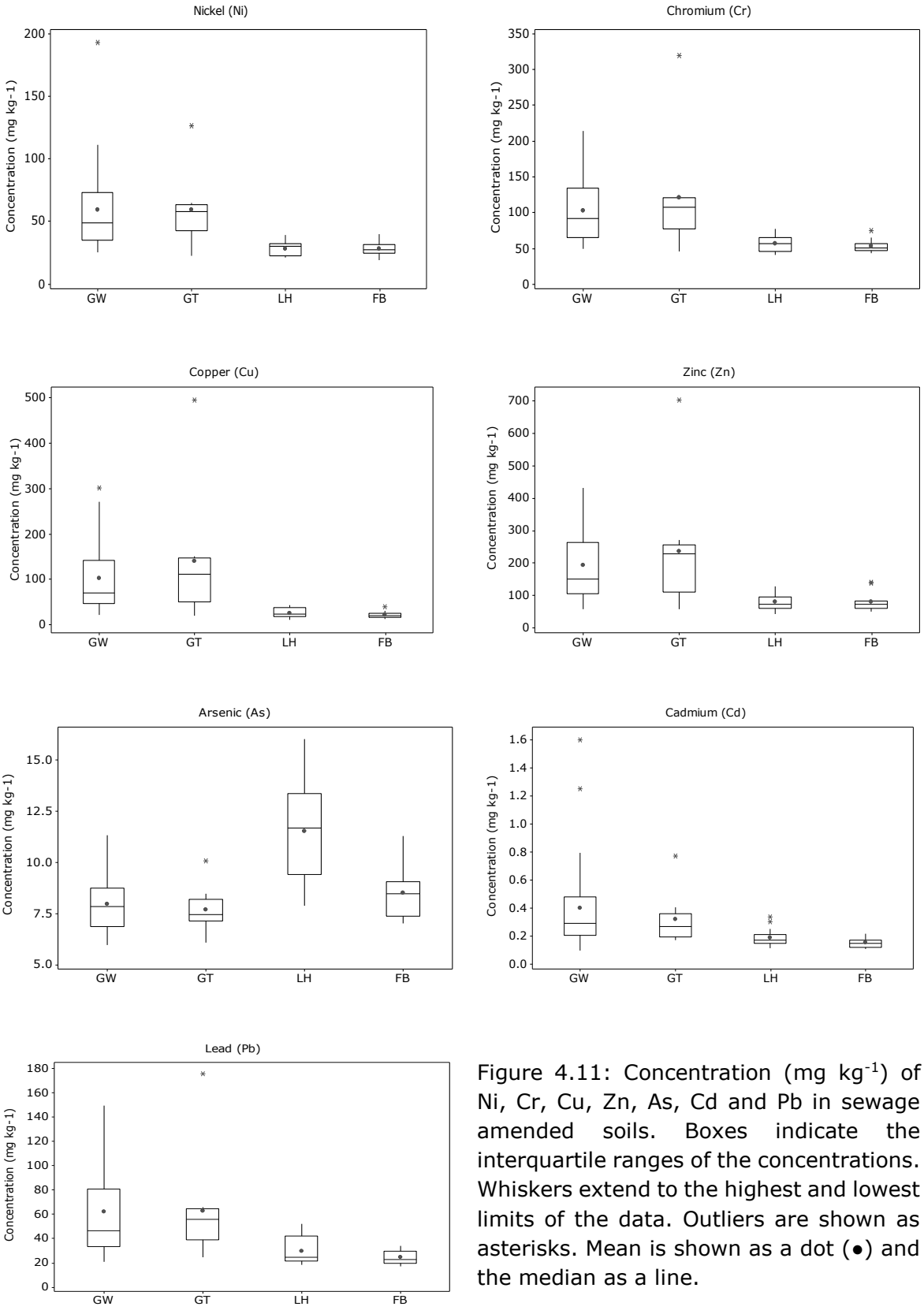


Figure 4.11: Concentration (mg kg^{-1}) of Ni, Cr, Cu, Zn, As, Cd and Pb in sewage amended soils. Boxes indicate the interquartile ranges of the concentrations. Whiskers extend to the highest and lowest limits of the data. Outliers are shown as asterisks. Mean is shown as a dot (●) and the median as a line.

The range of concentrations of Ni, Cu, Cr, Zn, As, Cd and Pb in GW and GT districts were similar. Nickel, Cr, Cu, Zn, Cd and Pb have similar concentrations in LH and FB but were different from those in GW and GT (p=0.000). Arsenic concentrations in LH were higher (i.e., 11.5 mg kg^{-1}) and significantly different (p=0.000) from the other three districts. Mean Cr, Cu and Zn concentrations exceeded threshold values (100, 100 and 200 mg kg^{-1} respectively) set by the European Commission (EC-DG, 2009) in some districts. Further comparison of the concentration ranges for the different trace metals (i.e., Ni, Cr, Cu, Zn, As, Cd and Pb) in Pakistan sewage amended soils with sewage sludge samples collected from Nottingham (e.g. Ng14 and Ng15; section 4.4.1.1) revealed that in the UK sewage samples the concentration of trace metals was higher more likely as a result of a longer history of industrialization.

4.4.3.2 Cluster Analysis

Cluster analysis is shown in Figure 4.12. There were two main groups, within group I three sub-groups were observed. In sub-group (i) Pb_{petrol} and $Pb_{geogenic}$ were closely clustered with Sn, Cr, Cu, Zn, Sb, Ni and Mo. The other sub-groups were (ii) P, Ag, Se, U and (iii) Mg, Ca, Sr, Ti, Nb, Hf. Most elements in group I appear to originate from anthropogenic sources and may be a result of pollutant release from industrial sites in GW, GT, LH and FB districts including textile, leather, electroplating, steel re-rolling, ceramics, fabrication and consumer industries (Rehman et al., 2008). Waste water and effluents are directly disposed to rivers and streams or are used in suburban areas for irrigation in order to increase the yield of crops (Kunhikrishnan et al., 2012) providing a source of contamination to agricultural land (Qadir et al., 2000, Singh et al., 2004, Mapanda et al., 2005). Fertilizers and foliar spray are also applied to correct nutrient deficiencies and may enhance concentrations of e.g. U, over long timescales (Jones and Jarvis, 1981).

Elements clustered in group II are most likely of natural origin and related to clay and oxide minerology.

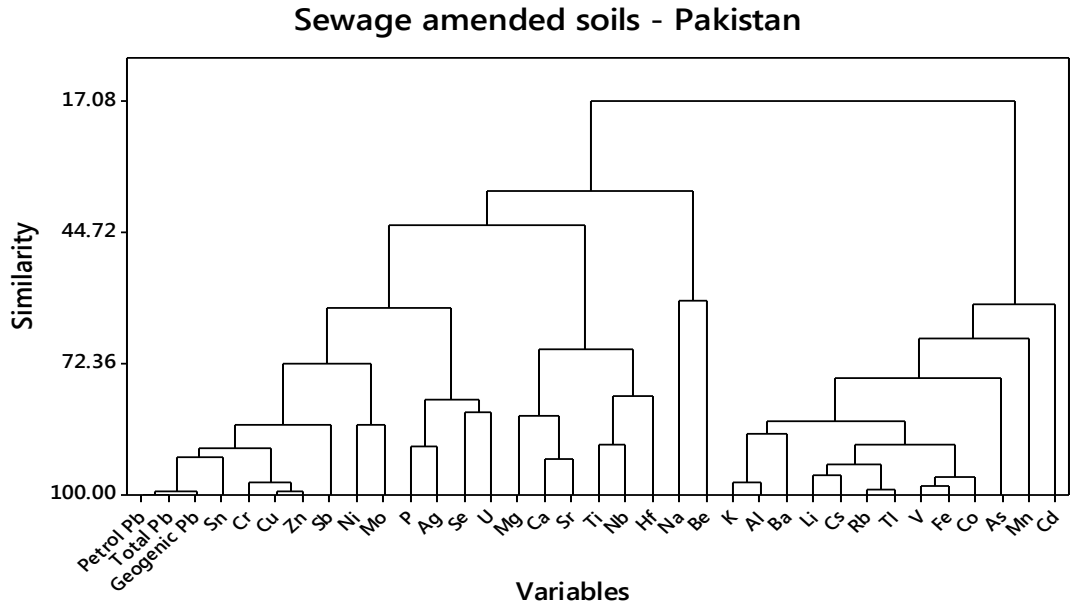


Figure 4.12: Dendrogram of cluster analysis of elements in Pakistan sewage amended soils.

4.4.3.3 Isotopic characterisation of Pb in Pakistan sewage amended soils and source apportionment

A Pb isotope binary plot is given in Figure 4.13 with upper continental crust and Australian ore 'end-members'. The two major suppliers of alkyl-Pb for the production of leaded petrol use Pb ores from either the Broken Hill type deposits in Australia or the Mississippi Valley type Pb deposit in USA (Bollhöfer and Rosman, 2001). In Pakistan Associated Octel supplied the Pb additive which was used in gasoline by most of the refineries until 2001. The ore to make the Pb additive was from Australia and therefore, Australian ore is used here as a proxy for Pb_{petrol}. Average upper continental crust isotopic signature (UCC) is used as a proxy for geogenic source (Millot et al., 2004). The range of isotopic signature of Pb

($^{206}/^{207}$Pb) in soils from different districts are shown in Figure 4.14. The Pb isotopic signature of most soils falls on, or close to, the mixing line between the end members but typically closer to the geogenic end member.

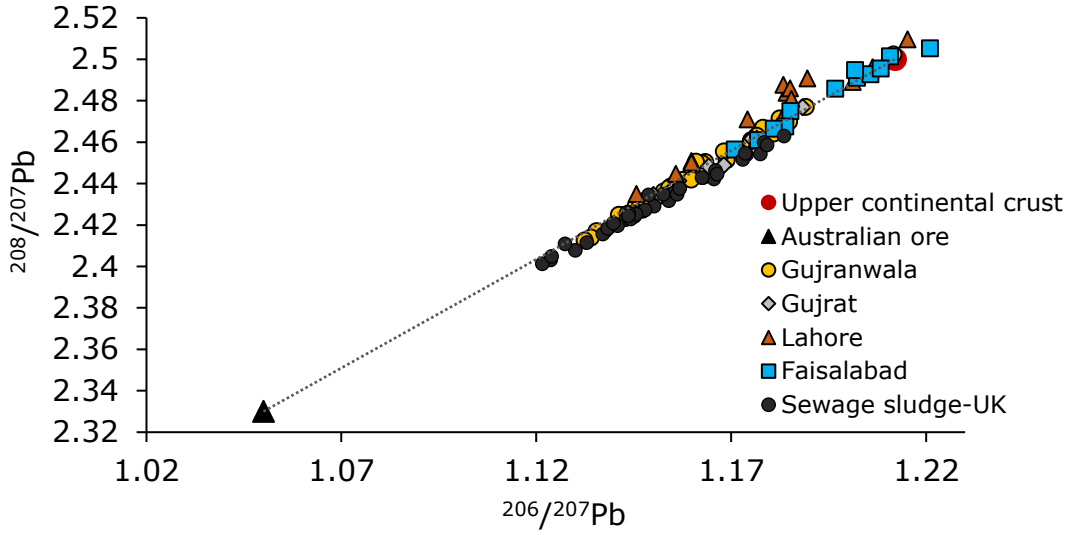


Figure 4.13: Binary plot of isotopic ratios $^{206}/^{207}$Pb vs $^{208}/^{207}$Pb for sewage amended soils.

In Figure 4.13 comparison is also made with sewage amended soils (n=38) collected from a sewage processing farm (Nottinghamshire, UK). The sewage amended soils from UK were plotted on the same graph with the same members because in past UK also imported Australian ore which was mainly used in the leaded gasoline (Sugden et al., 1993). The isotopic composition of these soils overlaps with the sewage amended soils from Pakistan. In particular a similar range of isotopic composition is observed when soils from GW and GT districts are compared with the UK soils. The mean proportion of Pb_{petrol} in the UK soils was slightly higher (27%) than the mean for all districts in Pakistan (25%). It has been previously reported by Atkinson et al. (2011a), that sewage farm soils have a more mixed Pb isotopic signature and are contaminated from Pb_{petrol} from recent inputs including road run-off.

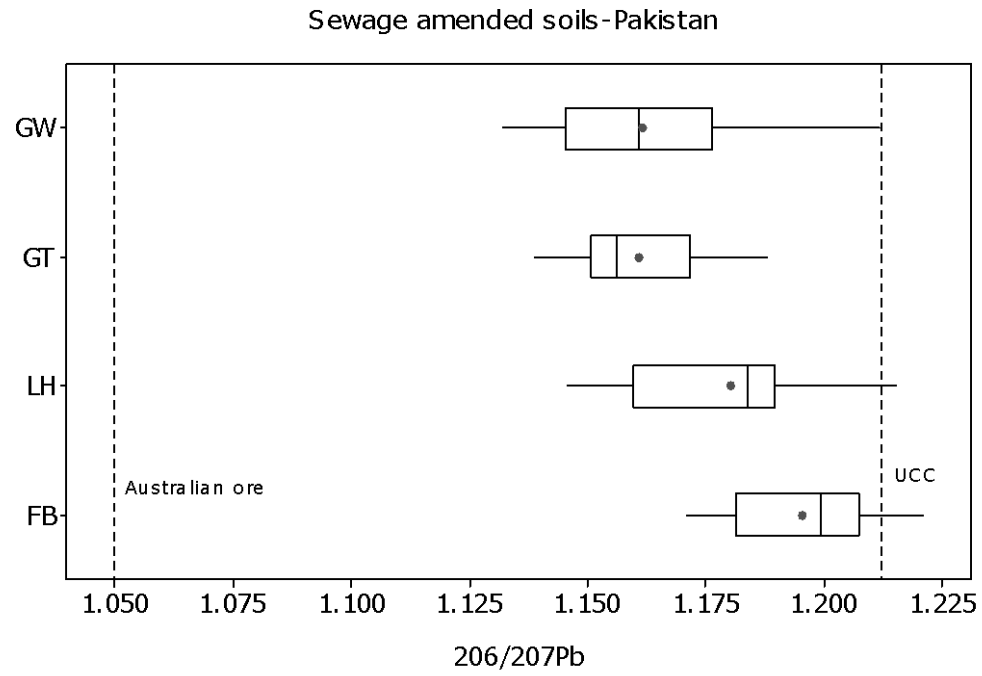


Figure 4.14: Lead isotopic ratio $^{206}/^{207}$Pb in sewage amended soils of different districts of Pakistan. Mean is shown as a (●) and median as a line. Broken lines indicate the range of reference sources (Australian ore as a proxy for Pb_{petrol} and UCC for $Pb_{geogenic}$).

The relationship of $^{206}/^{207}$Pb ratio with Pb_{total} for soils collected from the different districts is shown in Figure 4.15. A significantly strong correlation of $^{206}/^{207}$Pb and Pb_{total} was observed in all districts; GW (-0.874, $p=0.000$), GT (-0.782, $p<0.05$), LH (-0.858, $p=0.000$) and FB (-0.952, $p=0.000$). Soils with lower concentrations of Pb had Pb isotopic ratios closer to the $Pb_{geogenic}$ whereas soils with higher concentrations of Pb were more inclined towards the Australian ore isotopic composition.

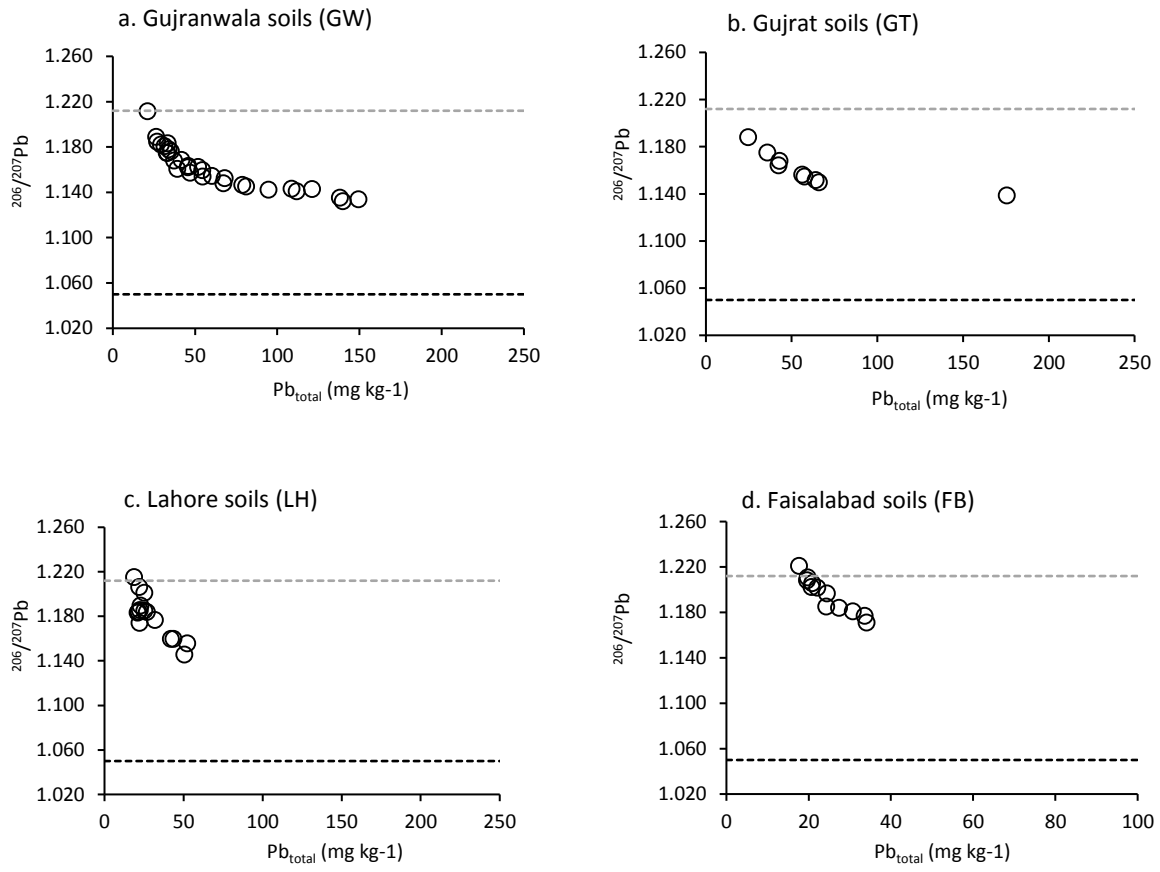


Figure 4.15: Relationship of Pb_{total} concentration and isotope ratio $^{206}/^{207}Pb$ in Pakistan sewage amended soils from different districts (a) GW (b) GT (c) LH and (d) FB. Grey and black dashed lines represents the ratios in UCC and Australian ore respectively.

Most of the soils were contaminated with Pb_{petrol} (Figure 4.16). The average proportion of Pb_{petrol} calculated in GW and GT sewage soils was similar at 31%, in LH it was 20% and in FB 11%. This demonstrates that although leaded-gasoline is no longer a legacy remains particularly in LH and FB soils.

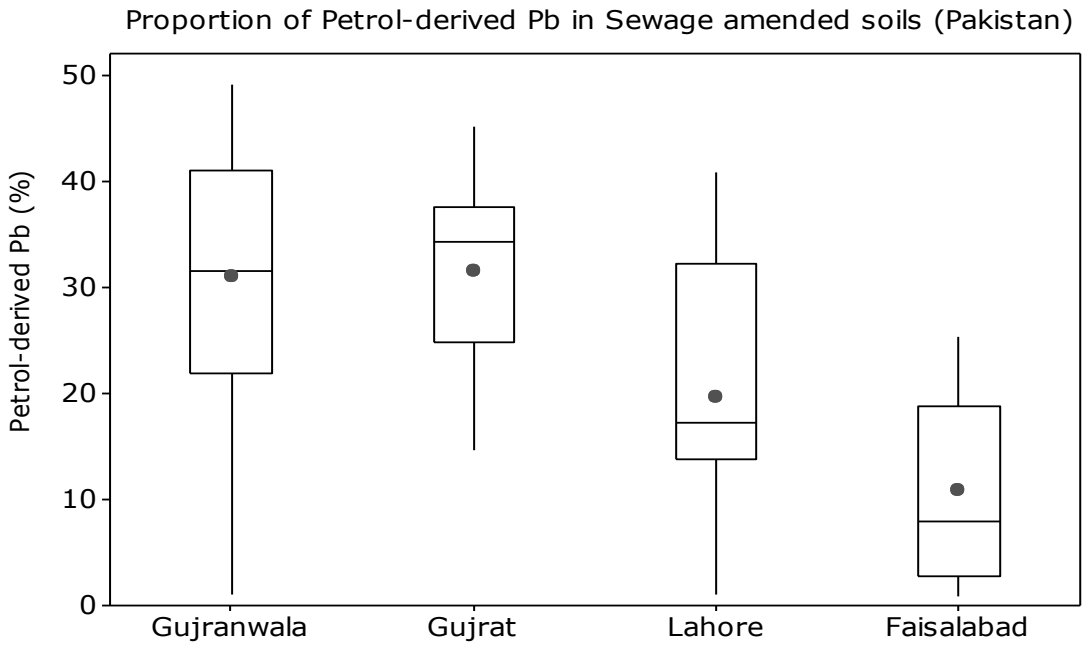


Figure 4.16: Proportion of Pb_{petrol} in Sewage amended soils

4.5 Conclusions

In urban soils from Nottingham, Wolverhampton (UK) and sewage amended soils (Pakistan) variation in trace element concentrations were mostly attributable to a combination of land use, a legacy of historical contamination and recent pollution sources. Cluster analysis in combination with source apportionment of Pb into petrol and geogenic forms was helpful in revealing a combined influenced of multiple anthropogenic sources (e.g. industrial and traffic emissions, waste disposal) and a natural background. Determination of isotopic ratios was helpful in characterizing Pb isotopic signatures with regards to assumed end-members and it confirmed that Pb_{petrol} and $Pb_{geogenic}$ were the dominant sources of Pb in these soils. Samples with greater concentrations of Pb_{total} were also more influenced by Pb_{petrol}.

The approaches used in this chapter were to some extent helpful in identifying generic sources but they were unable to help in the unique identification of individual contaminant sources. To develop this forensic approach further additional information is required. Considering a greater range of trace element signatures e.g. REEs or PGEs might provide information that will assist in improving the identification of specific sources. For example REEs are increasingly used in modern technology e.g. in mobile phones (Hurst, 2010) and the REEs signature of petrol is known to differ depending upon the source of the crude oil from which it originated (Olmez and Gordon, 1985). Release of PGEs into the environment is mainly associated with the use of catalytic convertors in car exhaust systems (Moldovan et al., 2002).

5 Chapter 5: Identification of contaminant sources in urban allotment soils

5.1 Introduction

In gardens and allotments a range of pollutants arise from agronomic operations, such as application of pesticides, fungicides, organic and inorganic manure, biosolids (sewage sludge) and fertilizers over extended periods of time (Lau, 1994, Huang et al., 2006). In urban areas, soils are also affected by pollutants from industrial and transport activities depending on their location i.e., either in the city centre or in the suburbs. Allotments are commonly located near roadsides, railway lines, former or present industrial areas etc. (Bell et al., 2016). Key sources include a large range of present and past industrial activities, traffic emissions and waste disposal of various kinds. Sometimes contributions of trace elements from other sources can also occur due to site levelling, leisure activities and run-off water from roads (Alloway, 2004). Recently the increased demand for PGEs and REEs for a range of applications, mainly in catalytic converters, electronic industries and agriculture, has also resulted in accumulation of these elements in urban environments. These trace elements (including RGEs and REEs) may pose risks to humans and to the environment. Contaminants from these soils can easily come into contact with humans through direct contact or as a result of transfer through the food chain, drinking of contaminated water and re-suspension (re-deposition) of soil and dust (McLaughlin et al., 2000, Cui et al., 2005, Zhang et al., 2007).

Effective conservation and rehabilitation of soil ecosystems polluted by trace elements first requires quantification and characterization. Part of this process is determining the origin of dispersed contaminants - source apportionment. Soil characterization helps in providing information regarding trace elements speciation and bioavailability whereas source apportionment of pollutants is more associated with identifying the source (Kabata-Pendias, 2010). Environmental protection legislation often requires data that characterizes the chemical properties of pollutants especially those that are present in food products (Alexander et al., 2006, Wuana and Okieimen, 2011).

5.2 Objectives

For source apportionment of pollutants in soil, determination of the spectrum of trace elements present is important. In order to get a clearer picture about pollutant sources, it may be necessary to investigate more obscure elements, such as REEs and PGEs. Both REEs and PGEs have been increasingly used (e.g. industrial, transport and fertilizers) for the last few decades and are now reported to occur as contaminants in a range of environmental media. Therefore, one aim of this chapter was to extend determination of the more commonly measured range of elements to include REEs and PGEs in urban allotment soils. Objectives were to (i) determine a wide range of elements, in order to estimate the likely potential sources of pollutants by using cluster analysis and correlation, (ii) assess the crust-normalized pattern, enrichment factors and correlations among REEs to identify possible sources and (iii) investigate aspects of the analysis of PGEs using ICP-QQQ-MS techniques (i.e., He gas mode, $NH_{3(on\text{-}mass)}$ and $NH_{3(mass\text{-}shift)}$ gas modes) to optimise interference removal and accuracy (iv) characterize the isotopic signature of Pb ($^{206}/^{207}$ Pb

and $^{208}/^{207}$Pb) to investigate the relative contribution of Pb_{petrol} and $Pb_{geogenic}$ in the urban allotment soils.

5.3 Materials and methods

5.3.1 Soil sampling

A set of urban allotments topsoil and subsoil samples (n=269) collected from 9 different allotment sites in Nottingham have been used in this chapter (more detail given in Chapter 2, section 2.2). The locations and descriptions of the sites are given in Table 5.1.

Table 5.1: Nottingham allotment sites and their descriptions

Allotment sites	Description	Latitude (N)	Longitude (W)
Old Park Farm (PF)	Railway line, near to Wollaton road (A609)	52°57′38.24″	1°13′18.23″
St Ann's (ST)	Oldest allotment, closer to city centre, near to major road (A60)	52°58′9.55″	1°8′7.64″
Canal (CN)	Railway line, near to Wollaton road (A609)	52°57′32.70″	1°12′7.34″
Mapperly (MP)	Closer to city centre	52°57′59.99″	1°8′53.37″
Moorfields (MR)	Railway line, closer to city centre and closer to Wollaton road (A609)	52°57′28.69″	1°11′20.22″
Blenheim (BH)	Relatively new allotment	53°0′39.30″	1°12′51.87″
Sneinton Dale (SN)	Closer to city centre, near to major road (A60) and near to the River Trent	52°57′18.20″	1°7′3.65″
Woodthorpe (WT)	Closer to Mansfield road	52°58′54.27″	1°8′21.61″
Windmill (WM)	Older allotment, closer to city centre and also near to the River Trent	52°57′7.82″	1°7′49.01″

Satellite views (Google Earth) of the nine allotment sites are given below; the major potential pollutant sources in close proximity to each allotment site are also highlighted.

a. Old Park Farm (PF)



b. St. Ann's (ST)



c. Canal (CN)



d. Mapperly (MP)



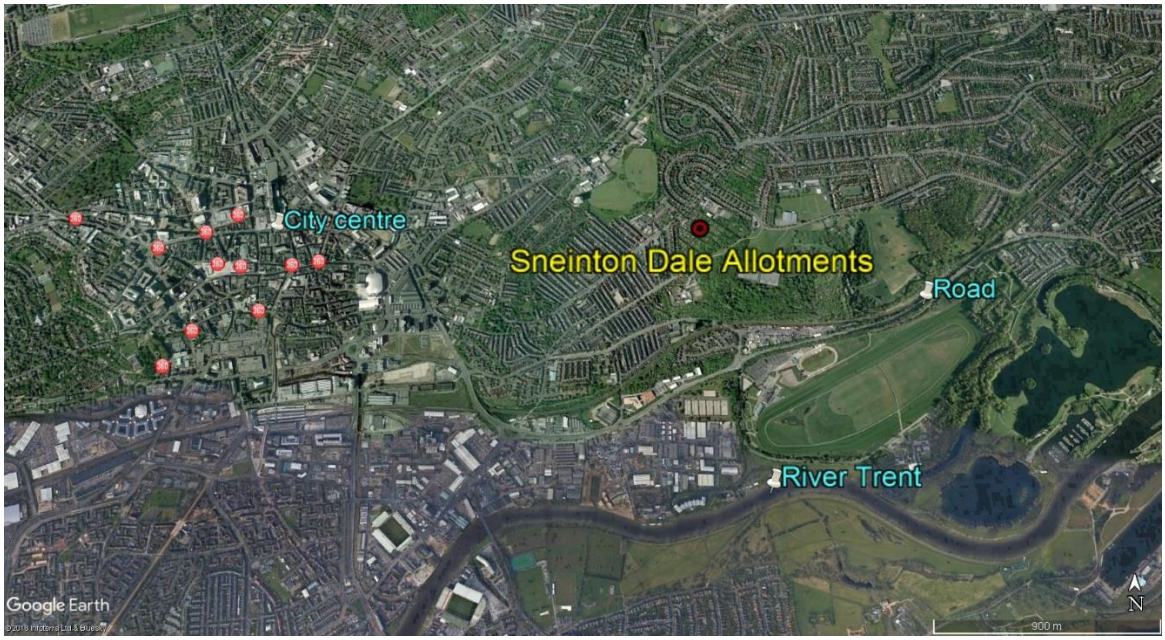
e. Moorfields (MR)



f. Blenheim (BH)



g. Sneinton Dale (SN)



h. Woodthorpe (WT)



i. Windmill (WM)



5.3.2 Sample analysis

The total concentrations of major and trace elements including the REEs in allotment soils were determined following a mixed acid (HF, $HClO_4$, HNO_3) digestion method. Soil digests were diluted prior to analysis using ICP-QMS in KED mode to remove interferences (details in Chapter 2, Section 2.7.1). Platinum group elements were analysed using an Agilent 8900 triple quadrupole instrument (ICP-QQQ-MS) at BGS Keyworth, using three different modes of operation: i.e., He, $NH_{3(on\text{-}mass)}$ and $NH_{3(mass\text{-}shift)}$ modes (details given in Chapter 2, Section 2.7.2.).

Isotopic abundances of Pb in Pb_{total} were measured according to the methodology described in Chapter 3. Also the relative contributions of Pb from different sources, particularly Pb_{petrol} and $Pb_{geogenic}$, were calculated according

to a simple binary mixture model, proposed by Monna et al. (1997) (Chapter 2 Section 2.8).

5.3.3 Statistical analysis for variation of heavy metals concentration between allotment sites

The variation in heavy metal/metalloid concentrations (Cr, Ni, Cu, Zn, As, Cd and Pb) among different allotment sites was investigated by analysis of variance (ANOVA; Minitab vs.17.2.1). Initially the normality of data was assessed using the Anderson-Darling method. Concentrations of Cr, Ni, Zn and As were normally distributed whereas concentration of Cu, Cd and Pb were positively skewed and were transformed using the Box-Cox transformation in order to reduce the skewness of data. In the ANOVA, Tukey analysis was carried out to establish the levels of significance of differences between different allotment sites.

5.3.4 Enrichment factors (EFs)

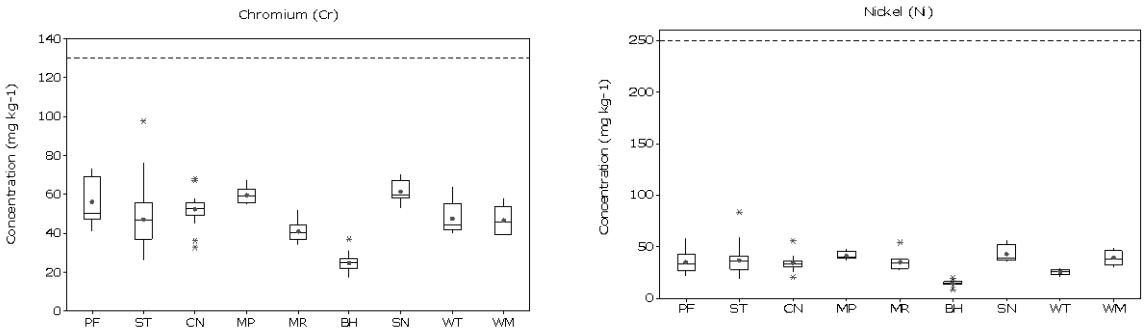
The EFs were calculated to assess the anthropogenic impact of the studied elements including REEs in the topsoil of different allotment. This approach is commonly used to estimate the heavy metals enrichment in soils. In this study EFs was calculated for all elements by dividing topsoil concentrations by their corresponding subsoils concentrations. In general, when an EF values are around or less than 1, it indicates depletion whereas EF values greater than 1 indicates elements enrichment in the soils. In case of REEs, the crust-normalized REEs patterns were also evaluated to estimate the enrichment of REEs relative to upper continental crust in topsoils.

5.4 Results and discussion

5.4.1 Major and trace element concentrations in allotment soils

The mean concentrations of major and trace elements, standard deviation and ranges (min and max) in top soils of different allotment sites are presented in Table A3 (see Appendix A). For some of the elements the larger standard deviation indicated heterogeneity between soils samples collected from the same sampling area. The concentrations of some of the most common heavy metals (Cr, Ni, Cu, Zn, As, Cd and Pb) are also shown as boxplots in Figure 5.1. The metal concentrations were significantly different ($p < 0.000$) between the different allotment sites (Two-way ANOVA).The mean concentrations of Cr, Ni and As in soils from different allotment sites were lower than the UK soil guideline values, SGVs (EA, 2009). Although the SGVs are now dated and are replaced in 2013 but they still have some validity as indicative of potential risks. The concentration of Cr was highest at site SN (61.7 mg kg^{-1}) and was lowest at site BH (24.8 mg kg^{-1}). The concentrations of Cr in the different allotments sites were in the following decreasing order: SN>MP>PF>CN>ST>WT>WM>MR>BH. Similarly the highest concentration of Ni was observed at site SN (43.1 mg kg^{-1}) and was lowest at site BH (14.8 mg kg^{-1}) and it followed the order: SN>MP>WM>PF>ST>MR>CN>WT>BH. In the case of As, the concentration was highest at site WM (21.5 mg kg^{-1}) and was lowest at site BH (9.7 mg kg^{-1}) and the concentration was in the following decreasing order: WM>MP>MR>CN>ST>SN>PF>WT>BH.The concentration of Cu and Zn were compared to the sludge (use in Agriculture) regulation values (1989) as there is no assessment criteria for Zn and Cu

from the EA. Some of the allotment sites were observed to exceed the threshold levels i.e 300 mg kg^{-1} for Zn. The highest concentrations of Cu and Zn were observed at sites MR (i.e., 92.3 and 443 mg kg^{-1} respectively) and WM (79.9 and 513.8 mg kg^{-1} respectively) and the lowest were observed at site BH (i.e., 31.4 for Cu and 116.3 mg kg^{-1} for Zn). The concentrations of Cu and Zn in different allotment sites followed the order: MR>SN>MP>WM>ST> CN> PF> WT> BH and WM>MR>MP>ST>CN>SN>PF>WT>BH respectively. The concentration of Cd was only elevated in approximately 25% of soil samples at site CN, whereas for other allotment sites the mean concentration of Cd was lower than the UK SGV (i.e., 1.80 mg kg^{-1}) and the mean Cd concentration at different allotment sites fell in the following order: CN>MR>WM>PF>ST>SN>MP>WT>BH. In the case of Pb, the mean concentrations in some of the soil samples from different allotment sites were also elevated above the UK SGV (i.e., 450 mg kg^{-1}). The highest mean concentration was found at site WM (620.7 mg kg^{-1}) and lowest at site BH (51.8 mg kg^{-1}) and concentration at different allotment sites followed the order: WM>ST>MR>MP>CN>PF>SN>WT>BH.



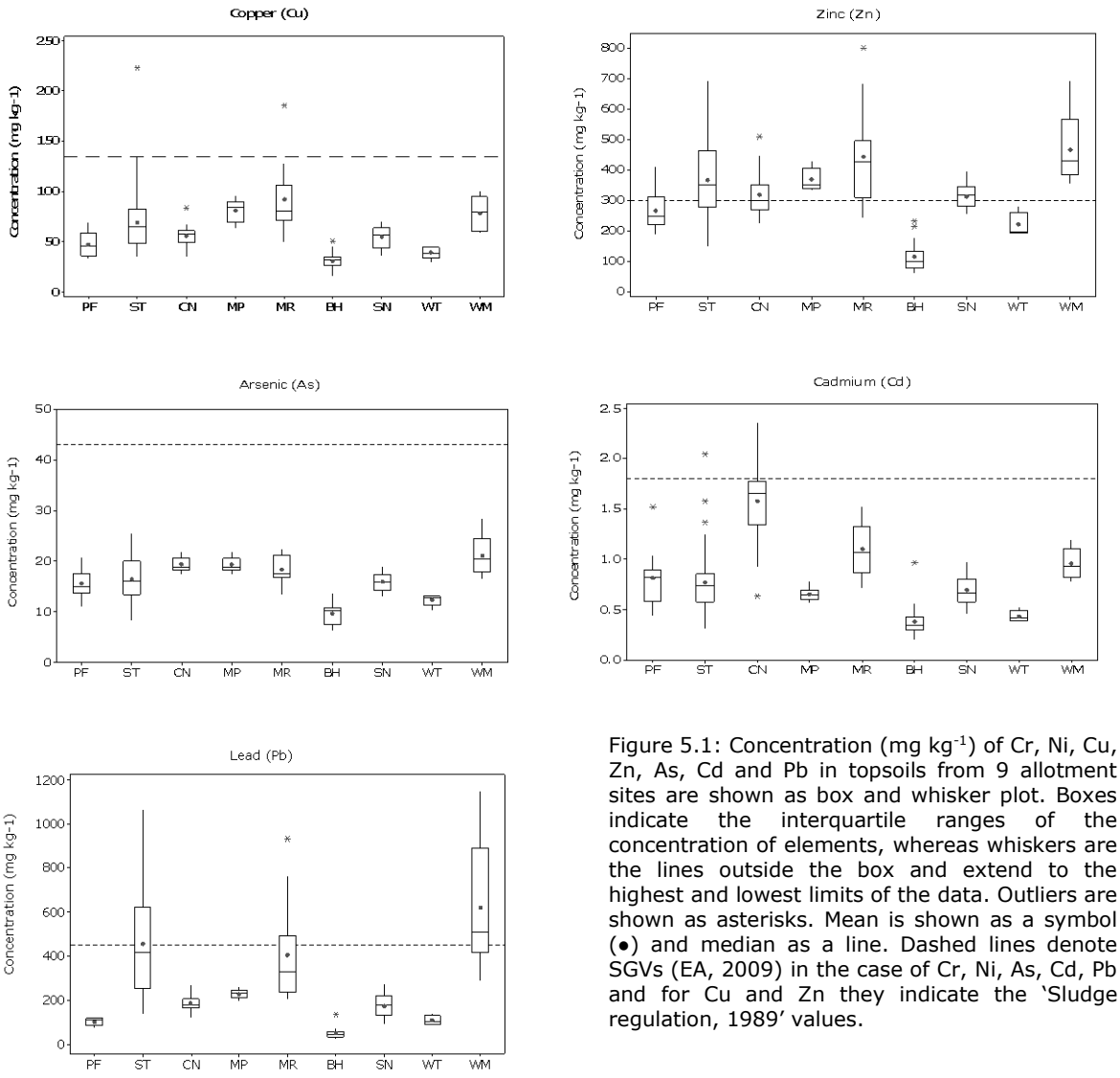


Figure 5.1: Concentration (mg kg^{-1}) of Cr, Ni, Cu, Zn, As, Cd and Pb in topsoils from 9 allotment sites are shown as box and whisker plot. Boxes indicate the interquartile ranges of the concentration of elements, whereas whiskers are the lines outside the box and extend to the highest and lowest limits of the data. Outliers are shown as asterisks. Mean is shown as a symbol (●) and median as a line. Dashed lines denote SGVs (EA, 2009) in the case of Cr, Ni, As, Cd, Pb and for Cu and Zn they indicate the 'Sludge regulation, 1989' values.

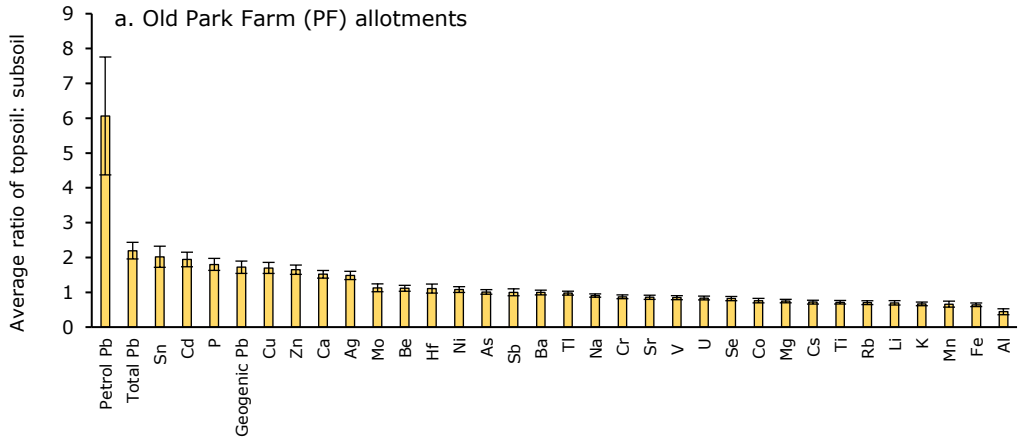
5.4.2 Enrichment factors (EFs)

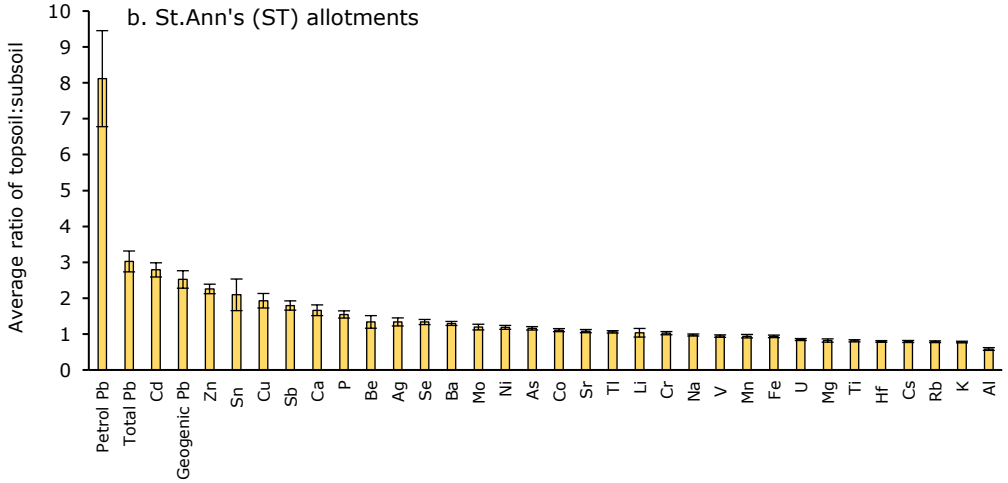
Enrichment factors can be used as an effective tool to distinguish metals originating from anthropogenic and natural sources in soils and to evaluate the degree of contamination from anthropogenic sources (Ye et al., 2011). Enrichment factors for individual elements were calculated by dividing the concentrations of elements in topsoils by their concentrations in the corresponding subsoils.

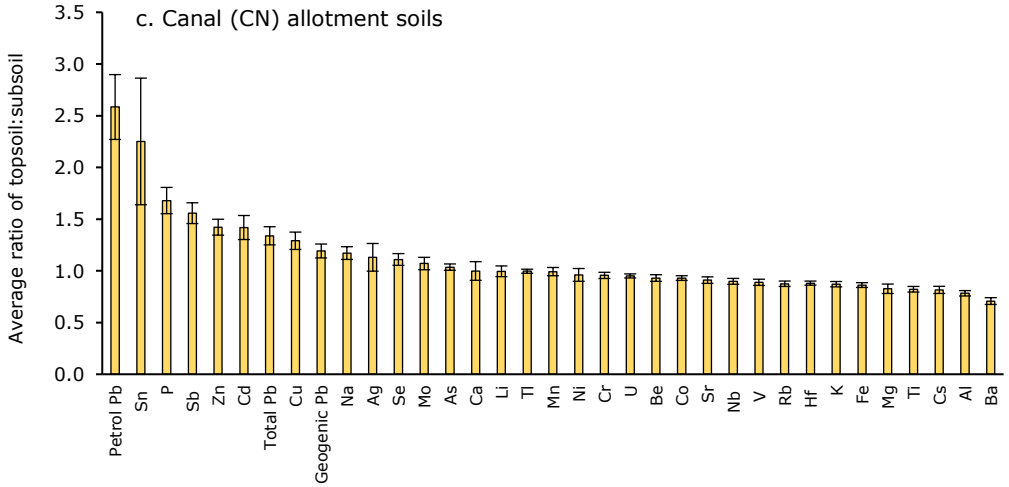
The average EFs for major and trace elements at each allotment sites are shown in Figure 5.2. It is considered that urban topsoils are usually more enriched with trace metals than subsoils due to intense anthropogenic activities. However, due to leaching effects and historic industrial or vehicular emissions deeper soil layers can also be contaminated with heavy metals (Luo et al., 2015). The range of EF values calculated for all sites (except site BH) suggested that typical urban elements such as Pb, Cd, Sn, Zn, Cu, Sb, Ag, Ca and P were more enriched in topsoils compared to subsoils. The enrichment of topsoils suggests that allotment soils had a combined influence from several sources such as vehicular and industrial emissions, coal burning and fertilizers application. The EF values also showed that Pb_{petrol} was more enriched in topsoils. In most of the allotment sites, the mean EF values calculated for Pb_{petrol} were in the range of 2.5 - 11.4 except at site BH where EF for Pb_{petrol} was 1.12. At different allotments, the variation among EFs for different elements may reflect differences in the site history and location. For example, BH was a new allotment site and is remote from major pollutant sources. Thus the mean EF values for most of the elements were closer to unity indicating that both topsoils and subsoils have approximately equal concentrations of these elements. By contrast, most of the allotments (PF, ST, CN, MP, MR, SN and WM) which were in close proximity to contaminant sources, such as main roads, the city centre, a railway line or industrial areas, were more highly enriched. Sites ST and WM were the oldest allotments so the enrichment of trace metals in these soils also suggested continuous accumulation of contaminants over many years (i.e., past historical contamination). Similarly the average EF calculated for $Pb_{geogenic}$ in most of the allotments was in the range of 2.0 - 5.6 except at site CN and BH where $Pb_{geogenic}$ in topsoils was

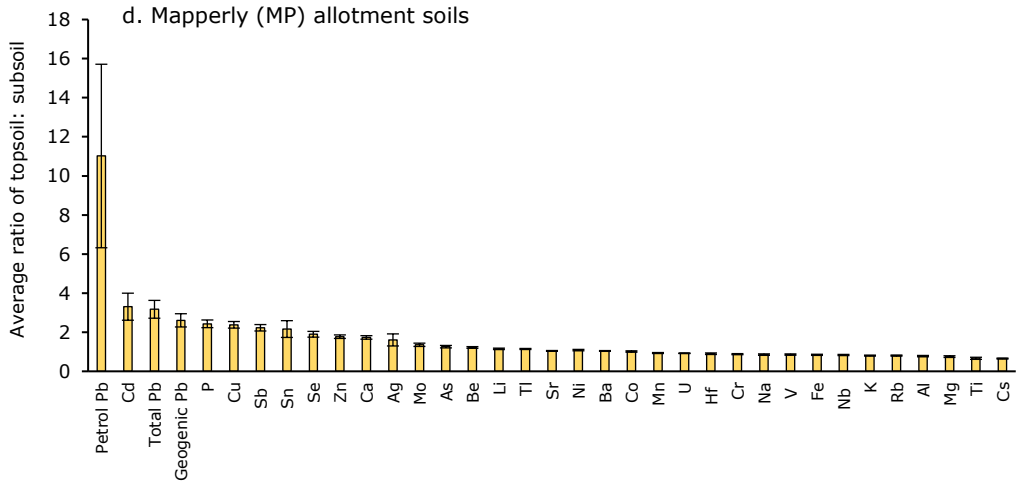
slightly enriched. Allotment site CN was closer to a railway line which would have been used for transportation of coal so these soils are likely to have a greater influence from $Pb_{geogenic}$ (mainly coal). It might also be possible that cultivation in allotments has reduced differences between topsoil and subsoil.

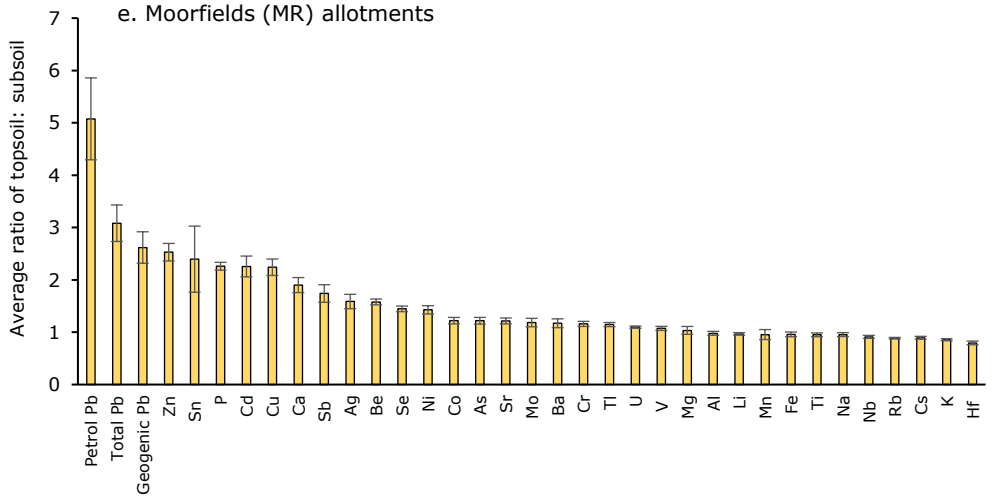
The relative contribution of Pb_{petrol} as compared to Pb_{coal} in topsoils (i.e., Pb_{petrol} /Pb_{coal}) was also calculated for all allotment sites. From the ratio values in Table 5.2, it could be concluded that in all allotment sites the contribution of Pb_{coal} to the soil Pb burden was greater than that of Pb_{petrol}. At site BH and CN, the ratio was lowest which indicated these allotments had the least influence from Pb_{petrol}. It is also important to mention that it was decided not to subtract subsoil values from topsoils to quantify the 'contaminant load' in topsoils because it was clear that the subsoils were not pristine and were substantially contaminated with both Pb_{petrol} and $Pb_{geogenic}$.

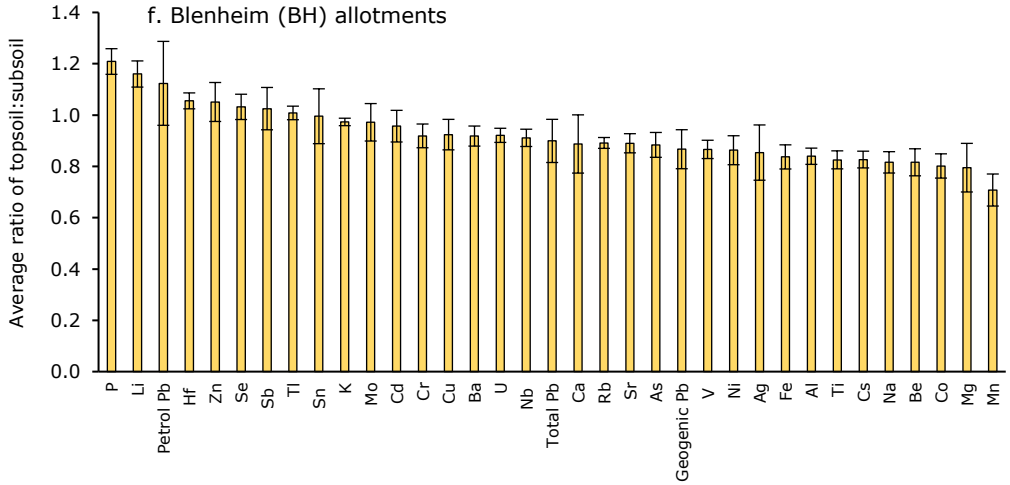

a. Old Park Farm (PF) allotments
Average ratio of topsoil: subsoil
0
1
2
3
4
5
6
7
8
9
Petrol Pb
Total Pb
Sn
Cd
P
Geogenic Pb
Cu
Zn
Ca
Ag
Mo
Be
Hf
Ni
As
Sb
Ba
Tl
Na
Cr
Sr
V
U
Se
Co
Mg
Cs
Ti
Rb
Li
K
Mn
Fe
Al


b. St.Ann's (ST) allotments
Average ratio of topsoil:subsoil
0
1
2
3
4
5
6
7
8
9
10
Petrol Pb
Total Pb
Cd
Geogenic Pb
Zn
Sn
Cu
Sb
Ca
P
Be
Ag
Se
Ba
Mo
Ni
As
Co
Sr
Tl
Li
Cr
Na
V
Mn
Fe
U
Mg
Ti
Hf
Cs
Rb
K
Al


c. Canal (CN) allotment soils
Average ratio of topsoil:subsoil
0.0
0.5
1.0
1.5
2.0
2.5
3.0
3.5
Petrol Pb
Sn
P
Sb
Zn
Cd
Total Pb
Cu
Geogenic Pb
Na
Ag
Se
Mo
As
Ca
Li
Tl
Mn
Ni
Cr
U
Be
Co
Sr
Nb
V
Rb
Hf
K
Fe
Mg
Ti
Cs
Al
Ba


d. Mapperly (MP) allotment soils
Average ratio of topsoil: subsoil
18
16
14
12
10
8
6
4
2
0
Petrol Pb
Cd
Total Pb
Geogenic Pb
P
Cu
Sb
Sn
Se
Zn
Ca
Ag
Mo
As
Be
Li
Tl
Sr
Ni
Ba
Co
Mn
U
Hf
Cr
Na
V
Fe
Nb
K
Rb
Al
Mg
Ti
Cs


e. Moorfields (MR) allotments
Average ratio of topsoil: subsoil
7
6
5
4
3
2
1
0
Petrol Pb
Total Pb
Geogenic Pb
Zn
Sn
P
Cd
Cu
Ca
Sb
Ag
Be
Se
Ni
Co
As
Sr
Mo
Ba
Cr
Tl
U
V
Mg
Al
Li
Mn
Fe
Ti
Na
Nb
Rb
Cs
K
Hf


f. Blenheim (BH) allotments
Average ratio of topsoil:subsoil
1.4
1.2
1.0
0.8
0.6
0.4
0.2
0.0
P
Li
Petrol Pb
Hf
Zn
Se
Sb
Tl
Sn
K
Mo
Cd
Cr
Cu
Ba
U
Nb
Total Pb
Ca
Rb
Sr
As
Geogenic Pb
V
Ni
Ag
Fe
Al
Ti
Cs
Na
Be
Co
Mg
Mn

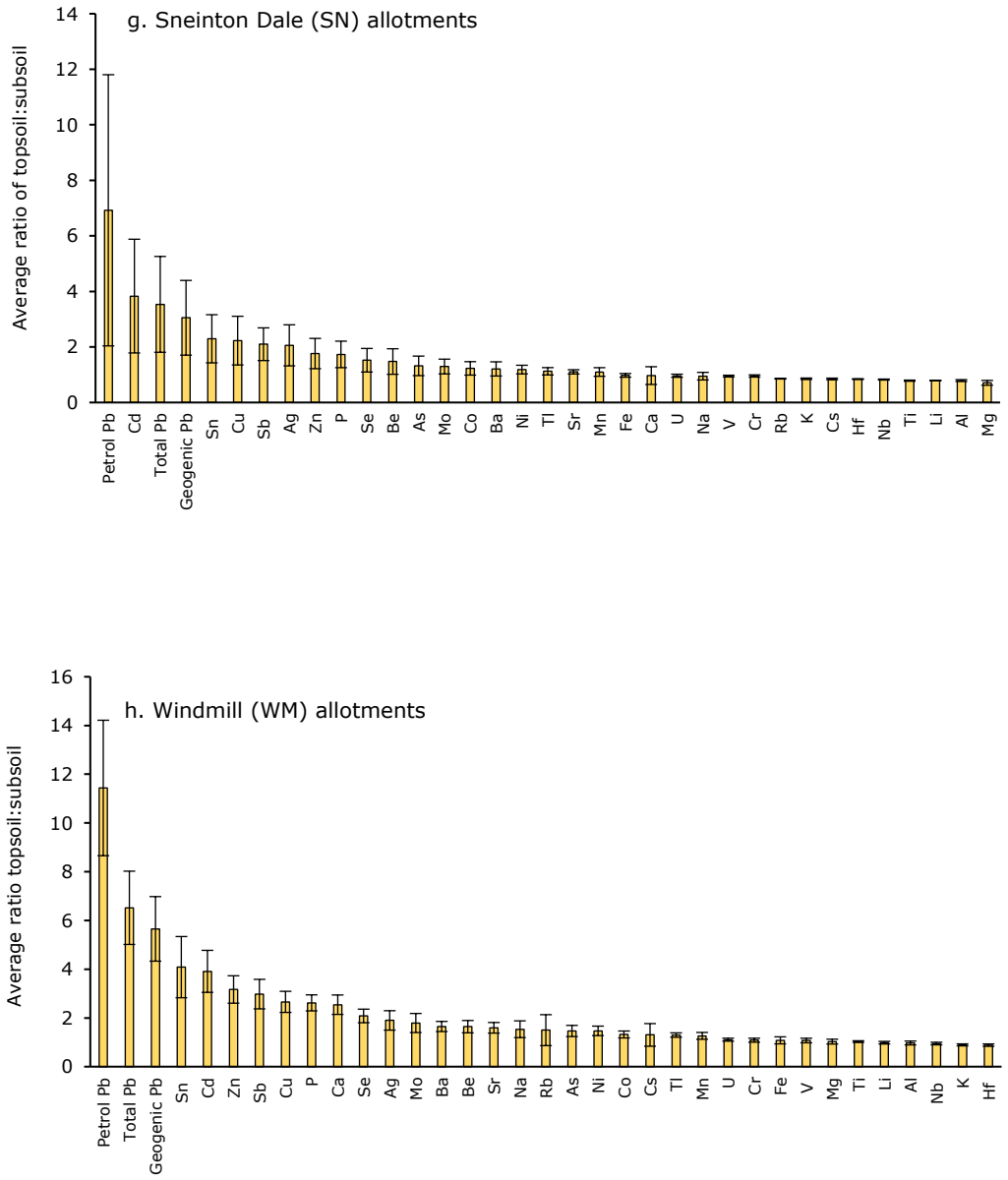


Figure 5.2: Average concentration ratios topsoil:subsoil (Enrichment factor, EF) for different elements in individual allotment sites. Vertical error bars denote the standard errors across all samples from individual sites.

Table 5.2 Average concentration ratios of Pb_{petrol} to Pb_{coal} in topsoils

Allotments	Pb_{petrol}/Pb_{coal}
Old Park farm (PF)	*0.59*
St Ann's (ST)	*0.42*
Canal (CN)	*0.28*
Mapperly (MP)	*0.33*
Moorfield (MR)	*0.50*
Blenheim (BH)	*0.26*
Sneinton Dale (SN)	*0.40*
Woodthorpe (WT)	*0.54*
Windmill (WM)	*0.36*

5.4.3 Cluster Analysis (CA)

In order to identify different possible sources of contaminants in allotment soils Pb_{petrol} and $Pb_{geogenic}$ were subject to cluster analysis with other elements based on their total concentration. The CA results are shown in Figure 5.3 as a dendrogram. From the clustering of different elements in groups it is cleared that allotment soils were influenced by both anthropogenic and natural sources. The different contaminant sources in allotment soils are discussed below.

Cluster Analysis results

There is a wide range of possible contaminants sources (both natural and anthropogenic) that can influence gardens and allotments which are commonly located in urban areas. The most significant sources are fertilizers and various agrochemicals, industrial emissions, fossil fuels combustion and vehicular exhaust (Alloway, 2004). In allotments application of fertilizers and various agrochemicals are a common practice to improve production and growth of plants. The different agronomic management practices of urban

gardens and allotments also include adding organic compost, manure, biosolids, lime and poultry litter. These fertilizers and agrochemicals are considered important sources of heavy metals in soils. In the UK inorganic fertilizers, especially phosphate, have been an important source of Cd (Järup et al., 1998). Also, in the past, fungicides and insecticides were based on compounds containing Cu, Zn, Mn and Pb (Wuana and Okieimen, 2011). For example, Cu-based fungicide sprays and Pb arsenate were used to control insect pests. Currently there are several coal power stations in Nottinghamshire that are still operational, and, in the past, coal used for domestic heating was the dominant source of Pb in the atmosphere. Coal burning was particularly important during the period of 1830-1930 when coal was the major energy source in the midlands and used for power stations and for domestic heating and industrial purposes (Farmer et al., 1999). This heavy coal mining and combustion has left a legacy of waste materials including trace elements, ash and slag, which has affected large areas (Bridge et al., 1997). Trace elements which are commonly found enriched in soils around coal burning power plants include Ti, Fe, Co, Cr, Ni, Cu, Zn, Cd and Hg (Bridge et al., 1997). The amendment of soil with ash is a common practice which is done in order to improve soil texture, adjust soil pH and to increase fertility (e.g. K). However, excessive application of ash can result in increased concentrations of trace elements (Carlson and Adriano, 1993). Coal ash is enriched in elements such as B, Be, V, Ni, Mn, Cu, Zn, Cd, Pb, Mo, As, Se, Sb and Te (Bridge et al., 1997, Mandal and Sengupta, 2006).

The rapid industrialization and urbanization during the 19th century has left a legacy of contamination in most urban areas of the UK (Bridge et al., 1997). For example in different industrial purposes many metals are used as alloys

such as Sn, Sb, Ag, Sr, Ca and Te and these are commonly alloyed with Pb. Similarly Zn is extensively used in the manufacturing of rubber, pharmaceuticals, textiles, plastics, electrical equipment, paints etc. (Kołodziejczak-Radzimska and Jesionowski, 2014). Allotments are also expected to be contaminated with traffic related metals (mechanical parts abrasion and wear and tear of tires) which are emitted in particulate form or dissolved form and are mostly transported to the ambient environment via air or road run-off (Bakirdere and Yaman, 2008, Werkenthin et al., 2014). The age and intensity of anthropic activity at each site is also considered an important factor responsible for increased concentration of contaminants over time (Imperato et al., 2003).

In allotment soils, definitive identification of all pollutant sources is very difficult, therefore a general 'expected' pattern of clusters arising from specified origins was established based on the most significant contaminant sources along with the common elements associated with each specific source (Table 5.3). Later in each allotment site, the relevant clusters were investigated on the basis of their established 'expected' pattern in order to identify possible contaminant sources.

Agriculture

The results of clustering patterns in the dendrograms (Figure 5.3) showed that in most of the allotment sites (PF, ST, MP, MR and BH), there was an apparent influence from fertilizers which was evidenced from close clustering of P and Ca together (Table 5.3). At sites CN and WM, the separate clustering of P and Ca also reflects some influence from agricultural activities. Whereas in allotment sites such as SN and WT, no obvious 'agricultural' cluster was

observed. Also in allotment soils, there was no obvious influence due to liming agents which suggested lime might not be added very often in allotment soils. Urban soils often have quite high pH values due to the presence of cement, concrete etc.

Coal

Among all the allotment sites, a cluster possibly attributed to coal was observed most strongly at sites ST and MR whereas in the other allotments there was a close association observed between $Pb_{geogenic}$ and Pb_{total}. The oldest allotments, such as ST, reflected a greater influence from past coal combustion. Similarly allotment sites such as PF, CN and MR were in close proximity to railway lines which used to run alongside a local canal, both in the past supplied coal to the locations within and beyond the city. The influence of the railway line could be observed most clearly at site MR.

Vehicular emission

In most of the allotment sites, there was a noticeable influence from traffic emissions, most strongly evidenced from the clustering of source-apportioned Pb (i.e., Pb_{petrol}) along with elements which are commonly emitted due to traffic exhaust. Most of the allotments were located close to major or other busy roads. Allotments ST, SN and WT lie close to the A60, whereas PF, CN and MR allotments are closer to the A609 (Wollaton road). Also the proximity of allotments ST and MR to the city centre might be an additional factor when considering contamination of these soils. At site BH, the separate clustering of Pb_{petrol} suggested only a minor influence from traffic; this site is comparatively new and well away from major roads. By contrast, the close association of Pb_{petrol} and Pb_{total} at site WT revealed vehicular emission as the dominant

source. At some of the allotment sites Pb_{petrol} was clustered with Sb and Ba. These elements have been used in more recent automotive technologies and have been reported to accumulate in the environment over time (Hjortenkrans et al., 2007). In UK, asbestos was banned in 1999 and it was later replaced by Sb in brake pads. Recently some studies have also reported Sb, Cu and Cd alongside other elements in roadside soils (Hjortenkrans et al., 2006, Apeagyei et al., 2011, Carrero et al., 2013). Hjortenkrans et al. (2007) in their study based in Stockholm, Sweden, calculated the elemental emissions from brake linings and tyres; the amounts of Sb released from brake linings and tire tread rubber were reported as 710 and 0.54 kg/year respectively. Similarly Ba, mostly as barium sulfate, also has been used by many manufacturers as filler material in brake pads (McKenzie et al., 2009).

Industrial emissions

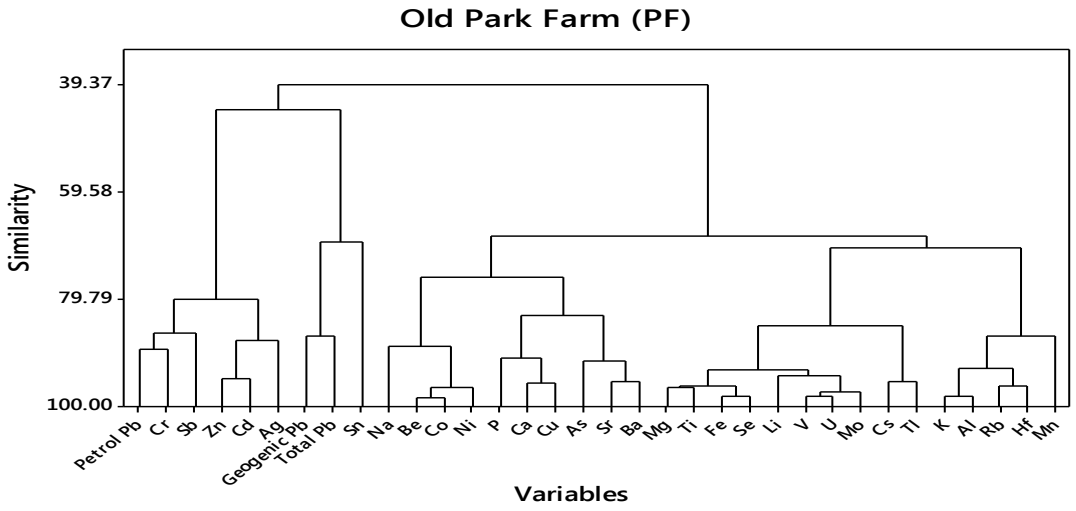
From the clustering pattern of different elements in most of the allotment sites (except WT) it can be seen that in allotment soils the distribution of heavy metals cannot be attributed solely to vehicular emissions. There was also a clear influence of industrial pollutants which was probably mainly due to past industrial processes within Nottingham. Furthermore, allotment sites SN and WM are quite close to the River Trent so it might be possible that these top soils were contaminated with river sediments or dredging operations etc. It has been suggested that >90% of heavy metal dispersal, both from point and diffuse sources, is via particulate-associated transport, mostly in flooded conditions (Macklin et al., 1997, Carter et al., 2006).

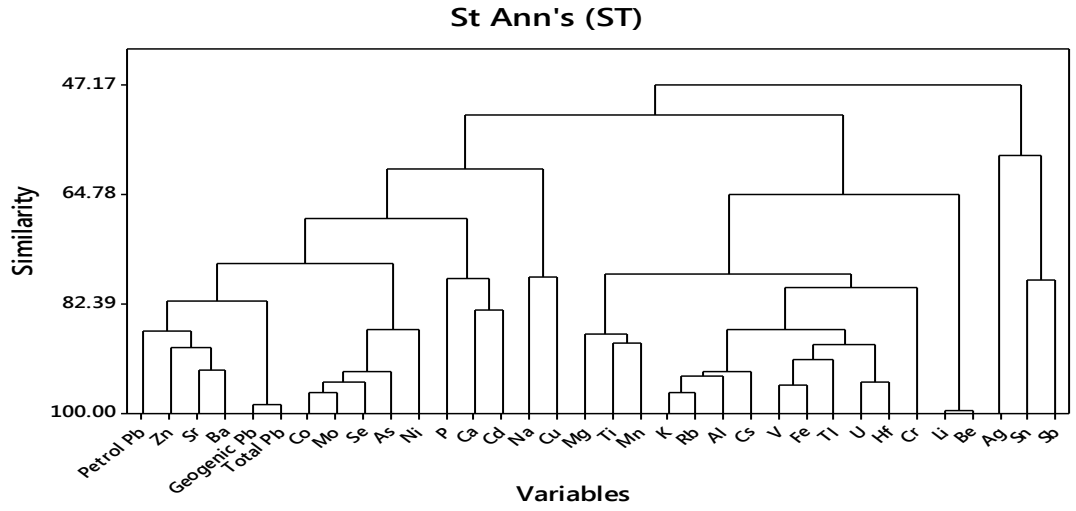
Natural sources

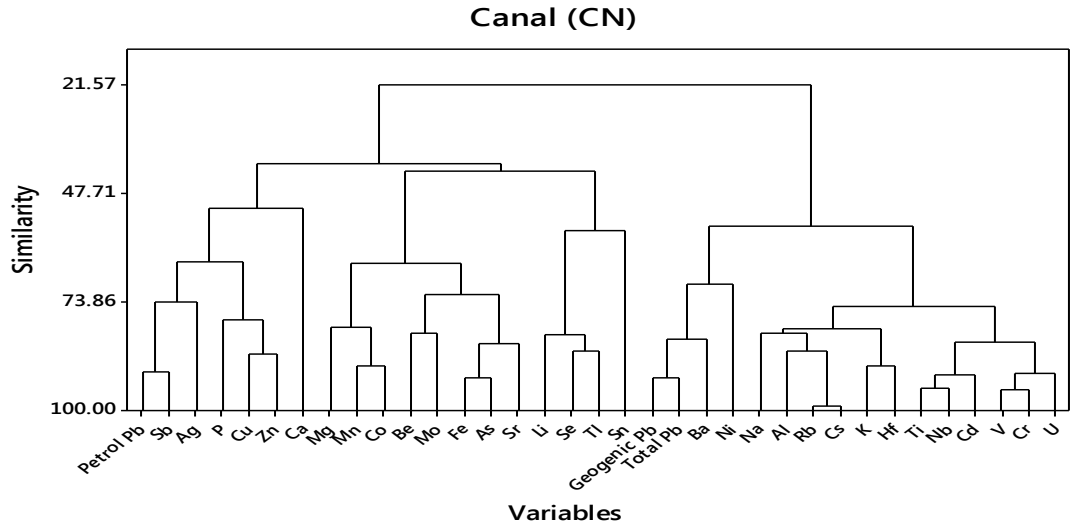
There was a strong geochemical grouping of elements observed in all allotment sites which were mostly indicators of clay mineralogy and associated exchangeable cations. Similarly Fe oxide minerology was also reflected in most of the allotment sites, where different elements such as V, Cr and Ti were strongly associated with Fe. It has already been revealed in the literature that the strong association of Fe with Ti, Al and V is an indication of contamination from soil dust on crops (Joy et al., 2017). Also clustering of Mn and Co was observed only at two allotment sites (CN and MR) which reflects the isomorphous substitution of Co into Mn oxides.

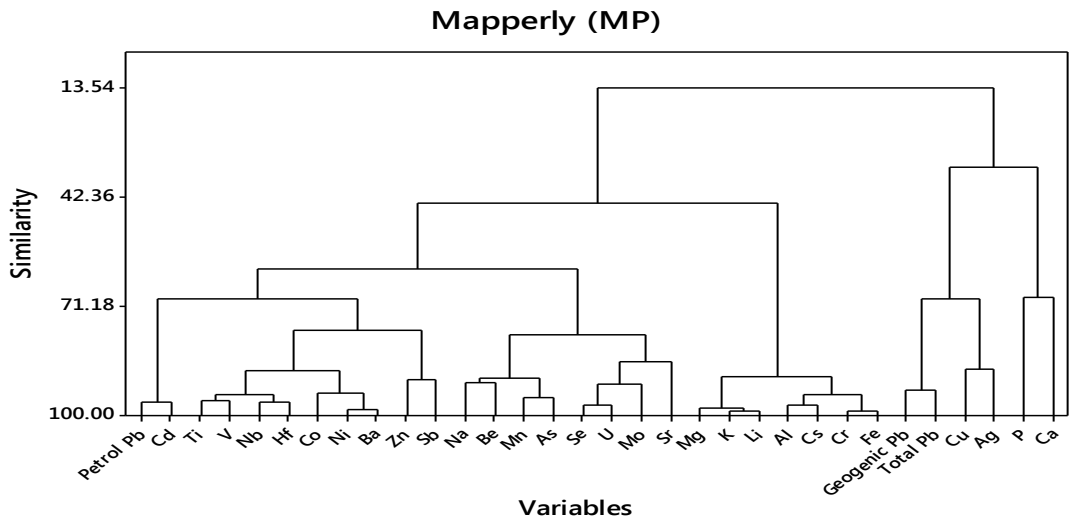
Table 5.3: Speculative association of elemental clusters with soil and contaminant sources for nine allotment sites

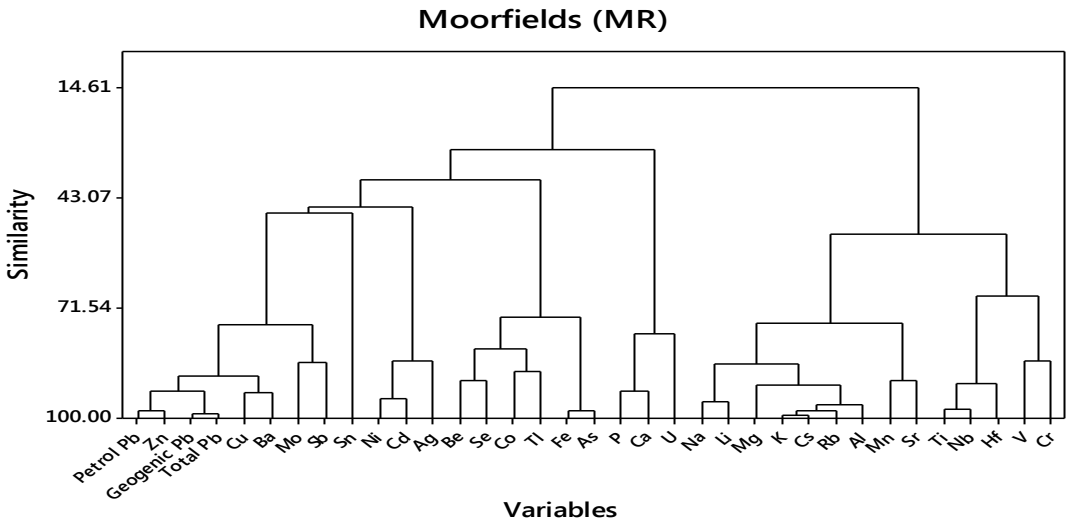
Possible source		Clays & Exchangeable cations	Fe oxides	Mn oxides	Lime	Agriculture	Coal	Vehicles	Industry
Sites/n		Al, K, Mg, Ca, Na, Cs, Li, Be, Rb	Fe, V, Ti, Cr, Mo	Mn, Co	Ca, Sr, U	P, Ca, Mg, K, As, Cu	Pb(G), As, Sb, V, Se, Mo, Ni	Pb(P), Cr, Sb, Zn, Ba, Cu, Cd	Cu, Zn, Ni, Cr, Cd, As, Pb
PF	*14*	K, Al, Rb	Fe, Ti, V, Mo	Mn		P, Ca, As	Pb(G), Pb(T)	Pb(P), Cr, Sb	Co, Ni, As, Cu<> Zn, Cd, Ag, Sb, Cr
ST	*50*	K, Rb, Al, Cs <> Li, Be	Fe, V, Cr			P, Ca, Cd	Pb(G), Pb(T), Zn, Co, Mo, Se, As, Ni	Pb(P), Zn	Ag, Sn, Sb
CN	*21*	Na, Al, Rb, Cs, K	Ti, V, Cr	Mn, Co		P, Cu, Zn <> Ca, Mg	Pb(G), Pb(T), Ni	Pb(P), Sb	Cu, Zn, Ag
MP	*9*	Mg, K, Li, Al, Cs	Ti, V, Co, Ni <> Cr, Fe			P, Ca	Pb(G), Pb(T)	Pb(P), Cd<> Zn, Sb	Cu, Ag
MR	*12*	Na, Li, Mg, K, Cs, Rb, Al	Ti <> V, Cr<> Fe, As	Mn, Co		P, Ca, U	Pb(G), Pb(T), Mo, Sb <> Se, Co	Pb(P), Zn, Cu, Ba	Ni, Cd, Ag
BH	*20*	Na, K, Rb, Cs <> Li, Be				P, Ca	Pb(G), Pb(T)	Pb(P) <> Cd, Ba, Zn	Cr, As, Ni, Cu, Sb
SN	*7*	K, Li, Cs	V, Cr, Fe, Co, Ni, As				Pb(G), Pb(T), Sb	Pb(P), Zn, Cd	Zn, Cd, Pb, Sb<> Cu
WT	*5*	Na, Li <> Mg, K, Rb, Cs, Al	Fe, V					Pb(P), Pb(T)	
WM	*6*	Mg, K, Rb, Cs, Al	V, Cr			P <> Ca	Pb(G), Pb(T), Se	Pb(P), Ba	Zn, As, Co, Ni, Cu, Cd, Fe

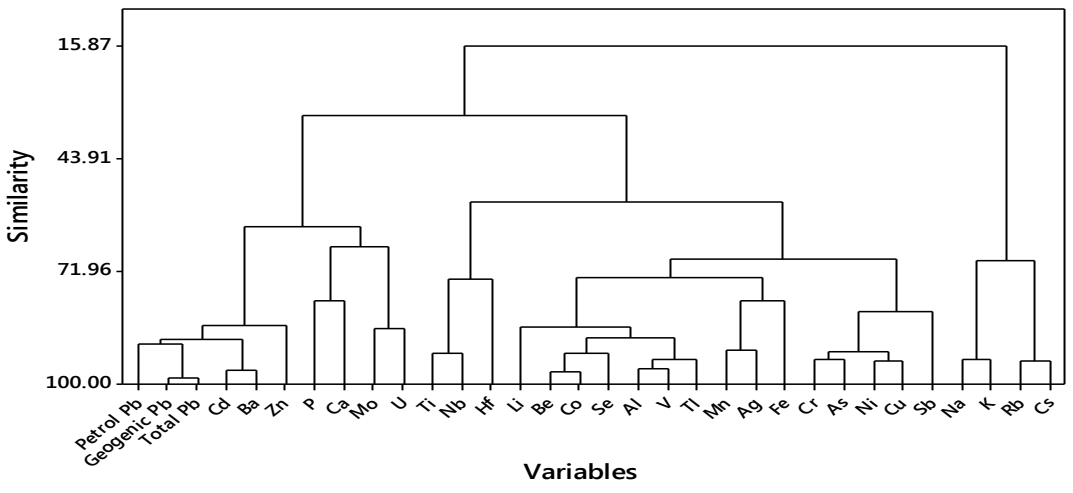

Old Park Farm (PF)
Similarity
39.37
59.58
79.79
100.00
Petrol Pb Cr Sb Zn Cd Ag Geogenic Pb Total Pb Sn Na Be Co Ni P Ca Cu As Sr Ba Mg Ti Fe Se Li V U Mo Cs Tl K Al Rb Hf Mn
Variables


St Ann's (ST)
Similarity
47.17
64.78
82.39
100.00
Petrol Pb Zn Sr Ba Geogenic Pb Total Pb Co Mo Se As Ni P Ca Cd Na Cu Mg Ti Mn K Rb Al Cs V Fe Tl U Hf Cr Li Be Ag Sn Sb
Variables


Canal (CN)
Similarity
21.57
47.71
73.86
100.00
Petrol Pb Sb Ag P Cu Zn Ca Mg Mn Co Be Mo Fe As Sr Li Se Tl Sn Geogenic Pb Total Pb Ba Ni Na Al Rb Cs K Hf Ti Nb Cd V Cr U
Variables


Mapperly (MP)
Similarity
13.54
42.36
71.18
100.00
Petrol Pb Cd Ti V Nb Hf Co Ni Ba Zn Sb Na Be Mn As Se U Mo Sr Mg K Li Al Cs Cr Fe Geogenic Pb Total Pb Cu Ag P Ca
Variables


Moorfields (MR)
Similarity
14.61
43.07
71.54
100.00
Petrol Pb Zn Geogenic Pb Total Pb Cu Ba Mo Sb Sn Ni Cd Ag Be Se Co Tl Fe As P Ca U Na Li Mg K Cs Rb Al Mn Sr Ti Nb Hf V Cr
Variables


Blenheim (BH)
Similarity
15.87
43.91
71.96
100.00
Petrol Pb Geogenic Pb Total Pb Cd Ba Zn P Ca Mo U Ti Nb Hf Li Be Co Se Al V Tl Mn Ag Fe Cr As Ni Cu Sb Na K Rb Cs
Variables

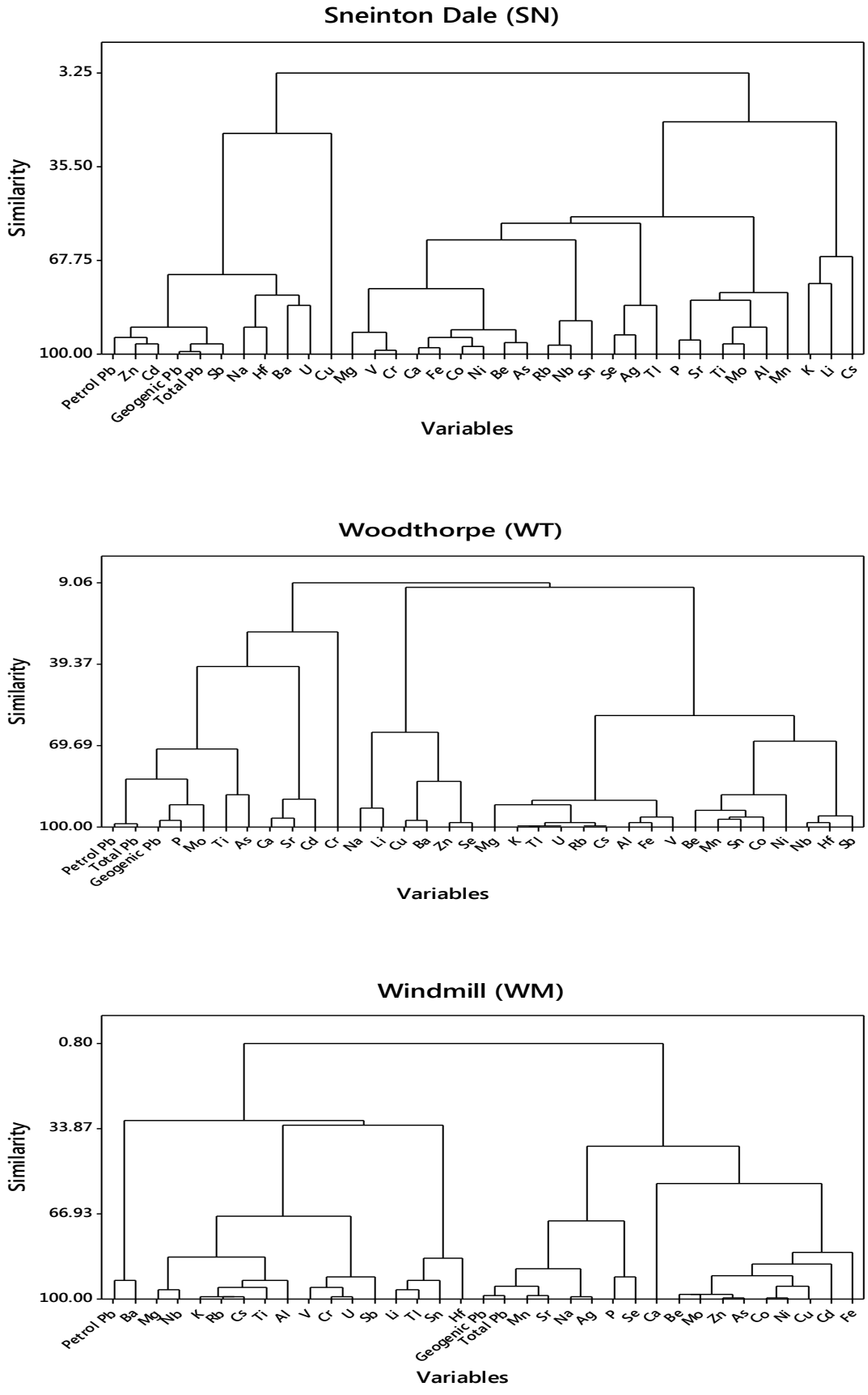


Figure 5.3: Dendrograms of topsoils elemental analysis from seven individual allotment sites.

5.5 Rare earth elements

5.5.1 Concentration of REEs in allotment soils

The average concentrations of REEs in both topsoils and subsoils followed the same order Ce>La>Nd>Y>Sc>Pr>Sm>Gd>Dy>Er>Yb>Eu>Tb>Ho>Tm>Lu. This sequence is in accord with the Oddo-Harkins rules i.e., elements with even atomic numbers are more abundant than elements with odd atomic number (Silva et al., 2016). The total REEs (∑REEs) concentrations in top soils ranged from 78–135 mg kg^{-1} with a mean value of 116 mg kg^{-1} and the mean concentrations of REEs in different allotments were in the following order: BH>WT>SN>ST>MR>WM>WM>MP>CN>PF as shown in Figure 5.4(a). In sub soils the total ∑REEs concentrations ranged from 74–150 mg kg^{-1} with mean value of 123 mg kg^{-1} and followed the sequence: MR>PF>ST>BH>SN>WM>MP>CN Figure 5.4(b). The total ∑REE concentrations in allotment soils were close to the reported values for European and Brazilian soils i.e., 125 and 108 mg kg^{-1} respectively (Sadeghi et al., 2013, Silva et al., 2016). The mean concentrations of LREEs (i.e., Ce, Eu, La, Nd, Pr and Sm) and HREEs (Dy, Er, Gd, Ho, Lu, Sc, Tb, Tm, Y and Yb) were different in topsoils and subsoils at all sites (Figure 5.5). The concentrations of LREEs in both topsoils and subsoils were higher than HREEs. In topsoils and subsoils, the mean concentrations of LREEs were 87.6 (58-103) and 84.5 (56-114) mg kg^{-1} respectively. The ratios of LREEs to HREEs in topsoils and subsoils were 3.095 and 2.826 respectively (Table A4 and A5, see Appendix A). In topsoils and subsoils, LREEs accounted for 76% and 85% respectively of the ∑REEs. In nature LREEs are relatively more abundant than HREEs and are the main cause of rare earth pollution in environment (de Sá Paye et al., 2016).

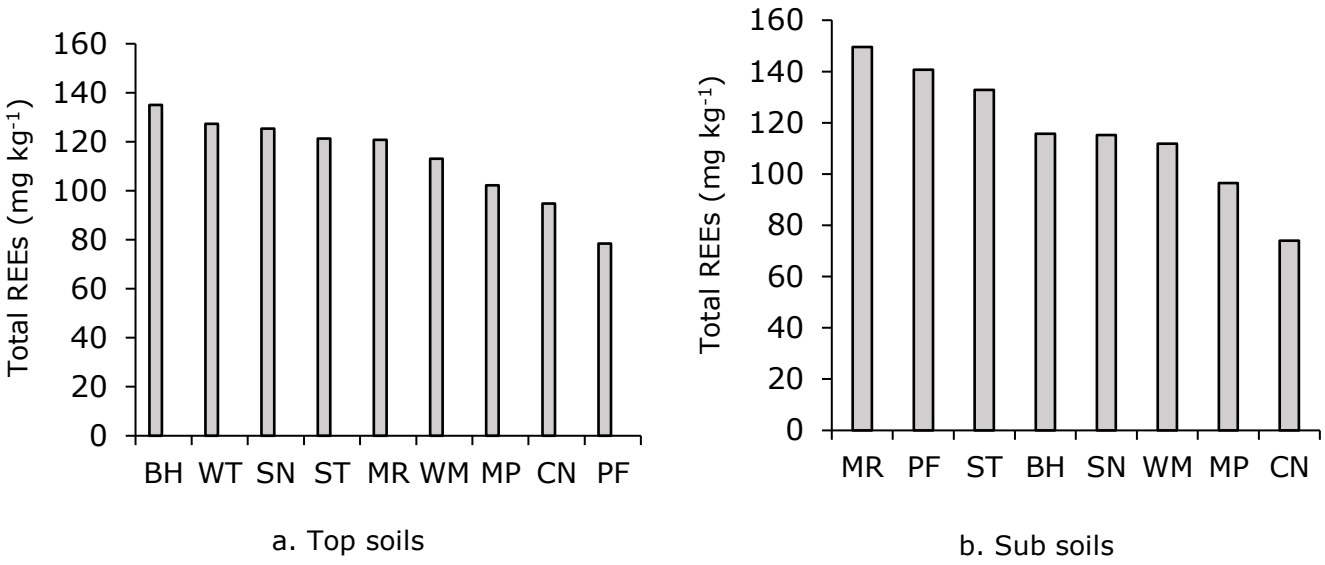


Figure 5.4: Concentration (mg kg^{-1}) of total REEs at different allotments sites (a) topsoils and (b) subsoils

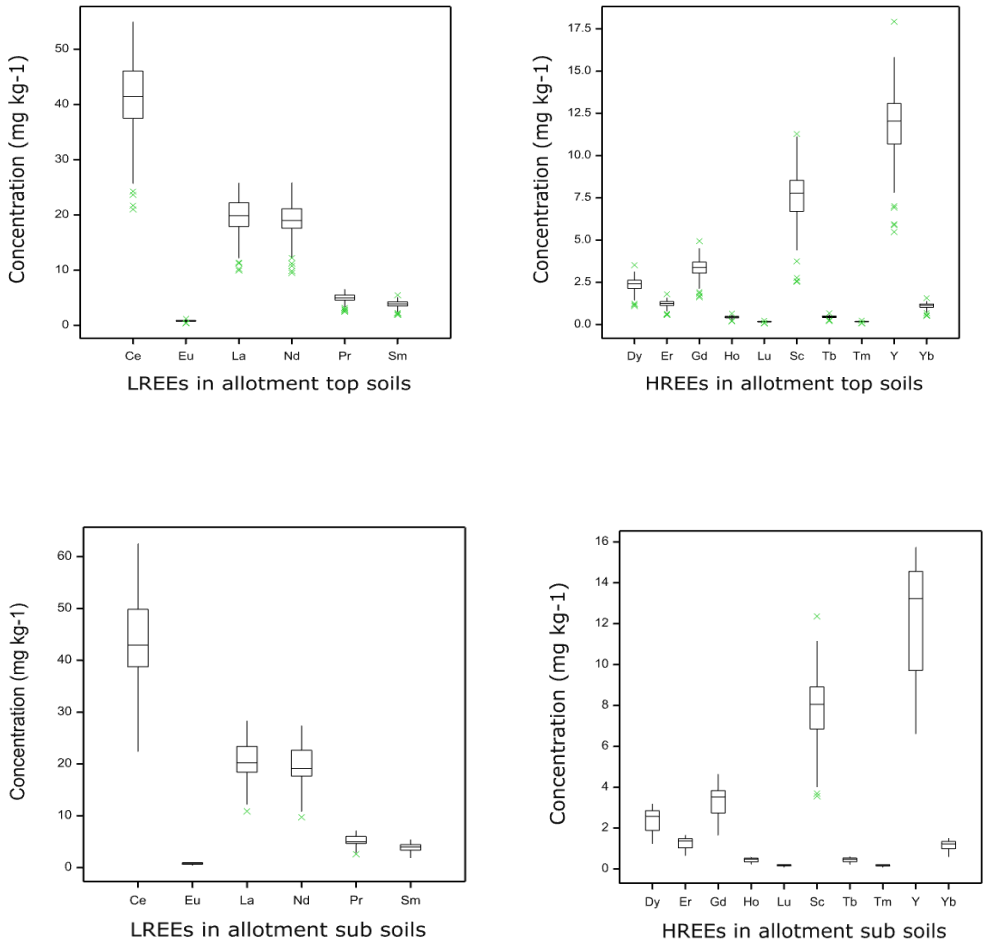
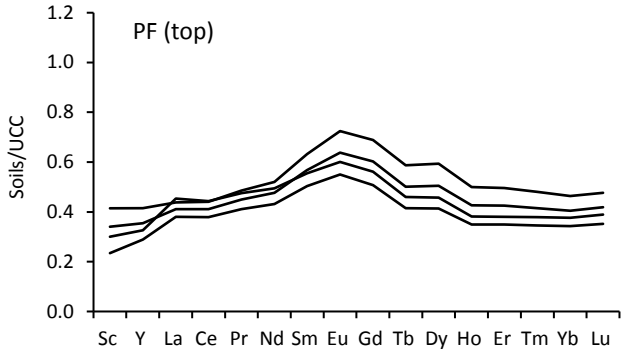
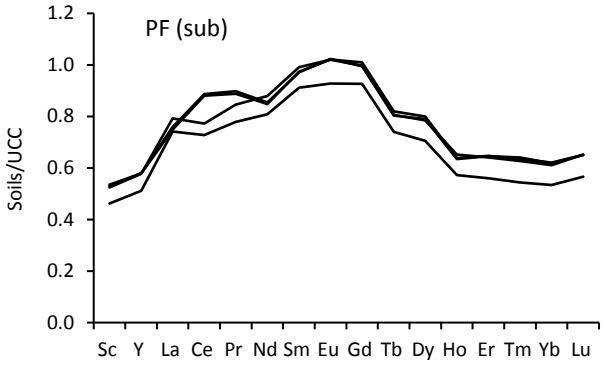


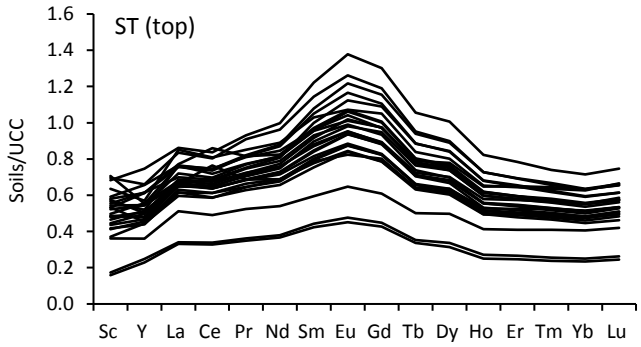
Figure 5.5: Average concentration (mg kg^{-1}) of LREEs and HREEs in topsoils and subsoils of allotments.

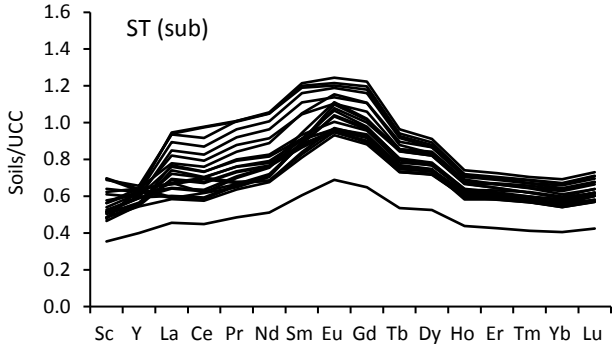
5.5.2 Crust-normalized REEs patterns for allotment soils

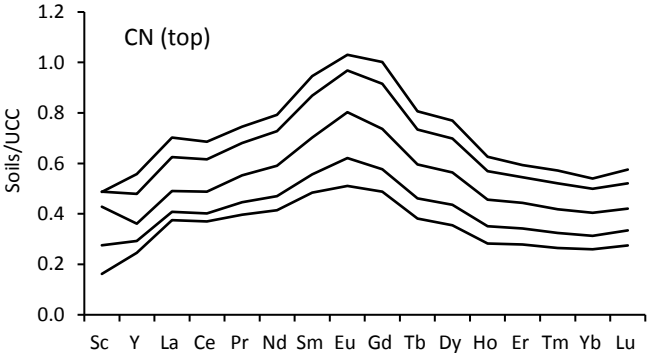
The abundance ratios of REEs in allotment topsoils and subsoils compared to the mean upper continental crust (UCC) values were calculated and shown in Figure 5.6. In this study, the mean values of UCC reported by Taylor and McLennan (1995) were used (Table A4 and A5, see Appendix A). The crust-normalized pattern of REEs is used to evaluate potential enrichment of selected REEs in soils. Soils that are not contaminated normally show a horizontal normalized pattern of REEs reflecting abundances in the crust whereas soils which are enriched in REEs show a different pattern from that of the normalized horizontal pattern; enriched elements normally show an anomaly (Kawasaki et al., 1998). Among LREEs, the concentrations of La, Pr, Nd and Ce in all top and sub soils showed a horizontal pattern and the concentration was lower than mean values of UCC. The pattern of Sm and Eu for most of the topsoils and subsoils was not flat but rather a positive anomaly was observed for these elements. These results are in agreement with findings of other studies where a positive Eu anomaly was also reported. For example Meryem et al. (2016) and Šmuc et al. (2012) showed a positive Eu anomaly in soils from smelting areas and in Kocani paddy soils. In another study conducted by de Sá Paye et al. (2016), a positive Eu anomaly was also reported in alkaline igneous rocks. Among HREEs, Sc, Y, Tb, Dy, Er, Tm, Yb, Lu and Ho showed a flat pattern and their concentrations were lower than UCC values whereas, only Gd showed a positive anomaly. In previous studies the mean concentration of Gd was also higher in Brazil soils (de Sá Paye et al., 2016).

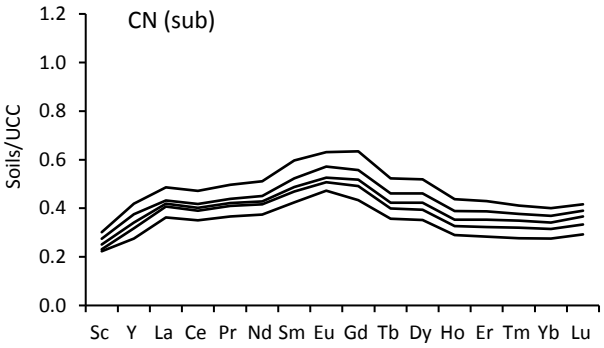

PF (top)
Soils/UCC
1.2
1.0
0.8
0.6
0.4
0.2
0.0
Sc Y La Ce Pr Nd Sm Eu Gd Tb Dy Ho Er Tm Yb Lu

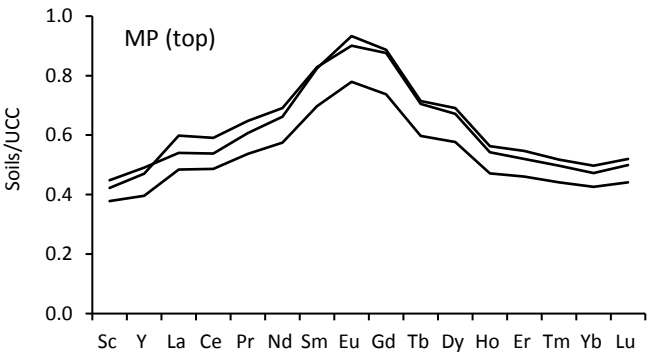

PF (sub)
Soils/UCC
1.2
1.0
0.8
0.6
0.4
0.2
0.0
Sc Y La Ce Pr Nd Sm Eu Gd Tb Dy Ho Er Tm Yb Lu

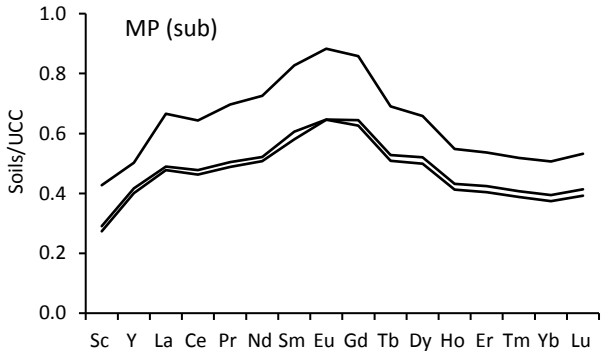

ST (top)
Soils/UCC
1.6
1.4
1.2
1.0
0.8
0.6
0.4
0.2
0.0
Sc Y La Ce Pr Nd Sm Eu Gd Tb Dy Ho Er Tm Yb Lu

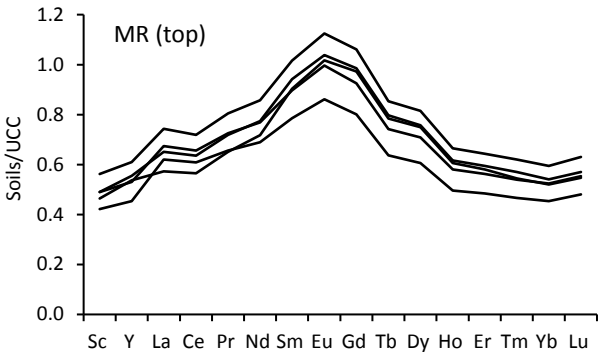

ST (sub)
Soils/UCC
1.6
1.4
1.2
1.0
0.8
0.6
0.4
0.2
0.0
Sc Y La Ce Pr Nd Sm Eu Gd Tb Dy Ho Er Tm Yb Lu

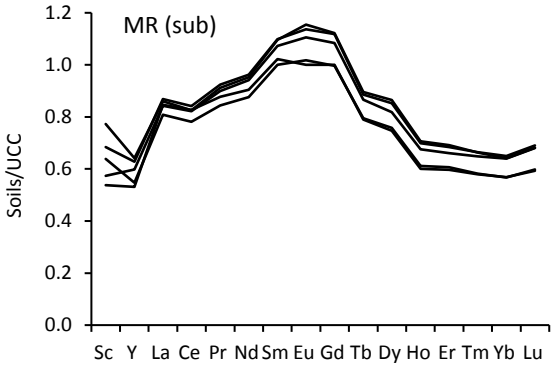

CN (top)
Soils/UCC
1.2
1.0
0.8
0.6
0.4
0.2
0.0
Sc Y La Ce Pr Nd Sm Eu Gd Tb Dy Ho Er Tm Yb Lu

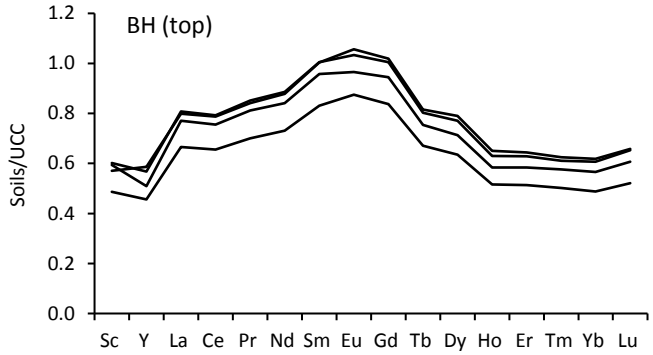

CN (sub)
Soils/UCC
1.2
1.0
0.8
0.6
0.4
0.2
0.0
Sc Y La Ce Pr Nd Sm Eu Gd Tb Dy Ho Er Tm Yb Lu

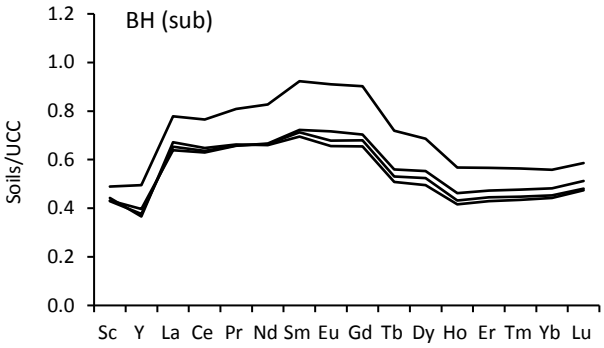

MP (top)
Soils/UCC
1.0
0.8
0.6
0.4
0.2
0.0
Sc Y La Ce Pr Nd Sm Eu Gd Tb Dy Ho Er Tm Yb Lu

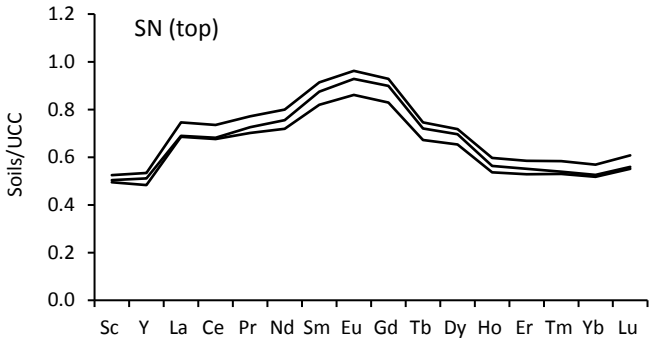

MP (sub)
Soils/UCC
1.0
0.8
0.6
0.4
0.2
0.0
Sc Y La Ce Pr Nd Sm Eu Gd Tb Dy Ho Er Tm Yb Lu

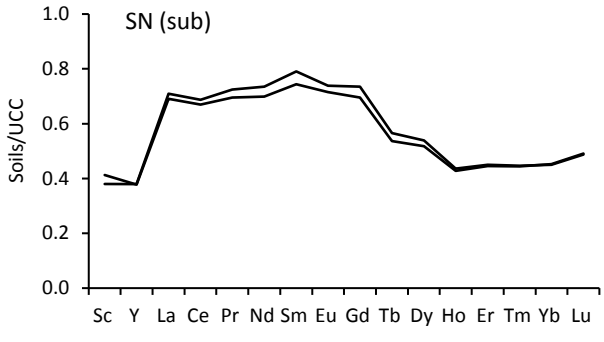

MR (top)
Soils/UCC
1.2
1.0
0.8
0.6
0.4
0.2
0.0
Sc Y La Ce Pr Nd Sm Eu Gd Tb Dy Ho Er Tm Yb Lu

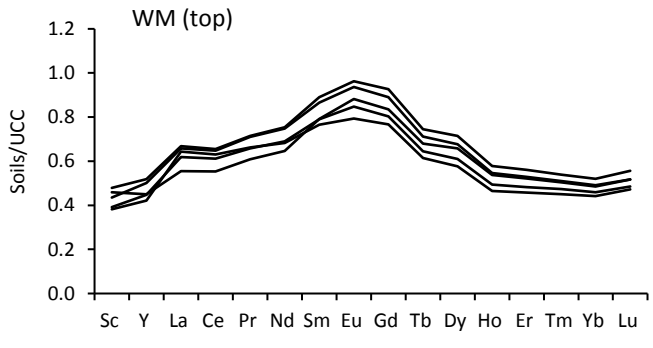

MR (sub)
Soils/UCC
1.2
1.0
0.8
0.6
0.4
0.2
0.0
Sc Y La Ce Pr Nd Sm Eu Gd Tb Dy Ho Er Tm Yb Lu

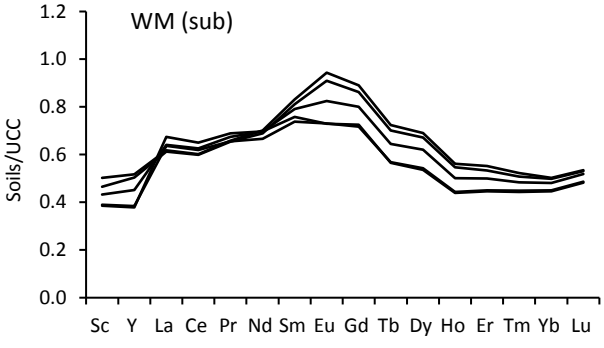

BH (top)
Soils/UCC
1.2
1.0
0.8
0.6
0.4
0.2
0.0
Sc Y La Ce Pr Nd Sm Eu Gd Tb Dy Ho Er Tm Yb Lu


BH (sub)
Soils/UCC
1.2
1.0
0.8
0.6
0.4
0.2
0.0
Sc Y La Ce Pr Nd Sm Eu Gd Tb Dy Ho Er Tm Yb Lu


SN (top)
Soils/UCC
1.2
1.0
0.8
0.6
0.4
0.2
0.0
Sc Y La Ce Pr Nd Sm Eu Gd Tb Dy Ho Er Tm Yb Lu


SN (sub)
Soils/UCC
1.0
0.8
0.6
0.4
0.2
0.0
Sc Y La Ce Pr Nd Sm Eu Gd Tb Dy Ho Er Tm Yb Lu


WM (top)
Soils/UCC
1.2
1.0
0.8
0.6
0.4
0.2
0.0
Sc Y La Ce Pr Nd Sm Eu Gd Tb Dy Ho Er Tm Yb Lu


WM (sub)
Soils/UCC
1.2
1.0
0.8
0.6
0.4
0.2
0.0
Sc Y La Ce Pr Nd Sm Eu Gd Tb Dy Ho Er Tm Yb Lu

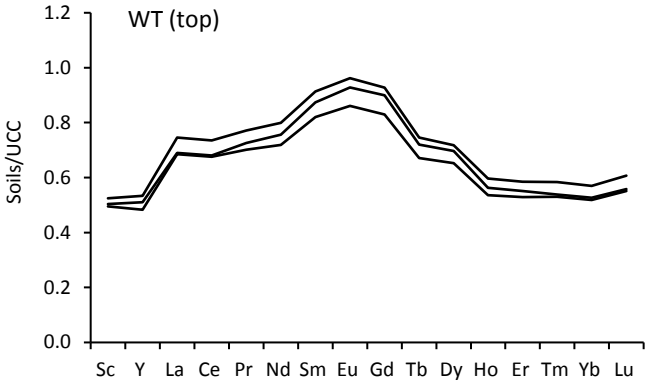
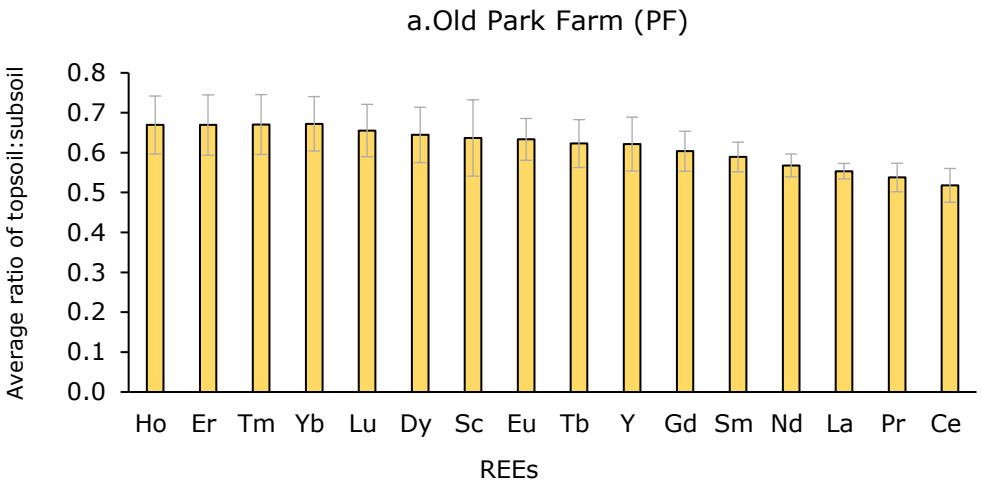
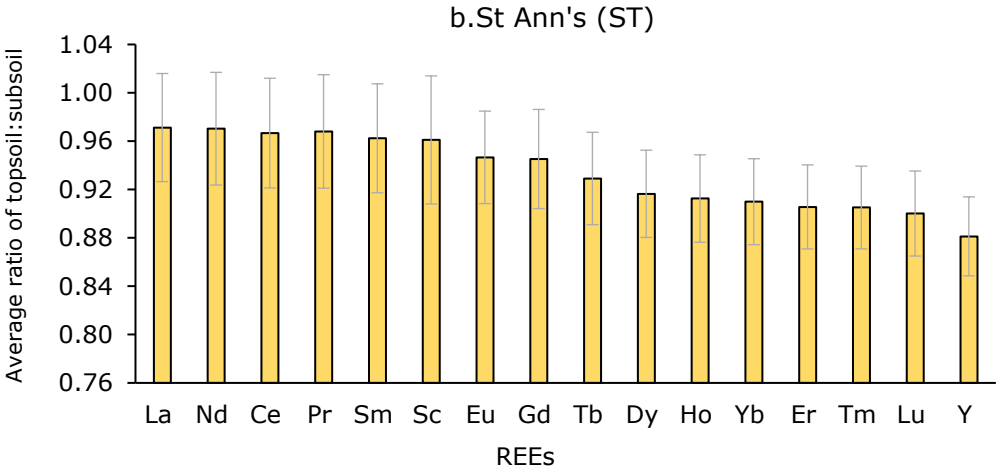


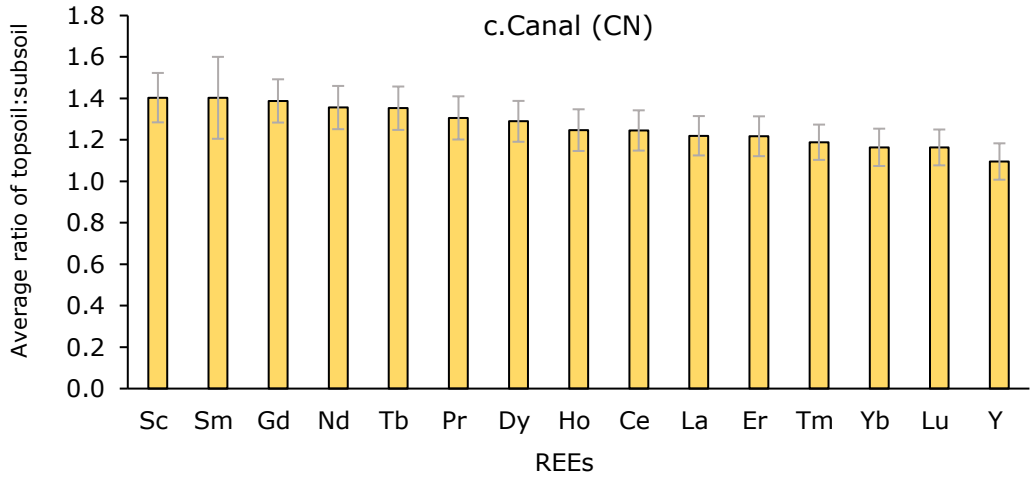
Figure 5.6: Crust-normalized REEs pattern for topsoils and subsoils of individual allotments.

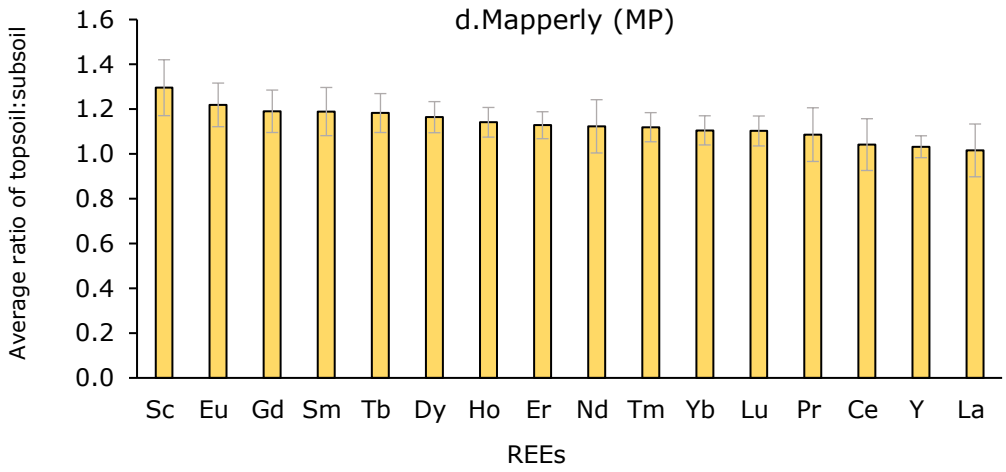
5.5.3 REEs Enrichment Factors

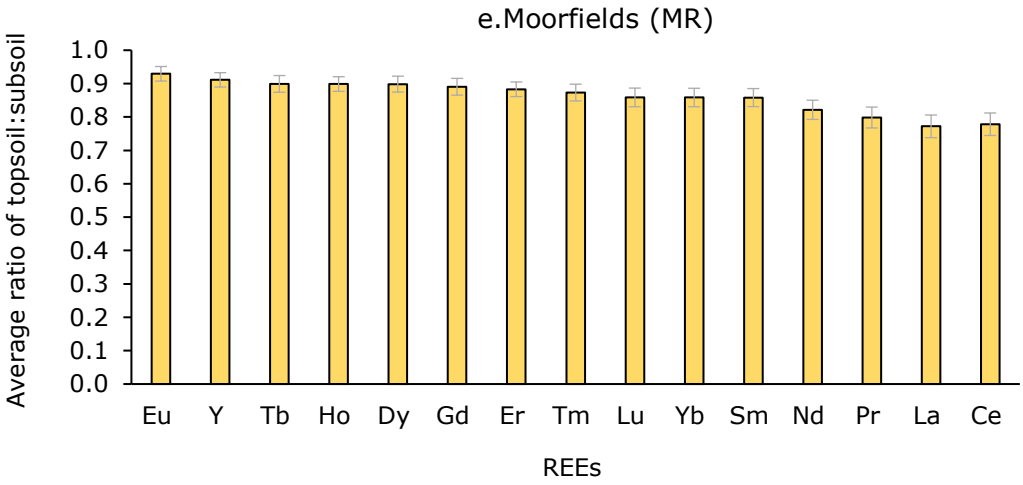
At allotment sites PF and MR, subsoils were more enriched with REEs than topsoils and so the EF values were <1.0. The mean EF value for REEs (mostly LREEs) at site ST was closer to unity, whereas HREEs were more enriched in subsoils. Topsoils of allotment sites CN, MP and BH were more enriched with REEs, the mean EF values for most of the REEs were > 1.0 as shown in Figure 5.7. Topsoils from sites SN and WM were mostly enriched in HREEs whereas most of the LREEs had EF values closer to unity.

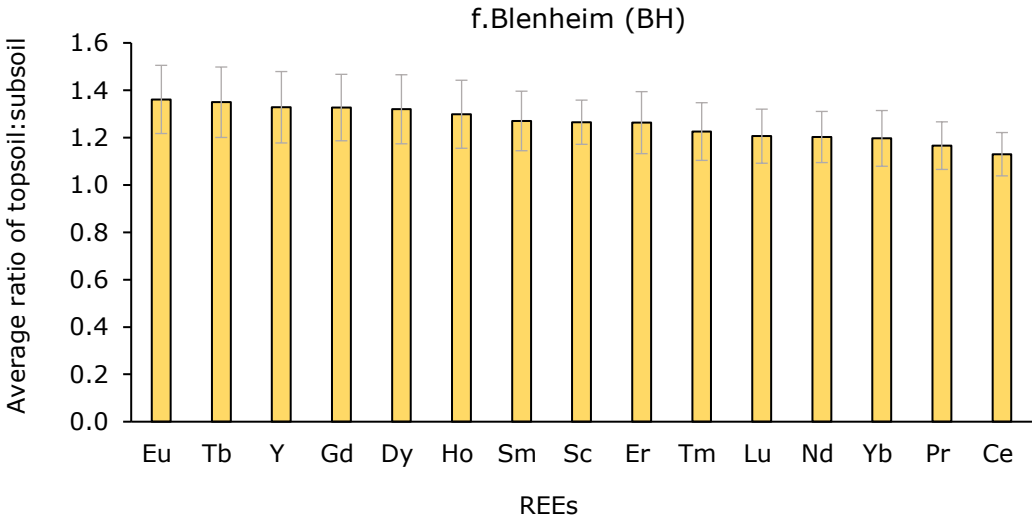

a.Old Park Farm (PF)
Average ratio of topsoil:subsoil
0.8
0.7
0.6
0.5
0.4
0.3
0.2
0.1
0.0
Ho Er Tm Yb Lu Dy Sc Eu Tb Y Gd Sm Nd La Pr Ce
REEs


b.St Ann's (ST)
Average ratio of topsoil:subsoil
1.04
1.00
0.96
0.92
0.88
0.84
0.80
0.76
La Nd Ce Pr Sm Sc Eu Gd Tb Dy Ho Yb Er Tm Lu Y
REEs


c.Canal (CN)
Average ratio of topsoil:subsoil
1.8
1.6
1.4
1.2
1.0
0.8
0.6
0.4
0.2
0.0
Sc Sm Gd Nd Tb Pr Dy Ho Ce La Er Tm Yb Lu Y
REEs


d.Mapperly (MP)
Average ratio of topsoil:subsoil
1.6
1.4
1.2
1.0
0.8
0.6
0.4
0.2
0.0
Sc Eu Gd Sm Tb Dy Ho Er Nd Tm Yb Lu Pr Ce Y La
REEs


e.Moorfields (MR)
Average ratio of topsoil:subsoil
1.0
0.9
0.8
0.7
0.6
0.5
0.4
0.3
0.2
0.1
0.0
Eu Y Tb Ho Dy Gd Er Tm Lu Yb Sm Nd Pr La Ce
REEs


f.Blenheim (BH)
Average ratio of topsoil:subsoil
1.6
1.4
1.2
1.0
0.8
0.6
0.4
0.2
0.0
Eu Tb Y Gd Dy Ho Sm Sc Er Tm Lu Nd Yb Pr Ce
REEs

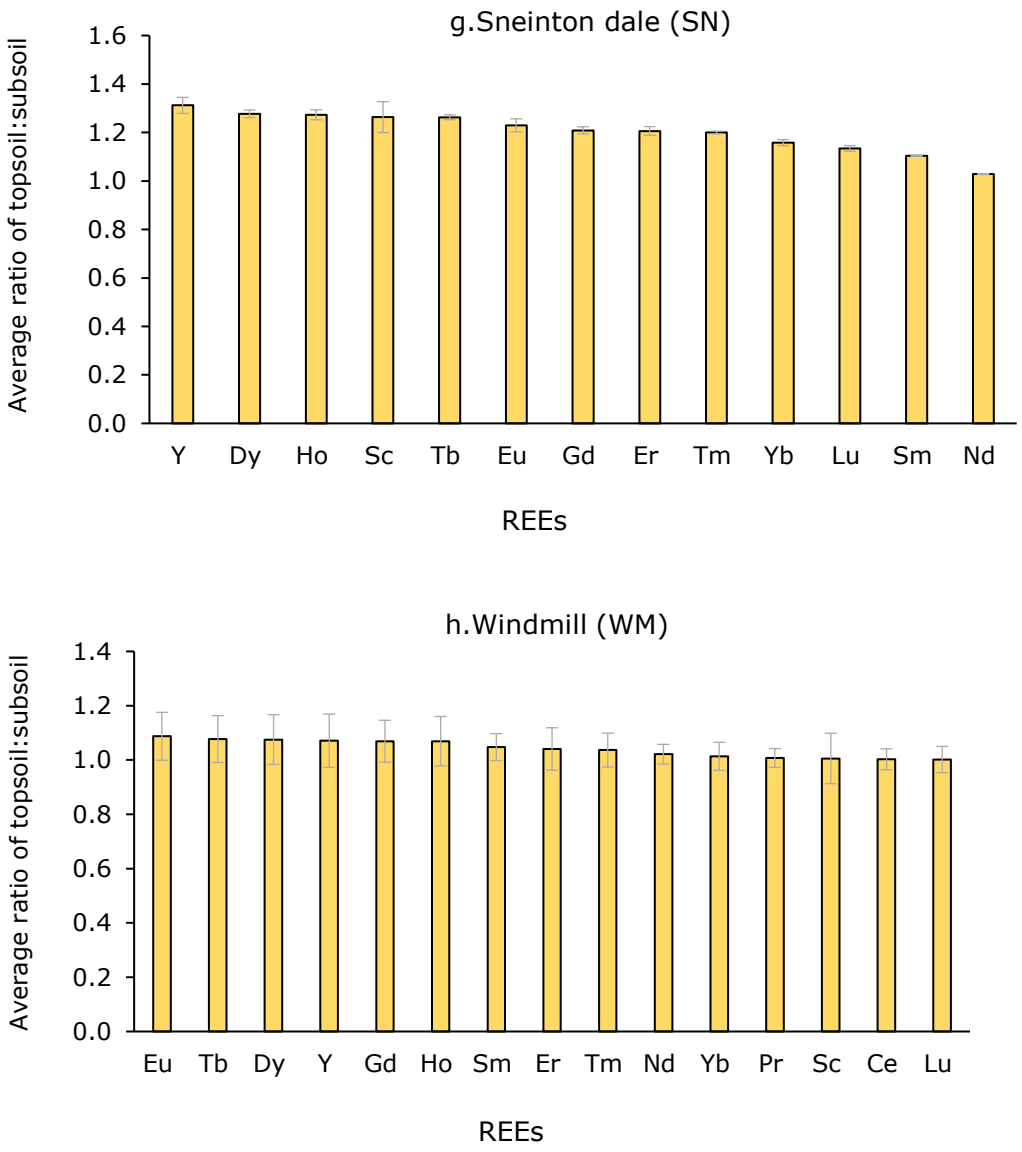


Figure 5.7: Average concentration ratio topsoil:subsoil (Enrichment factor, EF) for REEs in individual allotment sites. The vertical bars denote the average standard error.

5.5.4 Correlation analysis between REEs in soils

The Pearson's correlation coefficients for REEs in both topsoils and subsoils are shown in Tables 5.4 and 5.5. A strong significant positive correlation ($p<0.001$) was observed between LREEs (La-Eu) and HREEs (Gd-Sc) in both topsoils and subsoils, which indicates a common geochemical characteristic of these elements and possibly that they originate from similar sources.

Table 5.4: Correlation coefficients (r-values) between REEs (LREEs and HREEs) in allotment topsoils at $p \leq 0.001$.

	La	Ce	Pr	Nd	Sm	Eu	Gd	Tb	Dy	Ho	Er	Tm	Yb	Lu	Sc
Ce	0.984														
Pr	0.989	0.978													
Nd	0.978	0.961	0.996												
Sm	0.944	0.929	0.976	0.989											
Eu	0.9	0.887	0.942	0.963	0.989										
Gd	0.908	0.894	0.947	0.967	0.993	0.997									
Tb	0.897	0.883	0.938	0.959	0.988	0.996	0.999								
Dy	0.891	0.877	0.931	0.952	0.981	0.991	0.993	0.997							
Ho	0.889	0.874	0.927	0.947	0.974	0.985	0.986	0.993	0.998						
Er	0.901	0.883	0.934	0.951	0.971	0.976	0.978	0.985	0.993	0.997					
Tm	0.917	0.9	0.943	0.955	0.966	0.963	0.967	0.973	0.984	0.99	0.997				
Yb	0.923	0.905	0.944	0.953	0.957	0.95	0.954	0.961	0.973	0.981	0.991	0.998			
Lu	0.935	0.914	0.953	0.96	0.961	0.947	0.954	0.959	0.969	0.976	0.988	0.995	0.998		
Sc	0.916	0.901	0.932	0.934	0.925	0.911	0.911	0.915	0.927	0.935	0.95	0.963	0.968	0.966	
Y	0.906	0.904	0.94	0.954	0.974	0.981	0.983	0.986	0.987	0.986	0.98	0.974	0.964	0.959	0.911

Table 5.5: Correlation coefficients (r-values) between REEs (LREEs and HREEs) in allotment subsoils at $p \leq 0.001$.

	La	Ce	Pr	Nd	Sm	Eu	Gd	Tb	Dy	Ho	Er	Tm	Yb	Lu	Sc
Ce	0.975														
Pr	0.987	0.987													
Nd	0.982	0.966	0.992												
Sm	0.942	0.931	0.964	0.984											
Eu	0.814	0.812	0.855	0.893	0.957										
Gd	0.862	0.862	0.899	0.931	0.98	0.994									
Tb	0.813	0.818	0.856	0.892	0.956	0.997	0.995								
Dy	0.792	0.8	0.838	0.874	0.942	0.994	0.988	0.998							
Ho	0.787	0.789	0.833	0.871	0.938	0.991	0.984	0.995	0.998						
Er	0.82	0.827	0.864	0.894	0.951	0.989	0.987	0.993	0.996	0.997					
Tm	0.84	0.849	0.883	0.908	0.956	0.982	0.983	0.986	0.989	0.99	0.998				
Yb	0.873	0.879	0.911	0.932	0.969	0.974	0.982	0.978	0.978	0.979	0.991	0.997			
Lu	0.886	0.888	0.921	0.94	0.971	0.968	0.977	0.971	0.97	0.972	0.985	0.993	0.998		
Sc	0.874	0.861	0.896	0.924	0.955	0.943	0.953	0.938	0.93	0.928	0.936	0.936	0.943	0.944	
Y	0.69	0.705	0.735	0.773	0.862	0.958	0.939	0.965	0.975	0.972	0.966	0.952	0.928	0.917	0.865

5.5.5 Sources of REEs in allotment soils

In most of the allotment topsoils and subsoils, the main origin of the REEs was the soil parent material because the distribution of REEs in the environment under natural conditions is governed by the mineralogical composition of the parent material, along with geochemical and biological processes (Zhang et al., 2001). Weathered soils and rocks are also important sources of REEs in soils (Price, 1995). Soils which are developed on sandstones, acid and basic igneous rocks are more enriched in REEs as compared to soil which is developed on calcareous rocks (Hu et al., 2006, Laveuf and Cornu, 2009, de Sá Paye et al., 2016). It is considered that alkali feldspar (K-Feldspar) and plagioclase are important minerals present in sandstone which contain low abundances of REEs but also show a positive Eu-anomaly. This enrichment of Eu results from substitution of Eu^{2+} with Sr^{2+} due to its larger size as compared to other trivalent REEs (Edmunds et al., 1982, Taylor et al., 1985). Most soil in Nottingham is dominated by sandstones so it might be possible that K-Feldspar is a common factor explaining the positive anomaly of Eu observed in most of the allotment topsoils and subsoils.

The enrichment of most topsoils compared to subsoils indicated that, beside the main influence of parent material on the abundances of REEs, there were also other sources of REEs in the allotment soils. For example, application of fertilizers can be one of the sources responsible for enrichment of REEs. Phosphate fertilizers are known as the main direct source of REEs in agricultural soils because P-containing minerals (apatites) have a high affinity for REEs (Todorovsky et al., 1997). It has also been reported that the long term application of calcium superphosphate leads to increased concentrations of REEs

in surface soils (Zhang and YE, 2006). The other possible sources could be waste ash which can be applied to cultivated land as liming agent. In a study conducted on Japanese agricultural soils by Zhang et al. (2001) it was reported that the continuous application of waste ash, such as sewage sludge ashes and incinerator bottom ashes, could increase the concentration of Sc, Sm, Gd, Tb and Eu in soils. In the current study the positive anomalies of Sm, Eu and Gd in the crust-normalized pattern also showed some influence most likely due to application of fertilizers.

Atmospheric deposition is another important pathway for REEs to enter soils. Wet atmospheric deposition i.e., rainfall or snow is more significant as compared to dry deposition (Zhang et al., 1999). Studies have been conducted to distinguish between the different sources of REEs in the atmosphere through the use of REEs ratios (such as La/Sm, La/Ce etc.) which are normally used as tracers for identification of sources (Wang et al., 2001). Olmez and Gordon (1985) in their study reported that ratios of La to other REEs and V could be used to differentiate emission of REEs from petroleum-refinery and coal power plants. They found that the ratio of La to other REEs and V in coal-burning sources and in the crust are very similar. Nottingham is an old city with a history of heavy coal burning which must have had some influence on the REE composition of the allotment soils. The ratios of La to other REEs and V in topsoils and subsoils of individual allotment sites are shown in Table 5.6; it can be seen that, although there was variation between the sites, average values for La/Sm, La/Ce, La/Yb and La/V were very close to those reported for coal power plants by Olmez and Gordon (1985).

Table 5.6: Ratio of La to other REEs and V in topsoils and subsoils of individual allotment sites

Allotment sites	**La/Sm**	**La/Ce**	**La/Nd**	**La/Yb**	**La/Lu**	**La/V**
PF (top)	*5.0*	*0.47*	*1.01*	*14*	*96*	*0.19*
ST (top)	*5.1*	*0.48*	*1.04*	*18*	*116*	*0.38*
CN (top)	*4.9*	*0.48*	*1.00*	*18*	*115*	*0.25*
MP (top)	*4.6*	*0.47*	*0.97*	*16*	*104*	*0.22*
MR (top)	*4.8*	*0.48*	*0.99*	*17*	*110*	*0.37*
BH (top)	*5.3*	*0.48*	*1.05*	*18*	*117*	*0.72*
SN (top)	*5.4*	*0.48*	*1.08*	*18*	*116*	*0.30*
WT (top)	*5.4*	*0.49*	*1.08*	*19*	*125*	*0.43*
WM (top)	*5.1*	*0.48*	*1.03*	*18*	*116*	*0.34*
PF (sub)	*5.3*	*0.48*	*1.04*	*17*	*113*	*0.28*
ST (sub)	*5.1*	*0.48*	*1.03*	*17*	*109*	*0.38*
CN (sub)	*5.6*	*0.49*	*1.11*	*17*	*110*	*0.18*
MP (sub)	*5.4*	*0.48*	*1.07*	*17*	*114*	*0.19*
MR (sub)	*5.3*	*0.48*	*1.05*	*19*	*122*	*0.51*
BH (sub)	*6.0*	*0.48*	*1.12*	*19*	*125*	*0.54*
SN (sub)	*6.1*	*0.48*	*1.13*	*21*	*134*	*0.27*
WM (sub)	*5.4*	*0.48*	*1.06*	*18*	*117*	*0.35*
All sites (top soils)	*5.1*	*0.48*	*1.03*	*18*	*114*	*0.35*
All sites (sub soils)	*5.3*	*0.47*	*1.06*	*18*	*114*	*0.34*
Coal power plant	*5.2 ± 0.5*	*0.51 ± 0.04*	*1.6 ± 0.15*	*18 ± 4*	*80 ± 17*	*0.30 ± 0.08*

5.6 Platinum Group Elements

5.6.1 Investigation of interferences in the determination of PGEs by ICP-MS.

Details regarding the investigation of different interferences that are observed in the determination of PGEs in test samples are given in Appendix B. Also the results of PGEs determined in allotment soils in different modes have been compared.

5.6.2 Concentration of PGEs in allotment soils

The concentrations of PGEs measured in selected allotment topsoils and subsoils generally fell below the detection limits (DLs) of the ICP-QQQ-MS. This may indicate that allotment soils were not substantially influenced by PGEs, in contrast to other studies where PGEs have been reported at greater concentrations (Whiteley and Murray, 2003, Ladonin, 2018). The procedure used for soil digestion (HF, $HClO_4$, HNO_3) and the resulting dilutions required contributed to the low analytical concentrations of PGEs.

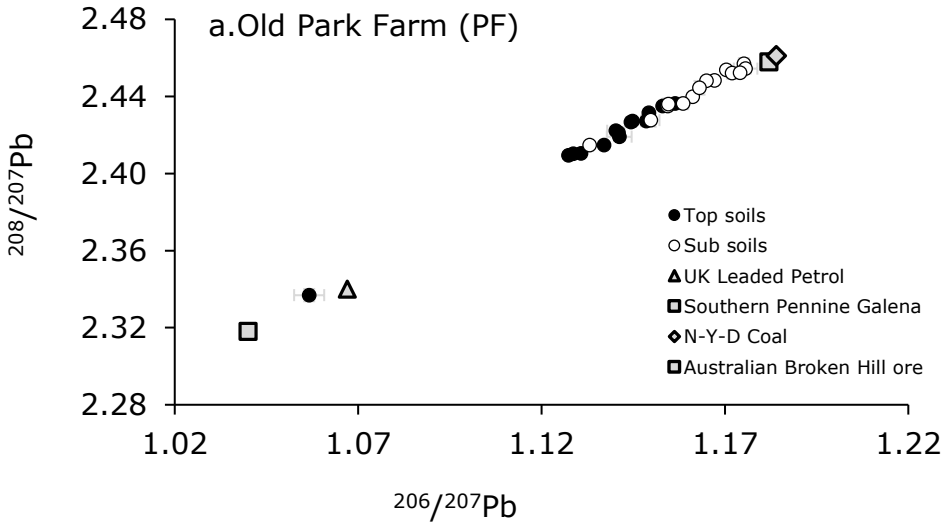
5.7 Characterisation of Pb isotopic signatures

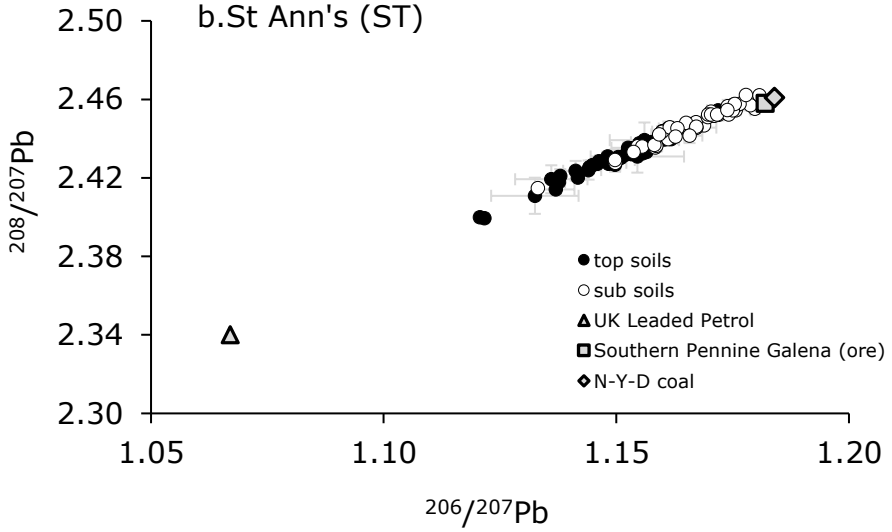
Binary plots ($^{206}/^{207}$Pb versus $^{208}/^{207}$Pb) for topsoils and subsoils for individual allotment sites are shown in Figure 5.8; major end member values for anthropogenic (i.e. leaded petrol) and geogenic sources of Pb such as local Pennine ore Pb and UK coal Pb are included. The measured Pb isotopic signatures for all topsoils from the allotments fell close to the general mixing line formed between Pb_{petrol} and $Pb_{geogenic}$ sources which confirmed these two end-members as the dominant sources of Pb in soils. The $^{206}/^{207}$Pb ratios in topsoils across all allotments were in the range of 1.106 - 1.177 (Figure 5.9),

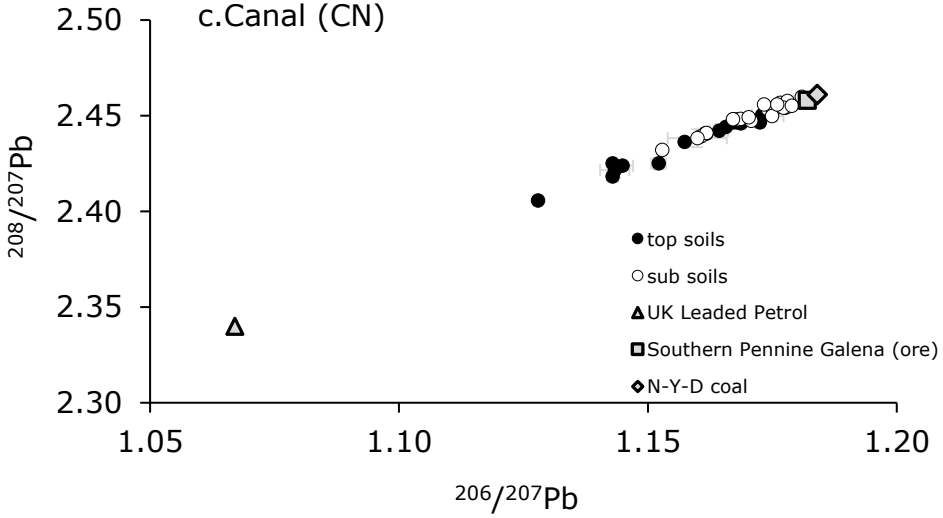
with the exception of only one soil sample from site PF-Q233 (ratio = 1.057). This range of values is in agreement with the isotopic composition of topsoils from rural roadsides and London soils measured by (Mao et al., 2014) i.e., $^{206}/^{207}$Pb in the range of 1.080-1.160. The sample (PF-Q233) with the lowest isotopic signature for $^{206}/^{207}$Pb (i.e., 1.057) appeared to reflect the isotopic signature of Australian (Broken Hill) ore (1.04), also shown in Figure 5.8 (a). A similar observation was made by Farmer et al. (2011), where a sample with a high concentration of Pb (2160 mg kg^{-1}) from an urban soil in Glasgow, Scotland had an isotopic signature close to that of Australian ore. The $^{206}/^{207}$Pb ratios in subsoils across all allotments also fell close to the general mixing line with values in the range 1.133 - 1.185. However, compared to topsoils, subsoils were clustered towards the geogenic sources.

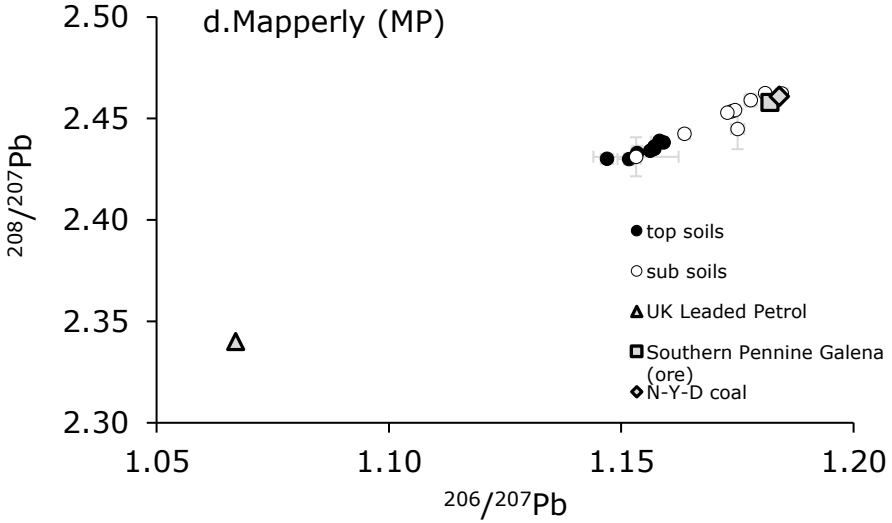
During the 1960s and 1970s, alkyl Pb additives became the most important sources of atmospheric Pb pollution throughout the world. However, despite the phasing out of leaded gasoline over the last three decades, Pb_{petrol} is still prevalent in soils, originally derived from atmospheric deposition (Cheng and Hu, 2010). Therefore, the contribution of Pb_{petrol} to Pb_{total} was also calculated for both topsoils and subsoils (excluding sample PF-Q233) (Figure 5.10). A t-test pairwise comparison showed that the mean proportion of Pb_{petrol} in most of the topsoils (except site BH) was significantly different from the proportion in subsoils ($p<0.001$). As expected, topsoils showed a greater contribution from Pb_{petrol} than subsoils. In topsoils the contribution of Pb_{petrol} to Pb_{total} was highest at sites PF, WT and MR where it was in the range of 30-35%; it was lowest (i.e., 18%) at the Blenheim (BH) and Canal (CN) sites. In all other allotments the contribution of Pb_{petrol} fell in the range 23-27%. Other studies have also shown higher concentrations of Pb_{petrol} in surface horizons as compared to deeper soils

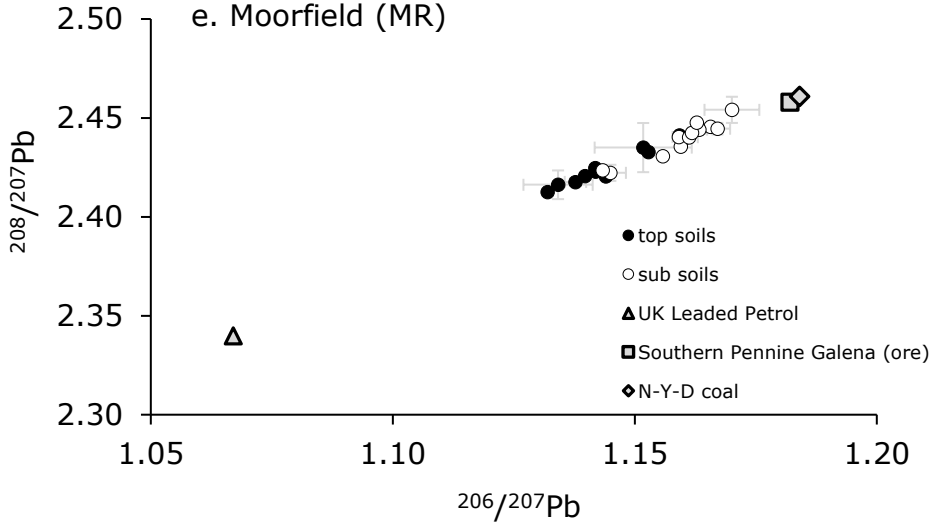
where natural Pb was mostly identified as the major source of Pb (Gulson et al., 1981). For example Hansmann and Köppel (2000) used Pb isotope ratios ($^{206}/^{207}$Pb, $^{206}/^{204}$Pb and $^{208}/^{204}$Pb) to identify different sources of anthropogenic and natural sources of Pb in urban soils of Switzerland. Anthropogenic sources of pollutants were found generally to be less radiogenic than the unpolluted soils and Pb_{petrol} from vehicular exhaust was the least radiogenic in composition across all anthropogenic sources.

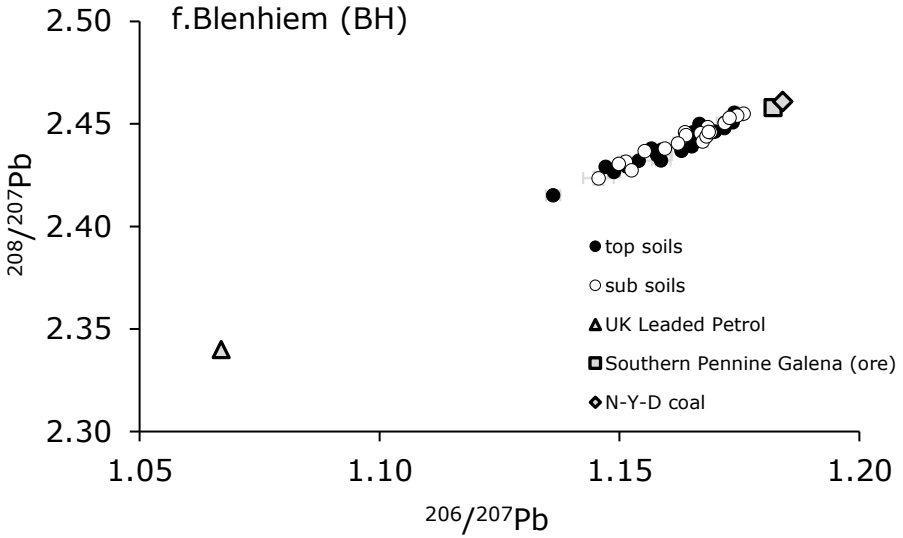

a.Old Park Farm (PF)
2.48
2.44
2.40
2.36
2.32
2.28
1.02
1.07
1.12
1.17
1.22
208/207Pb
206/207Pb
Top soils
Sub soils
UK Leaded Petrol
Southern Pennine Galena
N-Y-D Coal
Australian Broken Hill ore

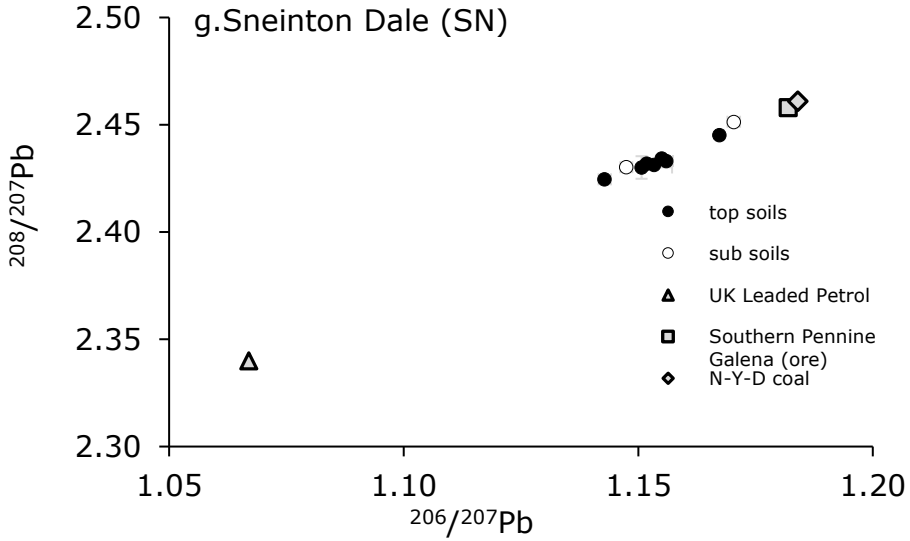

b.St Ann's (ST)
2.50
2.46
2.42
2.38
2.34
2.30
1.05
1.10
1.15
1.20
208/207Pb
206/207Pb
top soils
sub soils
UK Leaded Petrol
Southern Pennine Galena (ore)
N-Y-D coal

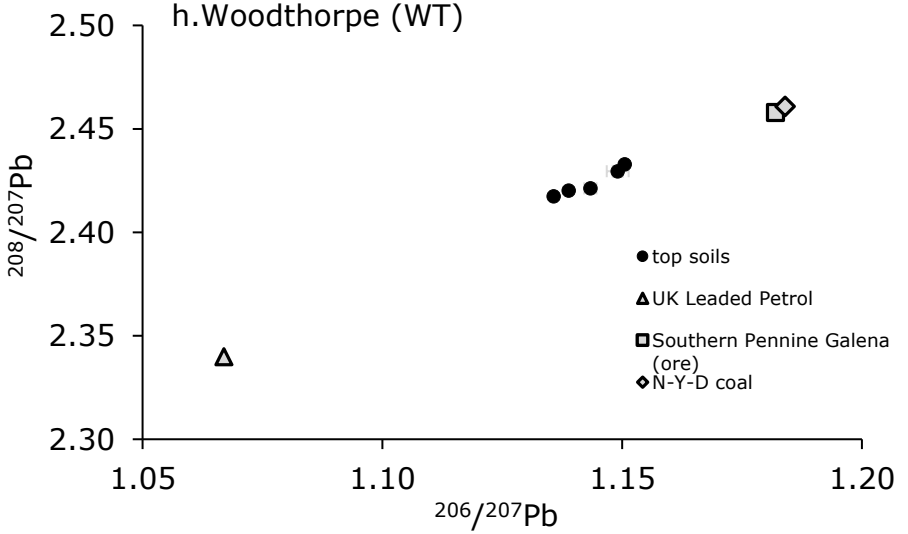

c.Canal (CN)
2.50
2.45
2.40
2.35
2.30
1.05
1.10
1.15
1.20
208/207Pb
206/207Pb
top soils
sub soils
UK Leaded Petrol
Southern Pennine Galena (ore)
N-Y-D coal


d.Mapperly (MP)
2.50
2.45
2.40
2.35
2.30
1.05
1.10
1.15
1.20
208/207Pb
206/207Pb
top soils
sub soils
UK Leaded Petrol
Southern Pennine Galena (ore)
N-Y-D coal


e. Moorfield (MR)
2.50
2.45
2.40
2.35
2.30
208/207Pb
1.05
1.10
1.15
1.20
206/207Pb
top soils
sub soils
UK Leaded Petrol
Southern Pennine Galena (ore)
N-Y-D coal


f.Blenhiem (BH)
2.50
2.45
2.40
2.35
2.30
208/207Pb
1.05
1.10
1.15
1.20
206/207Pb
top soils
sub soils
UK Leaded Petrol
Southern Pennine Galena (ore)
N-Y-D coal


g.Sneinton Dale (SN)
2.50
2.45
2.40
2.35
2.30
208/207Pb
1.05
1.10
1.15
1.20
206/207Pb
top soils
sub soils
UK Leaded Petrol
Southern Pennine Galena (ore)
N-Y-D coal


h.Woodthorpe (WT)
2.50
2.45
2.40
2.35
2.30
208/207Pb
1.05
1.10
1.15
1.20
206/207Pb
top soils
UK Leaded Petrol
Southern Pennine Galena (ore)
N-Y-D coal

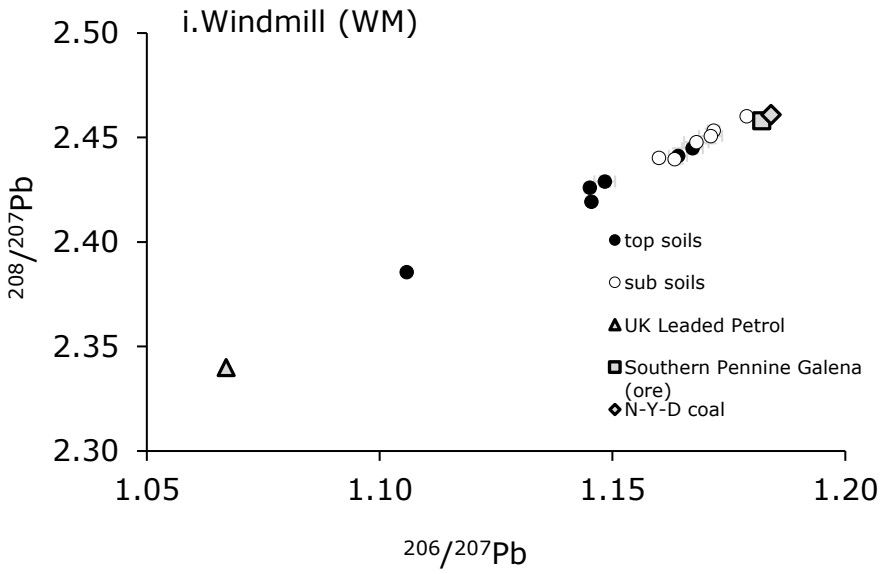


Figure 5.8: Binary plots showing the isotopic ratios $^{206}/^{207}$Pb vs $^{208}/^{207}$Pb for individual allotment topsoils and subsoils with median values from UK leaded petrol, Southern Pennine Pb ore (Galena) and N-Y-D coal shown for comparison.

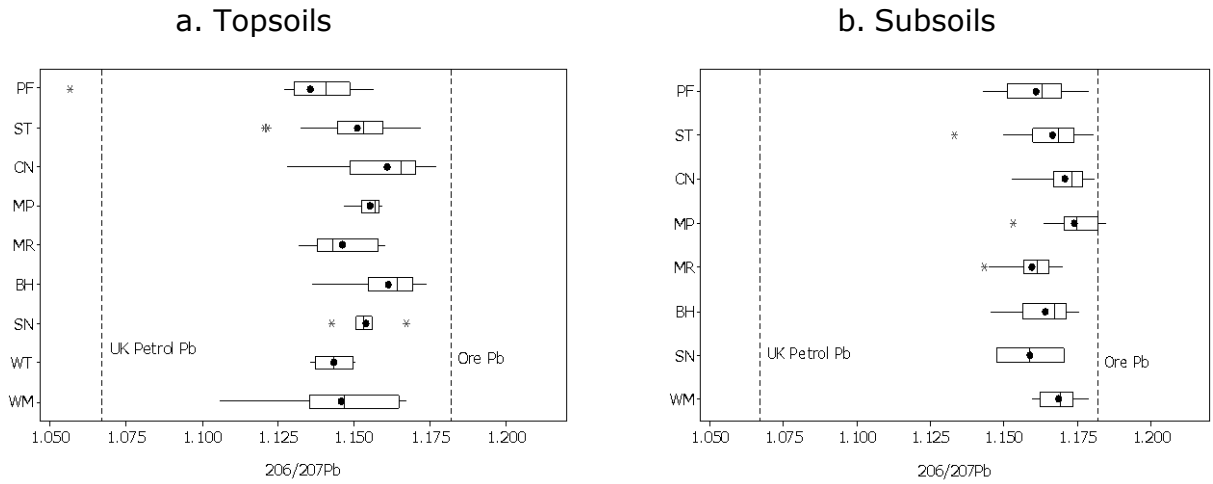


Figure 5.9: Lead isotopic ratio $^{206}/^{207}$Pb in (a) topsoils and (b) subsoils of individual allotment sites are shown as box and whisker plots. Outliers are shown as asterisks. Mean is shown as a symbol (•) and median as a line. The broken lines indicates the range of reference sources (UK ore and UK leaded petrol).

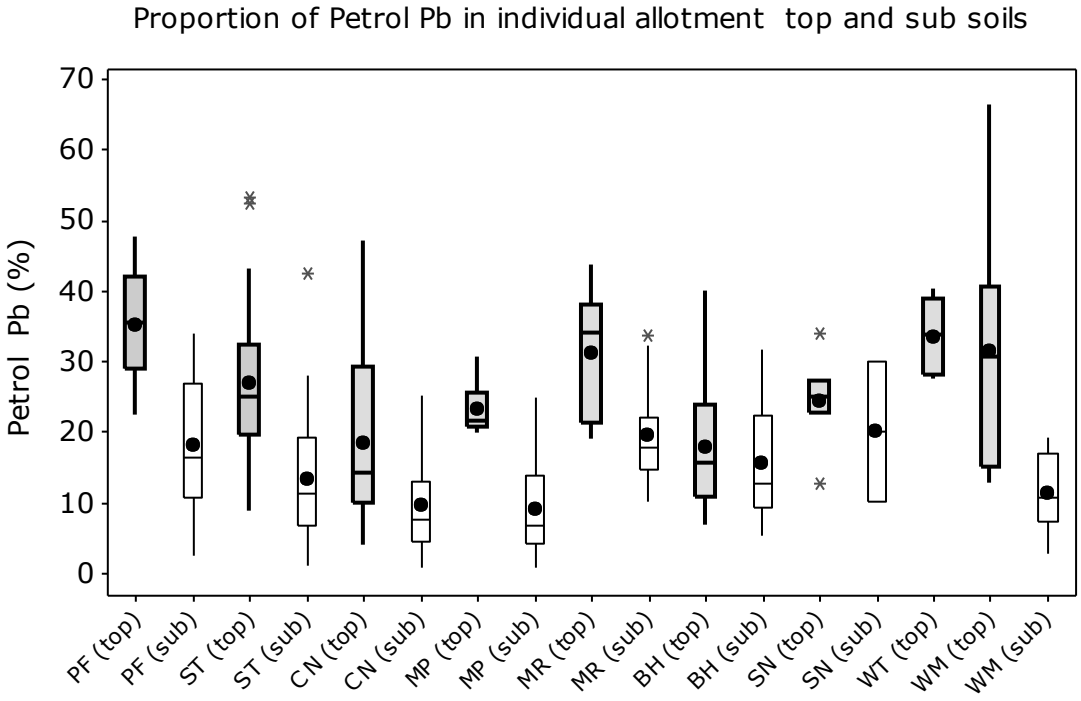


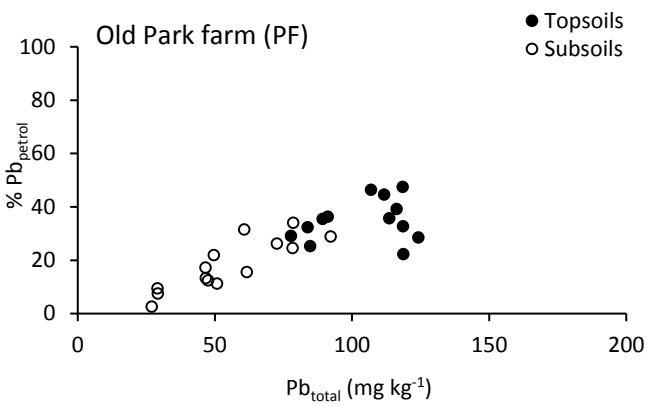
Figure 5.10: Proportion of Pb_{petrol} in allotment topsoils and subsoils

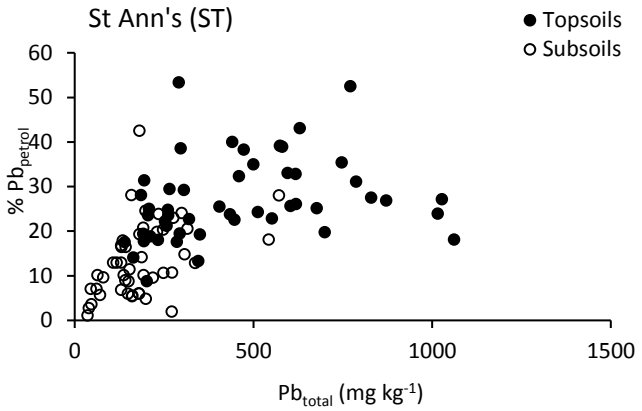
5.8 The relationship between Pb_{petrol} and Pb_{total} in top and subsoils

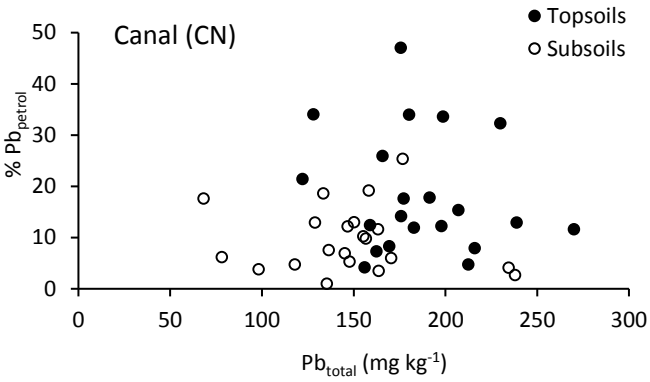
The relationship between Pb_{petrol} and Pb_{total} in both topsoils and subsoils of individual allotment sites was evaluated and is shown in Figure 5.11. A positive relationship between $\%Pb_{petrol}$ and Pb_{total} would suggests that past vehicular exhaust emissions were the main source determining soil Pb concentration at the site. Similarly a negative relationship would suggest that the dominant influence is from a geogenic source (e.g., coal). A flat trend would mean that the relative contribution from Pb_{petrol} and Pb_{coal} was constant across all soils despite, differences in total contaminant load, and a scattered pattern would indicate that there was local variation in relative inputs from the two main sources.

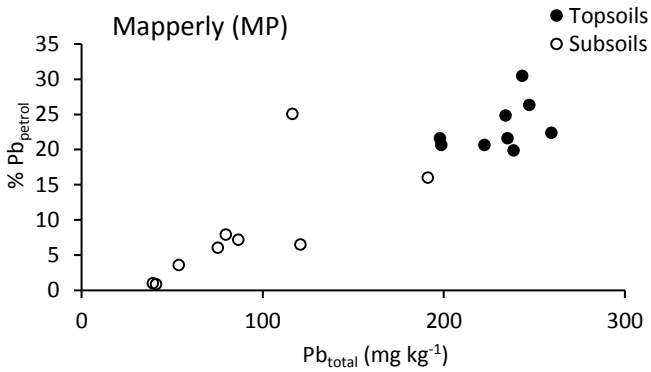
Among all allotments, an overall strong positive trend ($r= 0.828$ and $r = 0.892$, $p \leq 0.000$) was observed at sites PF and MP when both topsoils and subsoils were considered together. This showed that in these allotments there was same mix of Pb_{petrol} in both topsoils and subsoils and that the variation in soil Pb content was largely determined by Pb_{petrol}. At site ST and MP, there was also a positive trend but it was moderate ($r = 0.554$ and 0.586, $p = 0.000$). Furthermore, the contamination of subsoils with Pb_{petrol} indicated migration of Pb_{petrol} from topsoils to subsoils. Other studies have also shown the migration of anthropogenic Pb into deeper layers in soils. For example Izquierdo et al. (2012) in a study on alluvial soils showed evidence of translocation of Pb_{petrol} from the surface to soils layers of at least 35 cm depth. Similarly in a study conducted by Teutsch et al. (2001) they reported the migration of Pb_{petrol} into soil layers below the topsoil i.e., 20-30 cm. The migration velocity of Pb_{petrol} in

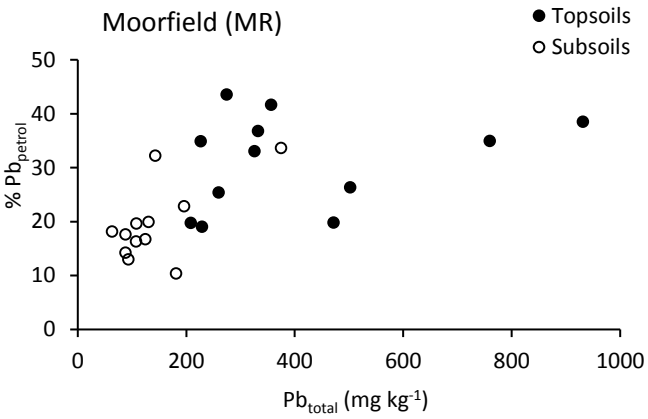
Mediterranean soils of Israel was determined as 0.5 cm year^{-1} by Erel et al. (1997). Another reason for contamination of subsoils with Pb_{petrol} might be due to the cultivation activities in the allotments, such as ploughing and deep incorporation of manures etc. which can result in mixing of topsoils with subsoils. In the topsoils from site WT a strong significant (i.e., $r = 0.835$, $p \leq 0.05$) positive trend was also observed which showed Pb_{petrol} was the dominant contaminant source in these soils. The strong relationship between Pb_{petrol} and Pb_{total} and the results of cluster analysis (section 5.4.3) where Pb_{petrol} was clustered separately makes it more evident that the closeness of the Mansfield road to this site was the main factor determining Pb contamination of these soils. In some of the allotments sites such as CN, SN, BH and WM there was no trend in both topsoils and subsoils. The data points were scattered which suggested the distribution pattern of different Pb sources (i.e., Pb_{petrol} and Pb_{coal}) varied locally depending upon the history and site location.

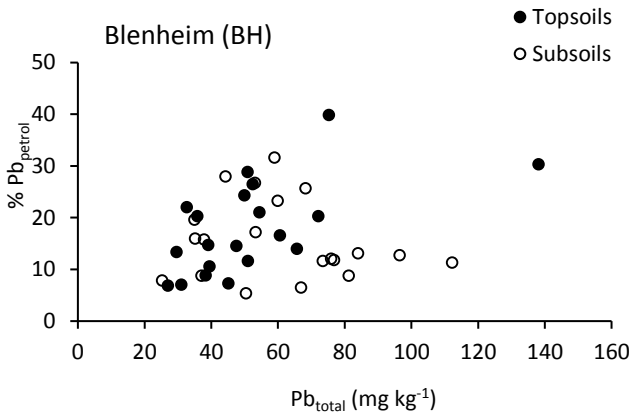

Old Park farm (PF)
Topsoils
Subsoils
% Pb$_{petrol}$
Pb$_{total}$ (mg kg^{-1})

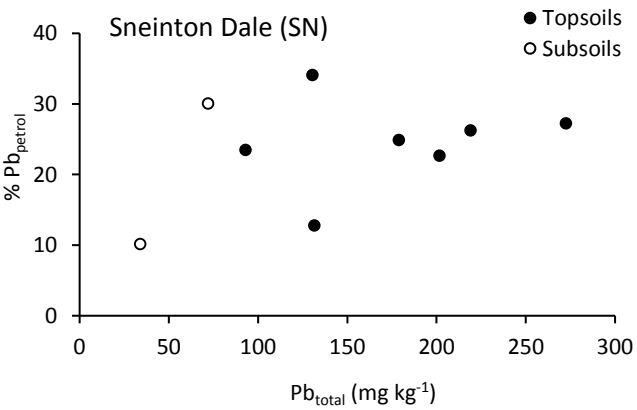

St Ann's (ST)
Topsoils
Subsoils
% Pb$_{petrol}$
Pb$_{total}$ (mg kg^{-1})

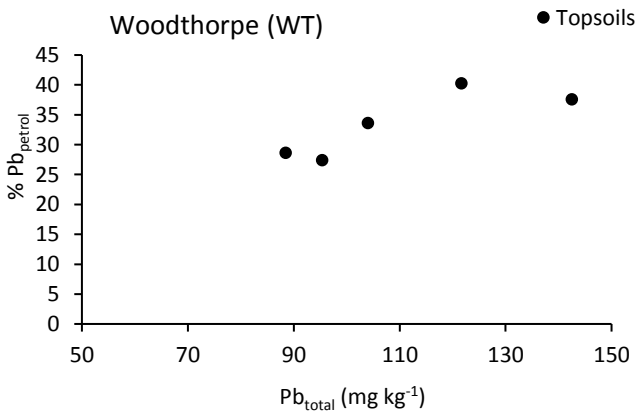

Canal (CN)
Topsoils
Subsoils
% Pb$_{petrol}$
Pb$_{total}$ (mg kg^{-1})


Mapperly (MP)
Topsoils
Subsoils
% Pb$_{petrol}$
Pb$_{total}$ (mg kg^{-1})


Moorfield (MR)
Topsoils
Subsoils
% Pb$_{petrol}$
Pb$_{total}$ (mg kg^{-1})


Blenheim (BH)
Topsoils
Subsoils
% Pb$_{petrol}$
Pb$_{total}$ (mg kg^{-1})


Sneinton Dale (SN)
Topsoils
Subsoils
% Pb$_{petrol}$
Pb$_{total}$ (mg kg^{-1})


Woodthorpe (WT)
Topsoils
% Pb$_{petrol}$
Pb$_{total}$ (mg kg^{-1})

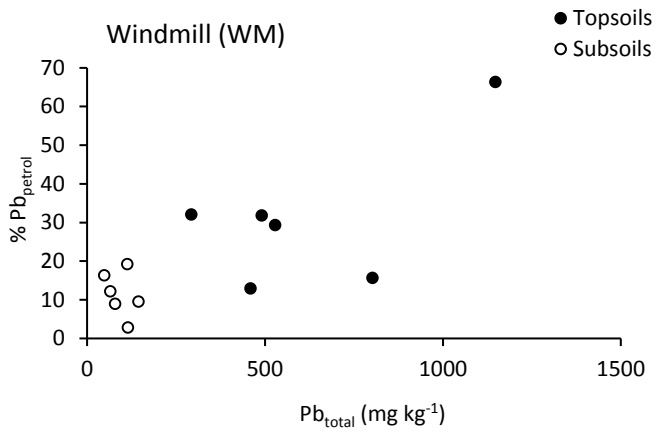


Figure 5.11: Relationship between $\%Pb_{petrol}$ and Pb_{total} in topsoils and subsoils of individual allotment sites.

5.9 Conclusions

Results showed that the topsoils of different allotment sites (except Blenheim; BH) were enriched with trace metals, relative to the subsoils, and the variation observed in trace metal concentrations among different allotment sites could be, in part, associated with allotment location and history. Allotments located in close proximity to potential pollutant sources were more highly contaminated although quantifying this relationship remains a challenge. A cluster analysis of multi elements in combination with source-apportionment of Pb from isotopic characteristics was helpful in attempting to understand the main anthropogenic sources. In the allotment soils the origin of REEs was primarily natural sources. However, a comparison of abundance ratios with those of the mean upper continental crust (UCC), and an examination of enrichment factors suggested that there was also a small influence from anthropogenic inputs, such as fertilizers. In the case of PGEs, the measured concentrations were below the DLs. Overall, the determination of REEs and PGEs in the allotment soils proved to be of limited value in helping to discriminate between specific sources of contamination.

The determination of Pb isotopic ratios in allotment topsoils and subsoils was most helpful in characterizing Pb sources and it confirmed that Pb_{petrol} and $Pb_{geogenic}$ were the dominant sources of Pb in these soils. In subsoils the presence of Pb_{petrol} revealed migration of mobile Pb_{petrol} from topsoils. The relationship between Pb_{petrol} and Pb_{total} further helped in identifying allotments (i.e., PF, ST, MP, MR and WT) where the main influence was from vehicles. Whereas the absence of trend observed at some of the allotments (i.e., CN, SN, BH and WM) suggested variation in the inputs of different sources.

An important finding from the examination of isotopic evidence in topsoils and subsoils was the extent to which Pb_{petrol} had apparently migrated down the soil profile into the subsoil. It is likely that the two main diffuse sources of Pb on the sites were coal burning and Pb_{petrol}, both arriving as aerial deposition (although coal ashes may also have been applied directly). It seems reasonable therefore to assume that the distribution of Pb in the soil from the two sources would be a function of the timing and magnitude of the inputs but also of the lability or solubility of the Pb in the two particulate materials.

In the following chapter this avenue of research is pursued further by determining the composition of soil 'fractions' using a SEP to isolate trace elements associated with particular soil phases, examine the Pb isotopic composition within the fractions and to determine 'reactivity' of trace metals by ID method.

6 Chapter 6: Use of common approaches to study behaviour and sources of pollutants in allotment soils

6.1 Introduction

The potential risk and toxicity of heavy metals in soil is a function of metal lability and bioavailability, which is associated with the different fractions of metal and the processes i.e., chemical and physical that control transformations between fractions (Schröder et al., 2005, Maas et al., 2010, Rodrigues et al., 2010). Total content of heavy metals in soil gives information only about possible enrichment and does not provide sufficient information regarding potential risk and toxicity of metals to the surrounding environment and human health (Nolan et al., 2003, Ure and Davidson, 2008). Heavy metals, after entering the soil system, are distributed into various soil constituents through different processes such as precipitation of contaminants, ion exchange, adsorption, complexation with organic matter. However, changes in environmental conditions can re-mobilise the metals to varying degrees (Yuan et al., 2004). The total concentrations of heavy elements may also be operationally divided into 'reactive' and 'non-reactive' fractions. The reactive fraction of heavy metals is most likely to be responsible for biologically harmful effects (Rieuwerts et al., 2006). In order to evaluate the toxic effects or deficiencies of heavy metals in the environment, it is important to understand the main processes controlling distribution of metals within the soil matrix (Nolan et al., 2003, Degryse et al., 2004, Peijnenburg et al., 2007). The major factors responsible for changes in reactivity or lability of trace metals are soil physicochemical properties (pH, redox potential, temperature etc.) and the nature of soil solid constituents, such as organic matter, clays, Fe/Mn oxides, phosphates, sulphides and carbonates (Ledin et al., 1996, Degryse et al., 2009,

Ottosen et al., 2009, Rodrigues et al., 2010). For example, the lability of trace metals in alkaline soil is generally low in contrast to acidic peat soils where lability is generally highest. In alkaline soils, the presence of mineral oxides and carbonates are responsible for reducing the reactivity of cationic trace metals by adsorption and co-precipitation (Degryse et al., 2004, Buekers et al., 2007). In contrast, the lability of Pb is reported to be limited due to the formation of discrete Pb-containing minerals such as Pb phosphates (e.g. chloropyromorphite, $Pb_5(PO_4)_3Cl$), which remains stable under a wide range of conditions (Zhang et al., 1997, Ryan et al., 2001, Miretzky and Fernandez-Cirelli, 2008).

The other major factor determining the lability of trace metals in soil is the source of contaminants (Ledin et al., 1996, Mao et al., 2014). Contaminants originating from sources, e.g. natural or anthropogenic sources, will have different intrinsic metal labilities (Atkinson et al., 2011b). It has been reported that Pb originating from petrol or coal combustion is more labile than Pb within primary minerals; geogenic Pb is mostly associated with 'residual' fractions in soils (Mao et al., 2014, Shetaya et al., 2018). Soil and trace metal contact time is also considered as an important factor that affects lability as both metal fixation in soil minerals and release from contaminant sources into soil can be slow processes (Tye et al., 2003). For example, the release of Pb from sulphide ore minerals in an aerobic topsoil environment occurs via very slow weathering processes, such as oxidation, over protracted contact times (Atkinson et al., 2011b).

Different approaches have been used to provide insight into these processes but the most commonly adopted techniques for characterizing the chemical fractions and reactivity of trace metals in soils are sequential extraction procedures (SEPs) and isotopic dilution (ID) techniques. The most widely applied sequential extractions procedures are the well-known Tessier procedure (Tessier et al., 1979)

and BCR approaches (Ure et al., 1993); many adaptations of these SEPs have been published (Campanella et al., 1995, Martin et al., 1998, Ariza et al., 2000, Smeda and Zyrnicki, 2002). In SEPs, trace elements are allocated to operationally defined geochemical fractions such as 'Exchangeable', 'Carbonate-bound', 'Oxide-bound', 'Organic matter or sulphide-bound' and 'Residual' (Degryse et al., 2011). In an SEP scheme, the order of different fractions (F) e.g., F1-F5, is essentially a sequence of decreasing solubility (Lu et al., 2003). The extraction steps in SEPs may vary from 3 to 7 depending on the aim of the study. Sequential extraction procedures can help in identifying the main binding sites of metals and their relative binding strength in different fractions of soil. Generally metals in the exchangeable and carbonate fractions are held by weak electrostatic forces on geocolloids and precipitated with carbonate minerals respectively. Metals in exchangeable and carbonate fractions are potentially the most available, particularly when environmental conditions in soil change - such as pH. Metals associated with oxides (Fe/Mn) and organic matter are considered relatively stable under normal conditions and metal ions in the residual phase are the least soluble (Wong et al., 2002, Kazi et al., 2005, Bakircioglu et al., 2011). In order to identify the different fractions in which metals may be present in soil, a series of extractants with increasing extraction strength is used to dissolve target metals (Degryse et al., 2011). Several researchers have highlighted the limitations of SEPs such as problems of incomplete dissolution and re-adsorption into different phases during extraction (Gleyzes et al., 2002). The problem of sensitivity of these procedures to minor changes for example, re-adsorption of metals has been found when there is a change in pH from the previous SEP step. This re-adsorption can result in 'carry over' and overestimation of subsequent metal fractions (Shan and Chen, 1993, Gleyzes et al., 2002, Labanowski et al., 2008, Degryse et al., 2011).

Also the application of SEPs in risk assessment for planning and developmental purposes is largely absent because the overall 'labile' fraction does not correspond to any single SEP fraction. Therefore, bioavailability of metals to plants is difficult to interpret only based on SEP results. The SEP data typically only gives some indication about the reactivity of metals because the most readily soluble species are generally extracted in the first fraction and most recalcitrant species in the later fractions (Harrison et al., 1981, Gibson and Farmer, 1986, Ottosen et al., 2009). Despite these inherent limitations the literature on SEPs is comparatively large compared to other more sophisticated approaches as the latter can be expensive and the equipment required may not be readily available (Degryse et al., 2011). A great deal of effort has been expended in the modification of SEPs in terms of reagent use, shaking time, soil:solution ratio etc. to obtain more discrete dissolution of the target fraction. In a few studies, different sources of Pb in individual fractions of SEPs have been investigated by measuring Pb isotope ratios. This combination of Pb partitioning in different fractions and Pb isotope ratios can also clarify the processes controlling behaviour of Pb in soil (Teutsch et al., 2001, Emmanuel and Erel, 2002, Bacon et al., 2006). For example, Emmanuel and Erel (2002) measured Pb isotope ratios in individual fractions of Czech forest soils to examine the mechanism of natural and anthropogenic Pb partitioning and revealed that natural Pb was mainly associated with residual and oxide fractions whereas anthropogenic Pb was in fractions associated with surface bound and organic matter phases. In a study by Wong et al. (2002), sources of Pb were identified in agricultural soils of the Pearl River Delta (South China) through the use of Pb isotopes and it was shown that Pb bound to Fe-Mn oxides and organic/sulphide fractions was the stable form of anthropogenic Pb after deposition to soil.

Isotopic dilution may be used to measure the reactive or 'labile' fraction, which is the amount of isotopically exchangeable metal in soil and is traditionally known as the E-value (Young et al., 2000b). The E-value may represent the fraction of metal that is in a readily available pool for plant uptake and transport (Ahnstrom and Parker, 2001). Isotopic dilution method is considered the most appropriate method for discriminating labile and non-labile pools of metals in soils and therefore could be used in site-specific risk assessments. However, due to operational limitations, this technique has been less preferred than SEPs (Young et al., 2005, Degryse et al., 2011). Initially ID was used to measure the availability of essential plant nutrients but later the technique was widely applied in studies of toxic elements and their reactivity in environment. Both radioactive and stable isotopes are used for measuring isotopically exchangeable pools of elements (Lopez and Graham, 1972, Echevarria et al., 1998, Smolders et al., 1999, Gäbler et al., 1999, Ahnstrom and Parker, 2001, Nolan et al., 2004). Recently use of stable isotopes have been preferred over radioactive isotopes because the latter are associated with disposal problems, exposure to radiation and also the non-availability of radioactive isotopes for some elements. With greater availability and widespread access to inductively coupled plasma mass spectrometry (ICP-MS) in the last two decades, it has been possible to expand the application of isotopic dilution techniques to those elements for which radioactive isotopes are not available (Montaser, 1998, Young et al., 2007, Huang et al., 2011, Izquierdo et al., 2012). Stable isotopes also have the advantage of allowing in-field isotopic experiments without environmental or health concerns (Hamon et al., 2008). Recently multi-element isotopic dilution approach has been developed and is used for simultaneous assessment of reactivity of different trace metals in soil (Marzouk et al., 2013b, Nazif et al., 2015, Izquierdo et al., 2017, Shetaya et al., 2018). This

simultaneous assessment of different trace metals using stable isotopes is considered more accurate and cost effective as compared to single and sequential extraction procedures.

To determine the isotopically exchangeable pool of trace metals, soil samples are suspended in dilute electrolyte such as $Ca(NO_3)_2$ or $CaCl_2$ for a specific period, known as a pre-equilibration time, after which a small amount of an isotope of the analyte is added to the suspensions. There are no guidelines available regarding the choice and concentration of stable isotopes to be used in ID methods but the amount of enriched stable isotope solution (spike) added should be sufficient to cause a significant change in the isotopic ratio of the spiked soil in comparison to the native/natural isotopic composition of the system. This added enriched stable isotope solution should not be large enough to perturb the pre-existing ratio of labile: non-labile metal of the soil. After a given reaction time, the extent to which this spike isotope has mixed with the indigenous soil metal is determined by analysis of isotopic ratios, usually in the soil solution phase. This permits quantification of the isotopically exchangeable metal concentration (Gäbler et al., 1999, Midwood, 2007, Hamon et al., 2008, Degryse et al., 2011). One complication to this approach is that the metal in the soil solution phase may not all be labile as some may be bound within suspended colloidal particles (SCPs <0.1 μm) in a non-labile form. The effect of non-labile metals bound within SCPs has been shown especially in soils with a large content of humus and carbonates (Marzouk et al., 2013a). Similarly, a range of studies has shown that non-labile SCP fractions were associated mostly with dissolved organic matter and hydrous oxide or carbonate particles (Lombi et al., 2003). Non-labile SCP fractions may not be readily available to plants but presumably can enhance the mobility of trace metals in soils. Therefore, the standard ID technique has been modified by several

researchers using a resin purification step in order to reduce the effect of non-labile metals in SCP and calculate the true isotopically exchangeable pool of metal (Lombi et al., 2003). In the 'resin purification' method, an ion-exchange 'chelex' resin is used and is introduced to separated filtered supernatant solution. This resin is then equilibrated, washed and eluted with acid to determine the true isotope ratios for the solution phase (and subsequently the E-value). The chelex resin purification method is based on the two assumptions that: i) the resin is not strong enough to extract non-labile metals from the SCPs and ii) the resin is cleaned of all colloidal particles prior to acid elution and isotope ratio analysis.

Studies have also been conducted using a combination of techniques in an attempt to provide insight into the complex interactions in the soils. This includes comparison of (and combination of) different methods such as ID and SEP (Atkinson et al., 2011b, Marzouk et al., 2013b, Mao et al., 2014). For example Degryse et al. (2011) compared three methods, including isotopic exchange (IE), speciation by XAFS spectroscopy and fractionation by sequential extraction for characterization of Zn in contaminated soils. Garforth et al. (2016) applied isotopic dilution *within* an SEP operation to assess the validity of each step of the SEP.

6.1.1 Aim of chapter

The aim of this chapter was to determine the fractionation of selected trace metals (Ni, Cu, Zn, Cd and Pb) in urban allotment soils. Experimental objectives included determination of the isotopically exchangeable fraction (E-value) by multi-element ID and fractionation of metals using the modified Tessier SEP. The degree of correspondence between these two methods (ID and SEP) was also investigated. The presence of non-labile metals associated with suspended colloidal particles (SCP) in submicron filtered (<0.22 μm) supernatant solutions was also tested by

comparing % E-values measured in filtered solutions (E_{soln}) and resin-treated solutions (E_{resin}).

The effect of common soil properties (pH, organic matter, available P and total elemental concentrations) and the long-term effect of Pb sources on lability of metals were evaluated. The relative contributions of different sources of Pb (i.e., Pb_{petrol} and $Pb_{geogenic}$) to labile and non-labile pools of soils was investigated to examine the influences of source and contact time on lability. The relative contributions of Pb_{petrol} and $Pb_{geogenic}$ in individual fractions of the SEP were calculated using measured Pb isotopic ratios ($^{206/207}$Pb and $^{208/207}$Pb) compared to expected end members (petrol and coal/ore Pb). Finally an attempt was also made to assess the behaviour of Pb_{petrol} with common soil properties in individual SEP fractions.

6.2 Materials and methods

6.2.1 Soil sampling

A set of 59 urban allotment top soils (i.e., ~ 15 cm soil depth; duplicates) from a total of 269 soil samples were selected in order to provide a range of Pb_{total} contents. In most of the soils (n=34) the Pb concentrations were > 400 mg kg^{-1}. As mentioned earlier in Chapter 2, allotment soils were previously collected (2014-2015) and analysed for a range of soil properties in another study by another researcher therefore the same data for basic soil properties including pH, organic matter content (SOM), soil organic carbon (SOC) and available phosphorus (P_{Olsen}) have also been used in this chapter.

6.2.2 Measurement of isotopically exchangeable Pb, Zn, Cd, Cu and Ni in soils using an ID technique

A multi-element isotopic dilution method used to determine the isotopically exchangeable pool (E-values) of five target metals is described in detail in Chapter 2 (Section 2.8). The presence of non-labile metal within SCPs was investigated using a 'Chelex purification method' described in Chapter 2 (Section 2.8.3). The underlying principle is that a cation exchange resin adsorbs only the labile metals which are normally present as free ions, soluble metal complexes and exchangeable metal ions adsorbed onto the surface of sub-micron colloids. The non-labile metal fractions within SCPs are not adsorbed by the resin and remain suspended in the soil solution (Lombi et al., 2003).

The E-values of Ni, Cu, Cd, Zn and Pb were calculated from the ratio of the main spike isotope to one of the non-spiked isotopes (Table 6.1). The E-value (mg kg^{-1}) was calculated according to Eq. (1) (Marzouk et al., 2013b). For comparison purposes, E-values (M_E) are often expressed as a proportion (%M_E) of the total metal content (M_{total}) in the soil, Eq. (2).

$$M_E = \left(\frac{M_{soil}}{W}\right)\left(\frac{C_{spike}\ V_{spike}}{M_{spike}}\right)\frac{\left({}^{Iso1}IA_{spike} - {}^{Iso2}IA_{spike}\, R_{ss}\right)}{\left({}^{Iso2}IA_{soil}\, R_{ss} - {}^{Iso1}IA_{soil}\right)}$$

Eq. (1)

Where M_{soil} and M_{spike} are the average atomic masses of metal in soil and spike, *W* is the weight of soil used (kg), C_{spike} is the gravimetric concentration of the metal in spike solution (mg L^{-1}), V_{spike} is the volume of spike added (L), IA_{spike} and IA_{soil} are the isotopic abundances on a mole basis in the spike and soil solution respectively and R_{ss} is the isotopic abundance ratio of the two isotopes (Iso1:Iso2)

in the spiked soil solution. Results reported for E-values in this study were averages of duplicates with coefficients of variation in the range of 0.06-4.4% for Ni, 0.02-19% for Cu, 0.2-11.9% for Zn, 0.12-18.5% for Cd and 0.06-14.6% for Pb.

$$\% \, \mathrm{M}_E = \frac{\mathrm{M_E}}{\mathrm{M_{total}}} \times 100$$

Eq. (2)

Table 6.1: Isotopic ratios (spiked and unspiked) and their natural isotopic ratio values

Enriched stable isotope (spike)	Isotope Ratio used for calculation	Natural isotopic ratio values
^{204}Pb	^{204}Pb:^{208}Pb	0.0272
^{108}Cd	^{108}Cd:^{111}Cd	0.0695
^{65}Cu	^{65}Cu:^{63}Cu	0.4457
^{70}Zn	^{70}Zn:^{66}Zn	0.0222
^{62}Ni	^{62}Ni:^{60}Ni	0.1386

6.2.3 Calculation of isotopic abundances (IAs) of non-labile metal

Prior to calculation of IAs of ^{206}Pb and ^{207}Pb in the non-labile fraction, it was important to calculate the IAs of ^{206}Pb and ^{207}Pb in Pb_{total} and in Pb_E by excluding the IA of isotope which was added to the samples (i.e., ^{204}Pb) because spiking the samples with ^{204}Pb changed the natural background of ^{204}Pb IA. For example, IA of ^{206}Pb in labile fraction was calculated according to Eq. (3). After calculation of

IAs of ^{206}Pb and ^{207}Pb in both Pb_{total} and Pb_E, IA in non-labile fraction was calculated according to Eq. (4) (Mao et al., 2014). Here an example is given for calculation of IA of ^{206}Pb in non-labile pool. From these IAs of ^{206}Pb and ^{207}Pb in non-labile pool, isotopic ratio ($^{206/207}Pb$) was finally calculated.

$$^{206}\mathrm{Pb}\ (\mathrm{IA}) = \frac{^{206}\mathrm{Pb}}{\mathrm{Sum}\ (^{206}\mathrm{Pb} + {}^{207}\mathrm{Pb} + {}^{208}\mathrm{Pb}\ )}$$

Eq. (3)

$$^{206}\mathrm{IA}_{\mathrm{NL}} = \frac{^{206}\mathrm{IA}_{\mathrm{total}} - (\ \ ^{206}\mathrm{IA}_{\mathrm{L}} \times \mathrm{P}_{\mathrm{L}}\ )}{(1 - \mathrm{P}_{\mathrm{L}}\ )}$$

Eq. (4)

Where $^{206}IA_{NL}$, $^{206}IA_{total}$, $^{206}IA_L$ are the isotopic abundances in non-labile, labile and total soil Pb respectively.P_L is the proportion of labile Pb calculated from $\%Pb_E$.

6.2.4 Proportion of Pb_{Petrol} and $Pb_{geogenic}$ in labile and non-labile pools

The proportion (%) of Pb_{petrol} and $Pb_{geogenic}$ in individual fractions of the SEP (exchangeable; F1, carbonate; F2, reducible; F3, oxidizable; F4 and residual; F5) were calculated using a simple binary mixing model (Chapter 2, Eq. 2). The relative contributions of Pb_{petrol} and $Pb_{geogenic}$ in the labile and non-labile pools were calculated according to Eq. (5) which is an extension of a binary mixture model.

$$\%\mathrm{Pb}_{(\text{labile petrol})} = \frac{\mathrm{IR}_{\mathrm{ore}} - \mathrm{IR}_{\mathrm{L}}}{\mathrm{IR}_{\mathrm{ore}} - \mathrm{IR}_{\mathrm{petrol}}} \times \frac{\mathrm{Pb}_{\mathrm{E}}}{\mathrm{Pb}_{\mathrm{total}}} \times 100$$

Eq. (5)

Where IR_{ore}, IR_{petrol} and IR_L are values of isotopic ratios ($^{206/207}Pb$ or $^{208/207}Pb$) in UK Pb ore, UK petrol and isotopically exchangeable Pb (labile pool) respectively; Pb_E and Pb_{total} are isotopically exchangeable Pb and total soil Pb.

6.2.5 Sequential extraction procedure

Fractionation of elements in a selected number of allotment topsoils (n=59; in duplicate) were carried out according to the SEP described in Chapter 2 (section 2.6). The recovery rates calculated for selected elements, measured against HF-$HClO_4$-HNO_3 digest assays, were as follows: Pb (128%), Cd (107%), Ba (119%), Tl (101%), U (110%), Mn (89.6%), Ca (110%), Mo (87.9%), Sr (83.5%), Zn (60%), Cu (65.4%), P (62.4%), V (56%), As (56.7%), Cr (50%), Co (54.2%), Fe (43.2%) and Ni (48.3%).

6.2.6 Analytical procedures for measurement of isotopic abundances in soils through ICP-QMS

Lead isotopic abundances in the individual fractions of SEP and Pb_{total} (HF-$HClO_4$-HNO_3) were measured following the methodology given in Chapter 3. Detail regarding determination of isotopic abundances of Ni, Cu, Zn, Cd and Pb in isotopic dilution assays of selected urban allotment soils (n=59) is given in Chapter 2, section 2.9.

6.3 Results and discussion

6.3.1 Lability (E-value) of trace elements (Ni, Cu, Zn, Cd and Pb) in soils

E-values (mg kg^{-1}) for allotment soil samples (n=59) ranged from 0.443 – 6.10 for Ni, 6.99 – 29.2 for Cu, 26.1 – 246 for Zn, 0.121- 0.541 for Cd and 11.0 – 223 for Pb. Mean and (Median) values (mg kg^{-1}) for Ni, Cu, Zn, Cd and Pb were 1.31 (1.13), 14.5 (13.8), 93.2 (87.9), 0.260 (0.239) and 106 (99.3) respectively.

Labilities of Ni, Cu, Zn, Cd and Pb expressed as a proportion (% E-value) of the total metal content are shown in Figure 6.1. The average labilities of all studied metals were below 50%. In theory E-values of different elements in soil should contribute to the evaluation of risk which could otherwise be overestimated if only total concentration of elements in soil are considered. A restricted range of metal lability in urban soils has also been reported in previous studies (Mao et al., 2014, Shetaya et al., 2018). The relative labilities of the five elements followed the order Cd> Pb ≥ Zn> Cu>Ni; a frequency distribution of % E-value of Ni, Cu, Zn, Cd and Pb is shown in Figure 6.2. The lability of Cd was generally higher than that of the other elements whereas lability of Ni was lowest; this is generally consistent with previous studies (Harrison et al., 1981, Gäbler et al., 2007, Marzouk et al., 2013a, Mao et al., 2017). Differences in lability of elements may arise due to differences in (i) original contaminant source characteristics and (ii) time-dependent mechanisms of interaction with soil constituents. The latter may include gradual stabilization of precipitates, slow adsorption on oxides/hydroxides (Fe and Mn) and clay, formation of increasingly stable complexes with organic matter, adsorption and co-precipitation on carbonates and in silicate lattices and diffusion of surface species into mineral micropores (Hamon and McLaughlin, 2002, Bradl, 2004, Ma et al., 2006a, Buekers et al., 2007). Heavy metals in soils have different affinities for adsorption to soil geocolloids. For example, Pb in soil is more strongly adsorbed to Fe-oxides compared to other heavy metals (Covelo et al., 2007). Similarly soils with $CaCO_3$ will retain more metals as carbonate precipitates than acidic soils (Garcia-Delgado et al., 1996, Zhang et al., 1998). Soil properties such as pH and total metal concentration influence the fixation rate of an element (Marzouk et al., 2013a). Buekers et al. (2007) in his study revealed that most of the variation in fixation rates of Cd, Zn and Ni was due to the effect

of pH and the presence or absence of carbonates. In another study Ma and Uren (1998) observed greater fixation of Zn in bentonites at large concentrations. There is also an association between fixation reaction and ionic radius of an element i.e., element with large ionic radius will have slower fixation reaction and vice versa (Trivedi and Axe, 2001, Degryse et al., 2007, Degryse et al., 2009). For example, the fixation rates for Ni and Zn are higher comparative to larger ions such as Pb and Cd (Xu et al., 2006, Buekers et al., 2008, Degryse et al., 2009). Besides the effects of fixation processes and soil properties, labilities of heavy metals in allotment soils might likely be influenced from different sources of pollutants. It has been shown that lability of metals varies between sources. For example, lability of metal will be lower in soil if the origin of metal is in less soluble form whereas lability of metal will be relatively higher if origin of metal is in more soluble form (Degryse et al., 2004).

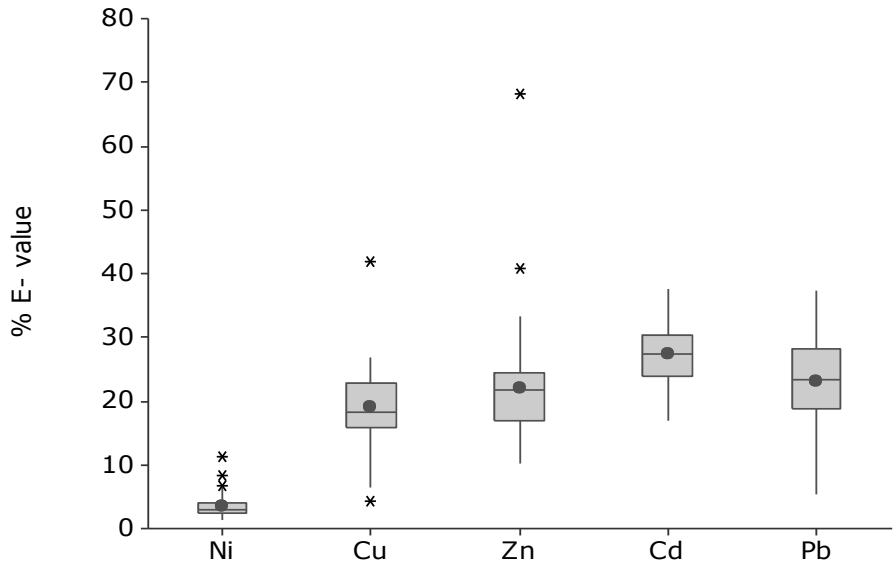


Figure 6.1: Box and whisker plot showing lability (% E-value) of Ni, Cu, Zn, Cd and Pb in allotment soils (n=59); the mean value (●) is also shown and outliers are marked as an asterix.

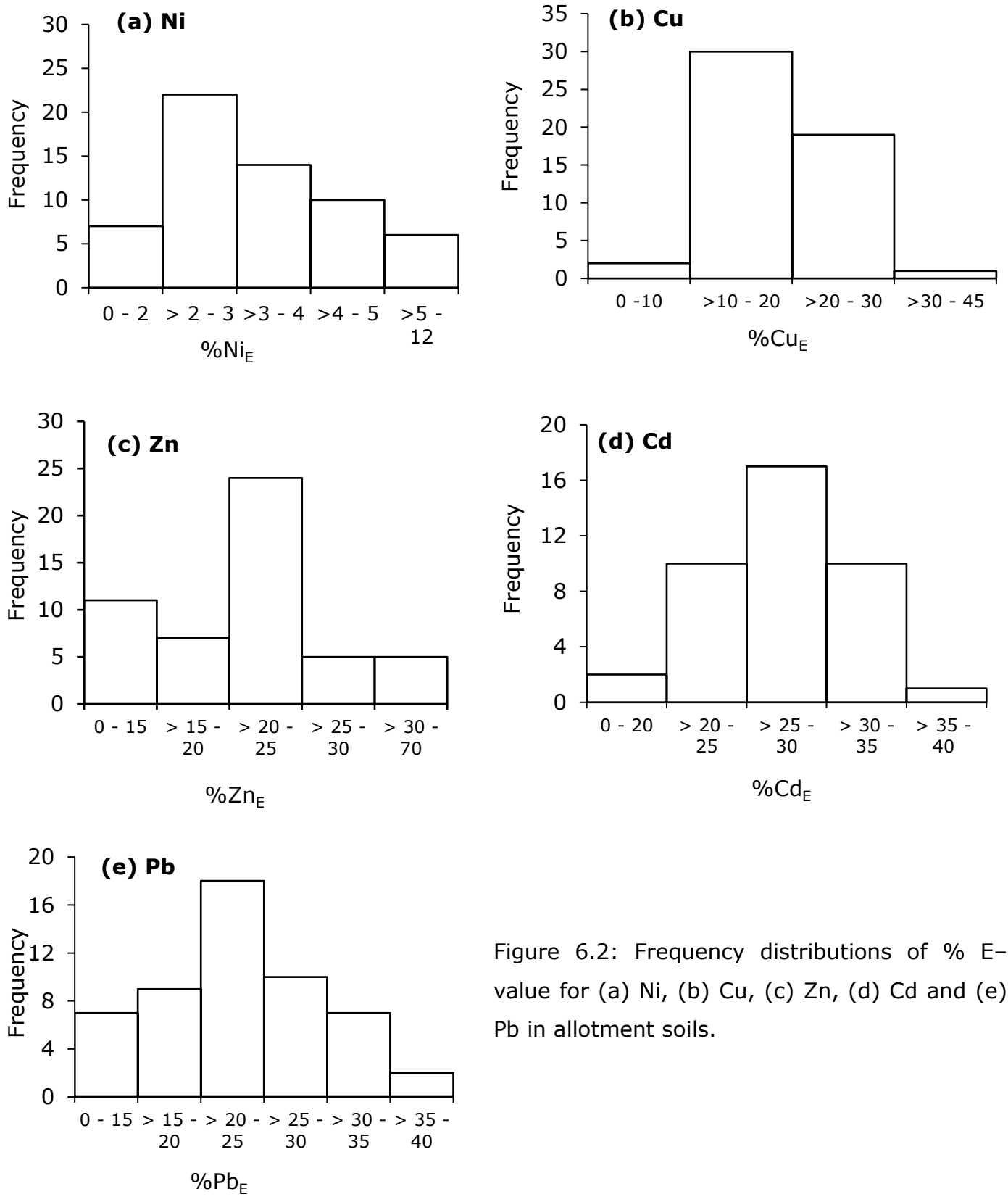


Figure 6.2: Frequency distributions of % E–value for (a) Ni, (b) Cu, (c) Zn, (d) Cd and (e) Pb in allotment soils.

6.3.2 Comparison of isotopically exchangeable (E-values) pool of different trace metals measured in filtered solutions (E_{soln}) and resin – treated solutions (E_{resin})

The presence of non-labile metals in suspended colloidal particles (SCP) in submicron filtered (<0.22 µm) supernatant solutions was tested by comparing %E-values measured in E_{soln} and E_{resin}. Results showed a good correlation between $\%E_{soln}$ and $\%E_{resin}$ for Ni, Cu and Zn with r values of 0.970, 0.908 and 0.980, respectively. These results were in agreement with findings of Mao et al. (2017) and Marzouk et al. (2013a) where, in most soils, non-labile metals associated with SCP were a minor constituent (average difference <2%) on E-values. However, in the case of Cd and Pb the resin-treated solutions appeared to greatly overestimate the E-value (Figure 6.3); this is the opposite of the expected trend in the presence of non-labile SCP metal. The mean %E-values, average standard deviation and average difference for Ni, Cu, Zn, Cd and Pb are also shown in Table 6.2. In the literature, the possible reasons suggested for overestimation of E_{resin} values include (i) experimental error arising from adsorption of colloids by the resin and their subsequent transfer to eluent due to inappropriate washing or (ii) the resin causing dissolution of non-labile metal associated with the SCP (Lombi et al., 2003). The overestimation of E_{resin} as compared to E_{soln} has also been previously reported. For example, Izquierdo et al. (2017) found higher concentration of Pb and Fe in resin-treated *unamended* soils; it was suggested that this was due to the sorption of non-exchangeable colloids i.e., DOC or Fe colloids by the resin. In this study, the reason for over-estimation of E_{resin} was probably contamination of the chelex-resin used with Pb and Cd (with normal isotopic abundances) which would then dilute the spike isotopes (^{204}Pb and ^{108}Cd) and thus inflate the apparent E-values. If there had simply been adsorption of SCP

by the resin, then the isotopic signature of both metals (Pb and Cd) in resin-treated and filtered solutions might be expected to be the same and so the resulting E-values would be similar. Thus the explanation of Izquierdo et al (2017) would not seem reasonable in this case. In order to investigate the contribution of chelex-resin to the background metal concentrations, a comparison of the most affected non-spiked isotopes (i.e. ^{111}Cd and ^{208}Pb, cps) analysed using both resin-treated and filtered soil solutions were made. A good correlation was found for both Cd and Pb measured by both resin-treated and filtered solutions with r values of 0.962 and 0.820 respectively. However, the intercept of a regression line for both Pb and Cd deviated from zero; in the case of Pb the intercept was at 45108 cps whereas for Cd, the intercept was at 232 cps (Figure 6.4). This indicates evidence of a constant level of contamination from chelex-resin with 'native' Pb and Cd (normal isotopic signature). Therefore, in further discussion in this chapter, only the non-chelex treated data is used.

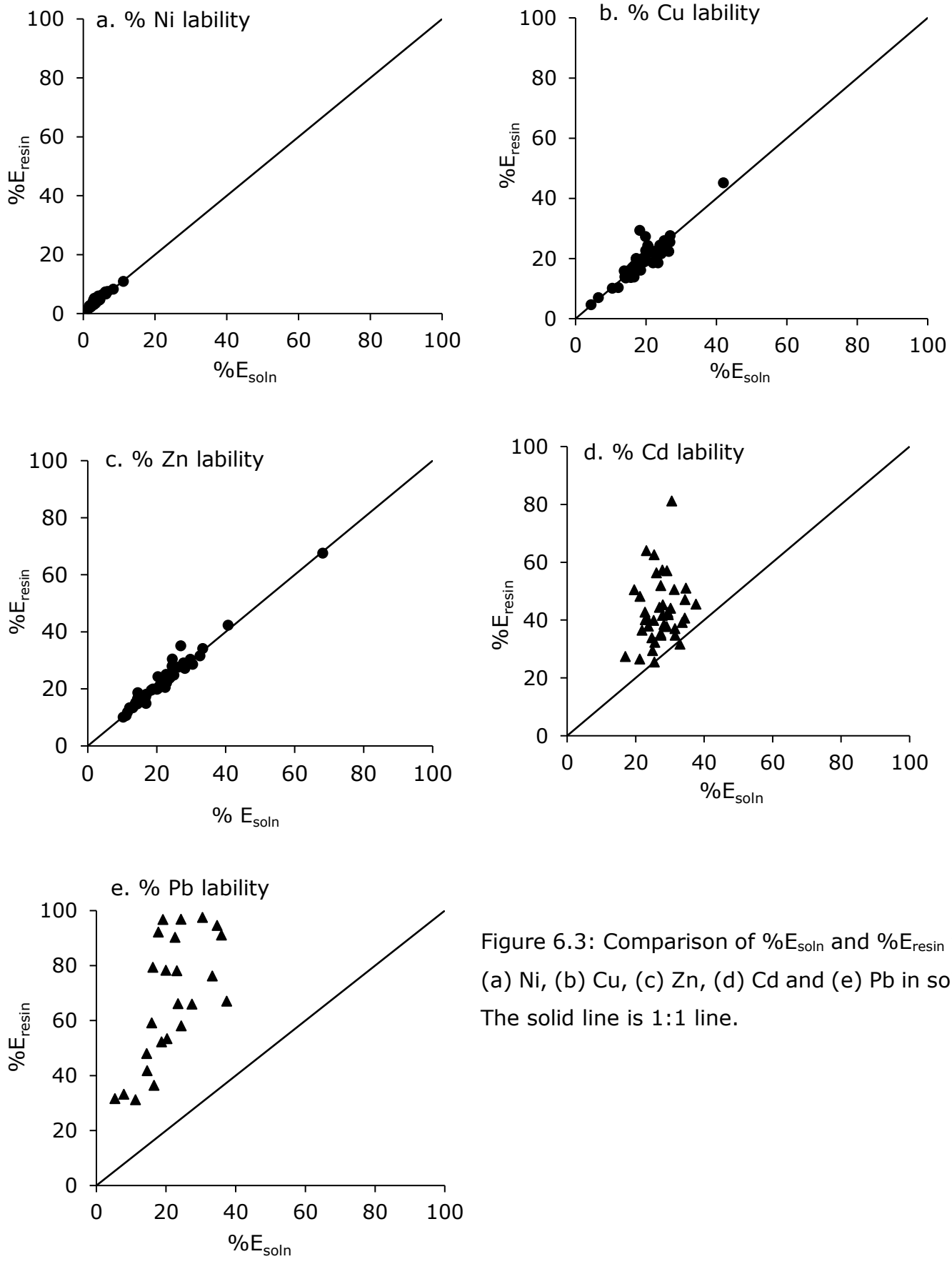


Figure 6.3: Comparison of $\%E_{soln}$ and $\%E_{resin}$ for (a) Ni, (b) Cu, (c) Zn, (d) Cd and (e) Pb in soils. The solid line is 1:1 line.

Table 6.2: Comparison of apparent labilities (%E-values), average standard deviations and average differences for Ni, Cu, Zn, Cd and Pb between resin-treated (E_{resin}) and filtered solutions (E_{soln}).

	Ni		Cu		Zn		Cd		Pb	
	%Esoln	*%Eresin*	*%Esoln*	*%Eresin*	*%Esoln*	*%Eresin*	*%Esoln*	*%Eresin*	*%Esoln*	*%Eresin*
% lability (mean)	3.43	3.92	19.0	19.2	21.9	22.8	27.7	43.2	23.1	316
Average standard deviation	0.02	0.05	1.06	1.13	2.91	4.96	0.02	0.04	4.37	123
Average difference	-0.50		-0.17		-0.96		-15.5		-367	

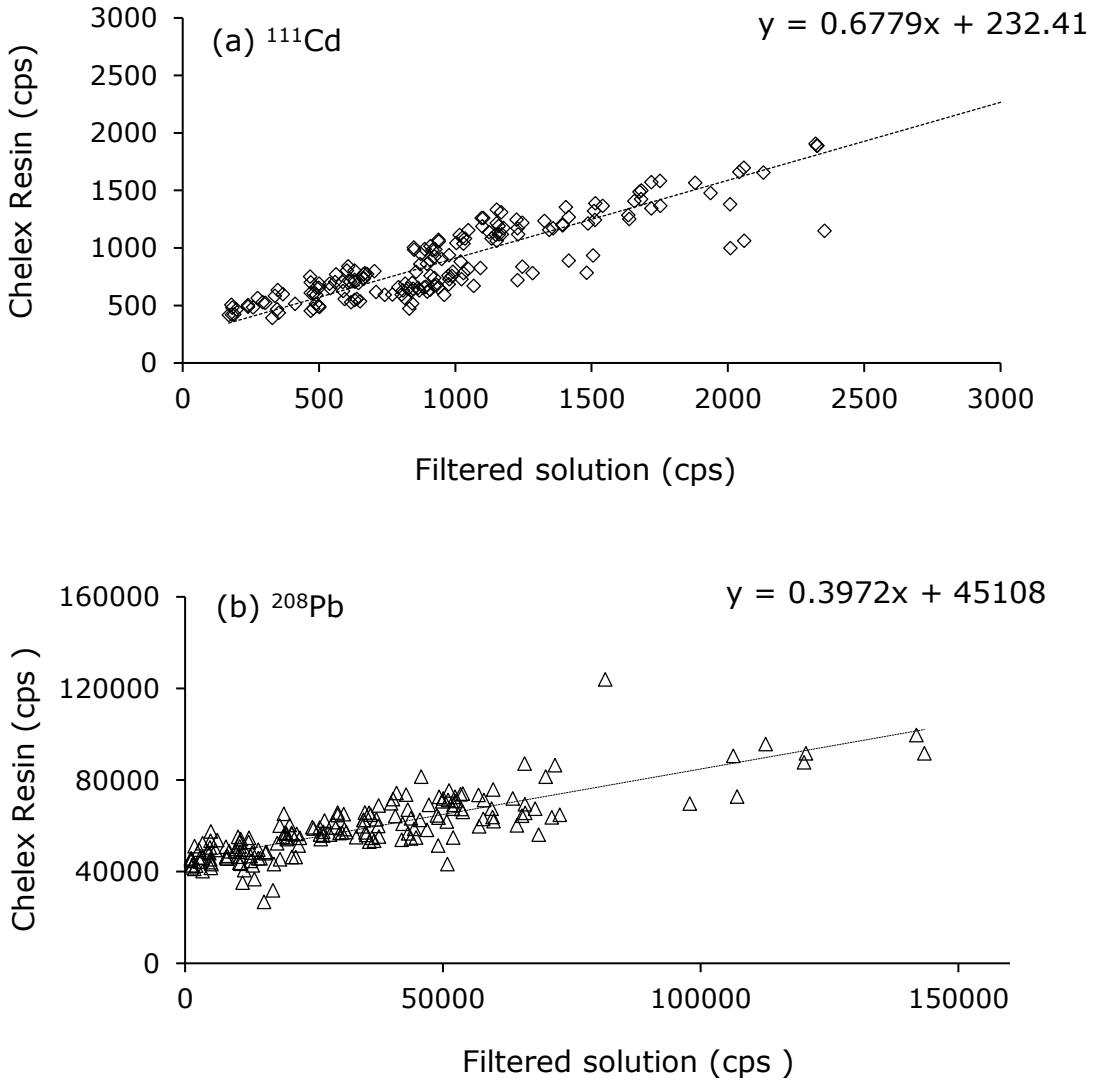


Figure 6.4 Comparison of non-spiked isotopes (a) ^{111}Cd and (b) ^{208}Pb; ICPMS intensities (cps) in resin-treated (E_{resin}) and filtered equilibrated soil solutions (E_{soln}).

6.3.3 Fractionations of multi-elements in allotment soils using a sequential extraction procedure (SEP)

The fractionation of trace and major elements in allotments soils (n=59) are discussed below and shown in Figure 6.12. These values are average percentage (%) distributions in each fraction (Table 6.3).

6.3.3.1 Copper

Copper was mainly in the F4 fraction (64%), followed by F5 and F3, which accounted for 23% and 10% respectively. A very small proportion of Cu was also held with F2 and F1 i.e., 2.5%.The strong association of Cu with the soil organic fraction is well established and has also been reported in other studies (Harrison et al., 1981, Gibson and Farmer, 1986, Li et al., 2001, Yin et al., 2002, Imperato et al., 2003, Lu et al., 2003). As compared to other elements, Cu has the highest affinity for soil organic matter and sulphide and forms highly stable organo-Cu complexes in humus. A significant correlation between Cu in F4 and soil organic matter content was also observed with r = 0.658 at $p \leq 0.000$ for a power relationship (Figure 6.5).

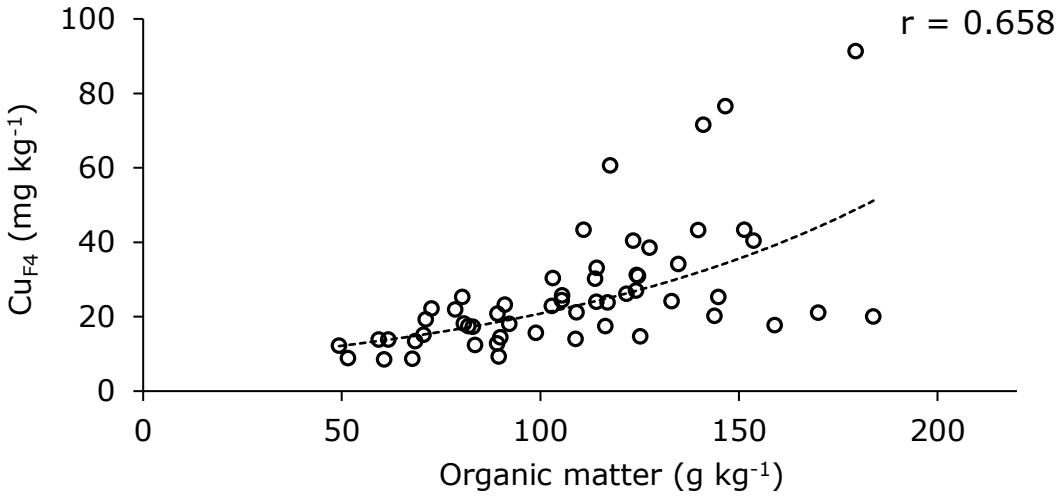


Figure 6.5: Correlation between concentrations of Cu associated with SEP fraction F4 (Cu_{F4}) and total organic matter content.

6.3.3.2 Zinc

The majority of Zn was found associated with F3 i.e., 53.5%, followed by F5 which accounted for 19.4%. This is in agreement with results reported by Li and Thornton (2001). A study conducted by Weng et al. (2001) and Buekers et al. (2008) showed that in acidic condition, the main sorbent for Zn is organic matter whereas in alkaline soils, Fe oxides (hydroxides) are considered as the main absorbent for Zn. Therefore, the highest proportion of Zn in allotment soils, which are mostly alkaline in nature (average pH = 6.99) was also found within Fe/Mn oxides. Zinc in F5 (19.4%) suggested its presence in primary minerals. The amount of Zn sorbed on F2 was 15.7%, while in F4 it was only 10.5% reflecting the relatively weak bond between Zn ions and humus. The least amount of Zn was found in F1 i.e., <1%.

6.3.3.3 Cadmium

The largest fraction of Cd was F3, i.e., average 42.7%, which suggests strong adsorption by Fe-Mn oxides. The first two fractions (F1 and F2) were also important for Cd; the combined proportion (%) of Cd held within the first two fractions (Cd_{F1+F2}) was 36.9%. The least amount of Cd was found associated with F4 i.e., 9.6%, whereas in F5, it was 10.7%. These findings are in good agreement with other investigations (Gibson and Farmer, 1986, Wilcke et al., 1999, Li and Thornton, 2001, Li et al., 2001). For example, Li and Thornton (2001) found the greatest proportion of Cd to be in first three fractions of soils close to Zn smelting sites i.e., 70% of total Cd. In this study, on average, 79.6% Cd was also associated with the first three fraction. Cadmium has some similarities with Ca, where a small proportion was found in F4 and F5 and most Ca was in the initial phases (F1-F3) of the SEP. The association of Cd with the more soluble phases also suggested the

greatest contribution was from anthropogenic sources rather than primary minerals.

6.3.3.4 Lead

Lead in soil is normally found to have very low mobility and mostly exists in unreactive forms albeit with the potential to become more mobile in acidic conditions (Alloway and Ayres, 1997, Miretzky and Fernandez-Cirelli, 2008). However, in the allotment soils, the predominant fraction of Pb was associated with *non-residual* fractions i.e., F4 (49.1%) and F3 (36.3%). There have been some studies in which Pb was also found to be associated mainly with oxides and the organic fraction (Emmanuel and Erel, 2002, Burt et al., 2003, Wilson et al., 2006). However, Pb in soils is often thought to be associated with phosphate; in F4 a significant correlation was found between P_{F4} and Pb_{F4} (r= 0.761 at $p \leq 0.000$; Figure 6.6). An association between P_{F4} and Pb_{F4} could be due to two possibilities. First, the correlation could be due to dissolution of pyromorphite, releasing both Pb and P ($Pb_5(PO_4)_3Cl$). Alternatively it might simply indicate the release of organically bound P and organically bound Pb. In order to investigate the source of P_{F4}, the ratio of C:P was calculated from measurement of soil organic carbon (SOC) and P_{F4} (Figure 6.7). The calculated slope value was 0.0074 which is reasonably close to a literature value of 0.016 (Tipping et al., 2016) for organic matter in fertile soils. Therefore, it seems likely that a large proportion of P_{F4} originated from the destruction of organic matter (humus) in F4. Fraction F5 accounted for only 9.6% of Pb which suggests a minor presence in primary mineral form; the least amount of Pb was in F1 and F2 i.e., 5.1%. This distribution patterns of Pb in allotment soils were in agreement with results previously reported by Bielicka-Giełdoń et al. (2013) for allotment soils.

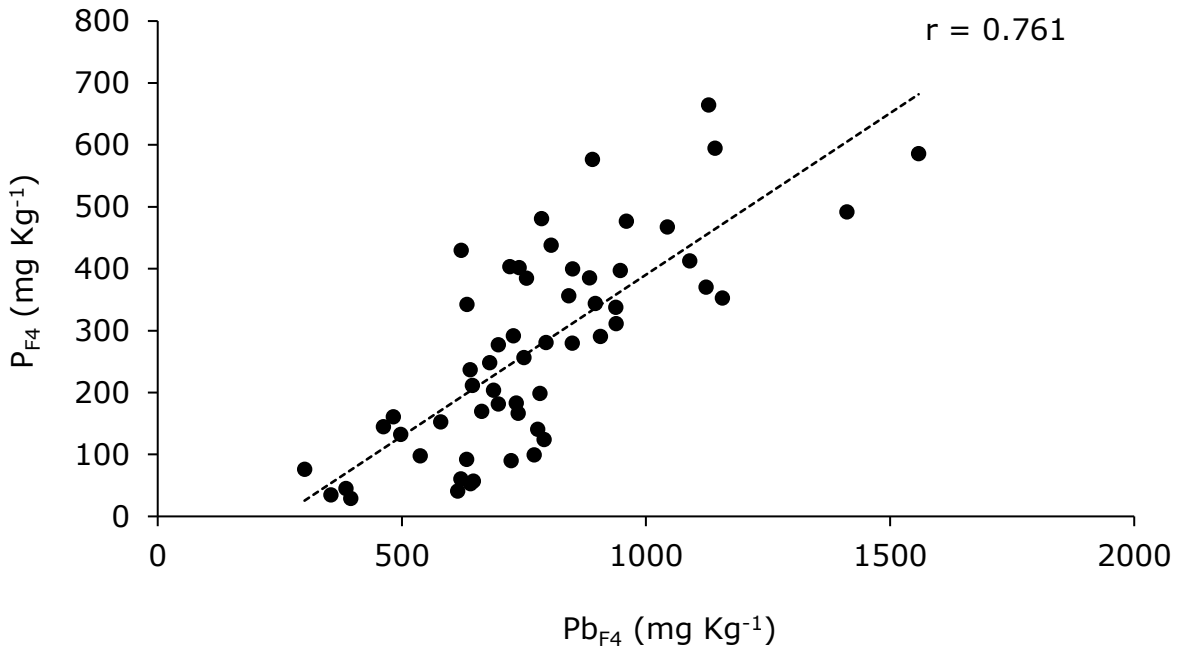


Figure 6.6: Correlation between Pb and P associated with F4 of the SEP

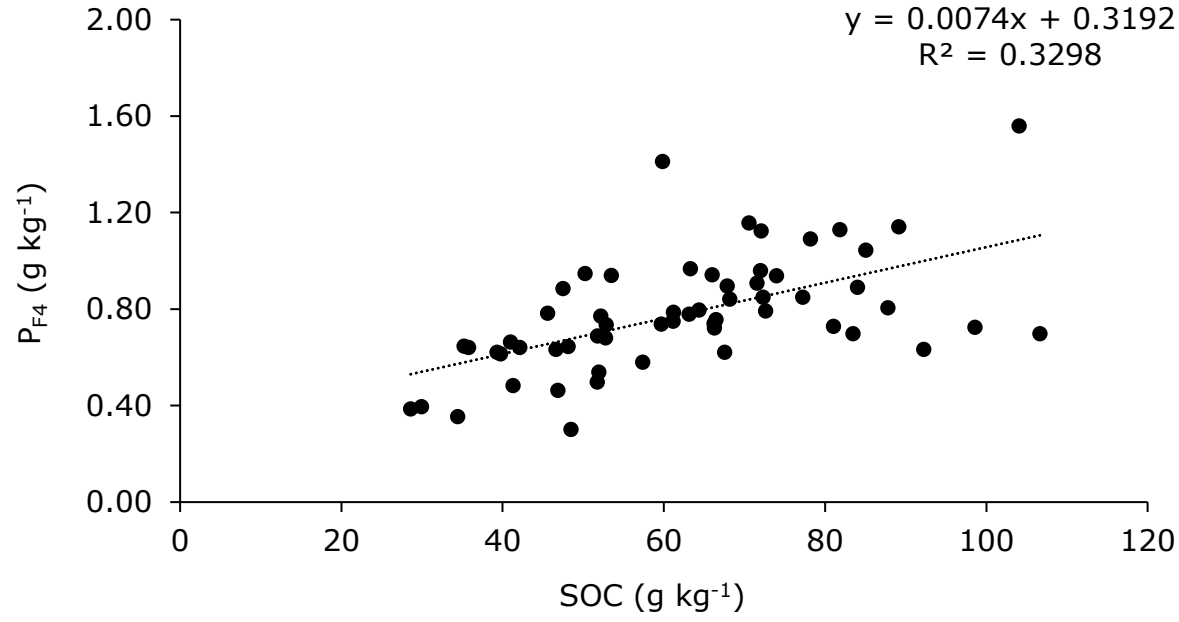


Figure 6.7: Correlation between SOC and concentration of P in F4 (P_{F4})

6.3.3.5 Nickel

The highest concentration of Ni was in F5, which accounted for 62% of total Ni on average. It was also found associated with F3 and F4, about 21% and 15% respectively. A very small amount of this metal was determined in F2 and F1 i.e., ~ 3%. These values of Ni except Ni associated with organic matter, were in general agreement with those reported by Bielicka-Giełdoń et al. (2013) for allotment soils in Koszalin, Poland. In other studies on urban soils, residual Ni was also found as the predominant fraction (Davidson et al., 1998, Wilcke et al., 1998, Davidson et al., 2006, Lu et al., 2007). This residual Ni is mostly lithogenic in nature and is held in silicates.

6.3.3.6 Manganese

As expected, manganese was found mostly associated with F3 which accounted for about 69.2%, whereas the least amount was present in F4 and F1 where it was < 5% in both cases. Other studies of urban soils also reported F4 as the most important fraction for Mn and suggested that this fraction is lithogenic in nature (Davidson et al., 2006, Bielicka-Giełdoń et al., 2013, Sagagi and Imam, 2017). In F2 and F5, the amount of Mn present was 13% and 11.4% respectively. Manganese oxides have an essential role in binding trace elements in soils, especially at low pH because of their low point of zero charge (pzc) (Bundt et al., 1997, Wilcke et al., 1998).

6.3.3.7 Iron

The largest proportion of Fe was found concentrated in F5 i.e., 69.3%. As for Mn, this was expected as Fe is present as a range of amorphous and crystalline Fe^{III} hydrous oxides. Iron was also held in F3 and F4 i.e., 18.8% and 11.9% respectively. In F1, no Fe was detectable whereas in F2 very small amounts were present i.e., 0.04%. These results corresponded very well with other studies (Li

and Thornton, 2001, Lu et al., 2007, Bielicka-Giełdoń et al., 2013, Sagagi and Imam, 2017).

6.3.3.8 Phosphorus

The highest percentage of P was associated with F4 where it accounted for about 55.9% probably due to the oxidation of humus; F3 and F2 contained 19.6% and 14.4% respectively. The association of P with F2 suggests it was released from Ca phosphates. A small amount of P was also found in F5, up to 8.1%. Whereas the smallest percentage of P was found in F1 i.e., 2%.

6.3.3.9 Calcium

The dominant fraction for Ca was F1 i.e., 37.5% followed by F3 and F2 i.e., 27.7% and 26.3% respectively. This is consistent with Ca^{2+} being the dominant exchangeable cation in cultivated soils subject to Ca inputs, such as lime and Ca phosphate. Calcium is not held by oxides but it presence in F3 showed possibly further dissolution of calcium carbonate ($CaCO_3$) or perhaps calcium phosphates. A small proportion of Ca was also present in F4 up to 6.3%, while F5 was least important with only 2.2% of Ca.

6.3.3.10 Strontium

The most important fraction observed for Sr was F5 where it was found to be about 39.6%. The other important fractions were the first two fractions, where the sum of Sr (Sr_{F1+F2}) held was 35.3%. In F3, the percentage of Sr was 17.1% whereas the least important fraction was F4 with only 8% of Sr. A further comparison of Sr and Ca in different fractions was also made as Ca is isomorphically substituted with Sr (Figure 6.8). Strontium and Ca in the first four fractions (F1-F4) followed the same trend which suggested these elements belonged to a common pool of reactive Sr and Ca in the soil. The Ca and Sr may have originated from several sources (eg. liming materials, Ca-phosphate, coal

ash, organic manure etc) but they appear to have fully mixed to have a common ratio of Ca:Sr in F1 – F4. By contrast, the trend observed in F5 was different, presumably representing the (much greater) Sr:Ca ratio in resistant primary minerals which had clearly not mixed with the cations in the other four fractions.

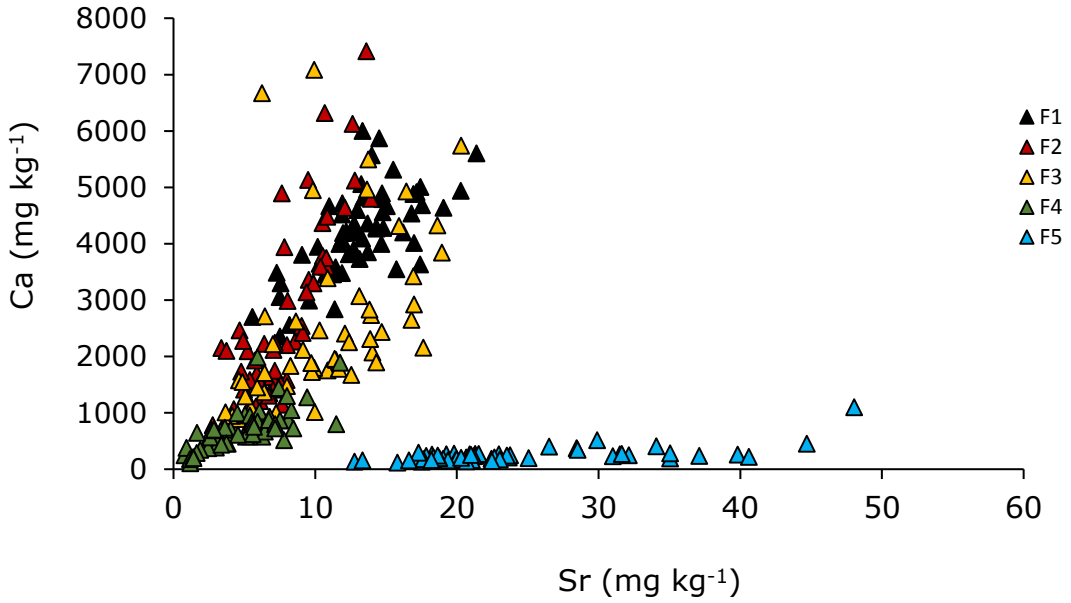


Figure 6.8: Comparison of Sr and Ca (mg kg^{-1}) in different fractions (F1-F5) of SEP.

6.3.3.11 Arsenic

The highest proportion of As was found in F5 and F4 which accounted for 41% and 32.4% respectively. In F3 it was present at an average proportion of 19.8% whereas both F1 and F2 contained < 1% of the soil As. A comparison of concentration of As and P in F3 (As_{F3} and P_{F3}) was made because arsenate and phosphate are similar in their geochemical behaviour – both are strongly adsorbed on Fe oxides (Jackson and Miller, 2000, Violante and Pigna, 2002). A significant correlation of As_{F3} and P_{F3} (i.e., r = 0.525, p=0.000) was observed which suggested their adsorption on Fe-oxides (Figure 6.9).

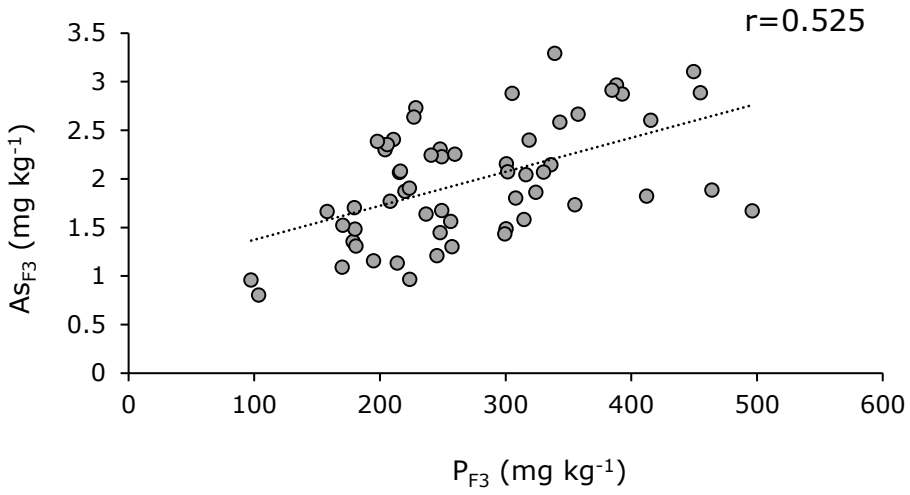


Figure 6.9: Correlation between concentration of As and P associated with F3 of the SEP.

6.3.3.12 Cobalt

The highest proportion of Co was found associated with F5 i.e., 49% and was followed by F3 which accounted for about 38.2%. In a study by McLaren et al. (1986), the largest proportion of Co was reported to be with Mn oxides in a study of Scottish soils due to the isomorphous substitution of Co for Mn in MnO_2. In the allotment soils there was also a significant moderate (r= 0.452, p = 0.000) association between Co and Mn in F3 (Figure 6.10). Some content of Co was also found in F4 i.e., 9.8%. Cobalt in F2 and F1 together accounted for <5%.

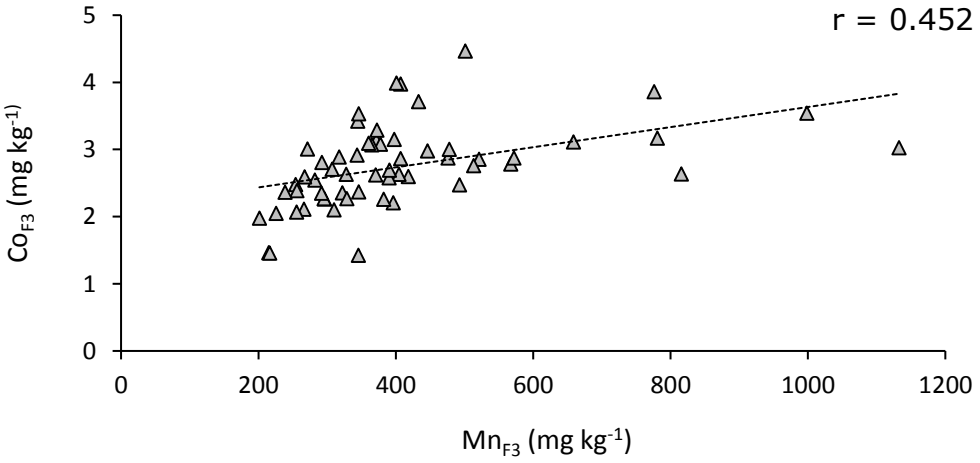


Figure 6.10: Correlation between concentration of Co and Mn held in F3.

6.3.3.13 Chromium

On average, Cr was predominantly in F5 (68.4%) followed by F4 (22.5%). These results are consistent with the findings of Köleli (2004) and Ottosen et al. (2009), where most Cr was also present in F4 and F5. Some Cr was also found associated with F3 i.e., 8.1%. Fraction 1 and F2 were the least important fractions for Cr i.e., <1%.

6.3.3.14 Barium

The highest proportion of Ba was present in the residual fraction, F5 (67.4%). This was followed by F3 and F4 which accounted for 14.7% and 10.28% respectively. The combined concentrations of Ba in the first two fractions (Ba_{F1+F2}) was 7.6%.

6.3.3.15 Uranium

The highest average proportion of U was associated with F5 i.e., 69.2%, followed by F4 and F3 which accounted for 16.1% and 10.10% respectively. Fractions F1 and F2 were lowest with U <5%.

6.3.3.16 Molybdenum

The highest concentration was found in F5 (51.8%), followed by F4 (35.3%). Molybdenum held in F3 was 9.4%. In F1, a small amount of Mo was also present i.e., 3.2%, whereas the least important fraction was F2 with Mo < 1%.

6.3.3.17 Vanadium

In the case of V, the highest proportion was associated with F5 (65.7%), this was followed by F4 and F3 which accounted for 18.2% and 15.5% respectively. A small amount of V was found in F2 i.e., 6.2% whereas in F1 < 1% was present. In soils V is reported to bind predominantly with Fe oxides due to isomorphous substitution of V^{3+} for Fe^{3+} and strong adsorption of vanadate (VO_4^{3-}) on Fe oxides (Schwertmann and Pfab, 1996). Therefore a comparison of V with Fe in the SEP

fractions (F1-F5) was also made (Figure 6.11). In the first two fractions, no significant correlation was observed between V and Fe whereas in the last three fractions moderate to strongly significant correlations were observed i.e., F3 (r=0.408, p=0.001), F4 (r=0.572, p=0.000) and F5 (r=0.827, p=0.000). Fraction F5 in particular suggests isomorphous substitution in primary mineral Fe oxides.

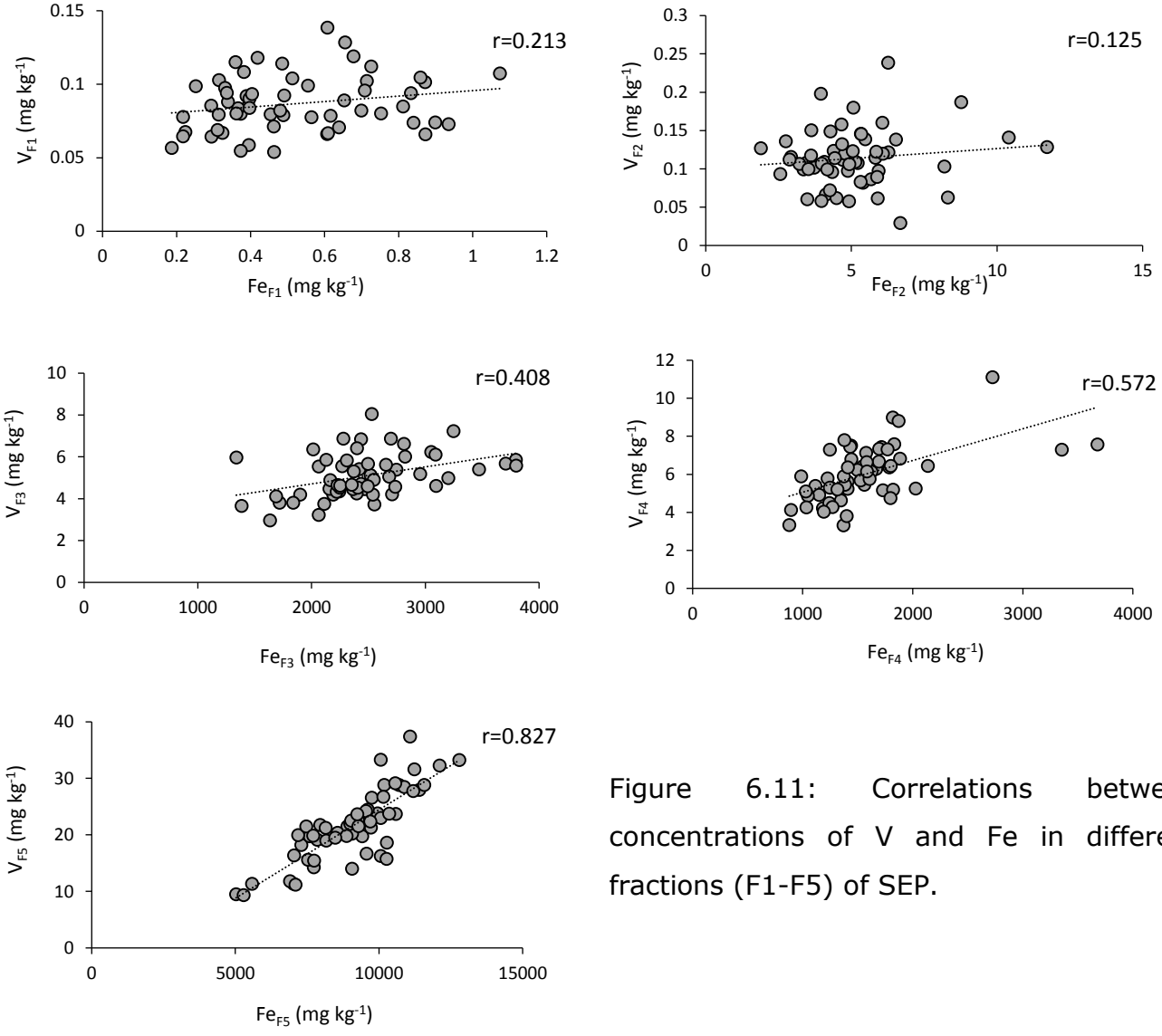


Figure 6.11: Correlations between concentrations of V and Fe in different fractions (F1-F5) of SEP.

6.3.3.18 Thallium

The highest concentration of Tl was found in F5 (82.2%), followed by F3 and F4 which accounted for about 10% and 6.2% respectively. In F1 and F2, Tl was less than <1% of the total soil Tl content.

Fractionation using the SEP revealed that only in the case of Cd, Sr and Ca were the highly available fractions F1 and F2 greatest indicating a potentially high bioavailability and solubility in the allotment soils. This suggests a strong association between Cd and Ca pools in the soils. Also a significant correlation of Cd and Ca in F1 and F2 i.e., $r=0.460$ and $r=0.471$ respectively at $p<0.001$ was observed. The proportions of other elements in the first two fractions were relatively low but in F3, the proportions of Pb, Zn, Cd, and Co were > 35% suggesting that these elements exist in association with Fe and Mn oxides. Thus, a change in environmental conditions, such as prolonged reducing conditions or soil acidification, could result in solubilisation of these trace metals. The high proportion of Pb, Cu, P, Mo, As (>30%) in F4 suggests a strong affinity with organic matter (and/or sulphide) and so availability to allotment plants may depend to some extent on management of soil humus levels by allotment holders. The SEP distribution patterns of Tl, Fe, V, Cr, Ni, Mo, Ba and U were similar with the dominant fraction (i.e., > 50%) present in F5. This indicates that the largest proportion of these metals are in the crystalline structure of primary minerals or other resistant components of the soil matrix and were in non-labile forms. In resisting solubilisation by acidification, oxidation and reduction, it is reasonable to say that this residual pool would not be available for plant uptake or transport. Trace elements in this phase may only become available to soil chemical and biological processes through the very slow processes associated with weathering.

Table 6.3: Average percentage (%) distribution of multi-elements in different fractions of sequential extraction procedure (SEP)

SEP Multi-elements	***Fraction 1*** Exchangeable (%)	***Fraction 2*** Carbonates (%)	***Fraction 3*** Reducible (%)	***Fraction 4*** Oxidizable (%)	***Fraction 5*** Residual (%)
Lead	0.02	5.09	36.4	48.9	9.57
Cadmium	16.9	19.1	42.8	9.77	11.3
Copper	0.73	1.77	9.60	62.6	25.4
Zinc	0.95	15.7	53.5	10.5	19.4
Nickel	0.56	2.01	21.1	15.3	61.1
Manganese	1.92	13.0	69.2	4.53	11.4
Phosphorus	2.01	14.4	19.6	55.9	8.08
Calcium	37.5	26.3	27.1	6.31	2.18
Iron	0.00	0.04	18.8	11.8	69.3
Strontium	22	13.3	17.1	8.03	39.6
Chromium	0.08	0.88	8.14	22.5	68.4
Cobolt	0.17	2.89	38.2	9.77	49.0
Molybdenum	3.23	0.32	9.38	35.3	51.8
Arsenic	0.67	6.19	19.8	32.4	41.0
Vanadium	0.26	0.35	15.5	18.2	65.7
Thalium	0.77	0.85	10.0	6.16	82.2
Barium	3.03	4.6	14.7	10.3	67.4
Uranium	0.06	4.6	10.1	16.1	69.2

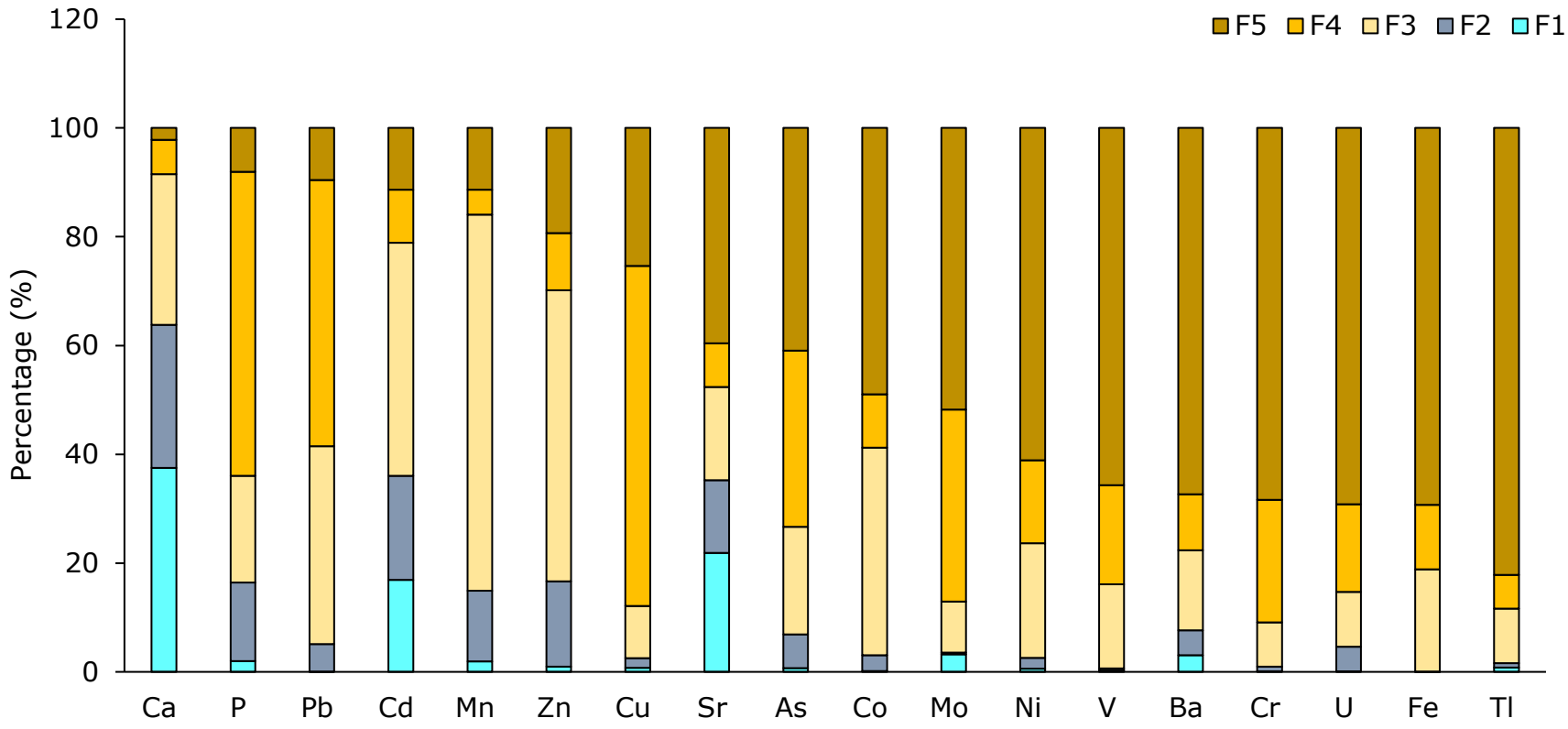


Figure 6.12: Fractionation (%) of elements in urban allotment topsoils determined by a sequential extraction procedures (SEP).

6.3.4 Labile and non-labile pools of Pb, Zn, Cd, Ni, and Cu: comparison of data from an isotopic dilution and SEP.

A comparison of SEP data with E-values for Ni, Cu, Zn, Cd and Pb (without resin cleaning) was made. No correspondence was observed between E-value and any single fraction of SEP which was in agreement with the results of Marzouk et al. (2013b) and Mao et al. (2014). However, a reasonable correspondence was found between metals extracted in combined fractions of SEP with E-values.

In the case of Pb, no consistent agreement was found between Pb_E and any individual fraction or combined fractions of SEP. Lead extracted in F1 and combined fractions (Pb_{F1-F2}) of the SEP were lower than Pb_E. However the combined amount of Pb extracted in the first three fractions (Pb_{F1-F3}) of the SEP was higher than Pb_E (Figure 6.13a). The difference found between combined SEP fractions (Pb_{F1-F3}) and Pb_E was 18.3%. This value might correspond to the amount of non-labile Pb in the first three fractions ($Pb_{F1-F3)}$. A similar finding was also reported by Huang et al. (2011) where Pb_E was lower than Pb_{F1-F3} of the BCR SEP. Good agreement was seen in the case of Zn, where $\%Zn_E$ was correlated with Zn_{F1-F2} i.e., r = 0.558 at $p \leq 0.000$ (Figure 6.13b). By contrast, non-labile Zn (78.5%) corresponded with the last three fractions i.e., Zn_{F3-F5} (Figure 6.14). This showed most non-labile Zn was retained within oxides or hydroxides, organic matter and mineral phases. These results agreed very well with previous studies (Young et al., 2005, Degryse et al., 2011). For Cd, no significant correspondence was observed between individual SEP fractions and %E-values (Figure 6.13c). Whereas, in a comparison of Cd_{F1-F2} with $\%Cd_E$, the former was higher; the difference $\%Cd_{F1-F2}$-$\%Cd_E$ was 9%. This difference might be due to non-labile Cd which is held in carbonate matrices. In the case of Ni, a significant correlation was

observed between SEP (Ni_{F1-F2}) and $\%Ni_E$ i.e., r = 0.709 at $p \leq 0.000$ (Figure 6.13d). This was in agreement with the findings of Mao et al. (2017), where a clear distinction between labile and non-labile Ni and the association of non-labile Ni with the residual phase in urban soils has also been made. For Cu, no correspondence between individual and combined SEP (Cu_{F1-F3}) was observed. Copper E-value was slightly higher than combined SEP (Cu_{F1-F3}) with a difference of 7.9% (Figure 6.13e). This might be some isotopically exchangeable Cu in the F4. However, most of the non-labile Cu (80.1%) agreed well with SEP combined fractions i.e., Cu_{F4+5} = 87.9% (Figure 6.14).

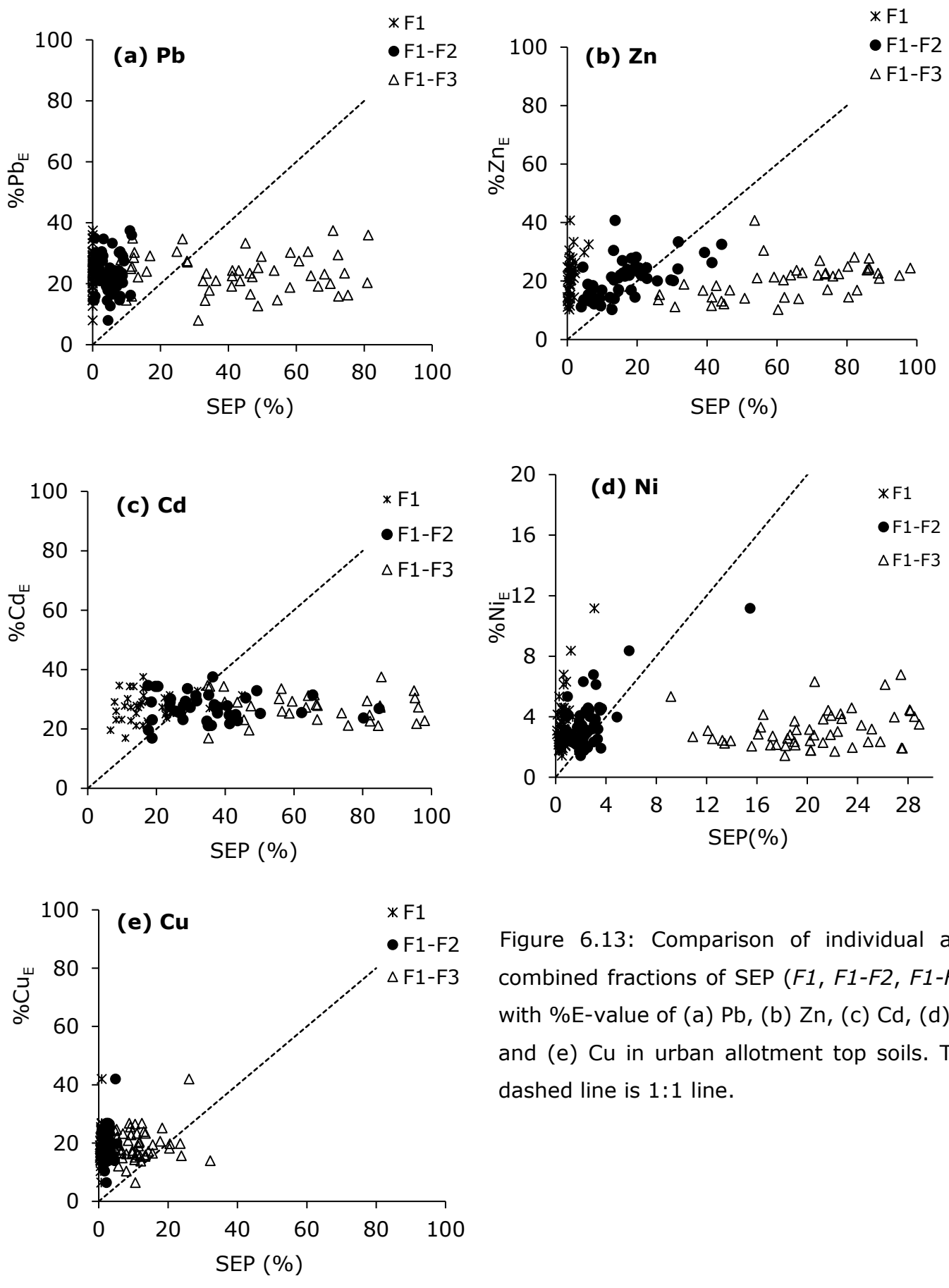


Figure 6.13: Comparison of individual and combined fractions of SEP (*F1*, *F1-F2*, *F1-F3*) with %E-value of (a) Pb, (b) Zn, (c) Cd, (d) Ni and (e) Cu in urban allotment top soils. The dashed line is 1:1 line.

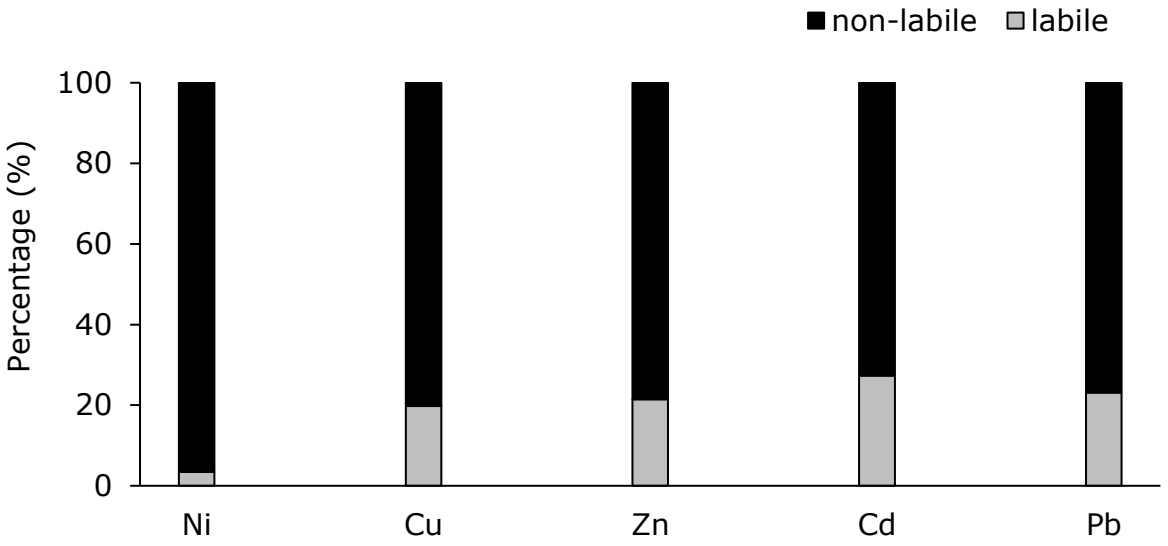


Figure 6.14: Average fractionation of labile and non-labile pools (% of total soil metal content) by isotopic dilution (ID) (n = 52 allotment soils).

6.3.5 Effects of soil properties on E-value of Ni, Cu, Zn, Cd and Pb

The effect of soil properties such as pH, organic matter and total metal content have been shown to explain some of the variation in %E-value (Ahnstrom and Parker, 2001, Ottosen et al., 2009, Marzouk et al., 2013a). The correlations between % E-value and (i) total metal content i.e., Ni, Cu, Zn, Cd and Pb, ii. pH, (iii) organic matter and (iv) available P are shown in Table 6.4. A weak negative correlation of %E-value with total metal content of Cu, Cd and Pb was found (Figure 6.15). For Ni, the relationship was negative but it was not significant. This might be due to few samples which showed opposite trend i.e., %E-value increased with increased in total Ni content. In the case of Zn a flat trend was observed. This negative relationship of total content of metals with % E-value indicated the larger proportion of native metals which were present in a non-reactive form. In a previous study Marzouk et al. (2013a), also observed a negative relationship between % E-value and total content of Zn, Cd and Pb in calcareous minespoil soils and was explained by a higher proportion of unreactive metals. Similarly a flat or slightly negative trend was also observed between pH

and % E-values for Ni, Cu, Zn and Pb but not for Cd, where pH was significantly negatively correlated with % E-value (Figure 6.16). Soil pH was observed to have a minor influence on % E-value and this might be due to the limited range of pH of soils found in urban soils generally and possibly allotment soils in particular which are managed to optimise vegetable growth (average pH = 6.99 ; standard deviation = 0.359). Organic matter content and available P were positively correlated with % E-value of Ni and Zn whereas for Cu, Cd and Pb a flat trend was observed (Figure 6.17 and 6.18). This positive correlation of organic matter with %E-value supports the hypothesis that labile Ni and Zn are held on humus. Overall, the soil properties appeared to have only a very weak relationship with lability of Ni, Cu, Zn, Cd and Pb. It has also been reported by Marzouk et al. (2013a) that in highly alkaline soils the presence of a larger proportion of non-reactive metals in the primary minespoil minerals decreases the potential of soil properties (except total content) to influence metal lability. This weak relationship of soil properties with lability of Ni, Cu, Zn, Cd and Pb also suggested a greater influence from original contaminant sources, originating either from parent materials or different anthropogenic sources. These results were in agreement with findings of Mao et al. (2014) and Marzouk et al. (2013b).

Table 6.4: Pearson correlation coefficients (r values) between %E-values of Ni, Cu, Zn, Cd and Pb with soil properties. Bold Figures represent significant *r* values at *p* values ≤ 0.05

Soil properties	Correlation coefficients values (*r*) of %E-values against soil properties				
	Ni_E	Cu_E	Zn_E	Cd_E	Pb_E
Total metal content	-0.228	**-0.498**	0.026	**-0.321**	**-0.396**
pH	-0.016	-0.014	-0.054	**-0.318**	-0.138
Organic matter	**0.323**	0.009	**0.527**	-0.067	-0.205
Available P	**0.325**	0.230	**0.585**	-0.019	-0.101

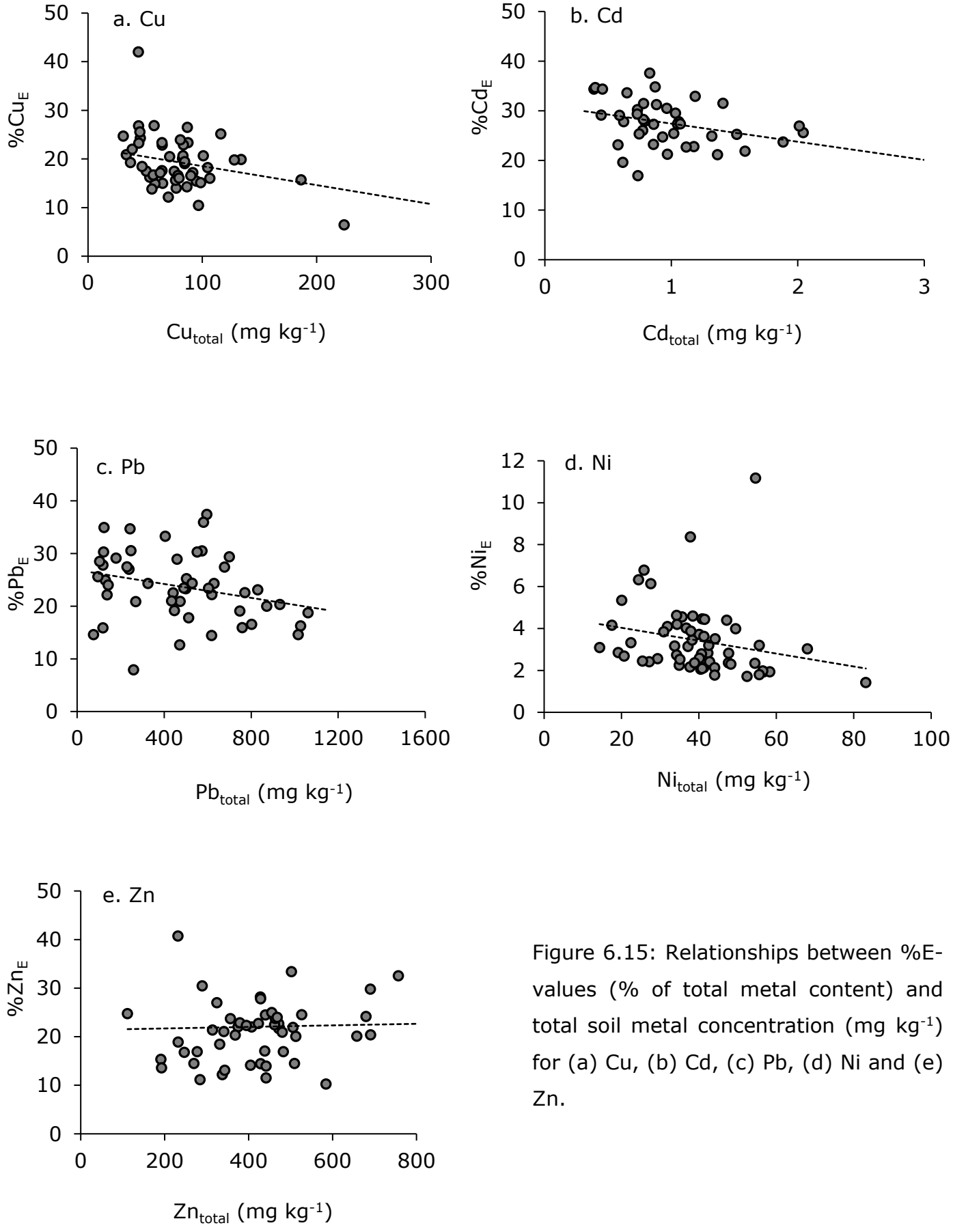


Figure 6.15: Relationships between %E-values (% of total metal content) and total soil metal concentration (mg kg^{-1}) for (a) Cu, (b) Cd, (c) Pb, (d) Ni and (e) Zn.

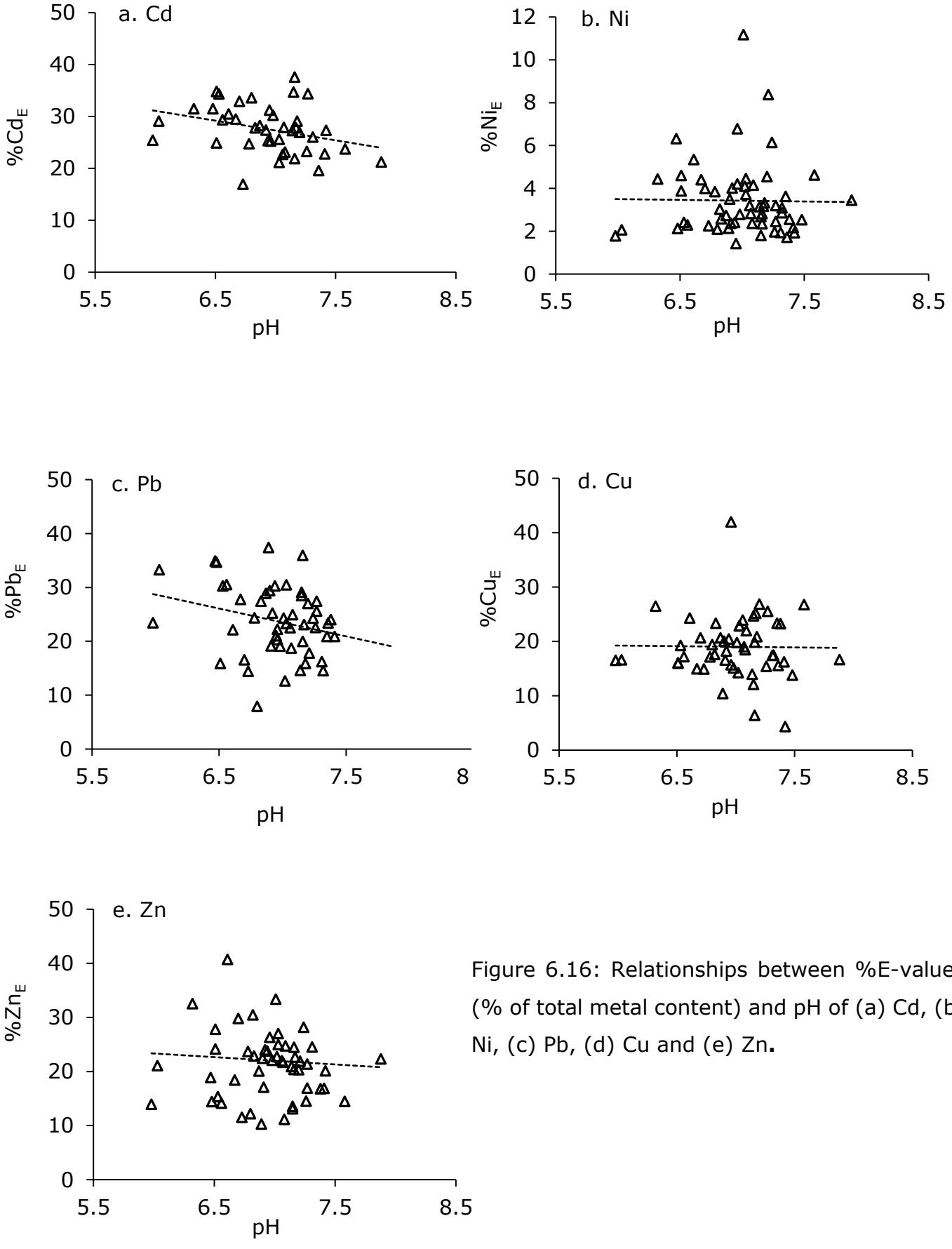


Figure 6.16: Relationships between %E-values (% of total metal content) and pH of (a) Cd, (b) Ni, (c) Pb, (d) Cu and (e) Zn**.**

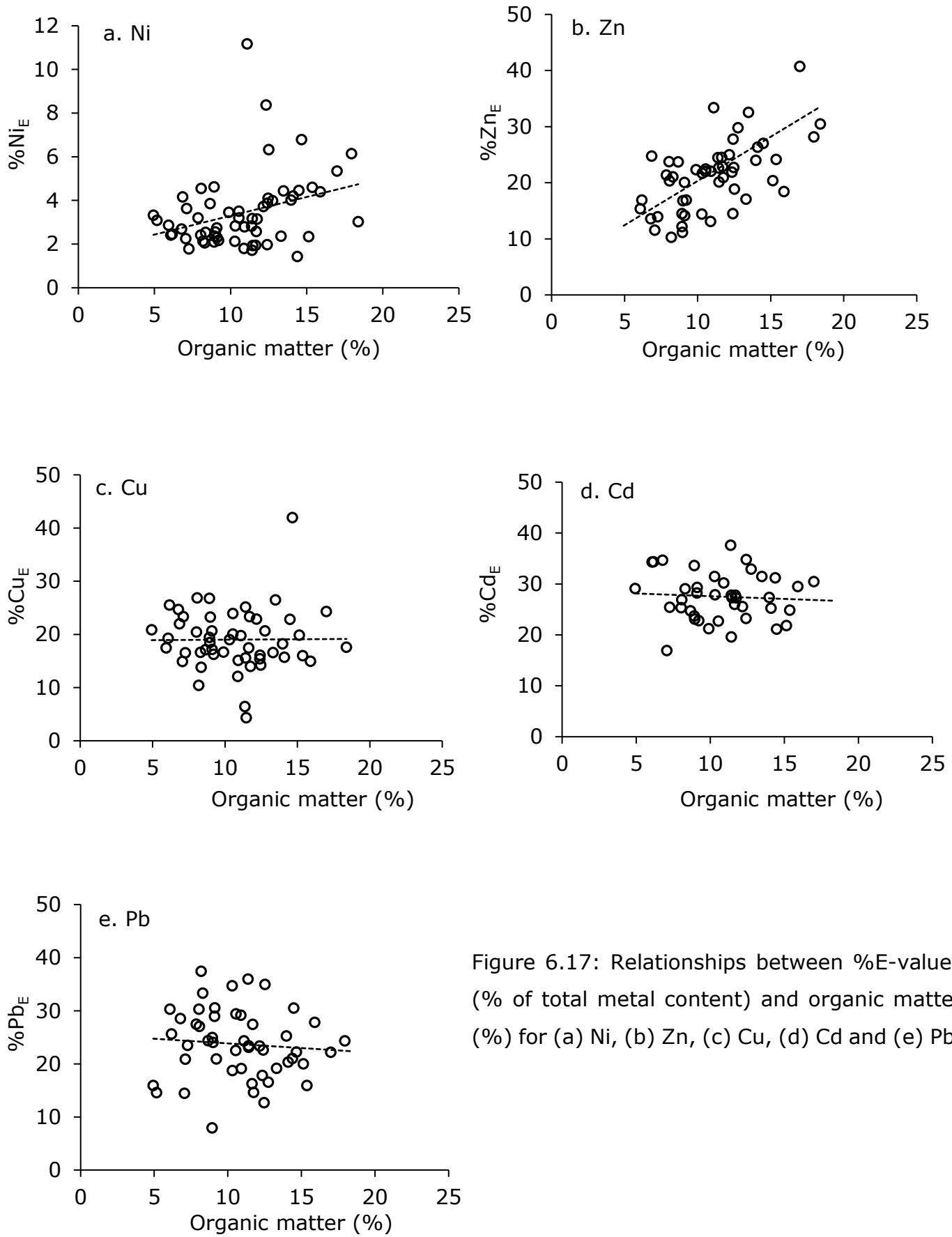


Figure 6.17: Relationships between %E-values (% of total metal content) and organic matter (%) for (a) Ni, (b) Zn, (c) Cu, (d) Cd and (e) Pb.

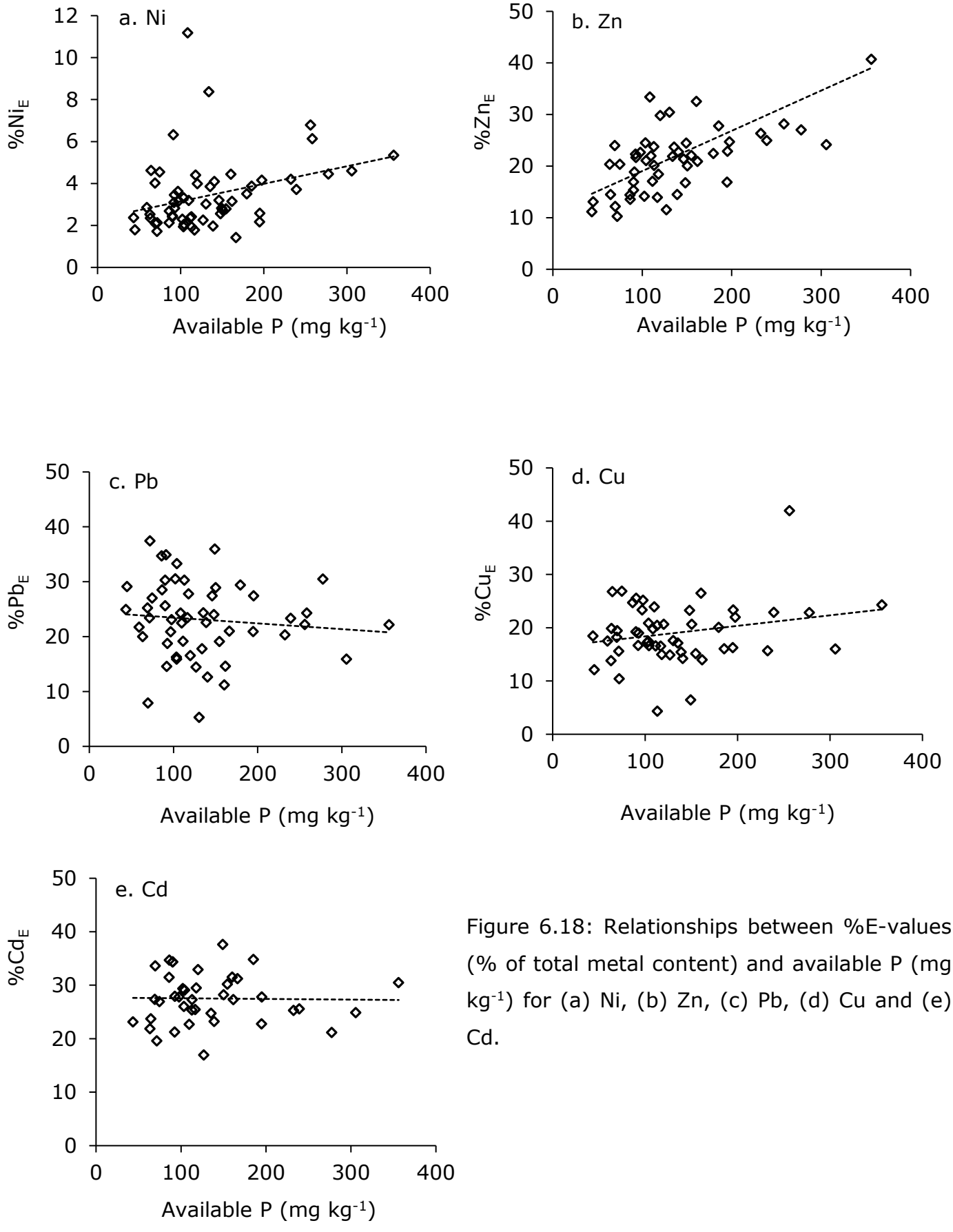


Figure 6.18: Relationships between %E-values (% of total metal content) and available P (mg kg^{-1}) for (a) Ni, (b) Zn, (c) Pb, (d) Cu and (e) Cd.

6.3.6 Source apportionment of labile/non-labile pools of lead urban allotment top soils

Lability of Pb has been observed to vary between pollutant sources (Mao et al., 2014, Shetaya et al., 2018). For example, Atkinson et al. (2011b) investigated the isotopic composition of labile and non-labile fractions of Pb in soils contaminated from a range of sources. Despite prolonged contact of the trace metals with the soil, they showed differences in the reactivity of Pb from the contaminant and native sources. In order to investigate the difference between isotopic signatures of labile and non-labile pools of Pb, the ratio of the isotopic ratios (IR) $^{206}/^{207}$Pb in non-labile (NL) and labile (L) pools (IR_{NL}/IR_{L}) was examined as a function of $^{206}/^{207}$Pb in Pb_{total}. The expectation might be that across the range of IR ($^{206}/^{207}$Pb) values there may be a difference in the lability of Pb originating from petrol or from geological sources; that would produce a value of IR_{NL}/IR_{L} which differed from 1.0. A value of IR_{NL}/IR_{L} greater than 1 would suggest that Pb from geological sources was less labile than Pb originating from petrol. However, in the allotment soils, there was no evidence of source-dependent differences in lability and there appeared to be an equal distribution of Pb_{petrol} and $Pb_{geogenic}$ in both labile and non-labile phases (Figure 6.19). This suggests that Pb originating from different sources must have mixed together into a common pool due to prolonged contact with soils. A few scattered samples observed below the horizontal line in Figure 6.19 with Pb_{total} IR values ≤ 1.14 (X-axis) indicate samples where Pb_{petrol} was less labile than $Pb_{geogenic}$. Similarly, a few samples which were scattered more above the horizontal line, with Pb_{total} IR values ≥ 1.14 (X-axis), represent soils where $Pb_{geogenic}$ was less labile than Pb_{Petrol}.

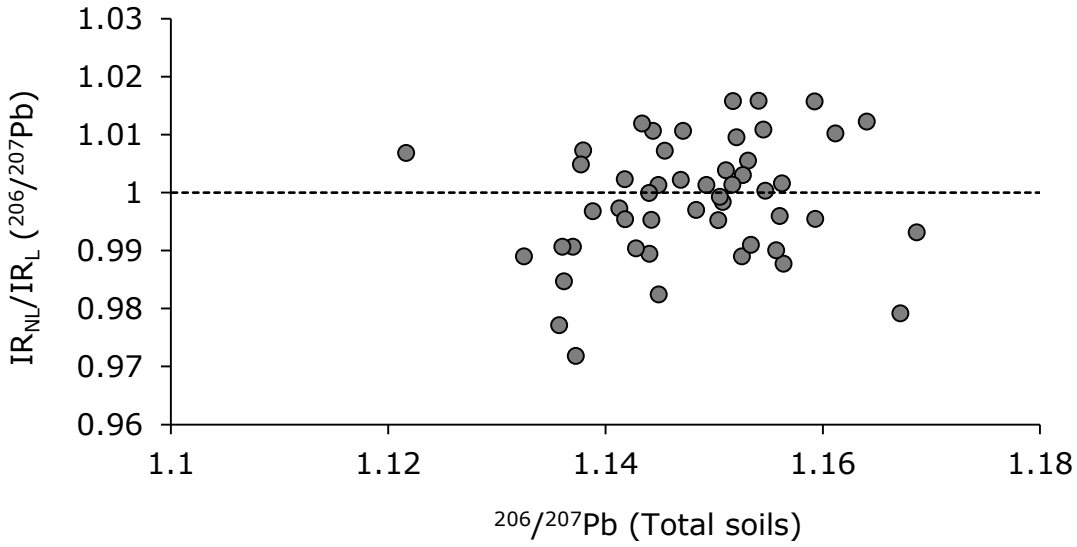


Figure 6.19: The ratio of non-labile to labile $^{206}/^{207}$Pb ratios (IR_{NL}/IR_L) as a function of $^{206}/^{207}$Pb of Pb_{total} in topsoils. The dashed horizontal line represents an IR_{NL}/IR_L ratio of 1.

The relative contributions of Pb_{petrol} and $Pb_{geogenic}$ to the labile and non-labile fractions of Pb_{total} were calculated (Figure 6.20) in order to investigate whether there was any evidence of source-dependent lability. The average proportion of the labile Pb pool derived from petrol was 23% whereas the average proportion of the non-labile Pb pool derived from petrol was 36%. This suggests that Pb_{petrol} is over-represented in the non-labile pool which is in contrast to a few other studies. For example, Mao et al. (2014) and Shetaya et al. (2018) reported slightly greater lability of Pb_{petrol} than $Pb_{geogenic}$ in topsoils which were collected from locations close to roads and industrial areas. The proportions (%) of petrol and geogenic Pb in labile and non-labile pools were also calculated (Figure 6.21); there were clear differences in lability of Pb from both sources confirming an apparently lower lability for petrol-derived Pb. The lower lability of Pb_{petrol} is surprising because it has probably been incorporated into the soil more recently and so has had less contact time with the allotment soils. Furthermore, it probably arrived at

the soil surface as sub-micron sized PbO particles which would be relatively soluble in soils (Olson and Skogerboe, 1975, Harrison, 2012). By contrast, the geogenic Pb would include coal ash and a wide range of industrial sources such as metal artefacts and paint which might be expected to retain an intrinsically less labile characteristic. The intrinsically greater lability of $Pb_{geogenic}$ was therefore an unexpected finding. Possible explanations might include (i) the arrival of $Pb_{geogenic}$ as fine aerial particles from centuries of domestic and industrial (power) coal burning and (ii) some of the apparently Pb_{petrol} actually originating from industrial products manufactured from imported Pb. It should also be acknowledged that the difference in lability between the two sources is quite small and the prevailing picture is one of almost complete mixing of all sources within the labile and non-labile pools of the soil Pb.

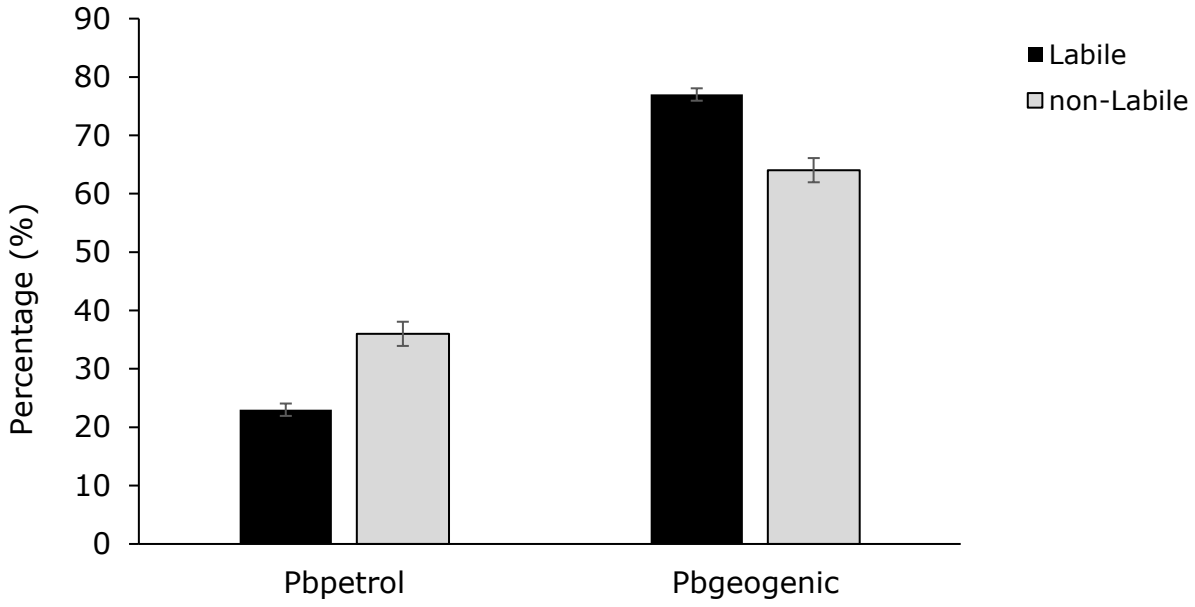


Figure 6.20: Proportion (%) of Pb_{petrol} and $Pb_{geogenic}$ in labile and non-labile pools in soils.

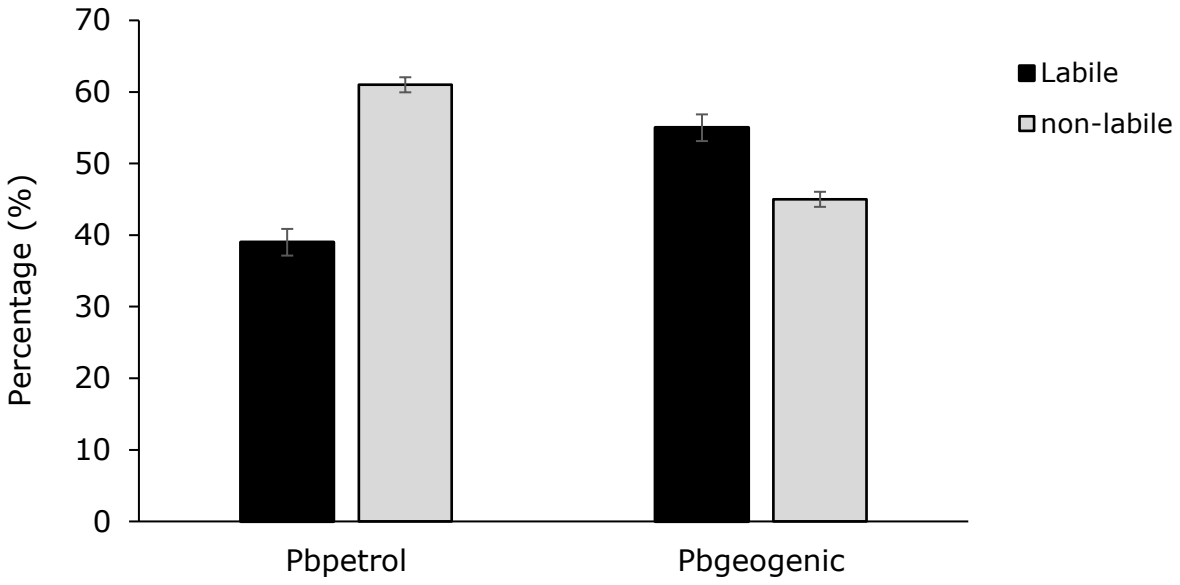


Figure 6.21: Intrinsic average percentage (%) of Pb_{petrol} and $Pb_{geogenic}$ in labile and non-labile pools of allotment topsoils.

6.3.7 Behaviour of Pb in individual fractions of an SEP in urban allotment topsoils

The use of Pb isotopic ratios for source-apportionment in the different fractions of the SEP is potentially a powerful forensic tool which may provide additional information regarding the behaviour of anthropogenic and natural Pb in soils (Teutsch et al., 2001, Emmanuel and Erel, 2002). Therefore, Pb isotopic ratios in individual fractions of the SEP scheme were also measured and are shown on a binary plot ($^{206}/^{207}$Pb versus $^{208}/^{207}$Pb) with reference values (end members) of UK leaded petrol and UK ore/coal (geogenic) to assess the likely contribution of Pb from these two major sources (Figure 6.22). Most of the data fell close to the mixing line between the two end-members. The proportion (%) of Pb_{petrol} and $Pb_{geogenic}$ in different fractions were also calculated according to Eq. (2) given in Chapter 2 (section 2.8) and was found to be slightly different in each fraction. All fractions had a greater proportion of $Pb_{geogenic}$ (> 67%) than Pb_{petrol} (Table 6.5).

The proportion (%) of $Pb_{geogenic}$ to Pb_{petrol} in individual fraction was lowest (2.04%) in F1 showing the presence of more Pb_{petrol} (33%) as compared to other SEP fractions. As expected, the highest (3.09%) ratio of $Pb_{geogenic}$ to Pb_{petrol} was found in F5 (Figure 6.23). However, the presence of *any* Pb_{petrol} in F5 is revealing of soil processes that have transformed Pb that was possibly originally soluble into a highly resistant form. In a previous study conducted by Teutsch et al. (2001), Pb_{petrol} was also shown to be associated more with the labile phases of soil whereas natural Pb was found in the stable minerals in soils. An attempt was also made to assess the behaviour of Pb_{petrol} with most common soil properties such as: pH, Pb_{total} content, organic matter and available P. Therefore, ratio of Pb_{petrol} in each fraction to Pb_{petrol} in fraction 5 (eg. ratio of % Pb_{petrol} (F1)/% Pb_{petrol} (F5)) was plotted against different soil properties. No relationship was seen in the distribution of Pb_{petrol} (%) across the SEP fractions as a function of pH. Again this may have been due to the very restricted pH range of the soil samples (pH=5.98-7.88; average = 6.99; standard deviation = 0.36), (Figure 6.24). The most significant relationship of the ratio of Pb_{petrol} (F1/F5) across the SEP fractions was with the organic matter content. A smaller ratio (F1/F5) for Pb_{petrol} was observed with increase in organic matter content (Figure 6.25). The same trend was also apparent in other fractions suggesting that soil humus (or organic matter addition to the soil) promotes the transfer of initially labile Pb_{petrol} into the residual phase. A role for soil humus in promoting Pb fixation has not been suggested previously, most studies suggest that fixation is more common in alkaline soils and soils with higher concentration of Fe oxides (hydroxides) (Ma et al., 2006b, Degryse et al., 2009). A trend was also observed between the ratio of Pb_{petrol} (F1/F5, F2/F5, F3/F5 and F4/F5) with Pb_{total} and available P concentration (Figures 6.26 and 6.27). Thus, transformation of Pb_{petrol} to F5 increased with the concentration of Pb_{total} and

available P. This again provides some circumstantial evidence that, with time, Pb_{petrol} can be transferred into residual forms through fixation processes such as precipitation of Pb in carbonates, pyromorphites or occlusion in other minerals. Another possibility might be the presence of resistant anthropogenic artefacts of (non-petrol) Pb such as paint flakes or particles of metallic Pb from wire, solders, pottery glazes, glass etc. that do not have the isotopic signature of 'geogenic Pb'. A study conducted by Mao et al. (2014), highlighted a soil sample collected during a survey of London which was highly contaminated from a 19th century 'white lead' works, using Pb imported from Australia or Canadia. The resulting soil Pb had an isotopic signature close to that of Pb_{petrol}. In the past, the UK has imported Pb from overseas for industrial use with isotopic signatures similar to that of UK Pb_{petrol} (Monna et al., 1997). In the Nottingham allotment soils this might contribute to the apparent presence of Pb_{petrol} in the F5 of the SEP.

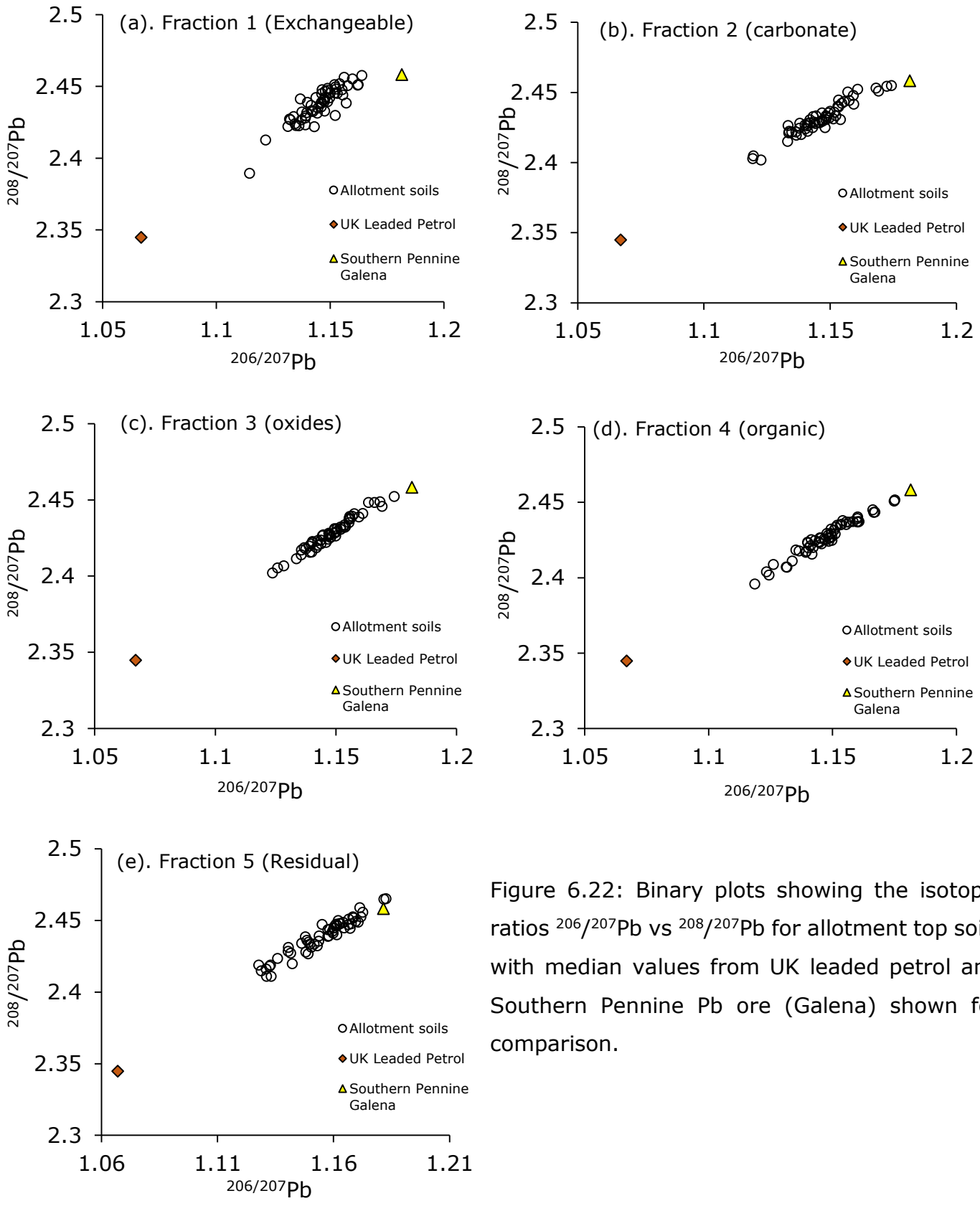


Figure 6.22: Binary plots showing the isotopic ratios $^{206}/^{207}$Pb vs $^{208}/^{207}$Pb for allotment top soils with median values from UK leaded petrol and Southern Pennine Pb ore (Galena) shown for comparison.

Table 6.5: Proportions (%) of Pb_{petrol} and $Pb_{geogenic}$ in individual fractions of SEP

SEP	Pb_{petrol} (%)	$Pb_{geogenic}$ (%)
Fraction 1	32.94	67.06
Fraction 2	32.07	67.93
Fraction 3	30.59	69.41
Fraction 4	30.99	69.01
Fraction 5	24.47	75.53

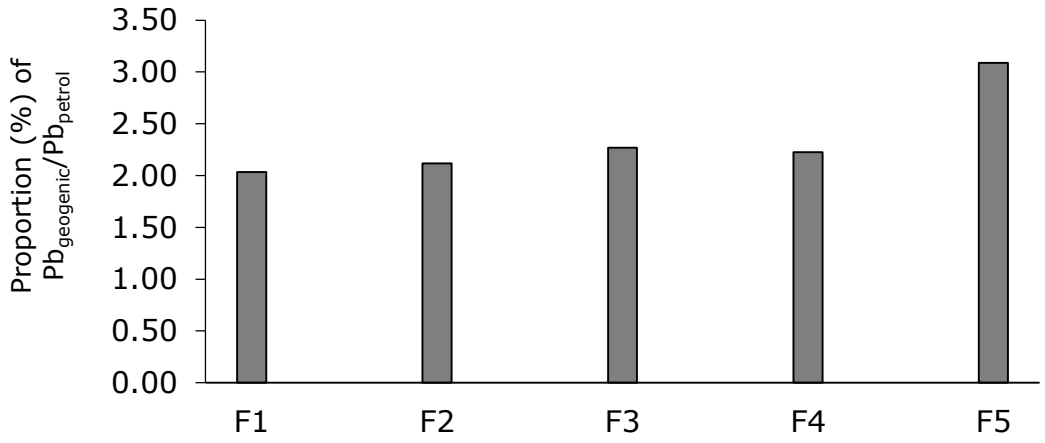


Figure 6.23: Proportion (%) of $Pb_{geogenic}$ to Pb_{petrol} in individual fractions of SEP

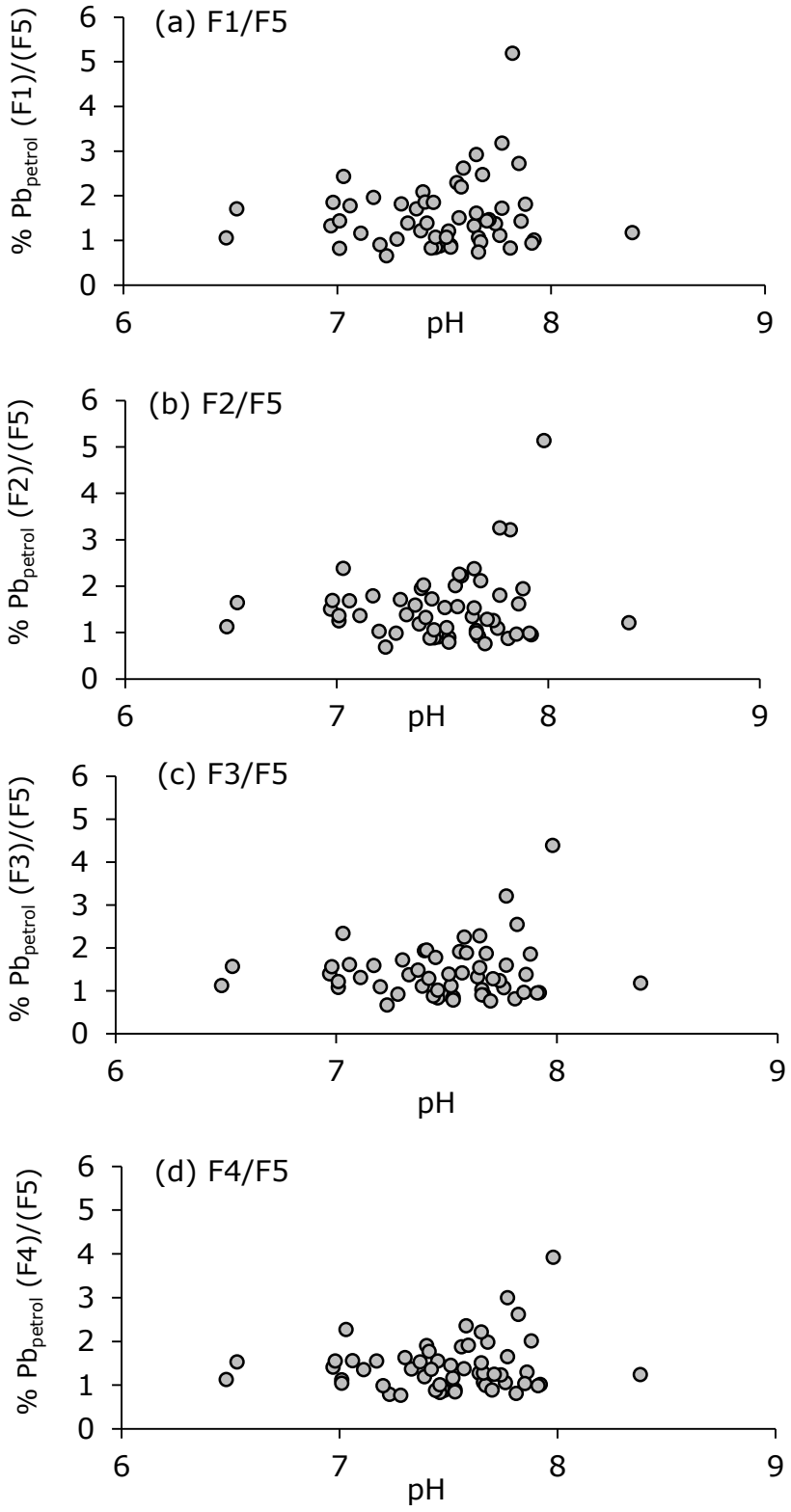


Figure 6.24: Effect of pH on Pb_{petrol} on (a) F1/F5, (b) F2/F5, (c) F3/F5 and (d) F4/F5.

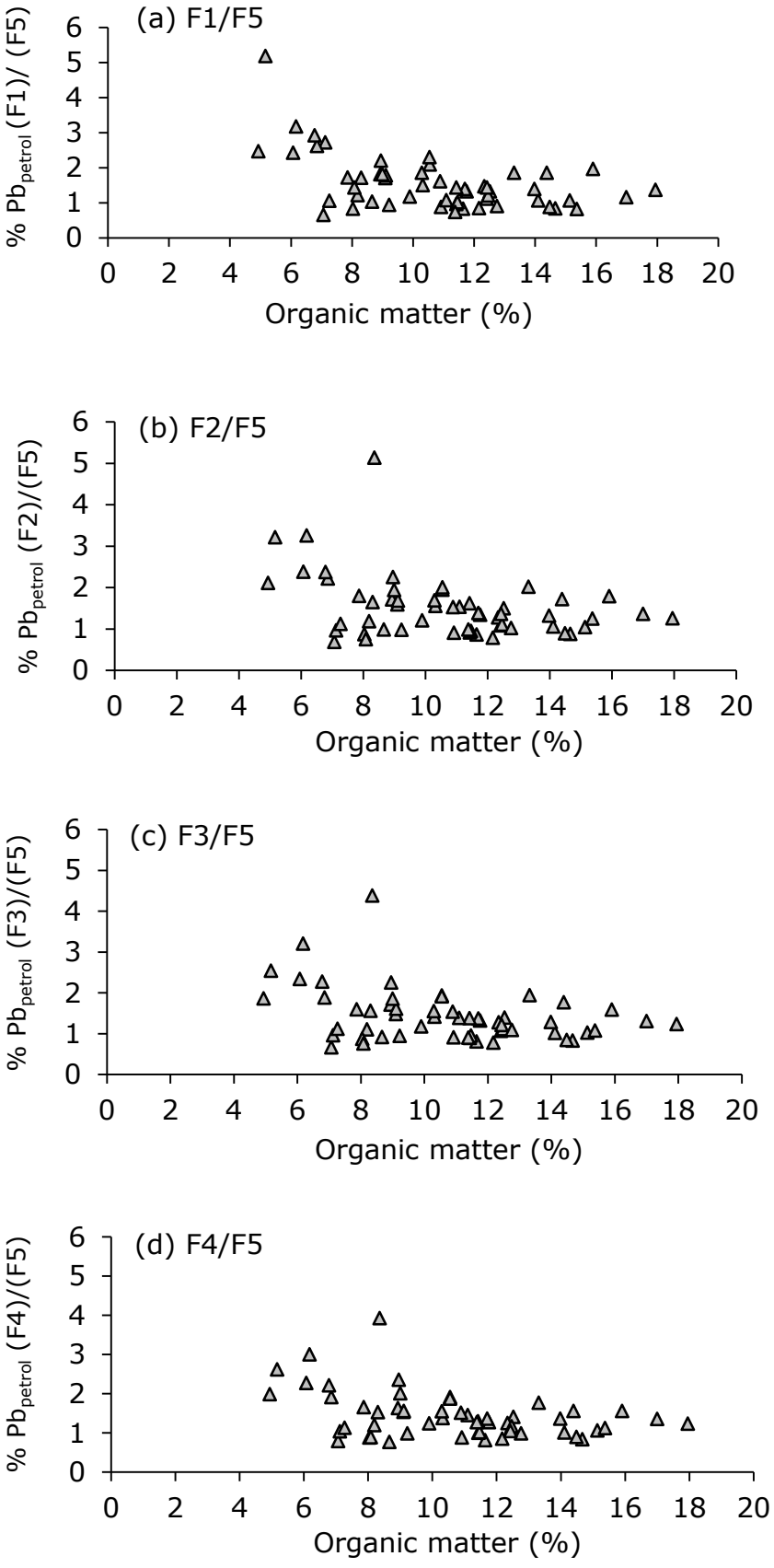


Figure 6.25: Effect of organic matter (mg kg^{-1}) on Pb_{petrol} on (a) F1/F5, (b) F2/F5, (c) F3/F5 and (d) F4/F5.

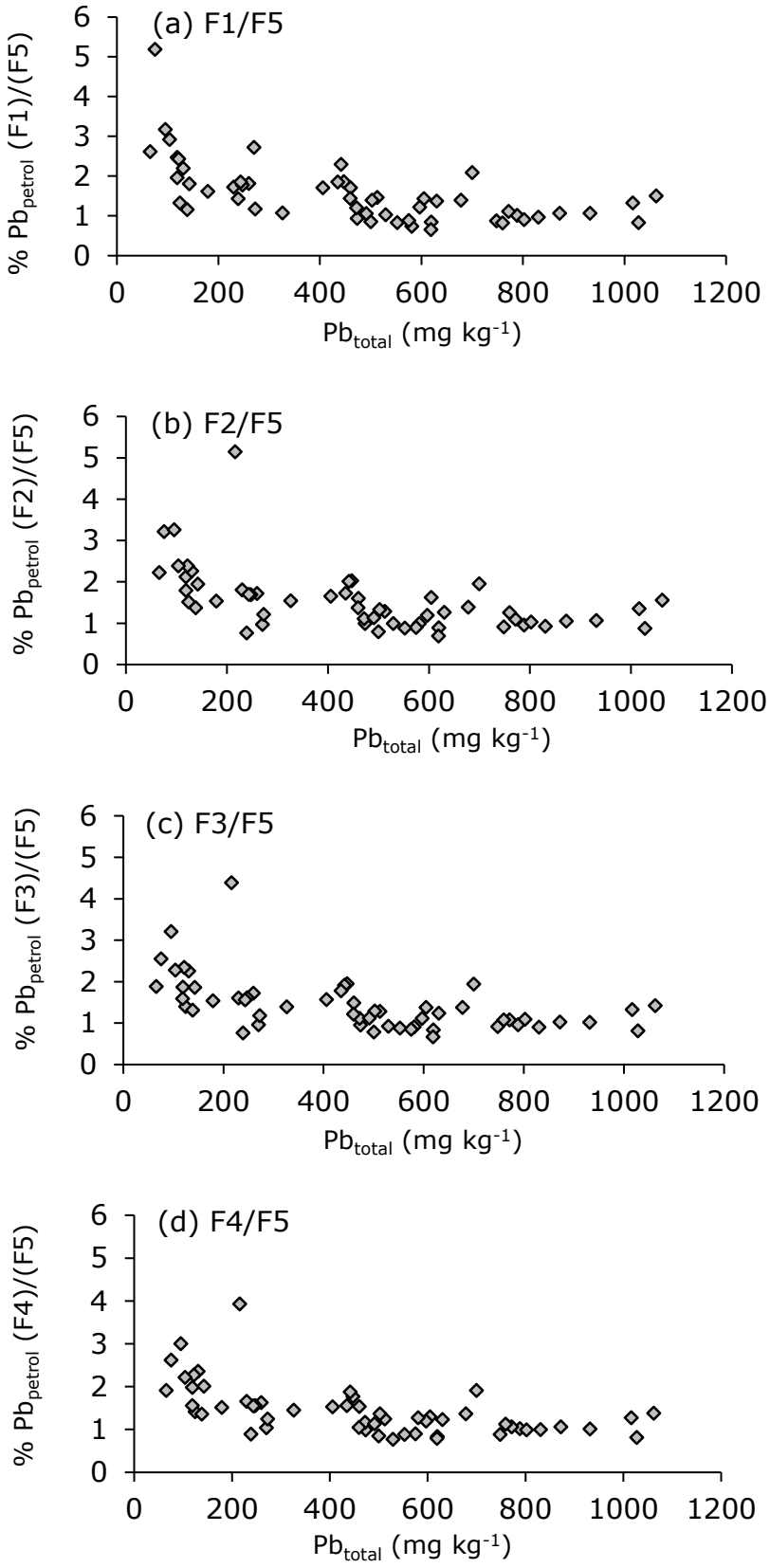


Figure 6.26: Effect of Pb_{total} content (mg kg^{-1}) on Pb_{petrol} on (a) F1/F5, (b) F2/F5, (c) F3/F5 and (d) F4/F5.

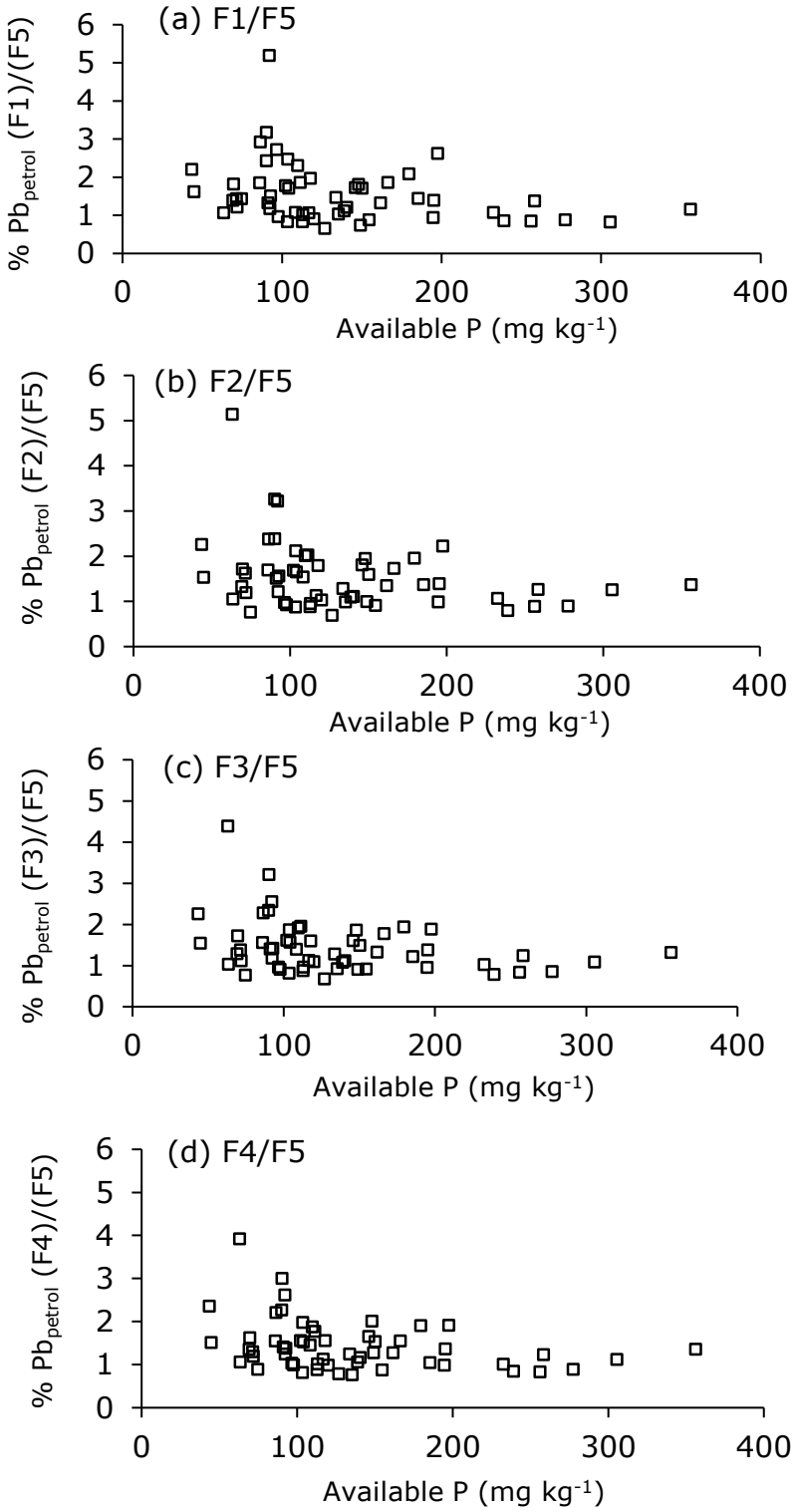


Figure 6.27: Effect of available P (mg kg^{-1}) on Pb_{petrol} on (a) F1/F5, (b) F2/F5, (c) F3/F5 and (d) F4/F5.

6.4 Conclusions

The results of multi-element isotopic dilution methods revealed that the average labilities of trace metals such as Ni, Cu, Zn, Cd and Pb were < 50%, where the highest lability was observed for Cd and lowest was for Ni. A comparison of E-values of trace metals (i.e., Ni, Cu and Zn) in E_{soln} and E_{resin} showed very little evidence of non-labile metals associated with suspended colloidal particles. Whereas, in the case of Pb and Cd, the overestimation of Pb_E and Cd_E in the resin treated solution indicated a constant level of contamination was from chelex-resin with 'native' Pb and Cd. There was only a weak relationship between soil properties and E-values for Ni, Cu, Zn, Cd and Pb in the allotment soils which might suggest a residual influence from the original contaminant source. Analysis of the sources of labile and non-labile Pb pools showed a greater contribution from $Pb_{geogenic}$ (possibly coal) to both labile and non-labile pools but, surprisingly, Pb from petrol had a lower intrinsic lability than Pb originating from geogenic sources.

Fractionation of different elements using a SEP was helpful in revealing that only Cd, Sr and Ca were highly bioavailable as these were found more enriched in fractions F1 and F2. Most trace metals were mainly associated with F3 and F4. In F3, the high fraction of the trace metals suggested mineral oxides were important adsorption phases for these metals while the presence of trace metals in F4 indicated their strong affinity with organic matter. The distribution pattern of elements such as Tl, Fe, V, Cr, Ni, Mo, Ba and U were similar with the greatest proportion associated with primary minerals (F5). A further comparison of SEP with E-values of Ni, Cu, Zn, Cd and Pb showed no consistent correspondence with any single fraction, however a reasonable correspondence was observed between trace metals extracted in combined fractions (F1+F2) with E-values for Zn and Ni.

In the case of Cu, the non-isotopically exchangeable fraction corresponded well with the combined last two fractions (Cu_{F4+F5}) of the SEP.

The isotopic characterization of Pb isotopes in the individual fractions of SEP was helpful in revealing that the relative contribution of $Pb_{geogenic}$ in all fractions was greater than Pb_{petrol}. The distribution of Pb_{petrol} across the SEP fractions showed the presence of Pb_{petrol} in F5; the proportion in F5 increased with the concentration of organic matter, Pb_{total} and available phosphorus. The presence of Pb_{petrol} in the most resistant fraction (F5) was surprising. This may indicate that, with time, the original soluble Pb_{petrol} has been transformed into a highly resistant form through reaction with soil constituents (e.g. precipitation as pyromorphites or occlusion within mineral phases). Alternatively this might indicate the presence of resistant anthropogenic artefacts of Pb with an isotopic signature similar to that of UK Pb_{petrol}. This would also be consistent with the finding that the isotopic exchangeability of 'petrol-Pb' was slightly less than that of geogenic Pb.

7 Chapter 7: General conclusions and future work

7.1 Overview

In the current study a forensic analysis of urban soils was undertaken by applying a "toolbox" of methods to identify different contaminant sources. A key part of the developmental work in the project was to refine a protocol, using the current generation ICP-QMS instrument, in order to maximise the accuracy and precise determination of Pb isotope ratios (chapter 3). The developed methodology was applied to a range of urban soils to enable soil Pb source apportionment and was further extended to utilize a full range of multi-elements (including REEs and PGEs) as an aid to investigate the other key potential sources of pollutant (Chapters 4 & 5). In order to provide more insight, the isotopically exchangeable fraction (E-value) by multi-element isotopic dilution (ID) and fractionation of metals by sequential extraction procedure (SEP) were determined to study the behaviour and sources of pollutants in selected allotment soils. The degree of correspondence between these two methods (ID and SEP) was also investigated (Chapter 6).

7.2 Main Findings

For several reasons, quadrupole-based mass spectrometers (ICP-QMS) are inferior to other mass spectrometers for measurement of Pb isotope ratios. In the current project, a refined protocol was developed for accurate and precise measurement of Pb isotope ratios in urban soils using a current-generation ICP-QMS. This was achieved by optimising several operating parameters including individual dilution of soil samples to the same Pb concentration,

identical to that of an external isotope standard (SRM-981, NIST), determination and setting of the dead time correction factor, optimisation of quadrupole dwell time and number of scans per sample using both internal (Tl) and external (SRM-981, NIST) standards for mass bias correction. The developed methodology benchmarked very well against MC-ICP-MS measurements on the same sample material. Average values and standard deviations of the Pb isotope ratios $^{207}/^{206}$Pb and $^{208}/^{206}$Pb in SRM-981 (NIST) were 0.91778 ± 0.00052 and 2.18142 ± 0.001757 respectively for the final developed protocol compared to the certified values of 0.91464 ± 0.00033 and 2.1681 ± 0.0008. In an analytical run where soil samples were analysed continually for five days, with SRM-981 standard repeats after every ten samples, the average standard deviations for Pb isotope ratios were $^{207}/^{206}$Pb = 0.91712 ± 0.00093 and $^{208}/^{206}$Pb = 2.17984 ± 0.00210 following in-sample Tl correction for mass bias. By contrast, the precision of Pb ratios involving the minor isotope (^{204}Pb) was not much improved even though interferences from ^{204}Hg were apparently negligible. This protocol for Pb isotopes ratio measurements can be particularly helpful in environmental applications that require analysis of large numbers of samples, in the minimum time utilizing simple sample preparation and operational techniques as compared to the relatively expensive (and for some, inaccessible) multi-collector mass spectrometers (MC-ICP-MS). This work can bring better source apportionment of Pb (at a time when there is renewed concern about Pb in cities) within the reach of laboratories with ICP-QMS because there are so very few labs with MC-ICP-MS and this is important as more labs are buying ICP-QMS as their analytical workhorses. Application of this protocol is limited in those cases

where very high precision is required, such as archaeological studies, or where the least abundant isotope (^{204}Pb) must also be included in the analysis.

The determination of Pb isotopic ratios in different sets of soils (urban soil, allotment soils and sewage amended soils) was very helpful in identifying the dominant sources of Pb (i.e., Pb_{petrol} and $Pb_{geogenic}$) and their relative contributions. The examination of isotopic ratios in both topsoils and subsoils of allotments was useful in revealing the apparent migration of Pb_{petrol} down the soil profile into the subsoil. Furthermore, the relationship of Pb_{petrol} with Pb_{total} helped in identifying allotments (i.e., PF, ST, MP, MR and WT) where the main influence was from vehicles or coal burning. Also the absence of trends at some allotment sites (i.e., CN, SN, BH and WM) was apparently due to variation in the inputs of different sources.

The measurement of Pb isotopes in individual fractions of the SEP was a useful approach in providing more detail regarding the estimation of dominant Pb sources (i.e., Pb_{petrol} and $Pb_{geogenic}$) associated with different phases. The relative contribution of $Pb_{geogenic}$ in all individual fractions appeared higher (>67%) than Pb_{petrol}. Whereas the greatest proportion (33%) of Pb_{petrol} was found associated with the most labile phase (F1). Lead isotopes in individual fractions of SEPs proved helpful in assessing the behaviour of Pb_{petrol} across the SEP fractions where it revealed the presence of Pb_{petrol} (24%) in the most resistant fraction (F5), which was surprising. The proportion of Pb_{petrol} in F5 was observed to be greatest in soils with greater concentration of organic matter, available P and Pb_{total}. This may reflect that with time, the original labile Pb_{petrol} has been transformed into a highly resistant form through reaction with soil constituents (e.g. precipitation as pyromorphites or occlusion in other minerals) or, alternatively it might be due to an artefact of resistant

anthropogenic (non-petrol) Pb with isotopic signatures similar to typical UK Pb_{petrol}.

The reactivities (E-values) calculated for trace metals such as Ni, Cu, Zn, Cd and Pb in allotment soils measured through multi-element isotopic dilution method were below 50% and the relative labilities of these elements followed the sequence Cd> Pb ≥ Zn> Cu>Ni. The overall weak relationship of common soil properties with E-values of different trace metals revealed a greater influence from contaminant sources. A further de-coupling of labile and non-labile fractions showed greater contribution of $Pb_{geogenic}$ (coal Pb) in both labile and non-labile fractions and surprisingly the intrinsic lability of Pb_{petrol} was observed to be lower. The greater lability of $Pb_{geogenic}$ was unexpected and a key finding which demonstrated coal Pb that entered into the allotment soils as aerial particulates were relatively in more reactive form compared to other sources such as coal ash.

The comparison of %E-values measured in E_{soln} and E_{resin} were very similar for Ni, Cu and Zn whereas in the case of Pb and Cd, there was an overestimation of E_{resin} because of systematic contamination from chelex-resin with 'native' Pb and Cd. It has been already reported that segregation of the true isotopic abundance from the labile pool using chelating resin may increase experimental error both as a result of resin contamination and because the metal concentration extracted by resin may be too small to be reliably measured. Therefore, when determining E-values for trace metals in soils the resin treated step may not be necessary.

A comparison of E-values for Ni, Cu, Zn, Cd and Pb with SEP data showed no correspondence with any single fraction whereas a reasonable correspondence

was observed between metals extracted in combined fractions – e.g. (F1+F1) with E-values for Zn and Ni. In the case of Cu, the non-isotopically exchangeable fraction correlated with the sum of the most resistant two fractions (F4+F5) of the SEP. Furthermore the comparison of Pb and Cd extracted in the combined fractions (F1+F2+F3) with E-values illustrated that SEP approach overestimated the lability of these metals most likely due to the mobilization of non-labile metals bound within the mineral oxides and carbonate matrices.

Approaches such as EFs and cluster analysis (dendrograms) in combination with source-apportionment of Pb (Pb_{petrol} and $Pb_{geogenic}$) were to some extent helpful in attempting to understand the major contaminant sources. As compared to urban soils (Nottingham and Wolverhampton), allotments with similar soil type, soil chemistry and closer sampling proximity, the cluster analysis approach identified more anthropogenic sources such as fertilizers, vehicles, coal and industrial. The attempt to extend the range of trace elements to other signatures (REEs and PGEs) in the allotment soils proved to be of limited value in providing additional information regarding the identification of specific sources of contaminants. In the allotment soils, PGEs were observed below DL which revealed two things: i) allotment soils might not be substantially contaminated by PGEs or ii) the procedure used for soil digestion were not optimised to generate measurable concentrations of PGEs. Comparison of REE abundance ratios with those of the mean upper continental crust (UCC), and an examination of EFs revealed only a small influence from anthropogenic inputs, such as fertilizers.

7.3 Future work

The main findings presented in this work suggest further investigation in the following areas:

- In the current study the existing attempt to define 3 or more sources of Pb through Pb isotopes was limited due to the lack of identification of reliable end members mainly due to regional factors. For example in the UK, the isotopic composition of a third end-member such as 'industrial' Pb is difficult to precisely define because it is likely that imported Pb with a range of isotopic signatures will have contributed to a wide range in Pb isotope compositions. Therefore in order to improve determination of Pb one possible future direction is to develop models that use the dataset itself to 'define' a range of end members in terms of their Pb isotopic abundances.
- The results of Pb isotopic characterization in individual fractions of the SEP revealed the presence of Pb_{petrol} in F5. The findings of this work suggested different soil processes would have transformed originally soluble Pb into a highly resistant form or possibly it might be resistant particles of industrial Pb with a similar isotopic signature to that of UK Pb_{petrol} that was not extracted in the first four fractions (F1-F4). Here there is a need of more insight to identify the possible nature of F5 particles through other techniques such as XAFS and SEM following isolation.
- The demand for REEs and PGEs in recent years has been increased mostly in industrial, commercial and residential appliances. As a result these elements are expected to increase in the environment over the next few decades. High concentrations of PGEs and REEs in the

environment are considered of serious concern due to possible adverse effects on human health and ecosystems but so far very little research has been undertaken on these elements. Therefore more information on sources and proper evaluation of REEs and PGEs is needed which could be forensically useful in future. Future investigation is also needed regarding the speciation characteristics of REEs in agricultural soils in order to assess possible adverse effects on soil fertility. Also there is a need to determine PGEs in soils by improved analytical techniques such as digestion of soils by aqua regia followed by matrix-separation and pre-concentration steps prior the analysis with ICP-QQQ.

- Future investigation is needed to keep pace with new inputs (pollutants) in terms of their composition and isotopic or elemental ratios. Therefore the possible use of MC-ICP-MS is necessary to examine the differences in isotopic signatures.

8 References

ADRIANO, D. C. 2001. Arsenic. *Trace elements in terrestrial environments.* Springer.

AGGARWAL, J., HABICHT-MAUCHE, J. & JUAREZ, C. 2008. Application of heavy stable isotopes in forensic isotope geochemistry: a review. *Applied Geochemistry,* 23**,** 2658-2666.

AHLBERG, G., GUSTAFSSON, O. & WEDEL, P. 2006. Leaching of metals from sewage sludge during one year and their relationship to particle size. *Environmental pollution,* 144**,** 545-553.

AHMAD, I., KHAN, B., KHAN, S., KHAN, M. T. & SCHWAB, A. P. 2018. Assessment of lead exposure among automobile technicians in Khyber Pakhtunkhwa, Pakistan. *Science of the Total Environment,* 633**,** 293-299.

AHNSTROM, Z. A. S. & PARKER, D. R. 2001. Cadmium Reactivity in Metal-Contaminated Soils Using a Coupled Stable Isotope Dilution−Sequential Extraction Procedure. *Environmental Science & Technology,* 35**,** 121-126.

ALEXANDER, P., ALLOWAY, B. & DOURADO, A. 2006. Genotypic variations in the accumulation of Cd, Cu, Pb and Zn exhibited by six commonly grown vegetables. *Environmental Pollution,* 144**,** 736-745.

ALFONSO, S., GROUSSET, F., MASSÉ, L. & TASTET, J.-P. 2001. A European lead isotope signal recorded from 6000 to 300 years BP in coastal marshes (SW France). *Atmospheric Environment,* 35**,** 3595-3605.

ALLOWAY, B. & AYRES, D. C. 1997. *Chemical principles of environmental pollution*, CRC press.

ALLOWAY, B. J. 2004. Contamination of soils in domestic gardens and allotments: a brief overview. *Land Contamination and Reclamation,* 12**,** 179-187.

ALLOWAY, B. J. 2013. Sources of heavy metals and metalloids in soils. *Heavy metals in soils.* Springer.

ALMEIDA, C. M. & VASCONCELOS, M. T. S. 2001. ICP-MS determination of strontium isotope ratio in wine in order to be used as a fingerprint of its regional origin. *Journal of Analytical Atomic Spectrometry,* 16**,** 607-611.

ANDER, E. L., JOHNSON, C. C., CAVE, M. R., PALUMBO-ROE, B., NATHANAIL, C. P. & LARK, R. M. 2013. Methodology for the determination of normal background concentrations of contaminants in English soil. *Science of the Total Environment,* 454**,** 604-618.

ANDERSEN, M., RAULUND RASMUSSEN, K., HANSEN, H. & STROBEL, B. 2002. Distribution and fractionation of heavy metals in pairs of arable and afforested soils in Denmark. *European Journal of Soil Science,* 53**,** 491-502.

APEAGYEI, E., BANK, M. S. & SPENGLER, J. D. 2011. Distribution of heavy metals in road dust along an urban-rural gradient in Massachusetts. *Atmospheric Environment,* 45**,** 2310-2323.

APPELBLAD, P. K. & BAXTER, D. C. 2000. A model for calculating dead time and mass discrimination correction factors from inductively coupled plasma mass spectrometry calibration curves. *Journal of Analytical Atomic Spectrometry,* 15**,** 557-560.

ARIZA, J. G., GIRALDEZ, I., SANCHEZ-RODAS, D. & MORALES, E. 2000. Metal sequential extraction procedure optimized for heavily polluted and iron oxide rich sediments. *Analytica Chimica Acta,* 414**,** 151-164.

ATKINSON, N., BAILEY, E., TYE, A., BREWARD, N. & YOUNG, S. 2011a. Fractionation of lead in soil by isotopic dilution and sequential extraction. *Environmental Chemistry,* 8**,** 493-500.

ATKINSON, N. R., BAILEY, E. H., TYE, A. M., BREWARD, N. & YOUNG, S. D. 2011b. Fractionation of lead in soil by isotopic dilution and sequential extraction. *Environmental Chemistry,* 8**,** 493-500.

ATSDR, U. 2007. Toxicological profile for lead. *US Department of Health and Human Services,* 1**,** 582.

AYRES, M. & HARRIS, N. 1997. REE fractionation and Nd-isotope disequilibrium during crustal anatexis: constraints from Himalayan leucogranites. *Chemical Geology,* 139**,** 249-269.

BÄCKSTRÖM, M., KARLSSON, S. & ALLARD, B. 2004. Metal Leachability and Anthropogenic Signal in Roadside Soils Estimated from Sequential Extraction and Stable Lead Isotopes. *Environmental Monitoring and Assessment,* 90**,** 135-160.

BACON, J., JONES, K. C., MCGRATH, S. & JOHNSTON, A. 1996. Isotopic character of lead deposited from the atmosphere at a grassland site in the United Kingdom since 1860. *Environmental science & technology,* 30**,** 2511-2518.

BACON, J. R., FARMER, J. G., DUNN, S. M., GRAHAM, M. C. & VINOGRADOFF, S. I. 2006. Sequential extraction combined with isotope analysis as a tool for the investigation of lead mobilisation in soils: application to organic-rich soils in an upland catchment in Scotland. *Environmental pollution,* 141**,** 469-481.

BAKIRCIOGLU, D., KURTULUS, Y. B. & IBAR, H. 2011. Investigation of trace elements in agricultural soils by BCR sequential extraction method and its transfer to wheat plants. *Environmental monitoring and assessment,* 175**,** 303-314.

BAKIRDERE, S. & YAMAN, M. 2008. Determination of lead, cadmium and copper in roadside soil and plants in Elazig, Turkey. *Environmental Monitoring and Assessment,* 136**,** 401-410.

BANDURA, D. R., BARANOV, V. I. & TANNER, S. D. 2000. Effect of collisional damping and reactions in a dynamic reaction cell on the precision of isotope ratio measurementsPresented at the 26th Annual Conference of the Federation of Analytical Chemistry and Spectroscopy Societies (FACSS), Vancouver, October 24–29, 1999. *Journal of Analytical Atomic Spectrometry,* 15**,** 921-928.

BARBASTE, M., ROBINSON, K., GUILFOYLE, S., MEDINA, B. & LOBINSKI, R. 2002. Precise determination of the strontium isotope ratios in wine by inductively coupled plasma sector field multicollector mass spectrometry (ICP-SF-MC-MS). *Journal of Analytical Atomic Spectrometry,* 17**,** 135-137.

BARBOSA JR, F., TANUS-SANTOS, J. E., GERLACH, R. F. & PARSONS, P. J. 2005. A critical review of biomarkers used for monitoring human exposure to lead: advantages, limitations, and future needs. *Environmental health perspectives,* 113**,** 1669-1674.

BAREFOOT, R. 1998. Determination of the precious metals in geological materials by inductively coupled plasma mass spectrometry. *Journal of Analytical Atomic Spectrometry,* 13**,** 1077-1084.

BARNES, S. J. 2004. Komatiites and nickel sulfide ores of the Black Swan area, Yilgarn Craton, Western Australia. 4. Platinum group element distribution in the ores, and genetic implications. *Mineralium Deposita,* 39**,** 752-765.

BAVEYE, P., MCBRIDE, M. B., BOULDIN, D., HINESLY, T. D., DAHDOH, M. S. & ABDEL-SABOUR, M. F. 1999. Mass balance and distribution of sludge-borne trace elements in a silt loam soil following long-term applications of sewage sludge. *Science of the total environment,* 227**,** 13-28.

BEGLEY, I. S. & SHARP, B. L. 1994. Occurrence and reduction of noise in inductively coupled plasma mass spectrometry for enhanced precision in isotope ratio measurement. *Journal of Analytical Atomic Spectrometry,* 9**,** 171-176.

BEGLEY, I. S. & SHARP, B. L. 1997. Characterisation and correction of instrumental bias in inductively coupled plasma quadrupole mass spectrometry for accurate measurement of lead isotope ratios. *Journal of Analytical Atomic Spectrometry,* 12**,** 395-402.

BELL, F., CULSHAW, M., FORSTER, A. & NATHANAIL, C. 2009. The engineering geology of the Nottingham area, UK. *Geological Society, London, Engineering Geology Special Publications,* 22**,** 1-24.

BELL, S., FOX-KÄMPER, R., KESHAVARZ, N., BENSON, M., CAPUTO, S., NOORI, S. & VOIGT, A. 2016. *Urban allotment gardens in Europe*, Routledge.

BENCS, L., RAVINDRA, K. & VAN GRIEKEN, R. 2003. Methods for the determination of platinum group elements originating from the abrasion of automotive catalytic converters. *Spectrochimica Acta Part B: Atomic Spectroscopy,* 58**,** 1723-1755.

BI, X., FENG, X., YANG, Y., QIU, G., LI, G., LI, F., LIU, T., FU, Z. & JIN, Z. 2006. Environmental contamination of heavy metals from zinc smelting areas in Hezhang County, western Guizhou, China. *Environment international,* 32**,** 883-890.

BI, X., LIU, J., HAN, Z. & YANG, W. 2015. Lead in Chinese villager house dust: geographical variation and influencing factors. *Environmental pollution,* 207**,** 183-189.

BIELICKA-GIEŁDOŃ, A., RYŁKO, E. & ŻAMOJĆ, K. 2013. Distribution, Bioavailability and Fractionation of Metallic Elements in Allotment Garden Soils Using the BCR Sequential Extraction Procedure. *Polish Journal of Environmental Studies,* 22.

BLAKE, L. & GOULDING, K. 2002. Effects of atmospheric deposition, soil pH and acidification on heavy metal contents in soils and vegetation of semi-natural ecosystems at Rothamsted Experimental Station, UK. *Plant and soil,* 240**,** 235-251.

BOGDANOV, K., FILIPOV, A. & KEHAYOV, R. 2005. Au-Ag-Te-Se minerals in the Elatsite porphyry-copper deposit, Bulgaria. *Geochem. Mineral. Petrol,* 43**,** 13-19.

BOLLHÖFER, A. & ROSMAN, K. 2001. Isotopic source signatures for atmospheric lead: the Northern Hemisphere. *Geochimica et Cosmochimica Acta,* 65**,** 1727-1740.

BOUTRON, C. F., GÖRLACH, U., CANDELONE, J.-P., BOLSHOV, M. A. & DELMAS, R. J. 1991. Decrease in anthropogenic lead, cadmium and zinc in Greenland snows since the late 1960s. *Nature,* 353**,** 153.

BRADL, H. B. 2004. Adsorption of heavy metal ions on soils and soils constituents. *Journal of colloid and Interface Science,* 277**,** 1-18.

BRÄNNVALL, M.-L., BINDLER, R., RENBERG, I., EMTERYD, O., BARTNICKI, J. & BILLSTRÖM, K. 1999. The Medieval metal industry was the cradle of modern large-scale atmospheric lead pollution in northern Europe. *Environmental Science & Technology,* 33**,** 4391-4395.

BRÄNNVALL, M.-L., KURKKIO, H., BINDLER, R., EMTERYD, O. & RENBERG, I. 2001. The role of pollution versus natural geological sources for lead enrichment in recent lake sediments and surface forest soils. *Environmental Geology,* 40**,** 1057-1065.

BRIDGE, D., BROWN, M. & HOOKER, P. 1997. Wolverhampton urban environmental survey: an integrated geoscientific case study.

BRUZZONITI, M., CAVALLI, S., MANGIA, A., MUCCHINO, C., SARZANINI, C. & TARASCO, E. 2003. Ion chromatography with inductively coupled plasma mass spectrometry, a powerful analytical tool for complex matrices: Estimation of Pt and Pd in environmental samples. *Journal of chromatography A,* 997**,** 51-63.

BUEKERS, J., DEGRYSE, F., MAES, A. & SMOLDERS, E. 2008. Modelling the effects of ageing on Cd, Zn, Ni and Cu solubility in soils using an assemblage model. *European Journal of Soil Science,* 59**,** 1160-1170.

BUEKERS, J., VAN LAER, L., AMERY, F., VAN BUGGENHOUT, S., MAES, A. & SMOLDERS, E. 2007. Role of soil constituents in fixation of soluble Zn, Cu, Ni and Cd added to soils. *European Journal of Soil Science,* 58**,** 1514-1524.

BUNDT, M., KRETZSCHMAR, S., ZECH, W. & WILCKE, W. 1997. Seasonal redistribution of manganese in soil aggregates of a Costa Rican coffee field. *Soil science,* 162**,** 641-647.

BURT, R., WILSON, M., KECK, T., DOUGHERTY, B., STROM, D. & LINDAHL, J. 2003. Trace element speciation in selected smelter-contaminated soils in Anaconda and Deer Lodge Valley, Montana, USA. *Advances in Environmental Research,* 8**,** 51-67.

BZDUSEK, P. A., LU, J. & CHRISTENSEN, E. R. 2006. PCB congeners and dechlorination in sediments of Sheboygan River, Wisconsin, determined by matrix factorization. *Environmental science & technology,* 40**,** 120-129.

CALLENDER, E. & RICE, K. C. 2000. The urban environmental gradient: anthropogenic influences on the spatial and temporal distributions of lead and zinc in sediments. *Environmental Science & Technology,* 34**,** 232-238.

CAMPANELLA, L., D'ORAZIO, D., PETRONIO, B. & PIETRANTONIO, E. 1995. Proposal for a metal speciation study in sediments. *Analytica Chimica Acta,* 309**,** 387-393.

CANFIELD, R. L., HENDERSON JR, C. R., CORY-SLECHTA, D. A., COX, C., JUSKO, T. A. & LANPHEAR, B. P. 2003. Intellectual impairment in children with blood lead concentrations below 10 μg per deciliter. *New England journal of medicine,* 348**,** 1517-1526.

CARLSON, C. L. & ADRIANO, D. C. 1993. Environmental impacts of coal combustion residues. *Journal of Environmental quality,* 22**,** 227-247.

CARRÉ, M., POUSSEL, E. & MERMET, J.-M. 1992. Drift diagnostics in inductively coupled plasma atomic emission spectrometry. Plenary lecture. *Journal of Analytical Atomic Spectrometry,* 7**,** 791-797.

CARRERO, J. A., ARRIZABALAGA, I., BUSTAMANTE, J., GOIENAGA, N., ARANA, G. & MADARIAGA, J. M. 2013. Diagnosing the traffic impact on roadside soils through a multianalytical data analysis of the concentration profiles of traffic-related elements. *Science of the Total Environment,* 458**,** 427-434.

CARRILLO-GONZÁLEZ, R., ŠIMŮNEK, J., SAUVE, S. & ADRIANO, D. 2006. Mechanisms and pathways of trace element mobility in soils. *Advances in agronomy,* 91**,** 111-178.

CARTER, J., WALLING, D. E., OWENS, P. N. & LEEKS, G. J. 2006. Spatial and temporal variability in the concentration and speciation of metals in suspended sediment transported by the River Aire, Yorkshire, UK. *Hydrological Processes,* 20**,** 3007-3027.

CASPARI, T., BÄUMLER, R., NORBU, C., TSHERING, K. & BAILLIE, I. 2006. Geochemical investigation of soils developed in different lithologies in Bhutan, Eastern Himalayas. *Geoderma,* 136**,** 436-458.

CHARALAMPIDES, G. & MANOLIADIS, O. 2003. IsoroPC TRACERs N susURFACE YDRoLoccAL. *Journal of Environmental Protection and Ecology,* 4**,** 777-782.

CHARSLEY, T., RATHBONE, P. & LOWE, D. 1990. Nottingham: A geological background for planning and development.

CHEN, J., TAN, M., LI, Y., ZHANG, Y., LU, W., TONG, Y., ZHANG, G. & LI, Y. 2005a. A lead isotope record of Shanghai atmospheric lead emissions in total suspended particles during the period of phasing out of leaded gasoline. *Atmospheric Environment,* 39**,** 1245-1253.

CHEN, T.-B., ZHENG, Y.-M., LEI, M., HUANG, Z.-C., WU, H.-T., CHEN, H., FAN, K.-K., YU, K., WU, X. & TIAN, Q.-Z. 2005b. Assessment of heavy metal pollution in surface soils of urban parks in Beijing, China. *Chemosphere,* 60**,** 542-551.

CHEN, T., LIU, X., ZHU, M., ZHAO, K., WU, J., XU, J. & HUANG, P. 2008. Identification of trace element sources and associated risk assessment in vegetable soils of the urban–rural transitional area of Hangzhou, China. *Environmental Pollution,* 151**,** 67-78.

CHEN, X., LU, X. & YANG, G. 2012. Sources identification of heavy metals in urban topsoil from inside the Xi'an Second Ringroad, NW China using multivariate statistical methods. *Catena,* 98**,** 73-78.

CHENERY, S., IZQUIERDO, M., MARZOUK, E., KLINCK, B., PALUMBO-ROE, B. & TYE, A. 2012. Soil–plant interactions and the uptake of Pb at abandoned mining sites in the Rookhope catchment of the N. Pennines, UK—A Pb isotope study. *Science of the total environment,* 433**,** 547-560.

CHENG, H. & HU, Y. 2010. Lead (Pb) isotopic fingerprinting and its applications in lead pollution studies in China: a review. *Environmental Pollution,* 158**,** 1134-1146.

CHOW, T. J. & JOHNSTONE, M. 1965. Lead isotopes in gasoline and aerosols of Los Angeles basin, California. *Science,* 147**,** 502-503.

CLARK, C., RAMPAL, K., THUPPIL, V., CHEN, C., CLARK, R. & RODA, S. 2006. The lead content of currently available new residential paint in several Asian countries. *Environmental Research,* 102**,** 9-12.

CLARK, H. F., HAUSLADEN, D. M. & BRABANDER, D. J. 2008. Urban gardens: lead exposure, recontamination mechanisms, and implications for remediation design. *Environmental Research,* 107**,** 312-319.

CLOY, J. M., FARMER, J. G., GRAHAM, M. C., MACKENZIE, A. B. & COOK, G. T. 2005. A comparison of antimony and lead profiles over the past 2500 years in Flanders Moss ombrotrophic peat bog, Scotland. *Journal of Environmental Monitoring,* 7**,** 1137-1147.

CLYMO, R. 1987. The ecology of peatlands. *Science Progress (1933-)***,** 593-614.

COVELO, E., VEGA, F. & ANDRADE, M. 2007. Competitive sorption and desorption of heavy metals by individual soil components. *Journal of Hazardous Materials,* 140**,** 308-315.

CUI, Y., ZHU, Y.-G., ZHAI, R., HUANG, Y., QIU, Y. & LIANG, J. 2005. Exposure to metal mixtures and human health impacts in a contaminated area in Nanning, China. *Environment International,* 31**,** 784-790.

DAVIDSON, C. M., DUNCAN, A. L., LITTLEJOHN, D., URE, A. M. & GARDEN, L. M. 1998. A critical evaluation of the three-stage BCR sequential extraction procedure to assess the potential mobility and toxicity of heavy metals in industrially-contaminated land. *Analytica Chimica Acta,* 363**,** 45-55.

DAVIDSON, C. M., URQUHART, G. J., AJMONE-MARSAN, F., BIASIOLI, M., DA COSTA DUARTE, A., DÍAZ-BARRIENTOS, E., GRČMAN, H., HOSSACK, I., HURSTHOUSE, A. S. & MADRID, L. 2006. Fractionation of potentially toxic elements in urban soils from five European cities by means of a harmonised sequential extraction procedure. *Analytica Chimica Acta,* 565**,** 63-72.

DAVIES, D., WATT, J. & THORNTON, I. 1987. Lead levels in Birmingham dusts and soils. *Science of the total environment,* 67**,** 177-185.

DAVIS, A. P., SHOKOUHIAN, M. & NI, S. 2001. Loading estimates of lead, copper, cadmium, and zinc in urban runoff from specific sources. *Chemosphere,* 44**,** 997-1009.

DAWSON, P. H. 2013. *Quadrupole mass spectrometry and its applications*, Elsevier.

DE SÁ PAYE, H., DE MELLO, J. W., DE MAGALHÃES MASCARENHAS, G. R. L. & GASPARON, M. 2016. Distribution and fractionation of the rare earth elements in Brazilian soils. *Journal of Geochemical Exploration,* 161**,** 27-41.

DEGRYSE, F., BUEKERS, J. & SMOLDERS, E. 2004. Radio-labile cadmium and zinc in soils as affected by pH and source of contamination. *European Journal of Soil Science,* 55**,** 113-122.

DEGRYSE, F., SMOLDERS, E. & PARKER, D. R. 2009. Partitioning of metals (Cd, Co, Cu, Ni, Pb, Zn) in soils: concepts, methodologies, prediction and applications – a review. *European Journal of Soil Science,* 60**,** 590-612.

DEGRYSE, F., VOEGELIN, A., JACQUAT, O., KRETZSCHMAR, R. & SMOLDERS, E. 2011. Characterization of zinc in contaminated soils: complementary insights from isotopic exchange, batch extractions and XAFS spectroscopy. *European journal of soil science,* 62**,** 318-330.

DEGRYSE, F., WAEGENEERS, N. & SMOLDERS, E. 2007. Labile lead in polluted soils measured by stable isotope dilution. *European Journal of Soil Science,* 58**,** 1-7.

DEMUTH, N. & HEUMANN, K. G. 1999. Determination of trace amounts of boron in rainwater by ICP-IDMS and NTI-IDMS and the dependence on meteorological and anthropogenic influences. *Journal of Analytical Atomic Spectrometry,* 14**,** 1449-1453.

DÍAZ-SOMOANO, M., CALVO, M., ANTÓN, M. A. L., SUAREZ-RUIZ, I., GARCÍA, R., MOINELO, S. R. & MARTÍNEZ-TARAZONA, M. R. 2007. Lead isotope ratios in a soil from a coal carbonization plant. *Fuel,* 86**,** 1079-1085.

DJINGOVA, R., KOVACHEVA, P., WAGNER, G. & MARKERT, B. 2003. Distribution of platinum group elements and other traffic related elements among different plants along some highways in Germany. *Science of the Total Environment,* 308**,** 235-246.

DOE, B. & STACEY, J. S. 1974. The application of lead isotopes to the problems of ore genesis and ore prospect evaluation: a review. *Economic Geology,* 69**,** 757-776.

DÖRR, H. & MÜNNICH, K. O. 1991. Lead and cesium transport in European forest soils. *Water, Air, and Soil Pollution,* 57**,** 809-818.

DUDKA, S. & ADRIANO, D. C. 1997. Environmental impacts of metal ore mining and processing: a review. *Journal of environmental quality,* 26**,** 590-602.

DUNLAP, C. E., STEINNES, E. & FLEGAL, A. R. 1999. A synthesis of lead isotopes in two millennia of European air. *Earth and Planetary Science Letters,* 167**,** 81-88.

DUZGOREN-AYDIN, N. S. 2007. Sources and characteristics of lead pollution in the urban environment of Guangzhou. *Science of the Total Environment,* 385**,** 182-195.

Environmental Agency (EA) (2009a) 'Contaminants in soil: updated collation of toxicological data and intake values for humans. Inorganic arsenic.' (Environment Agency: Rio House, Waterside Drive, Aztec West, Almondsbury, Bristol, BS32 4UD).

EA (2009b) Soil Guideline Values for cadium in soil. (Environment Agency: Rio House, Waterside Drive,

Aztec West, Almondsbury, Bristol, BS32 4UD).
EA (2009c) Soil Guideline Values for nickel in soil. (Environment Agency: Rio House, Waterside Drive, Aztec West, Almondsbury, Bristol, BS32 4UD).
EA (2009d) 'Updated technical background to the CLEA model'. Environment Agency, Rio House, Waterside Drive, Aztec West, Almondsbury, Bristol BS32 4UD.
EA (2009e) 'Contaminants in soil: updated collation of toxicological data and intake values for humans. Nickel.' (Environment Agency: Rio House, Waterside Drive, Aztec West, Almondsbury, Bristol, BS32 4UD).
ECHEVARRIA, G., MOREL, J., FARDEAU, J. & LECLERC-CESSAC, E. 1998. Assessment of phytoavailability of nickel in soils. *Journal of Environmental Quality,* 27**,** 1064-1070.
ECKEL, W. P., RABINOWITZ, M. B. & FOSTER, G. D. 2002. Investigation of unrecognized former secondary lead smelting sites: confirmation by historical sources and elemental ratios in soil. *Environmental Pollution,* 117**,** 273-279.
EDMUNDS, W. M., BATH, A. H. & MILES, D. L. 1982. Hydrochemical evolution of the East Midlands Triassic sandstone aquifer, England. *Geochimica et Cosmochimica Acta,* 46**,** 2069-2081.
EFCEL, Y. and Veron, A., 1997. Tracing the transport of anthropogenic lead in the atmosphere and in soils using isotopic ratios. *Geochimica et Cosmochimica Acta*, *61*(21), pp.4495-4505.
EK, K. H., MORRISON, G. M. & RAUCH, S. 2004. Environmental routes for platinum group elements to biological materials—a review. *Science of the Total Environment,* 334**,** 21-38.
ELLAM, R. 2010a. The graphical presentation of lead isotope data for environmental source apportionment. *Science of the total environment,* 408**,** 3490-3492.
ELLAM, R. M. 2010b. The graphical presentation of lead isotope data for environmental source apportionment. *Science of The Total Environment,* 408**,** 3490-3492.
EMMANUEL, S. & EREL, Y. 2002. Implications from concentrations and isotopic data for Pb partitioning processes in soils. *Geochimica et Cosmochimica Acta,* 66**,** 2517-2527.
ENCINAR, J. R., ALONSO, J. I. G., SANZ-MEDEL, A., MAIN, S. & TURNER, P. J. 2001. A comparison between quadrupole, double focusing and multicollector ICP-MS instruments Part I. Evaluation of total combined uncertainty for lead isotope ratio measurements. *Journal of Analytical Atomic Spectrometry,* 16**,** 315-321.
ENSINK, J. H., SIMMONS, R. & VAN DER HOEK, W. 2004. Wastewater use in Pakistan, the cases of Haroonabad and Faisalabad. *Wastewater use in irrigated agriculture: Confronting the livelihood and environmental realities,* 1**,** 91-99.
EQANI, S. A. M. A. S., KANWAL, A., BHOWMIK, A. K., SOHAIL, M., ULLAH, R., ALI, S. M., ALAMDAR, A., ALI, N., FASOLA, M. & SHEN, H. 2016a. Spatial distribution of dust–bound trace elements in Pakistan and their implications for human exposure. *Environmental pollution,* 213**,** 213-222.
EQANI, S. A. M. A. S., KHALID, R., BOSTAN, N., SAQIB, Z., MOHMAND, J., REHAN, M., ALI, N., KATSOYIANNIS, I. A. & SHEN, H. 2016b. Human lead (Pb) exposure via dust from different land use settings of Pakistan: A case study from two urban mountainous cities. *Chemosphere,* 155**,** 259-265.
EREL, Y., DUBOWSKI, Y., HALICZ, L., EREZ, J. & KAUFMAN, A. 2001. Lead concentrations and isotopic ratios in the sediments of the Sea of Galilee. *Environmental science & technology,* 35**,** 292-299.
EREL, Y., VERON, A. & HALICZ, L. 1997. Tracing the transport of anthropogenic lead in the atmosphere and in soils using isotopic ratios. *Geochimica et Cosmochimica Acta,* 61**,** 4495-4505.
ETTLER, V., MIHALJEVIČ, M. & KOMÁREK, M. 2004. ICP-MS measurements of lead isotopic ratios in soils heavily contaminated by lead smelting: tracing the sources of pollution. *Analytical and bioanalytical chemistry,* 378**,** 311-317.
FACCHINELLI, A., SACCHI, E. & MALLEN, L. 2001. Multivariate statistical and GIS-based approach to identify heavy metal sources in soils. *Environmental pollution,* 114**,** 313-324.
FARFEL, M. R., ORLOVA, A. O., LEES, P. S., ROHDE, C., ASHLEY, P. J. & CHISOLM JR, J. J. 2003. A study of urban housing demolitions as sources of lead in ambient dust: demolition practices and exterior dust fall. *Environmental Health Perspectives,* 111**,** 1228.

FARMER, J. G., BROADWAY, A., CAVE, M. R., WRAGG, J., FORDYCE, F. M., GRAHAM, M. C., NGWENYA, B. T. & BEWLEY, R. J. 2011. A lead isotopic study of the human bioaccessibility of lead in urban soils from Glasgow, Scotland. *Science of the total environment,* 409**,** 4958-4965.

FARMER, J. G., EADES, L. J. & GRAHAM, M. C. 1999. The lead content and isotopic composition of British coals and their implications for past and present releases of lead to the UK environment. *Environmental Geochemistry and Health,* 21**,** 257-272.

FAURE, G. 1986. Isotope systematics in two-component mixtures. *Principles of isotope geology***,** 141-153.

FAURE, G. 1998. *Principles and applications of geochemistry: a comprehensive textbook for geology students*, Prentice Hall.

FAVAS, P. J., PRATAS, J., GOMES, M. E. P. & CALA, V. 2011. Selective chemical extraction of heavy metals in tailings and soils contaminated by mining activity: environmental implications. *Journal of Geochemical Exploration,* 111**,** 160-171.

FERNANDEZ, C., LABANOWSKI, J., CAMBIER, P., JONGMANS, A. & VAN OORT, F. 2007. Fate of airborne metal pollution in soils as related to agricultural management. 1. Zn and Pb distributions in soil profiles. *European Journal of Soil Science,* 58**,** 547-559.

FERNANDEZ, C., MONNA, F., LABANOWSKI, J., LOUBET, M. & VAN OORT, F. 2008. Anthropogenic lead distribution in soils under arable land and permanent grassland estimated by Pb isotopic compositions. *Environmental Pollution,* 156**,** 1083-1091.

FINSTER, M. E., GRAY, K. A. & BINNS, H. J. 2004. Lead levels of edibles grown in contaminated residential soils: a field survey. *Science of the Total Environment,* 320**,** 245-257.

FOWLER, D., CAPE, J. & UNSWORTH, M. 1989. Deposition of atmospheric pollutants on forests. *Phil. Trans. R. Soc. Lond. B,* 324**,** 247-265.

FRITSCHE, J. & MEISEL, T. 2004. Determination of anthropogenic input of Ru, Rh, Pd, Re, Os, Ir and Pt in soils along Austrian motorways by isotope dilution ICP-MS. *Science of the Total Environment,* 325**,** 145-154.

FURUTA, N. 1991. Optimization of the mass scanning rate for the determination of lead isotope ratios using an inductively coupled plasma mass spectrometer. *Journal of Analytical Atomic Spectrometry,* 6**,** 199-203.

GÄBLER, H.-E., BAHR, A. & MIEKE, B. 1999. Determination of the interchangeable heavy-metal fraction in soils by isotope dilution mass spectrometry. *Fresenius' journal of analytical chemistry,* 365**,** 409-414.

GÄBLER, H. E., BAHR, A., HEIDKAMP, A. & UTERMANN, J. 2007. Enriched stable isotopes for determining the isotopically exchangeable element content in soils. *European Journal of Soil Science,* 58**,** 746-757.

GALE, W. K. V. 1966. *The Black Country iron industry: A technical history*, Iron & Steel Institute.

GALLEGO, J. L., ORDÓÑEZ, A. & LOREDO, J. 2002. Investigation of trace element sources from an industrialized area (Aviles, northern Spain) using multivariate statistical methods. *Environment International,* 27**,** 589-596.

GARCIA-DELGADO, R., GARCIA-HERRUZO, F., RODRÍGUEZ-MAROTO, J. & VEREDA, C. 1996. Influence of soil carbonates in lead fixation. *Journal of Environmental Science & Health Part A,* 31**,** 2099-2109.

GARFORTH, J. M., BAILEY, E. H., TYE, A. M., YOUNG, S. D. & LOFTS, S. 2016. Using isotopic dilution to assess chemical extraction of labile Ni, Cu, Zn, Cd and Pb in soils. *Chemosphere,* 155**,** 534-541.

GIBSON, M. & FARMER, J. 1986. Multi-step sequential chemical extraction of heavy metals from urban soils. *Environmental Pollution Series B, Chemical and Physical,* 11**,** 117-135.

GILLSON, G. R., DOUGLAS, D. J., FULFORD, J. E., HALLIGAN, K. W. & TANNER, S. D. 1988. Nonspectroscopic interelement interferences in inductively coupled plasma mass spectrometry. *Analytical Chemistry,* 60**,** 1472-1474.

GIUSTI, L. 2011. Heavy metals in urban soils of Bristol (UK). Initial screening for contaminated land. *Journal of soils and sediments,* 11**,** 1385-1398.

GLEYZES, C., TELLIER, S. & ASTRUC, M. 2002. Fractionation studies of trace elements in contaminated soils and sediments: a review of sequential extraction procedures. *TrAC Trends in Analytical Chemistry,* 21**,** 451-467.

GOMEZ, M., GOMEZ, M. & PALACIOS, M. 2000. Control of interferences in the determination of Pt, Pd and Rh in airborne particulate matter by inductively coupled plasma mass spectrometry. *Analytica Chimica Acta,* 404**,** 285-294.

GOMEZ, M., GOMEZ, M. & PALACIOS, M. 2003. ICP-MS determination of Pt, Pd and Rh in airborne and road dust after tellurium coprecipitation. *Journal of Analytical Atomic Spectrometry,* 18**,** 80-83.

GOYER, R. A. 1993. Lead toxicity: current concerns. *Environmental health perspectives,* 100**,** 177-187.

GULSON, B. L., TILLER, K. G., MIZON, K. J. & MERRY, R. H. 1981. Use of lead isotopes in soils to identify the source of lead contamination near Adelaide, South Australia. *Environmental Science & Technology,* 15**,** 691-696.

GÜNTHER, D., JACKSON, S. E. & LONGERICH, H. P. 1999. Laser ablation and arc/spark solid sample introduction into inductively coupled plasma mass spectrometers. *Spectrochimica Acta Part B: Atomic Spectroscopy,* 54**,** 381-409.

HAMON, R. E. & MCLAUGHLIN, M. J. 2002. Interferences in the determination of isotopically exchangeable P in soils and a method to minimise them. *Soil Research,* 40**,** 1383-1397.

HAMON, R. E., PARKER, D. R. & LOMBI, E. 2008. Chapter 6 Advances in Isotopic Dilution Techniques in Trace Element Research: A Review of Methodologies, Benefits, and Limitations. *Advances in Agronomy.* Academic Press.

HANSMANN, W. & KÖPPEL, V. 2000. Lead-isotopes as tracers of pollutants in soils. *Chemical Geology,* 171**,** 123-144.

HARRISON, R. 2012. *Lead pollution: causes and control*, Springer Science & Business Media.

HARRISON, R. M., LAXEN, D. P. & WILSON, S. J. 1981. Chemical associations of lead, cadmium, copper, and zinc in street dusts and roadside soils. *Environmental Science & Technology,* 15**,** 1378-1383.

HEINRICH, E., SCHMIDT, G. & KRATZ, K.-L. 1996. Determination of Platinum-Group Elements (PGE) from catalytic converters in soil by means of docimasy and INAA. *Fresenius' journal of analytical chemistry,* 354**,** 883-885.

HERNANDEZ, L., PROBST, A., PROBST, J. L. & ULRICH, E. 2003. Heavy metal distribution in some French forest soils: evidence for atmospheric contamination. *Science of the Total Environment,* 312**,** 195-219.

HEUMANN, K. G., GALLUS, S. M., RÄDLINGER, G. & VOGL, J. 1998. Precision and accuracy in isotope ratio measurements by plasma source mass spectrometry. *Journal of Analytical Atomic Spectrometry,* 13**,** 1001-1008.

HIRANO, S. & SUZUKI, K. T. 1996. Exposure, metabolism, and toxicity of rare earths and related compounds. *Environmental health perspectives,* 104**,** 85.

HJORTENKRANS, D., BERGBÄCK, B. & HÄGGERUD, A. 2006. New metal emission patterns in road traffic environments. *Environmental Monitoring and Assessment,* 117**,** 85-98.

HJORTENKRANS, D. S., BERGBÄCK, B. G. & HÄGGERUD, A. V. 2007. Metal emissions from brake linings and tires: case studies of Stockholm, Sweden 1995/1998 and 2005. *Environmental Science & Technology,* 41**,** 5224-5230.

HOODA, P. S. 2010. Assessing bioavailability of soil trace elements. *Trace elements in soils***,** 229-265.

HOUGH, R. L., BREWARD, N., YOUNG, S. D., CROUT, N. M., TYE, A. M., MOIR, A. M. & THORNTON, I. 2004. Assessing potential risk of heavy metal exposure from consumption of home-produced vegetables by urban populations. *Environmental health perspectives,* 112**,** 215.

HOWARD, G., PEDLEY, S., BARRETT, M., NALUBEGA, M. & JOHAL, K. 2003. Risk factors contributing to microbiological contamination of shallow groundwater in Kampala, Uganda. *Water research,* 37**,** 3421-3429.

HOZHABRI, S., WHITE, F., RAHBAR, M. H., AGBOATWALLA, M. & LUBY, S. 2004. Elevated blood lead levels among children living in a fishing community, Karachi, Pakistan. *Archives of Environmental Health: An International Journal,* 59**,** 37-41.

HU, Q., NOLL, R. J., LI, H., MAKAROV, A., HARDMAN, M. & GRAHAM COOKS, R. 2005. The Orbitrap: a new mass spectrometer. *Journal of mass spectrometry,* 40**,** 430-443.

HU, Y. & CHENG, H. 2016. A method for apportionment of natural and anthropogenic contributions to heavy metal loadings in the surface soils across large-scale regions. *Environmental Pollution,* 214**,** 400-409.

HU, Z., HANEKLAUS, S., SPAROVEK, G. & SCHNUG, E. 2006. Rare earth elements in soils. *Communications in Soil Science and Plant Analysis,* 37**,** 1381-1420.

HUANG, B., SHI, X., YU, D., ÖBORN, I., BLOMBÄCK, K., PAGELLA, T. F., WANG, H., SUN, W. & SINCLAIR, F. L. 2006. Environmental assessment of small-scale vegetable farming systems in peri-urban areas of the Yangtze River Delta Region, China. *Agriculture, Ecosystems & Environment,* 112**,** 391-402.

HUANG, Y., LI, T., WU, C., HE, Z., JAPENGA, J., DENG, M. & YANG, X. 2015. An integrated approach to assess heavy metal source apportionment in peri-urban agricultural soils. *Journal of hazardous materials,* 299**,** 540-549.

HUANG, Z.-Y., CHEN, T., YU, J., ZENG, X.-C. & HUANG, Y.-F. 2011. Labile Cd and Pb in vegetable-growing soils estimated with isotope dilution and chemical extractants. *Geoderma,* 160**,** 400-407.

HURST, C. 2010. China's rare earth elements industry: what can the West learn? : Institute for the Analysis of Global Security Washington DC.

HURSTHOUSE, A., TOGNARELLI, D., TUCKER, P., AJMONE-MARSAN, F., MARTINI, C., MADRID, L., MADRID DÍAZ, F. & DÍAZ BARRIENTOS, E. 2004. Metal content of surface soils in parks and allotments from three European cities: initial pilot study results.

IMPERATO, M., ADAMO, P., NAIMO, D., ARIENZO, M., STANZIONE, D. & VIOLANTE, P. 2003. Spatial distribution of heavy metals in urban soils of Naples city (Italy). *Environmental pollution,* 124**,** 247-256.

INGLE, C. P., SHARP, B. L., HORSTWOOD, M. S., PARRISH, R. R. & LEWIS, D. J. 2003. Instrument response functions, mass bias and matrix effects in isotope ratio measurements and semi-quantitative analysis by single and multi-collector ICP-MS. *Journal of Analytical Atomic Spectrometry,* 18**,** 219-229.

Instrument, S.U.S., 1989. The sludge (use in agriculture) regulations 1989. Statutory Instrument No. 1263.

IZQUIERDO, M., TYE, A. & CHENERY, S. 2012. Sources, lability and solubility of Pb in alluvial soils of the River Trent catchment, UK. *Science of the Total Environment,* 433**,** 110-122.

IZQUIERDO, M., TYE, A. & CHENERY, S. 2017. Using isotope dilution assays to understand speciation changes in Cd, Zn, Pb and Fe in a soil model system under simulated flooding conditions. *Geoderma,* 295**,** 41-52.

JACKSON, B. P. & MILLER, W. 2000. Effectiveness of phosphate and hydroxide for desorption of arsenic and selenium species from iron oxides. *Soil Science Society of America Journal,* 64**,** 1616-1622.

JACKSON, M. T., PRICHARD, H. M. & SAMPSON, J. 2010. Platinum-group elements in sewage sludge and incinerator ash in the United Kingdom: Assessment of PGE sources and mobility in cities. *Science of the total environment,* 408**,** 1276-1285.

JAMALI, M., KAZI, T., ARAIN, M., AFRIDI, H., MEMON, A., JALBANI, N. & SHAH, A. 2008. Use of sewage sludge after liming as fertilizer for maize growth. *Pedosphere,* 18**,** 203-213.

JÄRUP, L., BERGLUND, M., ELINDER, C. G., NORDBERG, G. & VANTER, M. 1998. Health effects of cadmium exposure–a review of the literature and a risk estimate. *Scandinavian journal of work, environment & health***,** 1-51.

JIANG, Y., CHAO, S., LIU, J., YANG, Y., CHEN, Y., ZHANG, A. & CAO, H. 2017. Source apportionment and health risk assessment of heavy metals in soil for a township in Jiangsu Province, China. *Chemosphere,* 168**,** 1658-1668.

JOHNSON, C. E., PETRAS, R. J., APRIL, R. H. & SICCAMA, T. G. 2004. Post-glacial lead dynamics in a forest soil. *Water, Air and Soil Pollution: Focus,* 4**,** 579-590.

JONES, L. & JARVIS, S. 1981. The fate of heavy metals. John Wiley & Sons: New York.

JOY, E. J., ANDER, E. L., BROADLEY, M. R., YOUNG, S. D., CHILIMBA, A. D., HAMILTON, E. M. & WATTS, M. J. 2017. Elemental composition of Malawian rice. *Environmental geochemistry and health,* 39**,** 835-845.

KABATA-PENDIAS, A. 2010. *Trace elements in soils and plants*, CRC press.

KADI, M. W. 2009. "Soil Pollution Hazardous to Environment": A case study on the chemical composition and correlation to automobile traffic of the roadside soil of Jeddah city, Saudi Arabia. *Journal of hazardous materials,* 168**,** 1280-1283.

KADIR, M. M., JANJUA, N. Z., KRISTENSEN, S., FATMI, Z. & SATHIAKUMAR, N. 2008. Status of children's blood lead levels in Pakistan: implications for research and policy. *Public health,* 122**,** 708-715.

KAWASAKI, A., KIMURA, R. & ARAI, S. 1998. Rare earth elements and other trace elements in wastewater treatment sludges. *Soil Science and Plant Nutrition,* 44**,** 433-441.

KAZI, T., JAMALI, M., KAZI, G., ARAIN, M., AFRIDI, H. & SIDDIQUI, A. 2005. Evaluating the mobility of toxic metals in untreated industrial wastewater sludge using a BCR sequential extraction procedure and a leaching test. *Analytical and Bioanalytical Chemistry,* 383**,** 297-304.

KELLY, J., THORNTON, I. & SIMPSON, P. 1996. Urban geochemistry: a study of the influence of anthropogenic activity on the heavy metal content of soils in traditionally industrial and non-industrial areas of Britain. *Applied geochemistry,* 11**,** 363-370.

KIMBROUGH, D. & CARDER, N. 1999. Off-site forensic determination of waterborne elemental emissions: a case study at a secondary lead smelter. *Environmental Pollution,* 106**,** 293-298.

KÖLELI, N. 2004. Speciation of chromium in 12 agricultural soils from Turkey. *Chemosphere,* 57**,** 1473-1478.

KOŁODZIEJCZAK-RADZIMSKA, A. & JESIONOWSKI, T. 2014. Zinc oxide—from synthesis to application: a review. *Materials,* 7**,** 2833-2881.

KOMÁREK, M., CHRASTNÝ, V. & ŠTÍCHOVÁ, J. 2007. Metal/metalloid contamination and isotopic composition of lead in edible mushrooms and forest soils originating from a smelting area. *Environment international,* 33**,** 677-684.

KOMÁREK, M., ETTLER, V., CHRASTNÝ, V. & MIHALJEVIČ, M. 2008. Lead isotopes in environmental sciences: a review. *Environment International,* 34**,** 562-577.

KOPPENAAL, D. W., EIDEN, G. C. & BARINAGA, C. J. 2004. Collision and reaction cells in atomic mass spectrometry: development, status, and applications. *Journal of Analytical Atomic Spectrometry,* 19**,** 561-570.

KUNHIKRISHNAN, A., BOLAN, N. S., MÜLLER, K., LAURENSON, S., NAIDU, R. & KIM, W.-I. 2012. The influence of wastewater irrigation on the transformation and bioavailability of heavy metal (loid) s in soil. *Advances in agronomy.* Elsevier.

KYLANDER, M. E., KLAMINDER, J., BINDLER, R. & WEISS, D. J. 2010. Natural lead isotope variations in the atmosphere. *Earth and Planetary Science Letters,* 290**,** 44-53.

LABANOWSKI, J., MONNA, F., BERMOND, A., CAMBIER, P., FERNANDEZ, C., LAMY, I. & VAN OORT, F. 2008. Kinetic extractions to assess mobilization of Zn, Pb, Cu, and Cd in a metal-contaminated soil: EDTA vs. citrate. *Environmental Pollution,* 152**,** 693-701.

LADONIN, D. 2018. Platinum-Group Elements in Soils and Street Dust of the Southeastern Administrative District of Moscow. *Eurasian Soil Science,* 51**,** 268-276.

LANPHEAR, B. P., DIETRICH, K., AUINGER, P. & COX, C. 2000. Cognitive deficits associated with blood lead concentrations< 10 microg/dL in US children and adolescents. *Public health reports,* 115**,** 521.

LAU, P. 1994. *A survey of heavy metal contents in children playgrounds in Hong Kong.* B. Sc. thesis, Hong Kong Baptist University, Hong Kong.

LAVEUF, C. & CORNU, S. 2009. A review on the potentiality of rare earth elements to trace pedogenetic processes. *Geoderma,* 154**,** 1-12.

LEDIN, M., KRANTZ-RÜLCKER, C. & ALLARD, B. 1996. Zn, Cd and Hg accumulation by microorganisms, organic and inorganic soil components in multi-compartment systems. *Soil Biology and Biochemistry,* 28**,** 791-799.

LI, X., COLES, B. J., RAMSEY, M. H. & THORNTON, I. 1995. Sequential extraction of soils for multielement analysis by ICP-AES. *Chemical Geology,* 124**,** 109-123.

LI, X., POON, C.-S. & LIU, P. S. 2001. Heavy metal contamination of urban soils and street dusts in Hong Kong. *Applied geochemistry,* 16**,** 1361-1368.

LI, X. & THORNTON, I. 2001. Chemical partitioning of trace and major elements in soils contaminated by mining and smelting activities. *Applied geochemistry,* 16**,** 1693-1706.

LI, Y.-H. 2007. Effects of mining activity on heavy metals in surface water in Lead-Zinc deposit area. *Journal of Agro-environment Science,* 26**,** 103-107.

LIN, Z., HARSBO, K., AHLGREN, M. & QVARFORT, U. 1998. The source and fate of Pb in contaminated soils at the urban area of Falun in central Sweden. *Science of the Total Environment,* 209**,** 47-58.

LOGAN, T., LINDSAY, B., GOINS, L. & RYAN, J. 1997. Field assessment of sludge metal bioavailability to crops: sludge rate response. *Journal of Environmental Quality,* 26**,** 534-550.

LOMBI, E., HAMON, R. E., MCGRATH, S. P. & MCLAUGHLIN, M. J. 2003. Lability of Cd, Cu, and Zn in Polluted Soils Treated with Lime, Beringite, and Red Mud and Identification of a Non-Labile Colloidal Fraction of Metals Using Isotopic Techniques. *Environmental Science & Technology,* 37**,** 979-984.

LOPEZ, P. L. & GRAHAM, E. 1972. LABILE POOL AND PLANT UPTAKE OF MICRONUTRIENTS: 1. DETERMINATION OF LABILE POOL OF MN, FE, ZN, CO, AND CU IN DEFICIENT SOILS BY ISOTOPIC EXCHANGE. *Soil Science,* 114**,** 295-299.

LU, X., WANG, L., LI, L. Y., LEI, K., HUANG, L. & KANG, D. 2010. Multivariate statistical analysis of heavy metals in street dust of Baoji, NW China. *Journal of hazardous materials,* 173**,** 744-749.

LU, Y., GONG, Z., ZHANG, G. & BURGHARDT, W. 2003. Concentrations and chemical speciations of Cu, Zn, Pb and Cr of urban soils in Nanjing, China. *Geoderma,* 115**,** 101-111.

LU, Y., ZHU, F., CHEN, J., GAN, H. & GUO, Y. 2007. Chemical fractionation of heavy metals in urban soils of Guangzhou, China. *Environmental Monitoring and Assessment,* 134**,** 429-439.

LUO, W., WANG, T., LU, Y., GIESY, J. P., SHI, Y., ZHENG, Y., XING, Y. & WU, G. 2007. Landscape ecology of the Guanting Reservoir, Beijing, China: multivariate and geostatistical analyses of metals in soils. *Environmental Pollution,* 146**,** 567-576.

LUO, X.-S., XUE, Y., WANG, Y.-L., CANG, L., XU, B. & DING, J. 2015. Source identification and apportionment of heavy metals in urban soil profiles. *Chemosphere,* 127**,** 152-157.

LUO, X., IP, C., LI, W., TAO, S. & LI, X. 2014. Spatial–temporal variations, sources, and transport of airborne inhalable metals (PM 10) in urban and rural areas of northern China. *Atmospheric Chemistry and Physics Discussions,* 14**,** 13133-13165.

MA, Y., LOMBI, E., NOLAN, A. & MCLAUGHLIN, M. J. 2006a. Determination of labile Cu in soils and isotopic exchangeability of colloidal Cu complexes. *European journal of soil science,* 57**,** 147-153.

MA, Y., LOMBI, E., OLIVER, I. W., NOLAN, A. L. & MCLAUGHLIN, M. J. 2006b. Long-term aging of copper added to soils. *Environmental science & technology,* 40**,** 6310-6317.

MA, Y. & UREN, N. 1998. Dehydration, diffusion and entrapment of zinc in bentonite. *Clays and Clay Minerals,* 46**,** 132-138.

MAAS, S., SCHEIFLER, R., BENSLAMA, M., CRINI, N., LUCOT, E., BRAHMIA, Z., BENYACOUB, S. & GIRAUDOUX, P. 2010. Spatial distribution of heavy metal concentrations in urban, suburban and agricultural soils in a Mediterranean city of Algeria. *Environmental pollution,* 158**,** 2294-2301.

MACKLIN, M., HUDSON-EDWARDS, K. & DAWSON, E. 1997. The significance of pollution from historic metal mining in the Pennine orefields on river sediment contaminant fluxes to the North Sea. *Science of the total Environment,* 194**,** 391-397.

MANDAL, A. & SENGUPTA, D. 2006. An assessment of soil contamination due to heavy metals around a coal-fired thermal power plant in India. *Environmental Geology,* 51**,** 409-420.

MAO, L. 2014. *Lability and solubility of trace metals in soils.* University of Nottingham.

MAO, L., BAILEY, E. H., CHESTER, J., DEAN, J., ANDER, E. L., CHENERY, S. R. & YOUNG, S. D. 2014. Lability of Pb in soil: effects of soil properties and contaminant source. *Environmental Chemistry,* 11**,** 690-701.

MAO, L. C., YOUNG, S. D., TYE, A. M. & BAILEY, E. H. 2017. Predicting trace metal solubility and fractionation in Urban soils from isotopic exchangeability. *Environmental Pollution,* 231**,** 1529-1542.

MAPANDA, F., MANGWAYANA, E. N., NYAMANGARA, J. & GILLER, K. 2005. The effect of long-term irrigation using wastewater on heavy metal contents of soils under vegetables in Harare, Zimbabwe. *Agriculture, Ecosystems & Environment,* 107**,** 151-165.

MARÉCHAL, C. N., TÉLOUK, P. & ALBARÈDE, F. 1999. Precise analysis of copper and zinc isotopic compositions by plasma-source mass spectrometry. *Chemical Geology,* 156**,** 251-273.

MARTIN, R., SANCHEZ, D. & GUTIERREZ, A. 1998. Sequential extraction of U, Th, Ce, La and some heavy metals in sediments from Ortigas river, Spain. *Talanta,* 46**,** 1115-1121.

MARTIN, S. & GRISWOLD, W. 2009. Human health effects of heavy metals. *Environmental Science and Technology briefs for citizens,* 15**,** 1-6.

MARTÍNEZ-CORTIZAS, A., PONTEVEDRA-POMBAL, X., NÓVOA MUÑOZ, J. C. & GARCÍA-RODEJA, E. 1997. Four thousand years of atmospheric Pb, Cd and Zn deposition recorded by the ombrotrophic peat bog of Penido Vello (Northwestern Spain). *Water, Air, and Soil Pollution,* 100**,** 387-403.

MARZOUK, E., CHENERY, S. & YOUNG, S. 2013a. Predicting the solubility and lability of Zn, Cd, and Pb in soils from a minespoil-contaminated catchment by stable isotopic exchange. *Geochimica et Cosmochimica Acta,* 123**,** 1-16.

MARZOUK, E. R., CHENERY, S. & YOUNG, S. 2013b. Measuring reactive metal in soil: a comparison of multi-element isotopic dilution and chemical extraction. *European journal of soil science,* 64**,** 526-536.

MAUQUOY, D. & BARBER, K. 1999. A replicated 3000 yr proxy-climate record from Coom Rigg Moss and Felecia Moss, the Border Mires, northern England. *Journal of Quaternary Science: Published for the Quaternary Research Association,* 14**,** 263-275.

MCCURDY, E. & WOODS, G. 2004. The application of collision/reaction cell inductively coupled plasma mass spectrometry to multi-element analysis in variable sample matrices, using He as a non-reactive cell gas. *Journal of Analytical Atomic Spectrometry,* 19**,** 607-615.

MCKENZIE, E. R., MONEY, J. E., GREEN, P. G. & YOUNG, T. M. 2009. Metals associated with stormwater-relevant brake and tire samples. *Science of the total environment,* 407**,** 5855-5860.

MCLAREN, R., LAWSON, D. & SWIFT, S. 1986. The forms of cobalt in some Scottish soils as determined by extraction and isotopic exchange. *European Journal of Soil Science,* 37**,** 223-234.

MCLAUGHLIN, M. J., ZARCINAS, B., STEVENS, D. & COOK, N. 2000. Soil testing for heavy metals. *Communications in Soil Science and Plant Analysis,* 31**,** 1661-1700.

MERYEM, B., HONGBING, J., YANG, G., HUAJIAN, D. & CAI, L. 2016. Distribution of rare earth elements in agricultural soil and human body (scalp hair and urine) near smelting and mining areas of Hezhang, China. *Journal of Rare Earths,* 34**,** 1156-1167.

MEZA-FIGUEROA, D., DE LA O-VILLANUEVA, M. & DE LA PARRA, M. L. 2007. Heavy metal distribution in dust from elementary schools in Hermosillo, Sonora, México. *Atmospheric Environment,* 41**,** 276-288.

MICÓ, C., RECATALÁ, L., PERIS, M. & SÁNCHEZ, J. 2006. Assessing heavy metal sources in agricultural soils of an European Mediterranean area by multivariate analysis. *Chemosphere,* 65**,** 863-872.

MIDWOOD, A. J. 2007. Stable Isotope Methods for Estimating the Labile Metal Content of Soils. *In:* WILLEY, N. (ed.) *Phytoremediation: Methods and Reviews.* Totowa, NJ: Humana Press.

MIELKE, H. W., GONZALES, C. R., SMITH, M. K. & MIELKE, P. W. 1999. The urban environment and children's health: soils as an integrator of lead, zinc, and cadmium in New Orleans, Louisiana, USA. *Environmental research,* 81**,** 117-129.

MIELKE, H. W. & REAGAN, P. L. 1998. Soil is an important pathway of human lead exposure. *Environmental health perspectives,* 106**,** 217.

MIJIĆ, Z., STOJIĆ, A., PERIŠIĆ, M., RAJŠIĆ, S., TASIĆ, M., RADENKOVIĆ, M. & JOKSIĆ, J. 2010. Seasonal variability and source apportionment of metals in the atmospheric deposition in Belgrade. *Atmospheric Environment,* 44**,** 3630-3637.

MILLER, P. E. & DENTON, M. B. 1986. The quadrupole mass filter: basic operating concepts. *Journal of chemical education,* 63**,** 617.

MILLOT, R., ALLÈGRE, C.-J., GAILLARDET, J. & ROY, S. 2004. Lead isotopic systematics of major river sediments: a new estimate of the Pb isotopic composition of the Upper Continental Crust. *Chemical Geology,* 203**,** 75-90.

MING-KAI, Q., WEI-DONG, L., ZHANG, C.-R., SHAN-QIN, W., YONG, Y. & LI-YUAN, H. 2013. Source apportionment of heavy metals in soils using multivariate statistics and geostatistics. *Pedosphere,* 23**,** 437-444.

MIRETZKY, P. & FERNANDEZ-CIRELLI, A. 2008. Phosphates for Pb immobilization in soils: a review. *Environmental Chemistry Letters,* 6**,** 121-133.

MOLDOVAN, M., PALACIOS, M., GOMEZ, M., MORRISON, G., RAUCH, S., MCLEOD, C., MA, R., CAROLI, S., ALIMONTI, A. & PETRUCCI, F. 2002. Environmental risk of particulate and soluble platinum group elements released from gasoline and diesel engine catalytic converters. *Science of the Total Environment,* 296**,** 199-208.

MOLDOVAN, M., RAUCH, S., MORRISON, G. M., GOMEZ, M. & ANTONIA PALACIOS, M. 2003. Impact of ageing on the distribution of platinum group elements and catalyst poisoning elements in automobile catalysts. *Surface and Interface Analysis: An International Journal devoted to the development and application of techniques for the analysis of surfaces, interfaces and thin films,* 35**,** 354-359.

MONNA, F., HAMER, K., LÉVÊQUE, J. & SAUER, M. 2000a. Pb isotopes as a reliable marker of early mining and smelting in the Northern Harz province (Lower Saxony, Germany). *Journal of geochemical exploration,* 68**,** 201-210.

MONNA, F., LANCELOT, J., CROUDACE, I. W., CUNDY, A. B. & LEWIS, J. T. 1997. Pb isotopic composition of airborne particulate material from France and the southern United Kingdom: implications for Pb pollution sources in urban areas. *Environmental Science & Technology,* 31**,** 2277-2286.

MONNA, F., LOIZEAU, J.-L., THOMAS, B., GUÉGUEN, C. & FAVARGER, P.-Y. 1998. Pb and Sr isotope measurements by inductively coupled plasma–mass spectrometer: efficient time management for precision improvement. *Spectrochimica Acta Part B: Atomic Spectroscopy,* 53**,** 1317-1333.

MONNA, F., LOIZEAU, J.-L., THOMAS, B., GUÉGUEN, C., FAVARGER, P.-Y., LOSNO, R. & DOMINIK, J. 2000b. Noise identification and sampling frequency determination for precise Pb isotopic measurements by quadrupole-based Inductively Coupled Plasma Mass Spectrometry. *Analusis,* 28**,** 750-757.

MONTASER, A. 1998. *Inductively coupled plasma mass spectrometry*, John Wiley & Sons.

MORTON, O., PUCHELT, H., HERNÁNDEZ, E. & LOUNEJEVA, E. 2001. Traffic-related platinum group elements (PGE) in soils from Mexico City. *Journal of Geochemical Exploration,* 72**,** 223-227.

MOSSOP, K. F. & DAVIDSON, C. M. 2003. Comparison of original and modified BCR sequential extraction procedures for the fractionation of copper, iron, lead, manganese and zinc in soils and sediments. *Analytica Chimica Acta,* 478**,** 111-118.

MUKAI, H., FURUTA, N., FUJII, T., AMBE, Y., SAKAMOTO, K. & HASHIMOTO, Y. 1993. Characterization of sources of lead in the urban air of Asia using ratios of stable lead isotopes. *Environmental Science & Technology,* 27**,** 1347-1356.

MURLEY, L. 1991. *Clean air around the world: National and international approaches to air pollution control*, International Union of Air Pollution Prevention Associations.

MURRAY, R., MILLER, D. J. & KRYC, K. 2000. Analysis of major and trace elements in rocks, sediments, and interstitial waters by inductively coupled plasma–atomic emission spectrometry (ICP-AES).

MURTAZA, G., GHAFOOR, A., QADIR, M., OWENS, G., AZIZ, M. & ZIA, M. 2010. Disposal and use of sewage on agricultural lands in Pakistan: A review. *Pedosphere,* 20**,** 23-34.

NADAL, M., SCHUHMACHER, M. & DOMINGO, J. 2004. Metal pollution of soils and vegetation in an area with petrochemical industry. *Science of the total environment,* 321**,** 59-69.

NANOS, N. & MARTÍN, J. A. R. 2012. Multiscale analysis of heavy metal contents in soils: spatial variability in the Duero river basin (Spain). *Geoderma,* 189**,** 554-562.

NATHANAIL, P., MCCAFFREY, C., OGDEN, R., FOSTER, N., GILLETT, A. & HAYNES, D. 2004. Uptake of arsenic by vegetables for human consumption: a study of Wellingborough allotment plots. *Land Contamination & Reclamation,* 12**,** 219-238.

NAZIF, W., MARZOUK, E., PERVEEN, S., CROUT, N. & YOUNG, S. 2015. Zinc solubility and fractionation in cultivated calcareous soils irrigated with wastewater. *Science of the Total Environment,* 518**,** 310-319.

NEEDLEMAN, H. 2004. Lead poisoning. *Annu. Rev. Med.,* 55**,** 209-222.

NELMS, S. 2005. Inductively coupled plasma mass spectrometry handbook. *Inductively Coupled Plasma Mass Spectrometry Handbook, Edited by Simon Nelms. Blackwell Publishing, 2005.*

NELMS, S. M. & BEAUCHEMIN, D. 2005. *Inductively coupled plasma mass spectrometry handbook*, Oxford, Boca Raton, FL.

NELMS, S. M., QUÉTEL, C. R., PROHASKA, T., VOGL, J. & TAYLOR, P. D. 2001. Evaluation of detector dead time calculation models for ICP-MS. *Journal of Analytical Atomic Spectrometry,* 16**,** 333-338.

NICHOLSON, F., SMITH, S., ALLOWAY, B., CARLTON-SMITH, C. & CHAMBERS, B. 2003. An inventory of heavy metals inputs to agricultural soils in England and Wales. *Science of the total environment,* 311**,** 205-219.

NOBLE, S. R., HORSTWOOD, M. S., DAVY, P., PASHLEY, V., SPIRO, B. & SMITH, S. 2008. Evolving Pb isotope signatures of London airborne particulate matter (PM 10)—constraints from on-filter and solution-mode MC-ICP-MS. *Journal of Environmental Monitoring,* 10**,** 830-836.

NOLAN, A. L., LOMBI, E. & MCLAUGHLIN, M. J. 2003. Metal bioaccumulation and toxicity in soils—why bother with speciation? *Australian Journal of Chemistry,* 56**,** 77-91.

NOLAN, A. L., MA, Y., LOMBI, E. & MCLAUGHLIN, M. J. 2004. Measurement of labile Cu in soil using stable isotope dilution and isotope ratio analysis by ICP-MS. *Analytical and Bioanalytical Chemistry,* 380**,** 789-797.

NOVAK, M., EREL, Y., ZEMANOVA, L., BOTTRELL, S. H. & ADAMOVA, M. 2008. A comparison of lead pollution record in Sphagnum peat with known historical Pb emission rates in the British Isles and the Czech Republic. *Atmospheric Environment,* 42**,** 8997-9006.

NRIAGU, J. O. 1990. The rise and fall of leaded gasoline. *Science of the total environment,* 92**,** 13-28.

NRIAGU, J. O. 1996. A history of global metal pollution. *Science,* 272**,** 223-223.

NRIAGU, J. O. & PACYNA, J. M. 1988. Quantitative assessment of worldwide contamination of air, water and soils by trace metals. *nature,* 333**,** 134-139.

OLMEZ, I. & GORDON, G. E. 1985. Rare earths: atmospheric signatures for oil-fired power plants and refineries. *Science,* 229**,** 966-968.

OLSON, K. W. & SKOGERBOE, R. K. 1975. Identification of soil lead compounds from automotive sources. *Environmental Science & Technology,* 9**,** 227-230.

OTTOSEN, L. M., HANSEN, H. K. & JENSEN, P. E. 2009. Relation between pH and desorption of Cu, Cr, Zn, and Pb from industrially polluted soils. *Water, air, and soil pollution,* 201**,** 295-304.

OUDIJK, G. 2010. The rise and fall of organometallic additives in automotive gasoline. *Environmental Forensics,* 11**,** 17-49.

PATTERSON, C. C. 1971. Native copper, silver, and gold accessible to early metallurgists. *American Antiquity,* 36**,** 286-321.

PEIJNENBURG, W. J., ZABLOTSKAJA, M. & VIJVER, M. G. 2007. Monitoring metals in terrestrial environments within a bioavailability framework and a focus on soil extraction. *Ecotoxicology and environmental safety,* 67**,** 163-179.

PRICE, D. G. 1995. Weathering and weathering processes. *Quarterly Journal of Engineering Geology and Hydrogeology,* 28**,** 243-252.

PROHASKA, T., WENZEL, W. & STINGEDER, G. 2005. ICP-MS-based tracing of metal sources and mobility in a soil depth profile via the isotopic variation of Sr and Pb. *International Journal of Mass Spectrometry,* 242**,** 243-250.

PRZYBYSZ, A., SÆBØ, A., HANSLIN, H. & GAWROŃSKI, S. 2014. Accumulation of particulate matter and trace elements on vegetation as affected by pollution level, rainfall and the passage of time. *Science of the Total Environment,* 481**,** 360-369.

PUSKÁS, I., PRAZSÁK, I., FARSANG, A. & MARÓY, P. 2008. Physical, chemical and biological aspects of human impacts on urban soils of Szeged (SE Hungary). *Journal of Environmental Geography,* 1**,** 11-21.

QADIR, M., GHAFOOR, A., MURTAZA, G. & MURTAZA, G. 2000. Cadmium concentration in vegetables grown on urban soils irrigated with untreated municipal sewage. *Environment, Development and Sustainability,* 2**,** 13-21.

QUÉTEL, C. R., THOMAS, B., DONARD, O. F. & GROUSSET, F. E. 1997. Factorial optimization of data acquisition factors for lead isotope ratio determination by inductively coupled plasma mass spectrometry. *Spectrochimica Acta Part B: Atomic Spectroscopy,* 52**,** 177-187.

RABINOWITZ, M. B. 2005. Lead isotopes in soils near five historic American lead smelters and refineries. *Science of the Total Environment,* 346**,** 138-148.

RAMOS, S. J., DINALI, G. S., OLIVEIRA, C., MARTINS, G. C., MOREIRA, C. G., SIQUEIRA, J. O. & GUILHERME, L. R. 2016. Rare earth elements in the soil environment. *Current Pollution Reports,* 2**,** 28-50.

RAURET, G., LOPEZ-SANCHEZ, J., SAHUQUILLO, A., RUBIO, R., DAVIDSON, C., URE, A. & QUEVAUVILLER, P. 1999. Improvement of the BCR three step sequential extraction procedure prior to the certification of new sediment and soil reference materials. *Journal of Environmental Monitoring,* 1**,** 57-61.

RAVINDRA, K., BENCS, L. & VAN GRIEKEN, R. 2004. Platinum group elements in the environment and their health risk. *Science of the Total Environment,* 318**,** 1-43.

RAZALI, N. M. & WAH, Y. B. 2011. Power comparisons of shapiro-wilk, kolmogorov-smirnov, lilliefors and anderson-darling tests. *Journal of statistical modeling and analytics,* 2**,** 21-33.

REHMAN, W., ZEB, A., NOOR, N. & NAWAZ, M. 2008. Heavy metal pollution assessment in various industries of Pakistan. *Environmental Geology,* 55**,** 353-358.

REIMANN, C., FLEM, B., ARNOLDUSSEN, A., ENGLMAIER, P., FINNE, T. E., KOLLER, F. & NORDGULEN, Ø. 2008. The biosphere: A homogeniser of Pb-isotope signals. *Applied Geochemistry,* 23**,** 705-722.

REIMANN, C., FLEM, B., FABIAN, K., BIRKE, M., LADENBERGER, A., NÉGREL, P., DEMETRIADES, A. & HOOGEWERFF, J. 2012. Lead and lead isotopes in agricultural soils of Europe–The continental perspective. *Applied Geochemistry,* 27**,** 532-542.

RENBERG, I., BRÄNNVALL, M.-L., BINDLER, R. & EMTERYD, O. 2002. Stable lead isotopes and lake sediments—a useful combination for the study of atmospheric lead pollution history. *Science of the Total Environment,* 292**,** 45-54.

REUER, M. K., BOYLE, E. A. & GRANT, B. C. 2003. Lead isotope analysis of marine carbonates and seawater by multiple collector ICP-MS. *Chemical Geology,* 200**,** 137-153.

RIEUWERTS, J., ASHMORE, M., FARAGO, M. & THORNTON, I. 2006. The influence of soil characteristics on the extractability of Cd, Pb and Zn in upland and moorland soils. *Science of the total Environment,* 366**,** 864-875.

RIEUWERTS, J. S., FARAGO, M., CIKRT, M. & BENCKO, V. 1999. Heavy metal concentrations in and around households near a secondary lead smelter. *Environmental Monitoring and Assessment,* 58**,** 317-335.

RODRIGUES, S., HENRIQUES, B., DA SILVA, E. F., PEREIRA, M., DUARTE, A. & RÖMKENS, P. 2010. Evaluation of an approach for the characterization of reactive and available pools of twenty potentially toxic elements in soils: Part I–The role of key soil properties in the variation of contaminants' reactivity. *Chemosphere,* 81**,** 1549-1559.

RODRÍGUEZ-CASTRILLÓN, J. Á., MOLDOVAN, M. & ALONSO, J. I. G. 2009. Internal correction of hafnium oxide spectral interferences and mass bias in the determination of platinum in environmental samples using isotope dilution analysis. *Analytical and bioanalytical chemistry,* 394**,** 351-362.

ROHL, B. M. 1996. Lead isotope data from the Isotrace Laboratory, Oxford: archaeometry data base 2, galena from Britain and Ireland. *Archaeometry,* 38**,** 165-180.

ROSMAN, K., CHISHOLM, W., BOUTRON, C., CANDELONE, J. & HONG, S. 1994. Isotopic evidence to account for changes in the concentration of lead in Greenland snow between 1960 and 1988. *Geochimica et Cosmochimica Acta,* 58**,** 3265-3269.

ROSSITER, D. & BURGHARDT, W. Classification of urban and industrial soils in the world reference base for soil resources: working document. Second International Conference of the working group Soil of Urban, Industrial, Traffic and Mining Areas (SUITMA) of the International Union of Soil Science (IUSS), Nancy, 2003.

RYAN, J. A., ZHANG, P., HESTERBERG, D., CHOU, J. & SAYERS, D. E. 2001. Formation of chloropyromorphite in a lead-contaminated soil amended with hydroxyapatite. *Environmental Science & Technology,* 35**,** 3798-3803.

SAAL, A., HART, S., SHIMIZU, N., HAURI, E., LAYNE, G. & EILER, J. 2005. Pb isotopic variability in melt inclusions from the EMI–EMII–HIMU mantle end-members and the role of the oceanic lithosphere. *Earth and Planetary Science Letters,* 240**,** 605-620.

SADEGHI, M., MORRIS, G. A., CARRANZA, E. J. M., LADENBERGER, A. & ANDERSSON, M. 2013. Rare earth element distribution and mineralization in Sweden: an application of principal component analysis to FOREGS soil geochemistry. *Journal of geochemical exploration,* 133**,** 160-175.

SAGAGI, B. & IMAM, T. 2017. Fractionation of potentially toxic elements (PTE) in soils irrigated with wastewater using modified BCR sequential extraction procedure. *Bayero Journal of Pure and Applied Sciences,* 10**,** 300-305.

SANBORN, M. D., ABELSOHN, A., CAMPBELL, M. & WEIR, E. 2002. Identifying and managing adverse environmental health effects: 3. Lead exposure. *Canadian Medical Association Journal,* 166**,** 1287-1292.

SANGSTER, D., OUTRIDGE, P. & DAVIS, W. 2000. Stable lead isotope characteristics of lead ore deposits of environmental significance. *Environmental Reviews,* 8**,** 115-147.

SANTOS, R., MACHADO, M. C., RUIZ, I., SATO, K. & VASCONCELOS, M. 2007. Space charge and mass discrimination effects on lead isotope ratio measurements by ICP-QMS in environmental samples with high uranium content. *Journal of Analytical Atomic Spectrometry,* 22**,** 783-790.

SAYED, S., ASHOUR, E. & YOUSSEF, G. 2003. Effect of sulfide ions on the corrosion behaviour of Al–brass and Cu10Ni alloys in salt water. *Materials Chemistry and Physics,* 78**,** 825-834.

SCHAEFER, K. & EINAX, J. W. 2016. Source apportionment and geostatistics: an outstanding combination for describing metals distribution in soil. *CLEAN–Soil, Air, Water,* 44**,** 877-884.

SCHRÖDER, T. J., HIEMSTRA, T., VINK, J. P. & VAN DER ZEE, S. E. 2005. Modeling of the Solid− Solution Partitioning of Heavy Metals and Arsenic in Embanked Flood Plain Soils of the Rivers Rhine and Meuse. *Environmental science & technology,* 39**,** 7176-7184.

SCHWERTMANN, U. & PFAB, G. 1996. Structural vanadium and chromium in lateritic iron oxides: genetic implications. *Geochimica et Cosmochimica Acta,* 60**,** 4279-4283.

SEN, I. S. & PEUCKER-EHRENBRINK, B. 2012. Anthropogenic disturbance of element cycles at the Earth's surface. *Environmental science & technology,* 46**,** 8601-8609.

SHAN, X. & CHEN, B. 1993. Evaluation of sequential extraction for speciation of trace metals in model soil containing natural minerals and humic acid. *Analytical Chemistry,* 65**,** 802-807.

SHETAYA, W., MARZOUK, E., MOHAMED, E., ELKASSAS, M., BAILEY, E. & YOUNG, S. 2018. Lead in Egyptian soils: Origin, reactivity and bioavailability measured by stable isotope dilution. *Science of The Total Environment,* 618**,** 460-468.

SHI, G., CHEN, Z., XU, S., ZHANG, J., WANG, L., BI, C. & TENG, J. 2008. Potentially toxic metal contamination of urban soils and roadside dust in Shanghai, China. *Environmental Pollution,* 156**,** 251-260.

SHOTYK, W., CHEBURKIN, A. K., APPLEBY, P. G., FANKHAUSER, A. & KRAMERS, J. D. 1996. Two thousand years of atmospheric arsenic, antimony, and lead deposition recorded in an ombrotrophic peat bog profile, Jura Mountains, Switzerland. *Earth and planetary science letters,* 145**,** E1-E7.

SHOTYK, W., WEISS, D., APPLEBY, P. G., CHEBURKIN, A. K., FREI, R., GLOOR, M., KRAMERS, J. D., REESE, S. & VAN DER KNAAP, W. O. 1998. History of Atmospheric Lead Deposition Since 12,370 ¹⁴C yr BP from a Peat Bog, Jura Mountains, Switzerland. *Science,* 281**,** 1635-1640.

SHUMAN, L. 1991. Chemical forms of micronutrients in soils. *Micronutrients in agriculture***,** 113-144.

SILVA, Y. J. A. B. D., NASCIMENTO, C. W. A. D., SILVA, Y. J. A. B. D., BIONDI, C. M. & SILVA, C. M. C. A. C. 2016. Rare Earth Element Concentrations in Brazilian Benchmark Soils. *Revista Brasileira de Ciência do Solo,* 40.

SIMPSON, L. A., THOMSEN, M., ALLOWAY, B. J. & PARKER, A. 2001. A dynamic reaction cell (DRC) solution to oxide-based interferences in inductively coupled plasma mass spectrometry (ICP-MS) analysis of the noble metals. *Journal of analytical atomic spectrometry,* 16**,** 1375-1380.

SINGH, K. P., MOHAN, D., SINHA, S. & DALWANI, R. 2004. Impact assessment of treated/untreated wastewater toxicants discharged by sewage treatment plants on health, agricultural, and environmental quality in the wastewater disposal area. *Chemosphere,* 55**,** 227-255.

SMEDA, A. & ZYRNICKI, W. 2002. Application of sequential extraction and the ICP-AES method for study of the partitioning of metals in fly ashes. *Microchemical Journal,* 72**,** 9-16.

SMIDT, G. A., KOSCHINSKY, A., DE CARVALHO, L. M., MONSERRAT, J. & SCHNUG, E. 2011. Heavy metal concentrations in soils in the vicinity of a fertilizer factory in Southern Brazil. *Agriculture and Forestry Research,* 61**,** 353-64.

SMOLDERS, E., BRANS, K., FÖLDI, A. & MERCKX, R. 1999. Cadmium fixation in soils measured by isotopic dilution. *Soil Science Society of America Journal,* 63**,** 78-85.

SMOLDERS, E. & DEGRYSE, F. 2002. Fate and effect of zinc from tire debris in soil. *Environmental Science & Technology,* 36**,** 3706-3710.

ŠMUC, N. R., DOLENEC, T., SERAFIMOVSKI, T., DOLENEC, M. & VRHOVNIK, P. 2012. Geochemical characteristics of rare earth elements (REEs) in the paddy soil and rice (Oryza sativa L.) system of Kočani Field, Republic of Macedonia. *Geoderma,* 183**,** 1-11.

SPADA, N., BOZLAKER, A. & CHELLAM, S. 2012. Multi-elemental characterization of tunnel and road dusts in Houston, Texas using dynamic reaction cell-quadrupole-inductively coupled plasma–mass spectrometry: evidence for the release of platinum group and anthropogenic metals from motor vehicles. *Analytica chimica acta,* 735**,** 1-8.

STRELOW, F. W. E. 1967. Application of ion exchange chromatography to accurate determination of lead, uranium, and thorium in tantaloniobates. *Analytical Chemistry,* 39**,** 1454-1455.

SUESS, D. T. & PRATHER, K. A. 1999. Mass spectrometry of aerosols. *Chemical Reviews,* 99**,** 3007-3036.

SUGDEN, C., FARMER, J. & MACKENZIE, A. 1993. Isotopic ratios of lead in contemporary environmental material from Scotland. *Environmental Geochemistry and Health,* 15**,** 59-65.

SUGIYAMA, N. & SHIKAMORI, Y. 2015. Removal of spectral interferences on noble metal elements using MS/MS reaction cell mode of a triple quadrupole ICP-MS. *Journal of Analytical Atomic Spectrometry,* 30**,** 2481-2487.

SURKAN, P. J., ZHANG, A., TRACHTENBERG, F., DANIEL, D. B., MCKINLAY, S. & BELLINGER, D. C. 2007. Neuropsychological function in children with blood lead levels< 10 μg/dL. *Neurotoxicology,* 28**,** 1170-1177.

SUTHERLAND, R. A. & TOLOSA, C. 2000. Multi-element analysis of road-deposited sediment in an urban drainage basin, Honolulu, Hawaii. *Environmental pollution,* 110**,** 483-495.

SUTHERLAND, R. A., TOLOSA, C. A., TACK, F. & VERLOO, M. 2000. Characterization of selected element concentrations and enrichment ratiosin background and anthropogenically impacted roadside areas. *Archives of Environmental Contamination and Toxicology,* 38**,** 428-438.

TACK, F. & VERLOO, M. G. 1995. Chemical speciation and fractionation in soil and sediment heavy metal analysis: a review. *International Journal of Environmental Analytical Chemistry,* 59**,** 225-238.

TAYLOR, P. D., DE BIÈVRE, P., WALDER, A. J. & ENTWISTLE, A. 1995. Validation of the analytical linearity and mass discrimination correction model exhibited by a multiple collector inductively coupled plasma mass spectrometer by means of a set of synthetic uranium isotope mixtures. *Journal of Analytical Atomic Spectrometry,* 10**,** 395-398.

TAYLOR, S., MCLENNAN, S., KEAREY, P. & BROOKS, M. 1985. An examination of the geochemical record preserved in sedimentary rocks. *The Continental Crust—Its Composition and Evolution*.

TAYLOR, S. R. & MCLENNAN, S. M. 1995. The geochemical evolution of the continental crust. *Reviews of Geophysics,* 33**,** 241-265.

TEMPLETON, D. M., ARIESE, F., CORNELIS, R., DANIELSSON, L.-G., MUNTAU, H., VAN LEEUWEN, H. P. & LOBINSKI, R. 2000. Guidelines for terms related to chemical speciation and fractionation of elements. Definitions, structural aspects, and methodological approaches (IUPAC Recommendations 2000). *Pure and applied chemistry,* 72**,** 1453-1470.

TESSIER, A., CAMPBELL, P. G. C. & BISSON, M. 1979. Sequential extraction procedure for the speciation of particulate trace metals. *Analytical Chemistry,* 51**,** 844-851.

TEUTSCH, N., EREL, Y., HALICZ, L. & BANIN, A. 2001. Distribution of natural and anthropogenic lead in Mediterranean soils. *Geochimica et Cosmochimica Acta,* 65**,** 2853-2864.

THIRLWALL, M. 2001. Inappropriate tail corrections can cause large inaccuracy in isotope ratio determination by MC-ICP-MS. *Journal of Analytical Atomic Spectrometry,* 16**,** 1121-1125.

THIRLWALL, M. F. 2002. Multicollector ICP-MS analysis of Pb isotopes using a 207pb-204pb double spike demonstrates up to 400 ppm/amu systematic errors in Tl-normalization. *Chemical Geology,* 184**,** 255-279.

THOMAS, P. J., CARPENTER, D., BOUTIN, C. & ALLISON, J. E. 2014. Rare earth elements (REEs): effects on germination and growth of selected crop and native plant species. *Chemosphere,* 96**,** 57-66.

THORNTON, I. 1993. Environmental geochemistry and health in the 1990s: a global perspective. *Applied geochemistry,* 8**,** 203-210.

THORNTON, I., FARAGO, M. E., THUMS, C. R., PARRISH, R. R., MCGILL, R. A., BREWARD, N., FORTEY, N., SIMPSON, P., YOUNG, S. & TYE, A. 2008. Urban geochemistry: research strategies to assist risk assessment and remediation of brownfield sites in urban areas. *Environmental Geochemistry and Health,* 30**,** 565-576.

THUMS, C. R., FARAGO, M. E. & THORNTON, I. 2008. Bioavailability of trace metals in brownfield soils in an urban area in the UK. *Environmental Geochemistry and Health,* 30**,** 549-563.

TIPPING, E., SOMERVILLE, C. J. & LUSTER, J. 2016. The C: N: P: S stoichiometry of soil organic matter. *Biogeochemistry,* 130**,** 117-131.

TODOROVSKY, D. S., MINKOVA, N. L. & BAKALOVA, D. P. 1997. Effect of the application of superphosphate on rare earths' content in the soil. *Science of the total environment,* 203**,** 13-16.

TONG, S., SCHIRNDING, Y. E. V. & PRAPAMONTOL, T. 2000. Environmental lead exposure: a public health problem of global dimensions. *Bulletin of the World Health Organization,* 78**,** 1068-1077.

TRIVEDI, P. & AXE, L. 2001. Predicting divalent metal sorption to hydrous Al, Fe, and Mn oxides. *Environmental science & technology,* 35**,** 1779-1784.

TYE, A., YOUNG, S., CROUT, N., ZHANG, H., PRESTON, S., BARBOSA-JEFFERSON, V., DAVISON, W., MCGRATH, S., PATON, G. & KILHAM, K. 2003. Predicting the activity of Cd 2+ and Zn 2+ in soil pore water from the radio-labile metal fraction. *Geochimica et Cosmochimica Acta,* 67**,** 375-385.

UPTON, C. 1998. *A history of Wolverhampton*, Phillimore.
URE, A., QUEVAUVILLER, P., MUNTAU, H. & GRIEPINK, B. 1993. Speciation of heavy metals in soils and sediments. An account of the improvement and harmonization of extraction techniques undertaken under the auspices of the BCR of the Commission of the European Communities. *International journal of environmental analytical chemistry,* 51**,** 135-151.
URE, A. M. & DAVIDSON, C. M. 2008. *Chemical speciation in the environment*, John Wiley & Sons.
VALLELONGA, P., VAN DE VELDE, K., CANDELONE, J.-P., MORGAN, V., BOUTRON, C. & ROSMAN, K. 2002. The lead pollution history of Law Dome, Antarctica, from isotopic measurements on ice cores: 1500 AD to 1989 AD. *Earth and Planetary Science Letters,* 204**,** 291-306.
VAN GEEL, B., BUURMAN, J. & WATERBOLK, H. T. 1996. Archaeological and palaeoecological indications of an abrupt climate change in The Netherlands, and evidence for climatological teleconnections around 2650 BP. *Journal of Quaternary Science,* 11**,** 451-460.
VAN HEUZEN, A. A., HOEKSTRA, T. & VAN WINGERDEN, B. 1989. Precision and accuracy attainable with isotope dilution analysis applied to inductively coupled plasma mass spectrometry: theory and experiments. *Journal of Analytical Atomic Spectrometry,* 4**,** 483-489.
VAN OORT, F., BALABANE, M., GAULTIER, J., HARDY, R. & BOURENANNE, H. 2001. Dissemination and spatial variability of metal pollutants generated by past metallurgical activity of a zinc smelter complex in surrounding agricultural land (Mortagne-du-Nord, northern France). *Mémoires des Sciences de la Terre,* 40**,** 157-160.
VANHAECKE, F., DE WANNEMACKER, G., MOENS, L., DAMS, R., LATKOCZY, C., PROHASKA, T. & STINGEDER, G. 1998. Dependence of detector dead time on analyte mass number in inductively coupled plasma mass spectrometry. *Journal of Analytical Atomic Spectrometry,* 13**,** 567-571.
VEYSSEYRE, A. M., BOLLHÖFER, A. F., ROSMAN, K. J., FERRARI, C. P. & BOUTRON, C. F. 2001. Tracing the origin of pollution in French Alpine snow and aerosols using lead isotopic ratios. *Environmental science & technology,* 35**,** 4463-4469.
VILE, M. A., WIEDER, R. K. & NOVÁK, M. 1999. Mobility of Pb inSphagnum-derived peat. *Biogeochemistry,* 45**,** 35-52.
VIOLANTE, A. & PIGNA, M. 2002. Competitive sorption of arsenate and phosphate on different clay minerals and soils. *Soil Science Society of America Journal,* 66**,** 1788-1796.
WAHEED, S., RAHMAN, A., KHALID, N. & AHMAD, S. 2006. Assessment of air quality of two metropolitan cities in Pakistan: Elemental analysis using INAA and AAS. *Radiochimica Acta,* 94**,** 161-166.
WALDER, A. J. & FREEDMAN, P. A. 1992. Communication. Isotopic ratio measurement using a double focusing magnetic sector mass analyser with an inductively coupled plasma as an ion source. *Journal of Analytical Atomic Spectrometry,* 7**,** 571-575.
WALRAVEN, N., VAN GAANS, P., VAN DER VEER, G., VAN OS, B., KLAVER, G. T., VRIEND, S., MIDDELBURG, J. & DAVIES, G. 2013. Tracing diffuse anthropogenic Pb sources in rural soils by means of Pb isotope analysis. *Applied geochemistry,* 37**,** 242-257.
WALRAVEN, N., VAN OS, B., KLAVER, G. T., BAKER, J. & VRIEND, S. 1997. Trace element concentrations and stable lead isotopes in soils as tracers of lead pollution in Graft-De Rijp, the Netherlands. *Journal of Geochemical Exploration,* 59**,** 47-58.
WANG, C., YANG, Z., ZHONG, C. & JI, J. 2016. Temporal–spatial variation and source apportionment of soil heavy metals in the representative river–alluviation depositional system. *Environmental pollution,* 216**,** 18-26.
WANG, C., ZHU, W., PENG, A. & GUICHREIT, R. 2001. Comparative studies on the concentration of rare earth elements and heavy metals in the atmospheric particulate matter in Beijing, China, and in Delft, the Netherlands. *Environment international,* 26**,** 309-313.
WANG, E. X. & BENOIT, G. 1997. Fate and transport of contaminant lead in spodosols: A simple box model analysis. *Water, Air, and Soil Pollution,* 95**,** 381-397.

WASEEM, A., ARSHAD, J., IQBAL, F., SAJJAD, A., MEHMOOD, Z. & MURTAZA, G. 2014. Pollution status of Pakistan: a retrospective review on heavy metal contamination of water, soil, and vegetables. *BioMed research international,* 2014.

WATANABE, T., ZHANG, Z.-W., QU, J.-B., GAO, W.-P., JIAN, Z.-K., SHIMBO, S., NAKATSUKA, H., MATSUDA-INOGUCHI, N., HIGASHIKAWA, K. & IKEDA, M. 2000. Background lead and cadmium exposure of adult women in Xian City and two farming villages in Shaanxi Province, China. *Science of the total environment,* 247**,** 1-13.

WEI, B. & YANG, L. 2010. A review of heavy metal contaminations in urban soils, urban road dusts and agricultural soils from China. *Microchemical Journal,* 94**,** 99-107.

WEISS, D., SHOTYK, W., APPLEBY, P. G., KRAMERS, J. D. & CHEBURKIN, A. K. 1999. Atmospheric Pb deposition since the industrial revolution recorded by five Swiss peat profiles: enrichment factors, fluxes, isotopic composition, and sources. *Environmental science & technology,* 33**,** 1340-1352.

WEISS, D. J., KOBER, B., DOLGOPOLOVA, A., GALLAGHER, K., SPIRO, B., LE ROUX, G., MASON, T. F., KYLANDER, M. & COLES, B. J. 2004. Accurate and precise Pb isotope ratio measurements in environmental samples by MC-ICP-MS. *International Journal of Mass Spectrometry,* 232**,** 205-215.

WENG, L., TEMMINGHOFF, E. J. & VAN RIEMSDIJK, W. H. 2001. Contribution of individual sorbents to the control of heavy metal activity in sandy soil. *Environmental Science & Technology,* 35**,** 4436-4443.

WERKENTHIN, M., KLUGE, B. & WESSOLEK, G. 2014. Metals in European roadside soils and soil solution–A review. *Environmental Pollution,* 189**,** 98-110.

WHITELEY, J. & MURRAY, F. 2003. Anthropogenic platinum group element (Pt, Pd and Rh) concentrations in road dusts and roadside soils from Perth, Western Australia. *Science of the Total Environment,* 317**,** 121-135.

WILCKE, W., LILIENFEIN, J., DO CARMO LIMA, S. & ZECH, W. 1999. Contamination of highly weathered urban soils in Uberlandia, Brazil. *Journal of Plant Nutrition and Soil Science,* 162**,** 539-548.

WILCKE, W., MÜLLER, S., KANCHANAKOOL, N. & ZECH, W. 1998. Urban soil contamination in Bangkok: heavy metal and aluminium partitioning in topsoils. *Geoderma,* 86**,** 211-228.

WILSON, C. A., CRESSER, M. S. & DAVIDSON, D. A. 2006. Sequential element extraction of soils from abandoned farms: an investigation of the partitioning of anthropogenic element inputs from historic land use. *Journal of Environmental Monitoring,* 8**,** 439-444.

WIXSON, B. G. & DAVIES, B. E. 1994. Guidelines for lead in soil. Proposal of the society for environmental geochemistry and health. *Environmental Science & Technology,* 28**,** 26A-31A.

WONG, C. S., LI, X. & THORNTON, I. 2006. Urban environmental geochemistry of trace metals. *Environmental Pollution,* 142**,** 1-16.

WONG, S., LI, X., ZHANG, G., QI, S. & MIN, Y. 2002. Heavy metals in agricultural soils of the Pearl River Delta, South China. *Environmental Pollution,* 119**,** 33-44.

WOODHEAD, J. 2002. A simple method for obtaining highly accurate Pb isotope data by MC-ICP-MS. *Journal of Analytical Atomic Spectrometry,* 17**,** 1381-1385.

WU, G., ZHU, J.-M., TAN, D., HAN, G., ZHANG, L. & REN, K. 2017. Accurate and precise determination of lead isotope composition in selected geochemical reference materials. *Acta Geochimica,* 36**,** 421-425.

WU, S., ZHAO, Y.-H., FENG, X. & WITTMEIER, A. 1996. Application of inductively coupled plasma mass spectrometry for total metal determination in silicon-containing solid samples using the microwave-assisted nitric acid–hydrofluoric acid–hydrogen peroxide–boric acid digestion system. *Journal of Analytical Atomic Spectrometry,* 11**,** 287-296.

WUANA, R. A. & OKIEIMEN, F. E. 2011. Heavy metals in contaminated soils: a review of sources, chemistry, risks and best available strategies for remediation. *Isrn Ecology,* 2011.

XIE, Y., MENG, J. & GUO, L. 2014. REE geochemistry of modern eolian dust deposits in Harbin city, Heilongjiang province, China: Implications for provenance. *Catena,* 123**,** 70-78.

XU, Y., BOONFUENG, T., AXE, L., MAENG, S. & TYSON, T. 2006. Surface complexation of Pb (II) on amorphous iron oxide and manganese oxide: Spectroscopic and time studies. *Journal of Colloid and Interface Science,* 299**,** 28-40.

YANAI, R. D., RAY, D. G. & SICCAMA, T. G. 2004. Lead reduction and redistribution in the forest floor in New Hampshire northern hardwoods. *Journal of environmental quality,* 33**,** 141-148.

YANG, J.-L. & ZHANG, G.-L. 2015. Formation, characteristics and eco-environmental implications of urban soils–A review. *Soil science and plant nutrition,* 61**,** 30-46.

YANG, L. 2009. Accurate and precise determination of isotopic ratios by MC-ICP-MS: A review. *Mass Spectrometry Reviews,* 28**,** 990-1011.

YANG, Z., LU, W., LONG, Y., BAO, X. & YANG, Q. 2011. Assessment of heavy metals contamination in urban topsoil from Changchun City, China. *Journal of Geochemical Exploration,* 108**,** 27-38.

YARLAGADDA, P. S., MATSUMOTO, M. R., VANBENSCHOTEN, J. E. & KATHURIA, A. 1995. Characteristics of heavy metals in contaminated soils. *Journal of environmental engineering,* 121**,** 276-286.

YE, C., LI, S., ZHANG, Y. & ZHANG, Q. 2011. Assessing soil heavy metal pollution in the water-level-fluctuation zone of the Three Gorges Reservoir, China. *Journal of hazardous materials,* 191**,** 366-372.

YIN, Y., IMPELLITTERI, C. A., YOU, S.-J. & ALLEN, H. E. 2002. The importance of organic matter distribution and extract soil: solution ratio on the desorption of heavy metals from soils. *Science of the Total Environment,* 287**,** 107-119.

YOUNG, S., CROUT, N., HUTCHINSON, J., TYE, A., TANDY, S. & NAKHONE, L. 2007. Techniques for measuring attenuation: isotopic dilution methods. *Natural attenuation of trace element availability in soils***,** 19-37.

YOUNG, S., TYE, A., CARSTENSEN, A., RESENDE, L. & CROUT, N. 2000a. Methods for determining labile cadmium and zinc in soil. *European Journal of Soil Science,* 51**,** 129-136.

YOUNG, S. D., TYE, A., CARSTENSEN, A., RESENDE, L. & CROUT, N. 2000b. Methods for determining labile cadmium and zinc in soil. *European Journal of Soil Science,* 51**,** 129-136.

YOUNG, S. D., ZHANG, H., TYE, A. M., MAXTED, A., THUMS, C. & THORNTON, I. 2005. Characterizing the availability of metals in contaminated soils. I. The solid phase: sequential extraction and isotopic dilution. *Soil Use and Management,* 21**,** 450-458.

YUAN, C.-G., SHI, J.-B., HE, B., LIU, J.-F., LIANG, L.-N. & JIANG, G.-B. 2004. Speciation of heavy metals in marine sediments from the East China Sea by ICP-MS with sequential extraction. *Environment International,* 30**,** 769-783.

ZEREINI, F., SKERSTUPP, B., ALT, F., HELMERS, E. & URBAN, H. 1997. Geochemical behaviour of platinum-group elements (PGE) in particulate emissions by automobile exhaust catalysts: experimental results and environmental investigations. *Science of the Total Environment,* 206**,** 137-146.

ZEREINI, F. & WISEMAN, C. L. 2015. *Platinum metals in the environment*, Springer.

ZHANG, C. 2006. Using multivariate analyses and GIS to identify pollutants and their spatial patterns in urban soils in Galway, Ireland. *Environmental pollution,* 142**,** 501-511.

ZHANG, F.-S., YAMASAKI, S. & KIMURA, K. 2001. Rare earth element content in various waste ashes and the potential risk to Japanese soils. *Environment International,* 27**,** 393-398.

ZHANG, J., ISHII, T., YOSHIDA, S., LIU, C. & ARMANNSSON, H. 1999. Rare earth element chemistry of rain water. *AA Balkema***,** 347-350.

ZHANG, P., RYAN, J. A. & BRYNDZIA, L. T. 1997. Pyromorphite formation from goethite adsorbed lead. *Environmental Science & Technology,* 31**,** 2673-2678.

ZHANG, P., RYAN, J. A. & YANG, J. 1998. In vitro soil Pb solubility in the presence of hydroxyapatite. *Environmental Science & Technology,* 32**,** 2763-2768.

ZHANG, Q., SHI, X., HUANG, B., YU, D., ÖBORN, I., BLOMBÄCK, K., WANG, H., PAGELLA, T. & SINCLAIR, F. 2007. Surface water quality of factory-based and vegetable-based peri-urban areas in the Yangtze River Delta region, China. *Catena,* 69**,** 57-64.

ZHANG, X., YANG, L., LI, Y., LI, H., WANG, W. & YE, B. 2012. Impacts of lead/zinc mining and smelting on the environment and human health in China. *Environmental Monitoring and Assessment,* 184**,** 2261-2273.

ZHANG, Y. & YE, W.-H. 2006. Does the long-term application of calcium superphosphate lead to an increase of the soil rare earth element contents? *Journal of Environmental Sciences,* 18**,** 130-134.

ZHAO, P., LI, J., ZHONG, L., SUN, S. & XU, J. 2014. A method for determination of PGE–Re concentrations and Os isotopic compositions in environmental materials. *Analytical Methods,* 6**,** 5537-5545.

ZHU, W., XU, S., ZHANG, H., SHAO, P., WU, D., YANG, W. & FENG, J. 1996. Investigation on the intelligence quotient of children in the areas with high REE background (Ⅰ)--REE bioeffects in the REE-high areas of southern Jiangxi Province. *Chinese science bulletin,* 41**,** 1977-1981.

ZIA, M. H., WATTS, M. J., NIAZ, A., MIDDLETON, D. R. & KIM, A. W. 2017. Health risk assessment of potentially harmful elements and dietary minerals from vegetables irrigated with untreated wastewater, Pakistan. *Environmental geochemistry and health,* 39**,** 707-728.

9 APPENDICIES

9.1 Appendix A Descriptive statistics

Table A1: Descriptive statistics for major and minor element concentrations in urban soils (Nottingham and Wolverhampton). All values are given in mg kg^{-1}.

Metal(loid)/ Urban soils		Nottingham (Ng)	Wolverhampton (Wv)	*NBCs
	n	20	30	
Sodium (Na)	Mean	1984	1975	
	SD	946	751	
	Min.	732	526	
	Max.	4431	4029	
Magnesium (Mg)	Mean	4978	3858	
	SD	2823	1662	
	Min.	2287	1284	
	Max.	14616	7413	
Potassium (K)	Mean	12046	12797	
	SD	3741	2877	
	Min.	4720	5745	
	Max.	19630	19755	
Calcium (Ca)	Mean	12037	9600	
	SD	11013	10958	
	Min.	2798	970	
	Max.	46281	50683	
Aluminium (Al)	Mean	31260	32088	
	SD	9047	11838	
	Min.	16462	14580	
	Max.	48552	58602	
Manganese (Mn)	Mean	749	606	
	SD	365	556	
	Min.	287	115	
	Max.	1551	3012	
Iron (Fe)	Mean	31171	24824	
	SD	11577	10730	
	Min.	16806	7930	
	Max.	56760	59249	
Phosphorus (P)	Mean	1882	1230	
	SD	2743	1648	
	Min.	233	399	
	Max.	11661	9572	
Lithium (Li)	Mean	42.8	51.1	
	SD	16.7	23.6	
	Min.	24.0	23.1	
	Max.	79.1	124	
Beryllium (Be)	Mean	3.96	2.36	
	SD	3.91	1.05	
	Min.	1.45	0.832	
	Max.	15.4	4.76	
Lead (Pb)	Mean	353	204	
	SD	301	187	
	Min.	18.1	27.9	820
	Max.	1108	841	
Cadmium (Cd)	Mean	4.77	2.03	
	SD	10.9	3.82	
	Min.	0.127	0.227	2.1
	Max.	46.9	21.4	
Zinc (Zn)	Mean	529	470	
	SD	490	622.4	
	Min.	35.9	66.2	
	Max.	1860	3431	
Copper (Cu)	Mean	230	177	
	SD	379	333	
	Min.	23.6	15.3	190
	Max.	1507	1879	
Nickel (Ni)	Mean	82.2	45.9	
	SD	99.5	40.4	
	Min.	17.4	12.5	40
	Max.	394	241	

Cobalt (Co)	Mean	19.3	14.6	
	SD	21.2	7.08	
	Min.	5.55	4.43	
	Max.	88.3	30.3	
Chromium (Cr)	Mean	186	66.4	
	SD	397	75.1	
	Min.	26.4	22.9	
	Max.	1661	450	
Vanadium (V)	Mean	67.2	78.5	
	SD	25.5	36.2	
	Min.	34.8	30.3	
	Max.	116	168	
Arsenic (As)	Mean	20.9	18.1	
	SD	11.1	14.3	
	Min.	6.86	8.53	
	Max.	50.5	88.1	
Molybdenum (Mo)	Mean	6.44	3.07	
	SD	10.5	1.54	
	Min.	1.38	1.25	
	Max.	39.1	6.65	
Antimony (Sb)	Mean	14.0	5.76	
	SD	19.0	4.83	
	Min.	1.58	1.11	
	Max.	76.1	19.0	
Tin (Sn)	Mean	41.1	33.8	
	SD	57.2	51.5	
	Min.	2.11	4.04	
	Max.	186	240	
Barium (Ba)	Mean	801	475	
	SD	348	176	
	Min.	381	246	
	Max.	1452	1049	
Hafnium (Hf)	Mean	2.78	1.89	
	SD	2.76	0.764	
	Min.	1.36	0.169	
	Max.	14.2	3.79	
Selenium (Se)	Mean	1.36	1.21	
	SD	0.614	0.649	
	Min.	0.512	0.481	
	Max.	3.02	3.15	
Rubidium (Rb)	Mean	54.5	58.7	
	SD	16.6	14.7	
	Min.	26.0	24.8	
	Max.	80.1	98.9	
Silver (Ag)	Mean	1.98	0.483	
	SD	4.61	0.965	
	Min.	0.097	0.121	
	Max.	18.3	5.494	
Titanium (Ti)	Mean	2380	2778	
	SD	859	1305	
	Min.	1389	1171	
	Max.	4118	5617	
Cesium (Cs)	Mean	3.22	3.53	
	SD	1.43	1.32	
	Min.	1.59	1.35	
	Max.	6.93	7.20	
Strontium (Sr)	Mean	107	105	
	SD	72.4	72.7	
	Min.	58.9	42.4	
	Max.	301	343	
Thallium (Tl)	Mean	0.569	0.576	
	SD	0.147	0.310	
	Min.	0.372	0.362	
	Max.	0.986	2.058	
Uranium (U)	Mean	2.35	1.71	
	SD	0.913	0.569	
	Min.	1.29	0.893	
	Max.	4.07	2.82	

32

*Normal background concentration values (NBCs), Ander et al. (2013)

Table A2: Descriptive statistics for major and minor element concentrations in sewage amended soils (Pakistan). All values are given in mg kg^{-1}.

Metal(loid)/ Sewage amended soils		Gujranwala (GW)	Gujrat (GT)	Lahore (LH)	Faisalabad (FB)	**EC-DG,2009**
	n	31	9	15	12	
Sodium (Na)	Mean	8715	8579	7685	9151	
	SD	542	670	1176	1036	
	Min.	7439	7414	6208	7400	
	Max.	9609	9770	10101	10940	
Magnesium (Mg)	Mean	7944	7378	8274	9193	
	SD	1745	1645	1227	1063	
	Min.	5245	5148	6161	7834	
	Max.	12856	10110	10489	11815	
Potassium (K)	Mean	16917	16250	16830	16484	
	SD	1087	809	1894	845	
	Min.	14913	14999	13079	15685	
	Max.	20009	17783	19807	18578	
Calcium (Ca)	Mean	14003	12363	11060	18678	
	SD	5285	5031	3016	6894	
	Min.	7117	6705	7741	9127	
	Max.	26853	20895	16246	32959	
Aluminium (Al)	Mean	52792	50267	52862	51442	
	SD	3777	2822	5504	2891	
	Min.	46667	47160	42277	48504	
	Max.	61572	54847	61125	57718	
Manganese (Mn)	Mean	528	496	542	503	
	SD	65	57	118	60	
	Min.	403	445	378	375	
	Max.	768	613	798	593	
Iron (Fe)	Mean	25179	23933	27277	25839	
	SD	3059	2753	3956	2604	
	Min.	20258	20392	21467	22892	
	Max.	31543	27156	34361	30152	
Phosphorus (P)	Mean	946	1012	723	943	
	SD	274	433	278	272	
	Min.	579	645	445	659	
	Max.	1608	2108	1236	1452	
Lithium (Li)	Mean	27.0	25.1	29.2	27.3	
	SD	3.64	3.34	3.67	2.56	
	Min.	21.0	21.6	22.6	24.2	
	Max.	35.1	30.3	36.3	31.1	
Beryllium (Be)	Mean	1.92	1.85	1.86	1.88	
	SD	0.100	0.082	0.219	0.157	
	Min.	1.69	1.78	1.47	1.70	
	Max.	2.17	2.02	2.26	2.22	
Lead (Pb)	Mean	62.5	62.7	29.8	24.6	
	SD	37.5	44.4	11.4	5.6	
	Min.	21.2	24.6	18.7	17.6	**100[a]**
	Max.	149	175	52.3	34.0	
Cadmium (Cd)	Mean	0.404	0.321	0.594	0.156	
	SD	0.323	0.185	1.551	0.032	
	Min.	0.100	0.175	0.121	0.114	
	Max.	1.60	0.776	6.20	0.223	
Zinc (Zn)	Mean	195	237	81	82	
	SD	113	189	24.9	29.6	
	Min.	58	60	43	51	**200[a]**
	Max.	431	702	129	142	
Copper (Cu)	Mean	103	140	26.8	22.4	
	SD	78	141	10.5	7.72	
	Min.	23.0	20.5	12.1	13.7	**100[a]**
	Max.	302	494	45	41	
Nickel (Ni)	Mean	60	59	28.5	28.5	
	SD	34.8	28.5	5.5	5.5	
	Min.	25.3	23.2	21.1	19.6	
	Max.	193	127	40	40	
Cobalt (Co)	Mean	8.29	7.72	9.07	8.47	
	SD	1.68	1.41	1.25	1.17	
	Min.	5.94	5.93	7.22	7.31	
	Max.	12.7	9.48	11.1	10.6	
Chromium (Cr)	Mean	103	121	57	53.6	
	SD	46	78	10.8	9.17	100[a]

	Min.	50	46	41	43
	Max.	215	319	77	75
Vanadium (V)	Mean	58.7	54.7	65.5	62.0
	SD	8.24	6.71	8.75	7.81
	Min.	46.7	47.6	52.1	53.6
	Max.	77.2	64.6	79.8	77.8
Arsenic (As)	Mean	7.94	7.67	11.5	8.51
	SD	1.33	1.10	2.42	1.35
	Min.	5.98	6.09	7.86	7.03
	Max.	11.3	10.1	16.0	11.3
Molybdenum (Mo)	Mean	1.71	1.59	0.906	0.770
	SD	0.74	0.916	0.502	0.428
	Min.	0.63	0.625	0.191	0.331
	Max.	3.63	3.59	1.69	1.91
Antimony (Sb)	Mean	1.58	1.60	1.04	0.867
	SD	0.92	0.85	0.54	0.226
	Min.	0.59	0.58	0.43	0.585
	Max.	5.33	3.56	2.72	1.33
Tin (Sn)	Mean	8.51	9.48	4.78	5.69
	SD	3.70	6.34	1.03	2.18
	Min.	3.49	3.71	3.19	3.97
	Max.	15.1	25.4	6.76	10.3
Barium (Ba)	Mean	468	457	493	442
	SD	40.8	44.2	64.6	41.2
	Min.	402	408	395	406
	Max.	541	523	593	536
Hafnium (Hf)	Mean	0.098	0.090	0.059	0.096
	SD	0.069	0.057	0.025	0.080
	Min.	0.002	0.008	0.030	0.010
	Max.	0.228	0.133	0.081	0.232
Selenium (Se)	Mean	0.514	0.506	0.499	0.574
	SD	0.050	0.092	0.038	0.080
	Min.	0.415	0.376	0.445	0.437
	Max.	0.637	0.714	0.571	0.713
Rubidium (Rb)	Mean	107	101	111	106
	SD	9.04	6.53	14.0	6.79
	Min.	92.0	90.8	85.4	99.2
	Max.	130	110	134	121
Silver (Ag)	Mean	0.357	0.354	0.180	0.312
	SD	0.224	0.317	0.173	0.277
	Min.	0.085	0.125	0.045	0.062
	Max.	0.936	1.16	0.611	0.919
Titanium (Ti)	Mean	3108	2968	3057	3287
	SD	276	241	168	172
	Min.	2656	2695	2833	3011
	Max.	3693	3487	3442	3601
Cesium (Cs)	Mean	6.28	5.87	7.39	6.99
	SD	0.93	0.86	1.22	0.74
	Min.	4.92	4.84	5.24	6.23
	Max.	8.57	7.12	9.83	8.30
Strontium (Sr)	Mean	120	114	89	147
	SD	28.8	24.7	20.7	31.4
	Min.	91	92	65	97
	Max.	235	164	136	196
Thallium (Tl)	Mean	0.489	0.464	0.528	0.502
	SD	0.042	0.036	0.068	0.034
	Min.	0.423	0.420	0.411	0.461
	Max.	0.607	0.514	0.648	0.57
Uranium (U)	Mean	1.92	1.93	1.61	2.11
	SD	0.43	0.60	0.34	0.34
	Min.	1.45	1.21	1.20	1.47
	Max.	3.06	3.35	2.26	2.66

[a]Europian Commission (EC-DG, 2009)

Table A3: Descriptive statistics for major and minor element concentrations in urban allotment topsoils in different allotment sites. All values are given in mg kg^{-1}.

Metal(loid)/ allotment sites topsoils		PF	ST	CN	MP	MR	BH	SN	WT	WM	SGV	Sludge regulations
	n	14	50	21	9	12	20	7	5	6		
Sodium (Na)	Mean	1503.8	1148.3	2324.3	1006.8	1776.7	952.8	940.7	1148.3	1167.0		
	SD	106.8	110.1	143.1	40.4	131.6	63.0	80.6	41.3	211.8		
	Min.	911.9	712.7	1195.9	879.4	1328.6	585.4	604.7	954.7	798.3		
	Max.	2353.2	1972.2	3076.1	1123.3	2151.7	1300.8	1281.4	1504.8	1691.2		
Magnesium (Mg)	Mean	2623.2	4806.3	4729.7	9443.8	2733.9	5323.1	17709.4	4942.0	4657.1		
	SD	133.8	306.0	178.7	368.2	98.8	143.8	801.6	101.4	131.5		
	Min.	1485.7	2401.3	2329.2	7005.8	1986.0	1473.6	8427.9	4626.7	3390.6		
	Max.	3954.8	10164.7	7191.1	11611.9	3691.2	12589.7	30522.8	5362.2	6437.4		
Potassium (K)	Mean	9641.2	18421.2	12973.4	26633.4	10079.2	7744.4	24936.8	1607.2	18558.3		
	SD	652.4	876.1	336.5	366.7	429.5	187.7	285.4	112.5	521.8		
	Min.	5050.8	9878.4	9739.6	23614.5	8241.6	6958.8	22693.2	1294.8	14378.1		
	Max.	14769.1	26550.3	15120.9	28412.6	12750.2	8949.4	26225.4	2149.4	23234.6		
Calcium (Ca)	Mean	6212.9	8759.4	12180.5	6875.6	11493.5	11191.9	16360.3	5754.2	7430.6		
	SD	527.3	567.7	663.4	215.6	416.6	311.0	509.5	153.8	259.7		
	Min.	3997.6	2402.3	6152.9	5568.9	8739.9	2448.7	7917.0	3805.8	5515.5		
	Max.	10387.1	21587.7	17899.6	7901.3	16131.6	25830.0	31548.1	8874.5	8902.2		
Aluminium (Al)	Mean	24259.5	28832.6	40203.6	53272.8	34481.9	21401.4	49860.5	38429.9	40372.9		
	SD	1504.3	2042.3	1772.2	954.4	1262.1	481.9	1098.8	2347.1	2737.4		
	Min.	8429.8	7192.6	28073.4	47406.2	27078.2	17498.5	36869.2	34809.0	31890.0		
	Max.	53485.3	56472.0	45493.3	60216.7	49101.0	25637.2	57603.3	45946.6	47976.3		
Manganese (Mn)	Mean	493.9	610.5	632.6	532.7	689.8	704.9	705.0	530.2	558.4		
	SD	34.4	35.1	33.5	11.8	25.8	20.2	6.5	15.0	15.6		
	Min.	306.2	290.8	475.4	495.0	575.7	309.1	542.5	423.6	500.9		
	Max.	797.8	1173.1	938.8	592.0	875.4	1234.9	864.5	623.7	651.2		
Iron (Fe)	Mean	30874.0	27312.7	30910.6	35088.0	34941.2	19490.3	33759.0	25078.9	32853.4		
	SD	1347.9	2053.3	1127.1	520.4	2012.5	1159.8	450.9	781.9	1414.5		
	Min.	17191.8	14938.5	25062.4	31454.7	27339.6	14993.3	28889.4	22305.2	26787.9		
	Max.	44701.7	43793.8	36797.0	40504.1	43294.0	24627.3	39671.7	29036.4	41140.7		
Phosphorus (P)	Mean	1444.7	1650.0	1714.9	2015.4	2558.4	1272.3	1532.0	1607.2	2358.9		
	SD	102.1	114.0	87.8	76.5	127.3	66.9	77.3	112.5	57.7		
	Min.	737.7	634.9	884.7	1604.1	1419.3	757.1	1036.5	1294.8	1599.9		
	Max.	2723.9	3194.7	2741.4	2336.5	3805.5	2739.7	1998.7	2149.4	2913.6		
Lithium (Li)	Mean	50.1	56.4	53.2	93.9	34.7	29.4	78.5	43.2	49.5		
	SD	2.6	13.1	1.6	1.1	0.8	0.6	2.5	0.5	1.6		
	Min.	23.4	28.4	30.0	79.9	28.6	18.0	53.4	41.4	35.4		
	Max.	82.0	466.5	69.0	101.4	41.3	36.1	112.7	46.9	72.6		
Beryllium (Be)	Mean	3.268	3.942	2.258	4.013	4.045	1.106	3.751	2.454	4.114		
	SD	0.186	1.043	0.072	0.098	0.250	0.046	0.078	0.020	0.144		
	Min.	1.693	1.711	1.624	3.370	3.208	0.674	2.758	2.111	3.282		
	Max.	5.417	33.933	2.990	4.753	4.854	1.621	4.955	2.672	5.267		
Lead (Pb)	Mean	176	457.5	186.6	230.8	406.7	51.8	175.3	110.4	620.7		
	SD	60	63.9	8.2	4.4	26.4	2.7	23.1	3.2	164.2		
	Min.	77.8	140.6	122.3	197.9	208.5	27.1	92.9	88.5	293.3	450[a]	
	Max.	1108	1062.1	270.2	259.5	931.7	138.2	272.6	142.5	1148.3		
Cadmium (Cd)	Mean	0.812	0.770	1.582	0.652	1.374	0.383	0.693	0.437	1.033		
	SD	0.105	0.060	0.045	0.020	0.046	0.024	0.033	0.010	0.068		
	Min.	0.444	0.317	0.635	0.576	0.725	0.206	0.470	0.388	0.780	1.80[a]	
	Max.	1.523	0.042	2.349	0.780	4.365	0.964	0.969	0.528	1.408		
Zinc (Zn)	Mean	268.6	366.6	316.8	368.2	443.0	116.3	313.8	220.8	513.8		
	SD	22.8	20.3	7.4	6.6	10.3	4.5	15.6	5.9	18.0		
	Min.	189.5	150.6	226.1	334.7	244.1	63.3	256.9	191.4	356.6		300[b]
	Max.	409.8	690.8	509.4	428.8	800.4	231.9	394.7	277.6	757.1		
Copper (Cu)	Mean	48.8	78.7	56.4	81.4	92.3	31.4	84.7	39.5	79.9		
	SD	3.2	17.2	1.8	1.2	10.8	1.3	1.0	0.7	4.4		
	Min.	33.5	35.8	35.4	63.7	50.2	16.3	36.3	30.8	58.9		135[b]
	Max.	69.3	545.7	83.5	96.0	186.3	50.9	262.3	45.5	100.9		
Nickel (Ni)	Mean	37.6	36.9	34.3	41.5	35.0	14.8	43.1	25.7	39.8		
	SD	3.2	4.2	2.6	1.2	2.1	1.3	2.0	1.7	2.6		
	Min.	22.4	19.6	21.0	36.6	27.7	8.4	36.2	20.7	30.9	250[a]	
	Max.	68.0	83.1	55.6	48.2	54.6	20.0	55.6	29.3	49.5		
Cobalt (Co)	Mean	13.4	12.9	11.6	14.4	12.0	6.2	14.7	9.7	14.0		
	SD	0.7	0.8	0.3	0.3	0.7	0.2	0.2	0.2	0.4		
	Min.	6.9	7.3	8.6	12.9	9.4	3.7	13.3	7.9	11.0		
	Max.	21.8	20.7	14.1	17.1	14.2	9.7	18.4	11.8	16.3		
Chromium (Cr)	Mean	55.9	47.3	52.4	59.5	41.2	24.8	61.7	47.8	45.4		
	SD	5.5	3.3	1.7	1.0	1.4	1.3	1.4	0.9	1.9		
	Min.	41.4	26.3	32.7	55.1	34.5	17.3	53.3	40.2	39.2	130[a]	
	Max.	73.2	97.4	68.2	67.1	52.0	37.3	70.0	63.7	58.0		

Vanadium (V)	Mean	67.7	53.3	62.2	73.7	52.6	31.6	71.1	51.6	55.4	
	SD	3.4	2.5	1.4	1.2	1.9	1.2	0.8	0.8	1.8	
	Min.	35.9	31.9	41.8	66.4	45.9	22.0	62.4	48.3	45.7	
	Max.	98.8	86.0	80.3	85.1	58.7	39.6	79.6	57.0	65.6	
Arsenic (As)	Mean	15.6	16.4	16.8	19.3	18.4	9.7	15.9	12.4	21.5	
	SD	0.8	1.0	0.4	0.5	1.1	0.3	0.3	0.4	0.8	
	Min.	11.2	8.4	12.5	17.6	13.6	6.4	13.1	10.4	16.4	**43[a]**
	Max.	20.7	25.5	23.1	21.8	22.3	13.7	18.9	13.3	28.4	
Molybdenum (Mo)	Mean	2.214	1.503	1.662	1.902	2.082	1.419	1.458	1.224	2.231	
	SD	0.196	0.192	0.062	0.049	0.103	0.084	0.118	0.035	0.103	
	Min.	0.434	0.434	1.076	1.674	1.833	0.820	0.958	1.017	1.568	
	Max.	4.063	2.924	2.387	2.138	2.454	2.499	1.825	1.429	3.805	
Antimony (Sb)	Mean	3.154	5.224	3.072	4.252	4.817	1.475	3.520	2.909	6.172	
	SD	0.264	0.453	0.248	0.139	0.452	0.098	0.269	0.294	1.293	
	Min.	2.012	1.668	1.144	3.571	2.875	0.709	2.071	1.693	3.896	
	Max.	4.769	17.580	6.006	5.388	6.498	2.924	5.955	3.784	8.742	
Tin (Sn)	Mean	6.910	13.609	10.606	13.372	17.218	2.388	14.700	8.434	17.931	
	SD	3.069	3.510	6.929	2.358	3.507	0.263	9.312	2.804	3.672	
	Min.	2.696	5.512	3.051	8.764	5.978	1.038	7.213	3.537	7.275	
	Max.	21.858	118.359	61.520	18.938	81.995	3.928	50.966	12.161	32.732	
Barium (Ba)	Mean	402.3	534.9	650.1	488.2	712.8	245.9	455.2	450.4	573.9	
	SD	24.1	29.3	30.3	11.8	30.4	16.4	9.7	3.6	15.6	
	Min.	320.3	282.2	483.1	459.7	484.4	199.8	406.9	406.3	495.9	
	Max.	497.4	998.5	813.8	515.3	1255.8	461.5	534.9	480.5	639.8	
Hafnium (Hf)	Mean	1.910	2.117	2.365	3.079	1.737	1.474	2.776	2.722	2.117	
	SD	0.105	0.106	0.084	0.073	0.057	0.070	0.078	0.187	0.077	
	Min.	1.188	1.247	1.715	2.931	1.386	1.125	2.378	2.320	1.703	
	Max.	2.696	3.014	2.840	3.311	2.230	1.706	3.249	2.939	2.624	
Selenium (Se)	Mean	1.22	1.13	1.24	1.64	1.45	0.70	1.06	0.87	1.39	
	SD	0.08	0.06	0.04	0.03	0.05	0.03	0.02	0.02	0.04	
	Min.	0.80	0.61	0.95	1.44	1.21	0.42	0.57	0.79	1.03	**120[a]**
	Max.	1.73	1.69	1.61	1.84	1.81	1.02	1.48	0.99	1.73	
Rubidium (Rb)	Mean	52.4	60.6	61.9	84.2	51.9	40.1	82.2	81.0	65.7	
	SD	3.4	3.2	2.5	2.0	1.2	1.0	4.3	1.9	2.2	
	Min.	26.1	33.6	42.1	76.7	43.3	31.6	72.2	77.1	51.0	
	Max.	75.1	85.1	71.2	94.9	65.8	44.7	96.0	93.7	79.1	
Silver (Ag)	Mean	0.34	0.35	0.28	0.36	0.40	0.15	0.28	0.24	0.46	
	SD	0.04	0.02	0.02	0.01	0.01	0.01	0.01	0.01	0.01	
	Min.	0.18	0.20	0.20	0.30	0.28	0.11	0.26	0.22	0.31	
	Max.	0.72	0.91	0.46	0.44	0.68	0.26	0.32	0.25	0.73	
Titanium (Ti)	Mean	731.8	638.5	776.6	887.8	614.8	370.2	953.3	761.6	695.0	
	SD	59.1	43.1	57.2	34.9	41.8	18.1	77.3	19.5	16.2	
	Min.	459.4	380.9	491.6	778.4	485.6	302.9	684.7	671.2	536.0	
	Max.	1128.3	1260.3	1029.2	1078.5	755.8	463.6	1240.3	814.8	956.6	
Cesium (Cs)	Mean	3.01	3.59	3.30	6.00	18.37	1.64	6.30	4.29	3.68	
	SD	0.21	0.20	0.16	0.12	1.06	0.05	0.22	0.08	0.12	
	Min.	1.47	2.09	2.04	5.16	13.60	1.25	5.30	3.94	2.39	
	Max.	4.50	6.02	4.01	6.87	22.34	1.87	7.65	5.20	5.02	
Strontium (Sr)	Mean	85.2	62.9	78.2	57.2	98.8	45.5	62.6	54.0	73.4	
	SD	4.8	3.8	2.6	1.1	4.1	2.3	1.2	1.1	2.7	
	Min.	52.7	31.2	66.0	53.4	79.4	35.2	50.5	50.5	64.7	
	Max.	122.5	101.0	100.7	62.4	122.0	58.2	76.9	62.2	92.5	
Thallium (Tl)	Mean	0.469	0.500	0.485	0.694	0.457	0.294	0.551	0.473	0.566	
	SD	0.031	0.022	0.013	0.008	0.010	0.007	0.016	0.021	0.018	
	Min.	0.289	0.329	0.399	0.657	0.378	0.223	0.472	0.449	0.515	
	Max.	0.647	0.666	0.534	0.757	0.541	0.334	0.608	0.545	0.623	
Uranium (U)	Mean	1.619	1.581	1.682	2.129	1.686	1.052	1.776	1.828	1.900	
	SD	0.086	0.081	0.046	0.030	0.047	0.043	0.026	0.017	0.069	
	Min.	0.882	0.823	1.316	2.011	1.468	0.854	1.567	1.731	1.706	
	Max.	2.476	2.310	2.012	2.317	1.965	1.200	2.094	2.046	2.201	

[a]Soil guideline values (SGVs, Environmental agency, 2009)
[b]The Sludge (Use in Agriculture) Regulations (1989)

Table A4: Descriptive statistics for rare earth elements (REEs) concentrations in different urban allotment topsoils. All values are given in mg kg^{-1}.

REEs allotment sites topsoils		PF	ST	CN	MP	MR	BH	SN	WT	WM	All sites	[a]UCC
	n	4	26	5	3	5	4	3	4	5		
La	Mean	12.63	20.09	15.60	16.23	19.57	22.82	21.21	22.00	18.87	19.23	30
	SD	0.62	1.16	1.50	0.08	1.44	0.89	1.39	0.15	0.72	1.01	
	Min.	11.42	9.95	11.25	14.53	17.18	19.99	20.55	19.54	16.66	9.95	
	Max.	13.62	25.86	21.07	17.94	22.29	24.23	22.38	23.91	20.06	25.86	
Ce	Mean	26.77	42.29	32.78	34.45	40.76	47.86	44.63	44.92	39.67	40.36	64
	SD	1.25	2.60	3.71	1.63	3.39	1.69	3.04	0.48	1.72	2.36	
	Min.	24.27	21.04	23.66	31.12	36.18	41.92	43.26	38.53	35.42	21.04	
	Max.	28.40	55.02	43.93	37.83	45.99	50.75	47.05	47.68	41.95	55.02	
Pr	Mean	3.24	5.03	4.01	4.24	5.05	5.69	5.20	5.35	4.76	4.84	7.1
	SD	0.15	0.27	0.30	0.04	0.17	0.20	0.36	0.06	0.20	0.22	
	Min.	2.92	2.48	2.81	3.82	4.62	4.97	4.98	4.60	4.32	2.48	
	Max.	3.45	6.61	5.29	4.60	5.72	6.05	5.48	5.68	5.08	6.61	
Nd	Mean	12.49	19.38	15.57	16.71	19.79	21.68	19.71	20.44	18.31	18.64	26
	SD	0.59	0.96	1.12	0.15	0.33	0.68	1.34	0.28	0.76	0.79	
	Min.	11.22	9.52	10.77	14.94	17.91	18.99	18.69	17.69	16.80	9.52	
	Max.	13.51	25.91	20.60	17.96	22.29	23.03	20.79	21.60	19.60	25.91	
Sm	Mean	2.54	3.94	3.20	3.53	4.09	4.27	3.91	4.06	3.69	3.78	4.5
	SD	0.09	0.20	0.23	0.02	0.03	0.10	0.25	0.08	0.15	0.15	
	Min.	2.27	1.90	2.18	3.14	3.53	3.74	3.69	3.62	3.44	1.90	
	Max.	2.85	5.50	4.26	3.73	4.57	4.52	4.11	4.24	4.01	5.50	
Eu	Mean	0.55	0.84	0.69	0.77	0.89	0.86	0.81	0.84	0.78	0.80	0.88
	SD	0.02	0.04	0.03	0.01	0.01	0.01	0.05	0.02	0.03	0.03	
	Min.	0.48	0.40	0.45	0.69	0.76	0.77	0.76	0.78	0.70	0.40	
	Max.	0.64	1.21	0.91	0.82	0.99	0.93	0.85	0.87	0.85	1.21	
Sc	Mean	5.16	7.94	5.89	6.66	7.77	9.01	8.12	7.95	6.87	7.49	16
	SD	0.29	0.42	0.21	0.19	0.22	0.11	0.29	0.13	0.19	0.30	
	Min.	3.75	2.54	2.59	6.05	6.75	7.78	7.92	7.34	6.11	2.54	
	Max.	6.63	11.28	7.81	7.17	8.99	9.62	8.39	8.29	7.66	11.28	
Y	Mean	8.31	12.24	9.29	10.86	12.89	12.71	12.21	12.17	11.23	11.65	24
	SD	0.18	0.70	0.46	0.21	0.74	0.32	0.97	0.14	0.29	0.54	
	Min.	6.93	5.48	5.88	9.51	10.88	10.95	11.59	10.59	10.12	5.48	
	Max.	9.97	17.93	13.39	11.78	14.63	14.06	12.80	13.07	12.46	17.93	
Gd	Mean	2.24	3.45	2.83	3.17	3.61	3.62	3.37	3.45	3.21	3.30	3.8
	SD	0.06	0.17	0.19	0.05	0.06	0.08	0.24	0.05	0.10	0.13	
	Min.	1.93	1.62	1.85	2.80	3.04	3.18	3.15	3.12	2.92	1.62	
	Max.	2.62	4.94	3.81	3.37	4.03	3.87	3.53	3.64	3.52	4.94	
Tb	Mean	0.31	0.47	0.38	0.43	0.49	0.49	0.46	0.46	0.43	0.45	0.64
	SD	0.01	0.02	0.02	0.01	0.01	0.01	0.03	0.00	0.01	0.02	
	Min.	0.27	0.22	0.24	0.38	0.41	0.43	0.43	0.42	0.39	0.22	
	Max.	0.38	0.68	0.52	0.46	0.55	0.52	0.48	0.49	0.48	0.68	
Dy	Mean	1.72	2.44	1.98	2.26	2.55	2.54	2.41	2.40	2.27	2.34	3.5
	SD	0.03	0.12	0.12	0.04	0.04	0.05	0.16	0.02	0.05	0.09	
	Min.	1.45	1.10	1.24	2.02	2.12	2.22	2.29	2.22	2.02	1.10	
	Max.	2.08	3.52	2.69	2.42	2.85	2.77	2.51	2.50	2.50	3.52	
Ho	Mean	0.33	0.45	0.37	0.42	0.47	0.48	0.45	0.45	0.42	0.44	0.8
	SD	0.01	0.02	0.03	0.01	0.01	0.01	0.03	0.00	0.01	0.02	
	Min.	0.28	0.20	0.23	0.38	0.40	0.41	0.43	0.42	0.37	0.20	
	Max.	0.40	0.66	0.50	0.45	0.53	0.52	0.48	0.46	0.46	0.66	
Er	Mean	0.95	1.27	1.01	1.17	1.32	1.36	1.28	1.26	1.17	1.22	2.3
	SD	0.02	0.06	0.06	0.03	0.02	0.03	0.09	0.02	0.02	0.04	
	Min.	0.80	0.57	0.64	1.06	1.11	1.18	1.22	1.19	1.05	0.57	
	Max.	1.14	1.80	1.37	1.26	1.48	1.48	1.35	1.30	1.29	1.80	
Tm	Mean	0.13	0.18	0.14	0.16	0.18	0.19	0.18	0.18	0.16	0.17	0.33
	SD	0.00	0.01	0.01	0.00	0.00	0.00	0.01	0.00	0.00	0.01	
	Min.	0.11	0.08	0.09	0.15	0.15	0.17	0.18	0.16	0.15	0.08	
	Max.	0.16	0.24	0.19	0.17	0.20	0.21	0.19	0.18	0.18	0.24	
Yb	Mean	0.87	1.14	0.89	1.02	1.16	1.25	1.18	1.14	1.06	1.10	2.2
	SD	0.01	0.05	0.05	0.02	0.02	0.03	0.08	0.02	0.02	0.04	
	Min.	0.75	0.52	0.57	0.94	1.00	1.07	1.14	1.07	0.97	0.52	
	Max.	1.02	1.57	1.19	1.09	1.31	1.36	1.25	1.19	1.14	1.57	
Lu	Mean	0.13	0.17	0.14	0.16	0.18	0.20	0.18	0.18	0.16	0.17	0.32
	SD	0.00	0.01	0.01	0.00	0.00	0.00	0.01	0.00	0.00	0.01	
	Min.	0.11	0.08	0.09	0.14	0.15	0.17	0.18	0.17	0.15	0.08	
	Max.	0.15	0.24	0.18	0.17	0.20	0.21	0.19	0.18	0.18	0.24	
LREEs		87.651										
HREEs		28.321										
ΣREEs		115.972										
LREEs/HEEs		3.095										

[a]Taylor and McLennan (1995)

Table A5: Descriptive statistics for rare earth elements (REEs) concentrations in different urban allotment subsoils. All values are given in mg kg^{-1}.

REEs allotment sites subsoils		PF	ST	CN	MP	MR	BH	SN	WM	All sites	[a]UCC
	n	4	26	5	3	5	4	3	5		
La	Mean	22.81	21.74	12.64	16.33	25.36	20.56	21.00	19.09	20.58	30
	SD	1.86	0.68	1.20	0.72	1.20	1.26	0.19	0.52	0.89	
	Min.	22.26	13.68	10.87	14.33	24.24	19.18	20.73	18.36	10.87	
	Max.	23.75	28.39	14.58	19.96	26.06	23.33	21.27	20.22	28.39	
Ce	Mean	52.29	45.72	26.01	33.78	52.42	42.85	43.44	39.64	43.34	64
	SD	4.10	1.39	2.39	1.44	2.07	2.80	0.54	1.12	1.82	
	Min.	46.59	28.68	22.44	29.58	49.97	40.29	42.89	38.38	22.44	
	Max.	56.75	62.58	30.18	41.15	53.83	48.93	44.00	41.64	62.58	
Pr	Mean	6.06	5.47	3.03	4.00	6.33	4.95	5.04	4.73	5.14	7.1
	SD	0.49	0.15	0.22	0.19	0.28	0.32	0.09	0.14	0.21	
	Min.	5.53	3.45	2.60	3.47	5.99	4.67	4.93	4.65	2.60	
	Max.	6.38	7.17	3.53	4.94	6.56	5.74	5.14	4.89	7.17	
Nd	Mean	22.04	21.02	11.34	15.21	24.10	18.32	18.64	17.94	19.50	26
	SD	1.85	0.52	0.78	0.64	1.04	1.13	0.30	0.56	0.75	
	Min.	21.01	13.27	9.73	13.19	22.78	17.14	18.16	17.31	9.73	
	Max.	22.87	27.44	13.28	18.87	25.01	21.52	19.12	18.21	27.44	
Sm	Mean	4.33	4.28	2.25	3.02	4.76	3.43	3.45	3.54	3.88	4.5
	SD	0.33	0.10	0.14	0.15	0.19	0.23	0.09	0.10	0.15	
	Min.	4.10	2.73	1.91	2.61	4.50	3.13	3.35	3.32	1.91	
	Max.	4.46	5.46	2.68	3.72	4.94	4.15	3.56	3.74	5.46	
Eu	Mean	0.88	0.92	0.48	0.64	0.95	0.65	0.64	0.73	0.81	0.88
	SD	0.06	0.02	0.02	0.02	0.03	0.03	0.02	0.01	0.02	
	Min.	0.82	0.61	0.42	0.57	0.88	0.58	0.63	0.64	0.42	
	Max.	0.90	1.10	0.56	0.78	1.02	0.80	0.65	0.83	1.10	
Sc	Mean	8.21	8.73	4.10	5.29	10.26	7.17	6.34	6.96	7.79	16
	SD	0.63	0.19	0.24	0.28	0.29	0.16	0.21	0.16	0.24	
	Min.	7.39	5.67	3.57	4.37	8.59	6.88	6.07	6.18	3.57	
	Max.	8.56	11.16	4.82	6.84	12.36	7.83	6.60	8.05	12.36	
Y	Mean	13.49	14.24	8.30	10.55	14.14	9.80	9.09	10.73	12.48	24
	SD	0.55	0.31	0.30	0.33	0.44	0.43	0.19	0.23	0.34	
	Min.	12.28	9.59	6.62	9.62	12.75	8.78	9.06	9.09	6.62	
	Max.	13.91	15.75	10.06	12.05	15.40	11.87	9.11	12.42	15.75	
Gd	Mean	3.73	3.78	2.00	2.70	4.04	2.79	2.72	3.04	3.37	3.8
	SD	0.23	0.09	0.11	0.10	0.15	0.17	0.07	0.08	0.11	
	Min.	3.52	2.47	1.65	2.38	3.79	2.49	2.64	2.73	1.65	
	Max.	3.84	4.65	2.41	3.26	4.26	3.43	2.79	3.38	4.65	
Tb	Mean	0.51	0.52	0.28	0.37	0.54	0.37	0.35	0.41	0.46	0.64
	SD	0.03	0.01	0.01	0.01	0.02	0.02	0.01	0.01	0.01	
	Min.	0.47	0.34	0.23	0.33	0.51	0.33	0.34	0.36	0.23	
	Max.	0.52	0.62	0.33	0.44	0.57	0.46	0.36	0.46	0.62	
Dy	Mean	2.69	2.75	1.50	1.96	2.83	1.98	1.85	2.14	2.43	3.5
	SD	0.11	0.06	0.06	0.06	0.10	0.09	0.05	0.04	0.07	
	Min.	2.47	1.84	1.23	1.75	2.61	1.73	1.81	1.88	1.23	
	Max.	2.80	3.19	1.82	2.31	3.03	2.40	1.89	2.42	3.19	
Ho	Mean	0.50	0.51	0.29	0.37	0.53	0.38	0.35	0.40	0.45	0.8
	SD	0.02	0.01	0.01	0.01	0.02	0.01	0.01	0.01	0.01	
	Min.	0.46	0.35	0.23	0.33	0.48	0.33	0.34	0.35	0.23	
	Max.	0.52	0.59	0.35	0.44	0.57	0.45	0.35	0.45	0.59	
Er	Mean	1.43	1.45	0.82	1.05	1.49	1.10	1.03	1.14	1.29	2.3
	SD	0.06	0.03	0.03	0.04	0.05	0.04	0.03	0.03	0.03	
	Min.	1.29	0.98	0.65	0.93	1.37	0.99	1.02	1.02	0.65	
	Max.	1.49	1.67	0.99	1.23	1.59	1.30	1.04	1.27	1.67	
Tm	Mean	0.20	0.20	0.11	0.14	0.21	0.16	0.15	0.16	0.18	0.33
	SD	0.01	0.00	0.00	0.01	0.01	0.01	0.00	0.00	0.00	
	Min.	0.18	0.14	0.09	0.13	0.19	0.14	0.15	0.15	0.09	
	Max.	0.21	0.23	0.14	0.17	0.22	0.19	0.15	0.17	0.23	
Yb	Mean	1.31	1.30	0.75	0.94	1.35	1.06	0.99	1.05	1.17	2.2
	SD	0.06	0.03	0.03	0.03	0.05	0.04	0.02	0.02	0.03	
	Min.	1.18	0.89	0.61	0.82	1.25	0.97	0.99	0.98	0.61	
	Max.	1.36	1.52	0.88	1.12	1.43	1.23	0.99	1.11	1.52	
Lu	Mean	0.20	0.20	0.11	0.14	0.21	0.16	0.16	0.16	0.18	0.32
	SD	0.01	0.00	0.00	0.01	0.01	0.01	0.00	0.00	0.01	
	Min.	0.18	0.14	0.09	0.13	0.19	0.15	0.16	0.15	0.09	
	Max.	0.21	0.23	0.13	0.17	0.22	0.19	0.16	0.17	0.23	
LREEs		84.509									
HREEs		29.904									
∑REEs		123.073									
LREEs/HEEs		2.826									

[a]Taylor and McLennan (1995)

9.2 Appendix B Investigation of interferences in the determination of PGEs by ICP-MS

B.1 Rhodium (Rh)

The calculated detection of limits (DLs), sensitivity (cps/ppb), background equivalent concentrations (BECs) and precision (%RSD) for different isotopes of Rh measured in three different modes (He, $NH_{3(on\text{-}mass)}$, $NH_{3(mass\text{-}shift)}$) of ICP-QQQ-MS are summarized in Table B.1, to investigate the efficiency of different cell gas modes in the elimination of spectral interferences. In the case of ^{103}Rh in He mode, the measured concentration in test samples was influenced more due to interference from Pb i.e. the signal was greater than the quantification limit QL, where QL is 10sd variation of the blanks. When a proportion of the Pb in the ICP forms Pb^{2+}, the doubly charged ^{206}Pb interferes with ^{103}Rh. The concentration of ^{103}Rh measured in test samples with $NH_{3(on\text{-}mass)}$ (103→103) and $NH_{3(mass\text{-}shift)}$ (103→171) modes were possibly interfered with by Sr i.e. a signal less than the QL but greater than the DL (3sd variation of the blanks), as some of the Sr in the ICP forms oxides ($^{87}Sr^{16}O^{+}$) that further interferes with ^{103}Rh. But in terms of precision (%RSD), it was observed equal in He and $NH_{3(on\text{-}mass)}$ (i.e., 2% RSD), whereas in the case of $NH_{3(mass\text{-}shift)}$ the precision was high (9% RSD). Among sensitivities calculated for the three different modes, it was found to be highest in $NH_{3(on\text{-}mass)}$ mode and was followed by He and $NH_{3(mass\text{-}shift)}$ modes. Therefore, $NH_{3(on\text{-}mass)}$ mode was considered preferable to the other modes of operation for the determination of ^{103}Rh due to higher sensitivity, better precision and likely reduced interference.

In Figure B.1, a comparison of ^{103}Rh measured in allotment soils in He and $NH_{3(on\text{-}mass)}$ modes are shown. It was observed that the concentration of ^{103}Rh

in most of the allotment samples measured in He-mode were above the DL (0.001 ppb) but this was due to overestimation of ^{103}Rh caused by interference by Pb^{2+}. In contrast the concentrations of ^{103}Rh (ppb) measured in $NH_{3(on\text{-}mass)}$ mode, were below the DL (0.0009 ppb).

Table B.1: Summary of ^{103}Rh results measured using different modes of ICP-QQQ

Transition Gas mode	**103 Rh** [He]	**103 -> 103 Rh** [NH_3]	**103 -> 171 Rh** [NH_3]
DL (ppb)	0.0010	0.0009	0.0012
DL (cps)	27	57	10
Sensitivity(cps/ppb)	87112	145930	40
BEC (ppt)	0.5	0.6	287
Accuracy	-2	-3	-12
Precision	2	2	9
Interference	**Pb^{2+}**	Sr?	Sr?

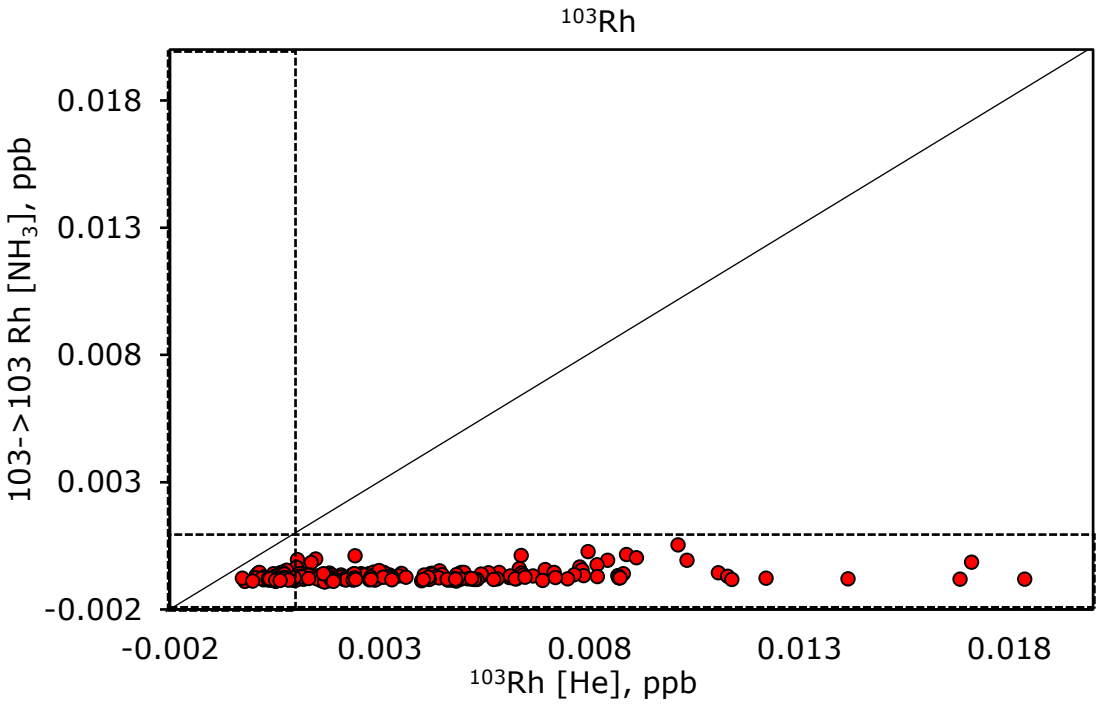


Figure B.1: Comparison of ^{103}Rh measured in allotment soils in He and $NH_{3(on\text{-}mass)}$ mode

B.2 Palladium (Pd)

Determination of ^{105}Pd was carried out in He and $NH_{3(on\text{-}mass)}$ (105→105) modes (Table B.2). In He mode, interferences were not completely eliminated in the determination of ^{105}Pd. The concentration of ^{105}Pd in test samples were seen to be affected by Cu and Sr (i.e., > DL), also interference was caused by Y i.e., > QL. Yttrium (Y) and Sr form oxides and hydro-oxides (YO^+ and $SrOH^+$) whereas Cu forms an argide ($CuAr^+$) which are responsible for interferences. In $NH_{3(on\text{-}mass)}$ (105→105) mode, the interferences observed were only due to Cu and Sr (i.e., > DL). But in both modes, $NH_{3(on\text{-}mass)}$ was comparatively better due to greater removal of spectral interferences; also the sensitivity was higher and precision (% RSD) was low in $NH_{3(on\text{-}mass)}$ mode.

Measurement of ^{108}Pd was carried out in three modes i.e., He, $NH_{3(on\text{-}mass)}$ (108→108) and $NH_{3(mass\text{-}shift)}$ (108→159). Concentration of ^{108}Pd measured in test samples in both He and $NH_{3(mass\text{-}shift)}$ modes were affected by Cu, W and Zr (i.e., > DL) due to the formation of an oxide and argide i.e., ZrO^+ and $CuAr^+$. Whereas $NH_{3(on\text{-}mass)}$ mode was better in terms of sufficient elimination of many interferences, except by Cu (>DL). Also the sensitivity was highest in $NH_{3(on\text{-}mass)}$ mode and precision (%RSD) was lowest i.e., 1% RSD. Therefore, it was a preferred mode for determination of ^{108}Pd.

In Figures B.2 and B.3, measurement of ^{108}Pd in allotment soils in He mode was compared with both $NH_{3(on\text{-}mass)}$ (108→108) and $NH_{3(mass\text{-}shift)}$ (108→159) modes. It was observed that concentration of ^{108}Pd in a few samples measured in He-mode were above the DL (0.009 ppb) which was due to the influence of spectral interferences. Whereas concentration of all samples measured in $NH_{3(on\text{-}mass)}$ mode were observed below the DL (0.03 ppb). In a comparison of He and $NH_{3(mass\text{-}shift)}$ modes, the concentration of ^{108}Pd in all samples, (except

one sample) in $NH_{3(mass\text{-}shift)}$ mode were observed to be below the DL (0.03 ppb).

Table B.2: Summary of Pd isotopes (^{105}Pd and ^{108}Pd) results measured using different modes of ICP-QQQ

Transition Gas mode	105 Pd [He]	108 Pd [He]	105->105 Pd [NH_3]	108 -> 108 Pd [NH_3]	108-> 159 Pd [NH_3]
DL (ppb)	0.009	0.009	0.03	0.03	0.03
DL (cps)	169	235	910	1120	71
Sensitivity(cps/ppb)	20839	27846	42098	54892	3552
BEC (ppt)	3	3	7	8	6
Accuracy	-1	-1	-2	-4	-16
Precision	2	2	1	1	9
Interference	**Y**,Cu?, Zr?	Cu?, Zr?	Cu?, Sr?	Cu?	Cu?, Zr?

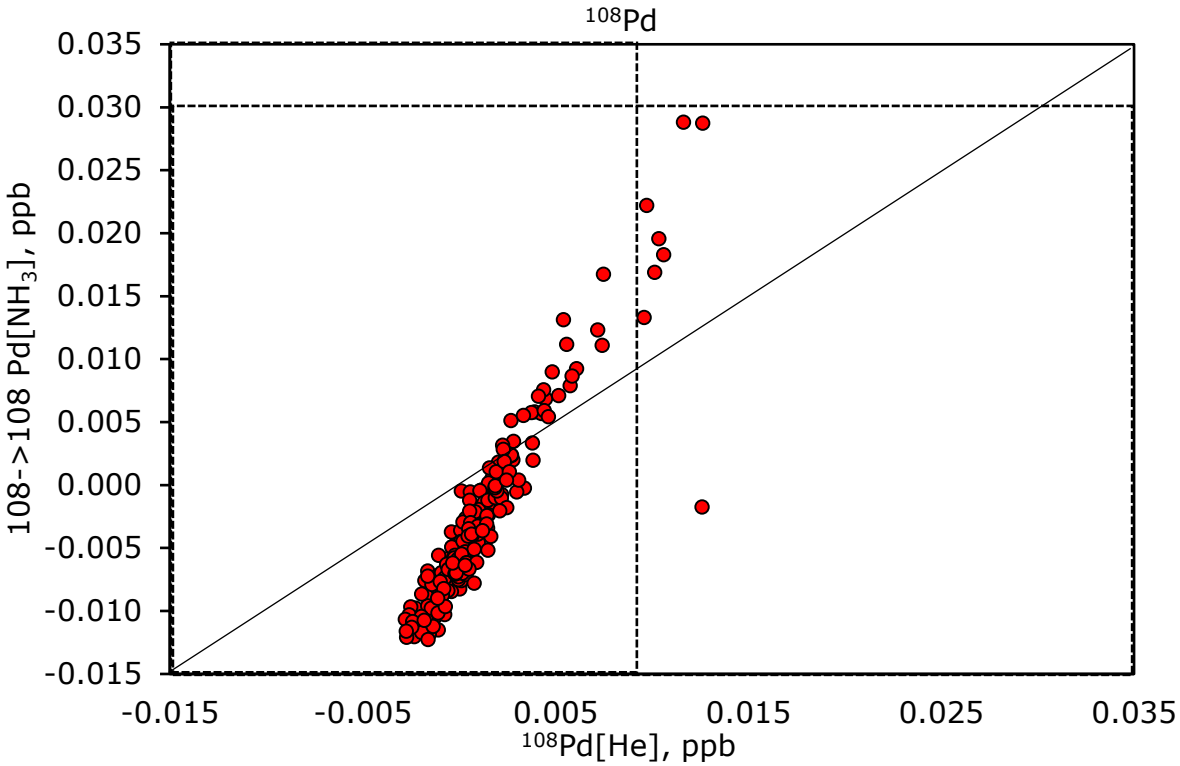


Figure B.2: Comparison of ^{108}Pd measured in allotment soils in He and $NH_{3(on\text{-}mass)}$ mode

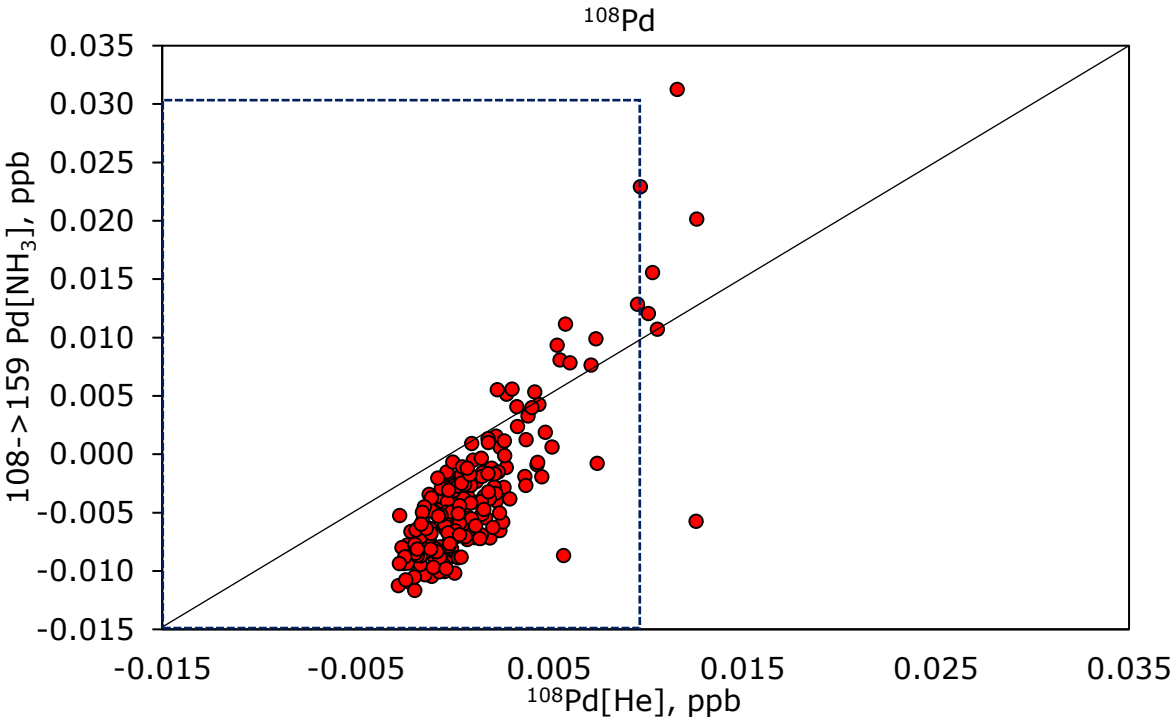


Figure B.3: Comparison of ^{108}Pd measured in allotment soils in He and $NH_{3(mass-shift)}$ mode

B.3 Iridium (Ir)

Determination of ^{191}Ir was carried out in all three modes i.e., He and $NH_{3(on-mass)}$ (191→191) and $NH_{3(mass-shift)}$ (191→206) modes in test samples (Table B.3). In He mode, the only interference observed was due to Cu and it was > DL. Whereas, in the case of $NH_{3(on-mass)}$ there was incomplete removal of interferences and an interference due to Cu, Sr and W (i.e., > DL) was seen. In $NH_{3(mass-shift)}$ mode, the concentration of ^{191}Ir in test samples was not influenced by any interferences. All measured values were within the DL. In terms of sensitivity it was very low in $NH_{3(mass-shift)}$ mode whereas in He and $NH_{3(on-mass)}$ modes, despite small interferences, the sensitivity of ^{191}Ir was high and precision (%RSD) was low. Therefore, both these modes were preferred in the determination of ^{191}Ir. Also the determination of ^{193}Ir in different modes i.e., He, $NH_{3(on-mass)}$ (193→193) and $NH_{3(mass-shift)}$ (193→208) and the potential

interfering species were also investigated. The interference-removal capability of both He and $NH_{3(on\text{-}mass)}$ modes was not effective and most severe interferences were observed due to Hf and W (i.e., > QL). Usually Hf and W form HfO^+ and WO^+ that further interfere with ^{193}Ir. In contrast $NH_{3(mass\text{-}shift)}$ mode was better in the removal of most of the interferences except for interference caused by Hf but again the sensitivity was comparatively very low.

In Figure B.4, a comparison is shown between He and $NH_{3(on\text{-}mass)}$ modes used to measure ^{191}Ir in allotment soils. In He mode only five samples were observed above the DL (0.003 ppb) and in $NH_{3(on\text{-}mass)}$ mode, only two samples were above the DL (0.005 ppb). Also comparison of ^{193}Ir measured in allotment soils in both He and $NH_{3(mass\text{-}shift)}$ modes is shown in Figure B.5. In He mode only five samples were above the DL (0.003 ppb) and in $NH_{3(mass\text{-}shift)}$ mode, concentration of ^{193}Ir in all samples were below the DL (0.01 ppb).

Table B.3: Summary of Ir isotopes (^{191}Ir and ^{193}Ir) results measured using different modes of ICP-QQQ

Transition Gas mode	191 Ir [He]	191 -> 191 Ir [NH_3]	191 -> 206 Ir [NH_3]	193 Ir [He]	193 -> 193 Ir [NH_3]	193 -> 208 Ir [NH_3]
DL (ppb)	0.003	0.005	0.02	0.003	0.005	0.01
DL (cps)	140	7	3	218	12	3
Sensitivity(cps/ppb)	66837	1987	204	114191	3522	338
BEC (ppt)	0.9	4	13	1	2	13
Accuracy	-4	-1	-1	-4	-1	-2
Precision	3	1	3	3	1	2
Interference	Cu?	Cu?, Sr?, W?		**Hf**	**Hf**	Hf?

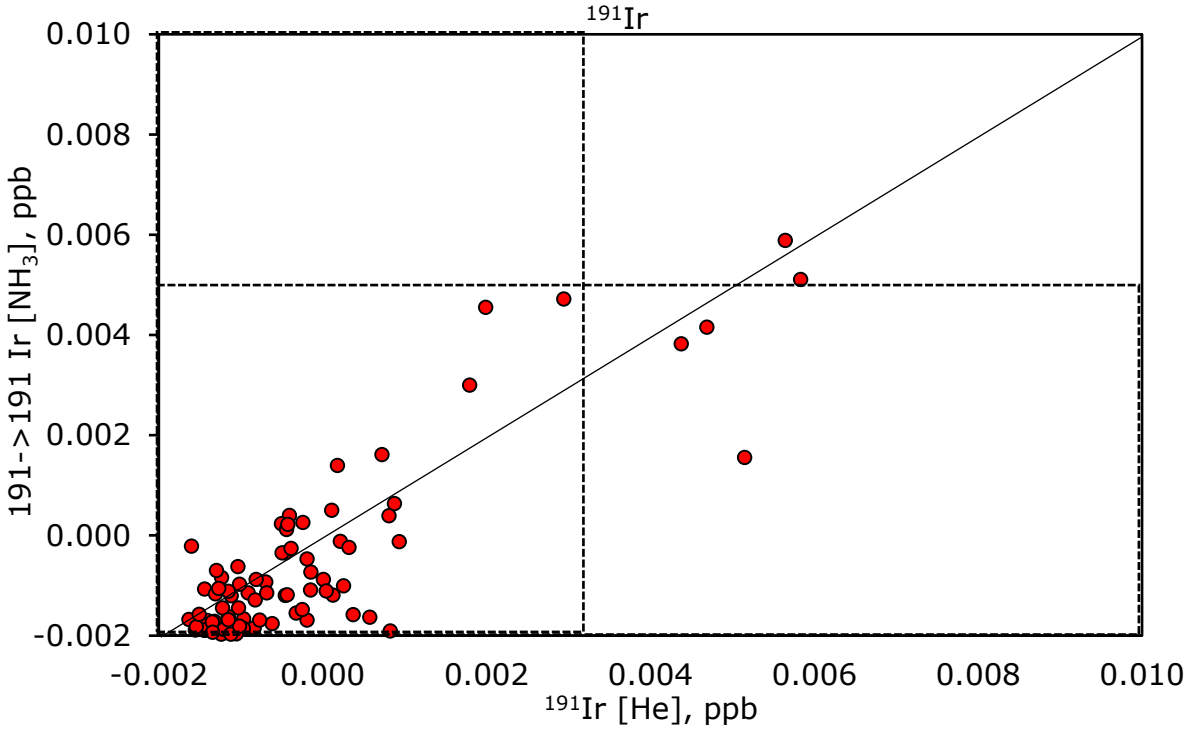


Figure B.4: Comparison of ^{191}Ir measured in allotment soils in He and $NH_{3(on-mass)}$ mode

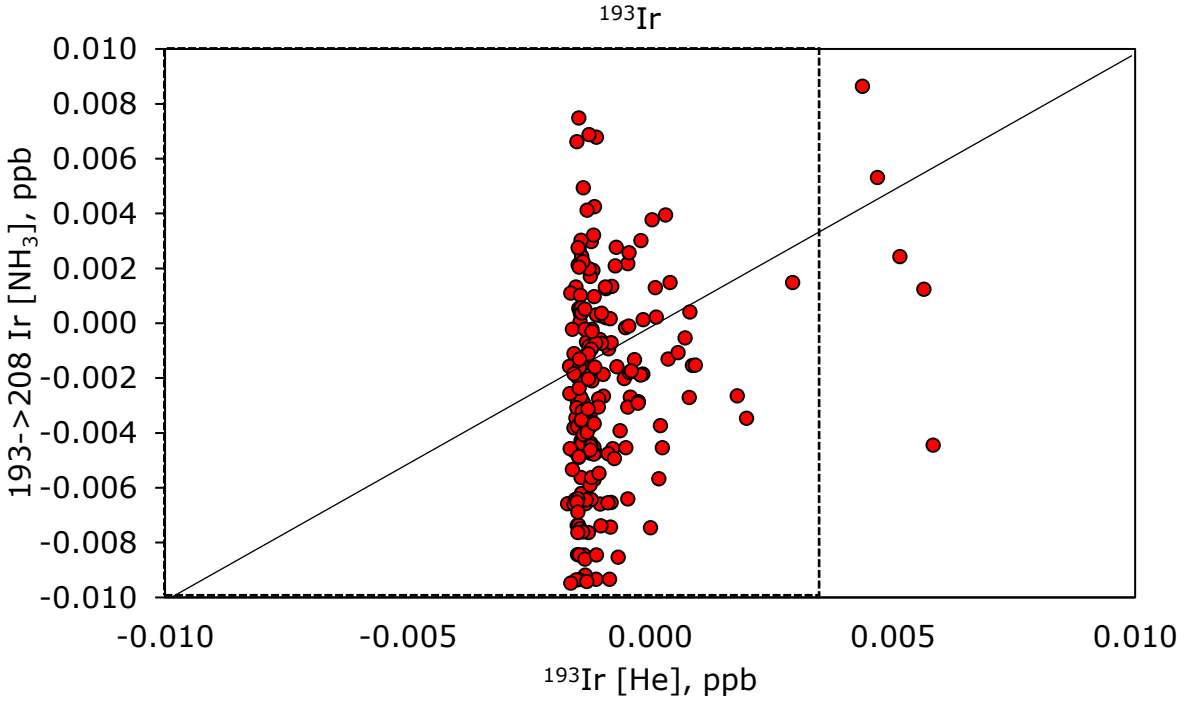


Figure B.5: Comparison of ^{193}Ir measured in allotment soils in He and $NH_{3(mass-shift)}$ mode

B.4 Platinum (Pt)

Determination of the isotopes ^{194}Pt, ^{195}Pt and ^{198}Pt measured in test samples in He mode were more affected by interferences, mostly from Hf, W, Zr and Ta with signals > QL due to oxides and hydro-oxides formed by these elements (Table B.4). The isotope ^{195}Pt was also measured in $NH_{3(on\text{-}mass)}$ (195→195) and $NH_{3(mass\text{-}shift)}$ (195→229) modes and interference by Hf and W with > QL was seen. The isotope ^{198}Pt was also determined in both these modes. In $NH_{3(on\text{-}mass)}$ mode, the common interference was due to W (>QL) and Ta (>DL). In contrast $NH_{3(mass\text{-}shift)}$ mode was more effective in eliminating interferences. In terms of sensitivity $NH_{3(mass\text{-}shift)}$ modes were better but lower than the sensitivity provided in $NH_{3(on\text{-}mass)}$ mode; nevertheless, $NH_{3(mass\text{-}shift)}$ mode was preferred for the analysis of ^{198}Pt in the allotment soils. A comparison between He and $NH_{3(mass\text{-}shift)}$ modes used in the measurement of Pt in allotment soils is shown in Figure B.6. In He mode, concentrations of ^{195}Pt in most of the allotment samples were above the DL (0.0003 ppb) due to the interferences which resulted in overestimation of ^{195}Pt concentration whereas in $NH_{3(mass\text{-}shift)}$ mode, only one sample was above the DL (0.0007 ppb).

Table B.4: Summary of Pt isotopes (^{195}Pt and ^{198}Pt) results measured using different modes of ICP-QQQ

Transition Gas mode	195 Pt [He]	195 -> 195 Pt [NH_3]	195 -> 229 Pt [NH_3]	198-> 198 Pt [NH_3]	198 -> 232 Pt [NH_3]
DL (ppb)	0.0003	0.0002	0.0005	0.0008	0.0007
DL (cps)	10	4	5	3	2
Sensitivity(cps/ppb)	44569	21705	13026	4757	2784
BEC (ppt)	0.09	0.2	0.2	0.5	0.4
Accuracy	-2	-7	-5	1	-5
Precision	3	1	3	1	4
Interference	**Hf, Ta, W,** Zr?	**Hf**,W?	**Hf, W**	**W,** Ta?	

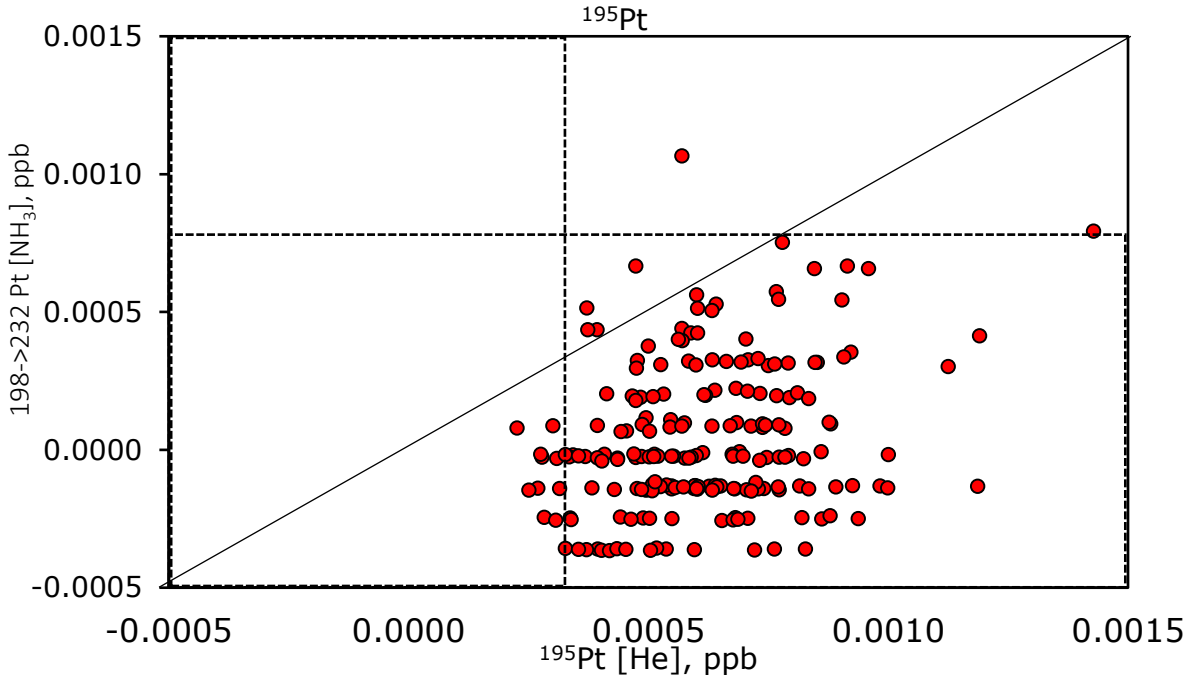


Figure B.6: Comparison of ^{195}Pt measured in allotment soils in He and $NH_{3(mass-shift)}$ mode

B.5 Gold (Au)

The ^{197}Au isotope was analysed in test samples using He, $NH_{3(on-mass)}$ (197→197) and $NH_{3(mass-shift)}$ (197→231) modes (Table B.5). Among these modes, He was not effective in removal of interferences which were mainly due to Cu, Hf, Ta, W (>QL) and Pb (>DL). The other two modes were more effective in the removal of most of the interferences except the interference caused by Cu (>QL). Interference by Cu on Au seems unlikely chance in all 3 acquisition modes; it may be that the Cu is a contaminant in the Au solution. Gold is often a bi-product of some Cu mining activities. Both $NH_{3(on-mass)}$ and $NH_{3(mass-shift)}$ were preferred for measurement of ^{197}Au. Also, a comparison of ^{197}Au analysed in He and $NH_{3(on-mass)}$ (197→197) modes in allotment soils are shown in Figure B.7. There were eleven samples observed which were above

the DL (0.004 ppb) when measured in He mode whereas, only four samples were above the DL (0.006 ppb) when measured in $NH_{3(on\text{-}mass)}$ mode.

Table B.5: Summary of ^{197}Au results measured using different modes of ICP-QQQ

Transition Gas mode	197 Au [He]	197 -> 197 Au [NH_3]	197->231 Au [NH_3]
DL (ppb)	0.004	0.006	0.006
DL (cps)	57	269	215
Sensitivity(cps/ppb)	78318	44335	39313
BEC (ppt)	0.7	2	2
Accuracy	-10	-18	-26
Precision	5	4	9
Interference	**Cu, Hf**, Pb?, **Ta**	**Cu,** Pb?, Sr?, Ta?	**Cu,** Pb?

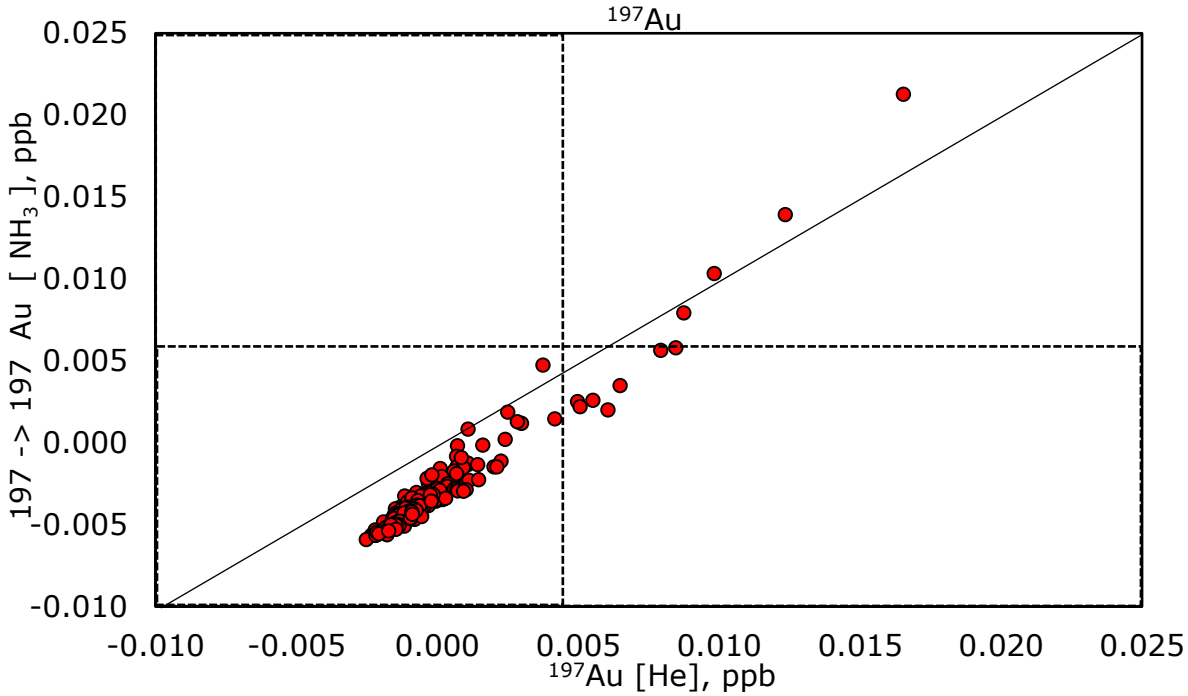


Figure B.7: Comparison of ^{197}Au measured in allotment soils in He and $NH_{3(on\text{-}mass)}$ mode.

A few samples had Au concentrations above the detection limit even in the preferred on-mass NH_3 mode. These were investigated further and it was observed that those samples above the DL were analysed immediately after

the 5 ppb QC solution. This strongly suggests that the Au had not been properly washed out of the system at the 0.005 ppb ($\mu g\ L^{-1}$) concentration level. It was therefore concluded that all the samples were probably below the detection threshold.

9.3 Publication

Part of this work (Chapter 3) has been published as:

Usman, A., Ander, E.L., Bailey, E.H., Nelms, S., Pashley, V., Young, S.D. and Chenery, S.R., 2018. Optimisation of a current generation ICP-QMS and benchmarking against MC-ICP-MS spectrometry for the determination of lead isotope ratios in environmental samples. *Journal of Analytical Atomic Spectrometry*, *33*(12), pp.2184-2194.